Pedestrian-induced lateral vibrations of footbridges

Experimental studies and probabilistic modelling

Einar Thór Ingólfsson

PhD Thesis

Department of Civil Engineering

2011

DTU Civil Engineering Report R-231 (UK)
January 2011

DTU Civil Engineering
Department of Civil Engineering

Pedestrian-induced lateral vibrations of footbridges

Experimental studies and probabilistic modelling

Einar Thór Ingólfsson

Ph.D. Thesis

Department of Civil Engineering
Technical University of Denmark

2011

Pedestrian-induced lateral vibrations of footbridges
Experimental studies and probabilistic modelling

Printed by DTU Tryk
Department of Civil Engineering
Technical University of Denmark
ISBN: 9788778778773104
ISSN: 1601-2917

Tileinkað nafna mínum og vini,

Hr. Einari Leifi Péturssyni

Preface

This thesis is submitted as a partial fulfilment of the requirements for the Danish Ph.D. degree. The work has been carried out at the Department of Civil Engineering at the Technical University of Denmark. The work took place in the period between September 2006 to June 2010, with Associate Professor Christos Georgakis as main supervisor and Professor Jeppe Jönsson as co-supervisor.

I gratefully acknowledge their constant support and guidance. I owe my deepest gratitude to Christos for his patience and encouragement throughout the entire course of this project and for entrusting me with the freedom to work in my own way.

Part of the work was carried out during a four month research visit (April-July, 2009) to the Inter-University Research Centre on Building Aerodynamics and Wind Engineering (CRIACIV) at the University of Firenze, Italy. The results that I collected during my research visit constitute a vital part of my thesis and would not have possible without the support of Associate Professor Francesco Ricciardelli, from the University of Reggio Calabrio. For that I am deeply indebted. Furthermore, I would like to thank Professor Claudio Borri, Director of CRIACIV, for hosting my research visit and a special gratitude is directed to Lorenzo Procino chief engineer at CRIACIV and his wife Alessandra Borsani for their assistance and kind hospitality during my visit. I also express my gratitude to Niccoló Bonanni graduate student at University of Florence for his substantial contribution and enthusiasm in recruiting test persons for my experimental campaign.

This thesis is based on scientific papers which have already been accepted for publication in relevant scientific journals or presented at international conferences with peer-review. Therefore, the thesis is subdivided into two separate parts. The first part is an extended synopsis, which summarises the main results of the research work and provides the link between the appended papers. The second part is a collection of papers which the thesis is based upon.

Lastly, I am grateful for the loving support of my friends and family, in particular my wife, Eva Dögg and our little girl Embla Björk, who spent a whole summer in Prato with me during my research visit to CRIACIV.

Kongens Lyngby, December, 2010

Einar Þór Ingólfsson

Preface to published version of thesis

The thesis was defended at a public defence on Thursday 20 January 2011. The official assessment committee consisted of Associate Professor Holger Koss (chairman), Technical University of Denmark, Professor James M.W. Brownhjohn, University of Sheffield and Reader John H.G. Macdonald, University of Bristol.

Compared to the original submitted version, a number of minor editorial corrections have been made to this version of the thesis based on the examiners' recommendations.

Kongens Lyngby, August, 2011

Einar Þór Ingólfsson

Abstract

The dissertation investigates the phenomenon of excessive pedestrian-induced lateral vibrations as observed on several high-profile footbridges. In particular, the temporary closures of both Paris' Solferino Bridge (1999) and the London Millennium Bridge (2000) have led to an understanding on the part of engineers and architects of the need to evaluate the potential for footbridge vibrations that can be attributed to pedestrians. Within the scientific community, the closures have also led to the initiation of a new tract of research, focused on the understanding of pedestrian loading, bridge response and their interaction. In the last decade, a significant amount of research has been carried out in this field. As a consequence, numerous other bridges of different length and type have been found prone to similar excessive lateral vibrations when exposed to large pedestrian crowds.

However, only few national and international codes of practice and official design guidelines currently exist to help the designer address this issue. Most of these are based on the main hypothesis, that pedestrian-induced lateral loads can be modelled as velocity proportional or as *negative dampers*, resulting from the *synchronised* lateral movement of pedestrians. This excitation mechanism is often characterised as Synchronous Lateral Excitation (SLE). Reports from a limited number of controlled pedestrian crowd tests have verified the existence of a transition point at which a rapid increase in the lateral bridge response is triggered. This disproportionate increase in the lateral vibration response is caused by a dynamic interaction between the pedestrian and the laterally moving structure, although the governing mechanism which generates the load is still disputed.

In this thesis, a comprehensive literature review is presented, solely focused on pedestrian-induced lateral forces, their effect on footbridges and existing theoretical models of human-structure interaction. It is shown that different hypotheses exist about the nature of this interaction, many of which are only supported by theoretical modelling and lack sufficient experimental evidence to support their applicability. Especially, the importance of human-structure synchronisation for the development of large footbridge vibrations is questionable.

Therefore, an extensive experimental campaign has been carried out to determine the lateral forces generated by pedestrians during walking on a laterally moving treadmill. Two different conditions are investigated; initially the treadmill is fixed and then it is laterally driven in a sinusoidal motion at varying combinations of frequencies (0.33 – 1.07 Hz) and amplitudes (4.5 – 48 mm). The experimental campaign involved 71 test subjects who covered approximately 55 km of walking distributed on almost 5000 individual tests. An in-depth analysis of the movement of the pedestrians that participated in the experimental campaign reveal that synchronisation is not a pre-condition for the

development of large amplitude lateral vibrations on footbridges, as walking frequencies remain largely unaffected by the lateral motion. Instead, large amplitude vibrations are the result of correlated pedestrian forces in the form of *negative damping* that can be generated irrespective of the relationship between the walking frequency and the frequency of the lateral movement. These forces are *self-excited* in the sense that they are generated by the movement of the body's centre of mass, which in turn is caused by the lateral acceleration of the underlying pavement.

Due to the random nature of the human-induced loadings and a large scatter in the experimental data, a novel stochastic load model for the frequency and amplitude dependent lateral forces is presented. The parameters in the model are based directly on the measured lateral forces from the experimental campaign. Thereby, the model is currently the most statistically reliable analytical tool for modelling of pedestrian-induced lateral vibrations. It is shown that the modal response of a footbridge subject to a pedestrian crowd is sensitive to the selection of the pacing rate distribution within the group, the magnitude of ambient loads and the total duration of the load event. The selection of these parameters ultimately affects the critical number of pedestrians needed to trigger excessive vibrations in a particular simulation.

Finally, a simplified frequency dependent stability criterion is presented, for which the critical number of pedestrians needed to cancel the inherent modal damping of a footbridge can be obtained.

Resumé

Denne afhandling omhandler vandrette fodgængerinducerede svingninger svarende til dem der bl.a. blev observeret på Londons præstigefulde gangbro, Millennium Bridge i året 2000 og Solferino-broen i Paris i 1999. I særdeleshed har den midlertidige lukning af førnævnte broer gjort ingeniører og arkitekter bevidste om de potentielle svingningsproblemer som fodgængere kan forårsage i gangbroer. Som en følge heraf er der opstået en ny forskningsretning som søger at forstå effekten af fodgængerinducerede laster på gangbroer og kvantificere interaktionen mellem fodgængere og et vandret bevægende underlag. I det sidste årti er antallet af videnskabelige publikationer indenfor dette område steget stødt og stadig flere tilfælde af broer der har oplevet lignende voldsomme svingninger er blevet offentliggjorte.

Til trods for dette findes der på verdensplan kun et fåtal normer og retningslinjer med vejledninger til undgåelse af disse problemer i nye gangbroer. Disse vejledninger bygger typisk på en antagelse om at fodgængerinducerede vandrette laster er proportionale med broens svingningshastighed, hvorfor deres effekt kan modelleres som *negative dæmpere* hidrørende fra en synkroniseret bevægelse af fodgængerne. Denne ekscitationsmekanisme er ofte karakteriseret som *Synkroniseret Vandret Ekscitation* (e. Synchronised Lateral Excitation – SLE). Observationer fra et begrænset antal fuldskala gruppeforsøg har eftervist forekomsten af en form for ustabilitet, karakteriseret ved en uforholdsmæssig stigning i den vandrette respons ved en forøgelse af antallet (udover et kritisk antal) af fodgængere på broen. Fænomenet skyldes en form for interaktion mellem fodgængerne og den vandrette bevægelse af broen, men de styrende mekanismer i forbindelse med lastfrembringelsen debatteres stadig.

I denne afhandling præsenteres et omfattende litteraturstudie der omhandler fodgængerinducerede vandrette laster, deres effekt på gangbroer og teoretiske modeller af interaktionen derimellem (e. Human-Structure Interaction). Det vises her at der eksisterer forskellige hypoteser vedrørende interaktionens karakter. Mange af disse beror udelukkende på teoretiske modeller og mangler fyldestgørende empirisk dokumentation til at understøtte og retfærdiggøre deres anvendelse. I særdeleshed betvivles vigtigheden af personers synkronisering til broens svingninger som forudsætning for udvikling af voldsomme sideværts svingninger.

I dette studium er der udført eksperimentelle undersøgelser, hvis formål er at bestemme de laster som hidrører fra personers gang på et vandret bevægeligt underlag, nærmere betegnet et løbebånd. Lasterne er bestemt under to forskellige forhold. I den første del fastholdes løbebåndet mod vandret bevægelse hvorefter den anden del er karakteriseret ved en påtvungen sinusformet bevægelse ved forskellige kombinationer af frekvens (0.33-1.07 Hz) og amplitude (4.5-48 mm). Dette studie omfattede 71 personer der tilsammen

tilbagelagde 55 km fordelt på næsten 5000 individuelle forsøg. En detaljeret analyse af forsøgspersonernes bevægelsesmønstre afslørede at synkronisering mellem personen og det bevægelige underlag ikke er nødvendig for at forårsage store vandrette svingninger i gangbroer. Derimod fremkommer de store svingninger fra hastighedskorrelerede kræfter i form af negativ dæmpning, der kan opstå uafhængigt af forholdet mellem gangfrekvensen og frekvensen af den vandrette bevægelse. Disse kræfter fremkaldes af accelerationer af kroppens tyngdepunkt forårsaget af underlagets bevægelse, hvorfor de beskrives som selvinducerede (e. self-excited).

Grundet den store spredning i forsøgsresultaterne, samt det faktum af menneskeinducerede laster generelt er underlagt en stor usikkerhed, er der udviklet en stokastisk model der beskriver frekvens- og amplitudeafhængigheden af de vandrette laster hidrørende fra fodgængere. Parametrene i modellen er baseret direkte på forsøgsresultaterne og udgør dermed et robust og statistisk pålideligt værktøj til modellering af fodgængerinducerede vandrette vibrationer. Det demonstreres her, at responsen af gangborer udsat for last fra menneskegrupper er følsom over for valg af diverse inputparametre. Disse tæller blandt andet fordelingen af gangfrekvenser i gruppen, størrelsen af lasten fra de øvrige omgivelser eksempelvis vind, samt lastvarigheden. Valget af disse parametre har en afgørende betydning for antallet af fodgænger, der kan forårsage voldsomme svingninger i et givet scenarie.

Afslutningsvis præsenteres et forenklet stabilitetskriterium der kan anvendes til at bestemme det kritiske antal personer som kan ophæve konstruktionens dæmpning og dermed forårsage voldsomme svingninger.

Table of Contents

Additional work (not included in the thesis)

[1] Živanović S., Ingólfsson E.T., Pavic A. and Gudmundsson G.V.: 'Experimental Investigations of Reykjavik City Footbridge'. In proceedings: *International Modal Analysis Conference (IMAC-XXVIII), 2010, Orlando, Florida (USA).*

[2] Živanović S., Pavic A. and Ingólfsson E.T.: 'Modelling Spatially Unrestricted Pedestrian Traffic on Footbridges'. Published in: *ASCE Journal of Structural Engineering, Vol. 136 (10),1296-1306, 2010, doi:10.1061/(ASCE)ST.1943.541X.0000226.*

[3] Ingólfsson E.T., Georgakis C.T. and Svendsen M.N.: 'Vertical footbridge vibrations: details regarding and experimental validation of the Response Spectrum Methodology'. In proceedings: *of Footbridge 2008, Third International Conference, 2008, Porto (Portugal).*

[4] Georgakis C.T. and Ingólfsson E.T.: 'Vertical footbridge vibrations: the Response Spectrum Methodology'. In proceedings: *of Footbridge 2008, Third International Conference, 2008, Porto (Portugal).*

[5] Gudmundsson G.V., Ingólfsson E.T., Einarsson B. and Bessason B.: 'Serviceability assessment of three lively footbridges in Reykjavik'. In proceedings: *of Footbridge 2008, Third International Conference, 2008, Porto (Portugal).*

[6] Ricciardelli F., Briatico C., Ingólfsson E.T. and Georgakis C.T.: 'Experimental validation and calibration of pedestrian loading models for footbridges'. In proceedings: *Experimental Vibration Analysis for Civil Engineering Structures, 2007, Porto (Portugal).*

[7] Ingólfsson E.T., Georgakis C.T., Jönsson J. and Ricciardelli F.: 'Vertical footbridge vibrations: towards an improved and codifiable response evaluation'. In proceedings: *the third International Conference on Structural Engineering, Mechanics and Computation, 2007, Cape Town (South Africa).*

Part I

Extended summary

Chapter 1

Introduction

Traditional structural design is governed by the load carrying capacity of the structural members. General requirements in codes of practice are mostly based on verification of this, the so-called Ultimate Limit State. With recent advances in computer based modelling of structures and the use of high-strength materials, the ability of engineers to meet the architects' demand for long and lightweight spans has increased. However, as structures become longer and lighter, their susceptibility to vibration caused by dynamic forces increases. In fact, many modern structures which are designed for human occupants are prone to vibrations due to one or more natural frequencies within the range of typical human activity such as walking, running, bouncing or jumping. These structures are typically footbridges (Živanović et al., 2005a), open plan offices (Ohlsson, 1982; Pavic and Reynolds, 2002a,b), staircases (Kerr, 1998), gymnasia (Ji and Ellis, 1994; Bachmann et al., 1996a) or grandstands (Kasperski, 1996). Although cases of crowd related structural failure exist (Wolmuth and Surtees, 2003), vibrations caused by human occupants are in most cases a matter of comfort, rather than structural strength or integrity. With an increasing demand for service-life performance of modern structures and low tolerance for perceptible vibrations, *vibration serviceability* design of structures has become an increasingly important discipline in civil engineering.

1.1 Vibration serviceability of footbridges

Research within vibration serviceability of civil engineering structures covers a wide range of structures and potential excitation sources. A widely used terminology in vibration serviceability is that of the ISO 10137 standard (ISO 10137, 2007). Here distinction is made between the *vibration source*, the *transmission path* and the *vibration receiver* (Živanović et al., 2005a). The vibration source covers all possible sources to the dynamic loading but in the work presented in this thesis, the source is limited to human-induced excitation. The transmission path deals with a description of the structure, e.g. a footbridge, in which the vibration is transferred from the source to the receiver and is characterised by its mass, stiffness and damping properties. Finally, the receiver is the person or the object for which the vibrations should be assessed.

Early research into vibration serviceability of footbridges is dated back to the seventies, with the work of Blanchard et al. (1977) to define design guidelines for the assessment

Figure 1.1: *The London Millennium Footbridge (Picture from* `http://www.cambridge2000.com/gallery`*).*

of human-induced vertical vibrations of footbridges. His work was later incorporated into several international bridge design codes, such as BS5400 (BS 5400, 1978) the Ontario Highway code (OHBDC, 1983) and even the guidelines issued by the Danish Road Directorate (DRD, 2002). Although the effect of pedestrian crowds on footbridges was investigated by other researchers (Peterson, 1972; Matsumoto et al., 1978; Wheeler, 1981, 1982), only a simplified single pedestrian load scenario was included in the aforementioned standards. Furthermore, no provisions were deemed necessary for calculating the lateral response or the possibility of developing excessive crowd-induced lateral vibrations although this phenomenon was described by Peterson (1972) a few years earlier.

1.2 Excessive lateral vibrations of footbridges

Until the beginning of the new millennium, this entire research topic had not gained much public attention. Although the problems with current codes of practice had already been made clear by e.g. Rainer et al. (1988), Fujino et al. (1993), Pimentel and Waldron (1997), and Snæbjörnsson and Sigbjörnsson (1999), most modern design codes such as the British (BS 5400, 1978), American (AASHTO, 1997), Canadian (OHBDC, 1983), European (ENV 1995-2, 1997) and Scandinavian (DRD, 2002; Bro 2004, 2004) standards all relied on oversimplified methods for verification of footbridge serviceability.

On June 10$^{\text{th}}$, 2000, one of the world's most innovative pedestrian bridges was opened to the public for crossing. The London Millennium Bridge over the River Thames in London, designed by a team of world renowned architects Foster and Partners, sculptor Sir Anthony Caro and engineers Ove Arup Partnership. The structure is novel in that it is main suspension cables traverse below the bridge deck (Fig. 1.1) and it features a much smaller ratio sag-to-span ratio (around 1:60) than conventional suspension bridges. It was estimated that between 80 000 – 100 000 people crossed the bridge on the opening day, with up to 2000 people on the bridge at any one time (Dallard et al., 2001b). Within

minutes after its opening, the structure started moving laterally with amplitudes up to about 100 mm. These unexpected lateral vibrations caused city authorities to close the bridge only two days after its inauguration. In the following 18 months, Arup designed, tested and implemented a passive damping system to control the vibrations (Dallard et al., 2001a). Interestingly, it was realised that the lateral vibrations were not an artefact of the innovative design of the London Millennium Bridge, but had been observed on several occasions in the past. This included the prestigious Solferino Bridge in Paris, which was closed temporarily, immediately after its opening in 1999 (Dziuba et al., 2001).

None of the existing codes of practice or design guidelines were able to predict these excessive lateral vibrations. Therefore, a new branch of research within vibration serviceability initiated, to understand the potential negative effect of pedestrian crowds on footbridges. A series of international conferences were established, solely devoted to research and developments concerning footbridge structures. The first conference was established in Paris 2002, entitled *Footbridge 2002* and subsequently several national and international research projects were initiated to update current codes of practice and to develop design guidelines specifically for dynamic design of footbridges (FIB, 2005; Sétra, 2006; Butz et al., 2007; Willford and Young, 2006; Brownjohn et al., 2009; NA to BS EN 1991-2 UK, 2008).

1.3 The research problem

At this point it is well-known that both the pedestrian-induced load as well as the response of pedestrians to vibration is governed by randomness and depends on a vast number of biological, mechanical as well as psychological parameters. The main effects of this randomness are that (i) each pedestrian within a group will induce different load and react differently to a vibratory environment (inter-subject variability) and (ii) small variations in the walking pattern of each pedestrian (intra-subject variability) causes the load to be a narrow-band random process rather than a perfectly periodic one. In addition, the intra-subject variability can cause the same pedestrian to behave differently in two nominally identical situations (Griffin, 2004).

In relation to footbridges, a large amount of research has been published in recent years which can broadly be split into two categories, vertical and lateral pedestrian-induced vibrations. For the vertical direction the research has mainly been focused on the following:

- An accurate quantification of the loading and its randomness (Brownjohn et al., 2004b; Willford and Young, 2005; Sahnaci and Kasperski, 2005).
- The development of stochastic load models (Živanović, 2006; Tubino and Piccardo, 2008; Pedersen and Frier, 2010; Li et al., 2010).
- Simplified response evaluation techniques (Butz, 2006, 2008; Georgakis and Ingólfsson, 2008; Ingólfsson et al., 2008b).
- Analysis of footbridge response to normal pedestrian traffic (Živanović et al., 2005c; Kasperski, 2006; da Silva et al., 2007; Gudmundsson et al., 2008; Živanović et al., 2010).

The complexity of modelling pedestrian-induced loading is further increased as *human-human interaction* may force people to walk at a different speed when walking in a crowd compared to the normally preferred walking speed of the individuals. Furthermore, the interaction between the flexible structure and the pedestrians is not well understood. In particular, the effect of crowds on the apparent modal properties of bridges is currently an unknown quantity, although recent research suggests that the presence of pedestrians increase the damping of predominantly vertical vibration modes (Živanović et al., 2005b, 2009; Jørgensen, 2009).

For the lateral direction, the existence of a form of instability in which large lateral vibrations can develop under crowd loading has been observed and verified on numerous occasions (Brownjohn et al., 2008; Ingólfsson et al., 2010a). It is commonly accepted that this instability, which has become known as *Synchronous Lateral Excitation*, or simply SLE, occurs due to synchronisation (or lock-in) of the pedestrian movement to that of the footbridge. This human-structure synchronisation is in fact the most severe type of interaction, but recent research suggests that it is not a necessary condition for the development of SLE. When studying the published literature in this area, it may be divided into three categories:

1. Crowd tests of as-built bridges to verify the existence of SLE. Often a number of pedestrian crowd scenarios are presented and the results evaluated in terms of critical number of pedestrians to cause diverging vibration amplitudes.

2. Experimental tests using either instrumented platforms, shaking tables or other equipment to measure the lateral loads directly from a limited number of pedestrians at few combinations of vibration frequencies and amplitudes.

3. Theoretical load or response evaluation models, which are only partly supported by experimental studies or full scale measurements.

Each of the above mentioned research entities have provided valuably insight into the potential of crowds to cause large lateral footbridge vibrations. However, it is apparent that there is a general need for statistically reliable data on the pedestrian-induced lateral forces on a moving surface to verify existing models and demystify the governing mechanisms behind SLE. In particular, the question whether synchronisation is necessary for the development of SLE remains unanswered and little is known about the relationship between the pedestrian load and the frequency and amplitude of the lateral motion.

The working hypothesis is that in order to predict the lateral response of footbridges subject to crowd loading and thereby predict their potential to SLE, relies on an understanding of the interaction between the pedestrian and the laterally moving structure. In particular the development of motion-induced forces, i.e. forces which occur at the frequency of the structural vibrations and are caused by this interaction, are not well understood. Therefore, the main purpose of this thesis is to carry out extensive experimental investigations and provide statistically reliable data on the lateral pedestrian-induced load as a function of the lateral vibration frequency and amplitude. The measured forces will subsequently be used in a stochastic modelling framework, in which both the inter-subject and intra-subject variability are taken into account. Monte Carlo response simulations

are carried out to demonstrate the capabilities of the modelling framework and to test the sensitivity of the model to various input parameters. In the final part of this thesis, a frequency-dependent criterion for lateral stability of bridges subject to crowd loading is developed.

1.4 Thesis outline

The work presented in this thesis is structured into seven chapters (part I) and five scientific papers (part II). Part I is an extended summary, which provides the necessary references to and link between the appended papers.

In this first chapter (Chapter 1), a formal and broad introduction to the research topic in general has been given, and the scientific hypothesis which has driven this work was presented. In Chapter 2, a detailed background review relating to pedestrian-induced vibrations of footbridges is given, with main emphasis on pedestrian-induced lateral loads and their effect on low-frequency footbridges. The review includes past research into human-induced loadings, development of load models and vibration criteria as well as several examples of bridges which have experienced excessive lateral vibrations under crowd loading.

In Chapter 3, a preliminary experimental investigation is presented, utilising a laboratory platform, constructed at the laboratory of DTU Civil Engineering.

In Chapter 4, the results from an extensive experimental campaign are presented, which involve measured footfall forces from seventy-one individuals walking on both a rigid and laterally oscillating instrumented treadmill. In Chapter 5, the results from the experimental campaign were used to develop a novel stochastic time-domain pedestrian load model, for predicting the response of footbridges to crowd loading. Chapter 6 presents a simplified and conservative criterion for the determination of the the potential of excessive lateral vibrations.

Finally, a summary of the main conclusions from the research work as well as recommendations for future research are presented in Chapter 7.

Chapter 2

Background review

This chapter is primarily related to material presented in the literature review of Ingólfsson et al. (2010a) (Paper I of this thesis), which is focused on crowd-induced lateral loads and responses of bridges. The emphasis of Ingólfsson et al. (2010a) is placed on published cases of excessive bridge vibrations and the current state-of-the-art in the development of analytical load and response models. In this chapter an extended introduction to the topic is given starting with a short background on human locomotion and the generation of Ground Reaction Forces (GRFs). This section is an addition to the content presented by Ingólfsson et al. (2010a) and is essential for a full understanding of the research problem at hand. A brief summary of the content of the literature review (Ingólfsson et al., 2010a) is given with an extended section summarising different interaction mechanisms. Finally, a new section has been added relating to human response to lateral vibrations, which primarily contains references to research into human perception in high-rise buildings subject to wind-induced vibrations. With these additions, a broad introduction is given to the research field and is not restricted to the material published by Ingólfsson et al. (2010a).

2.1 Human locomotion

Walking is the fundamental form of human locomotion and the most common mean of non-vehicular transportation. Walking is an extremely complex process which has fascinated scientists throughout history, dating back to Aristotle's fundamental curiosity about the gait of animals (Aristotle, 350 B.C.), Leonardo da Vinci's (1452 – 1519) interest in the human body or Borelli's (1608 – 1679) pioneering work on the movement of humans and animals (Baker, 2007). Significant improvements in the field were made following World War II, caused by a need for an improved understanding of human locomotion for treatment of war veterans and the necessary development of protheses (Rose, 1983; Andriacchi and Alexander, 2000). In the last few decades, design of bipedal robots has contributed to an increased understanding and quantification of human balance control (Vaughan, 2003) and with the rapid development in modern technologies, techniques for clinical gait analysis have improved (Andriacchi and Alexander, 2000).

According to Perry (1992), walking can be characterised as a controlled fall where the body repeatedly falls forward from a stable position onto a contralaterally swinging limb.

This way, the driving forces of the locomotion are the fall of the body weight and the inertia force from the forward swing of the contralateral limb. The stance limb is used as a rocker to maintain the momentum created by the fall.

Different types of walking exist (normal walk, march, stroll etc.), but common for all is that at all times there is ground contact with at least one foot. A complete gait cycle (two successive footfalls) is characterised by two phases, the *stance phase* and the *swing phase* (Perry, 1992). The stance phase is the phase in which the foot is in contact with the ground, defined from initial contact (or heel strike) until the toe lifts off the ground (toe off). The swing phase is the subsequent phase in which the same foot is in the air until its heel strike, which completes the gait cycle (see Fig. 2.1). During a normal gait cycle, the stance phase lasts approximately 60 % of the time and during approximately 20 % of the time, both feet are in contact with the ground (during the initial and the terminal double limb stances respectively) (Perry, 1992). The exact duration of each period within the gait cycle depends on the walking speed as well as individual characteristics (Andriacchi et al., 1977). Particularly, the duration of the double support shortens as the walking speed increases (Racic et al., 2009). The stance phase may be further subdivided into five gait phases (Initial Contact, Loading Response, Mid-Stance, Terminal Stance and Preswing) whereas the swing phase is subdivided into three phases (Initial Swing, Mid-Swing and Terminal Swing) to fully characterise the gait cycle (see Fig. 2.1).

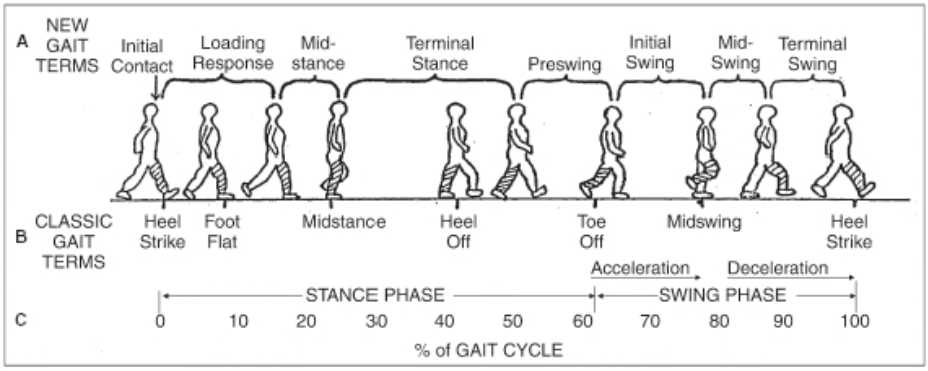

Figure 2.1: *Human gait cycle (reproduced from Uustal and Baerga (2004)).*

2.1.1 Human Ground Reaction Forces

During walking, the GRF occurs due to the acceleration and deceleration of the body's centre of mass. The GRF from a single footstep is transferred to the ground through contact with the foot during the stance phase of the gait. In general, the GRF is a three dimensional vector with varying length and direction, but is conveniently projected onto three (perpendicular) axes, determined by the forward direction of the walk. The principal directions are vertical (Superior-Inferior), longitudinal (Anterior-Posterior) and lateral (Medial-Lateral) (Racic et al., 2009). In Fig. 2.2, a characteristic shape of the GRF as projected onto the three main directions is shown, both for a single footstep as well as for repetitive (assumed identical) footsteps.

The largest component of the GRF is usually the vertical one which can be characterised by three local maxima/minima in the time history (F_7-F_9) (Andriacchi et al., 1977). The first maxima (F_7) occurs after the initial heel contact and the second maxima (F_9) occurs during the terminal stance whereas F_8 represents the local minimum between these two peaks. Similarly, with reference to Fig. 2.1, the time instances of the peaks in the horizontal loads can be linked to different phases of the gait cycle. In this thesis, the focus is on the medio-lateral component of the GRFs and a more elaborate discussion on the topic is provided by Ingólfsson et al. (2010a).

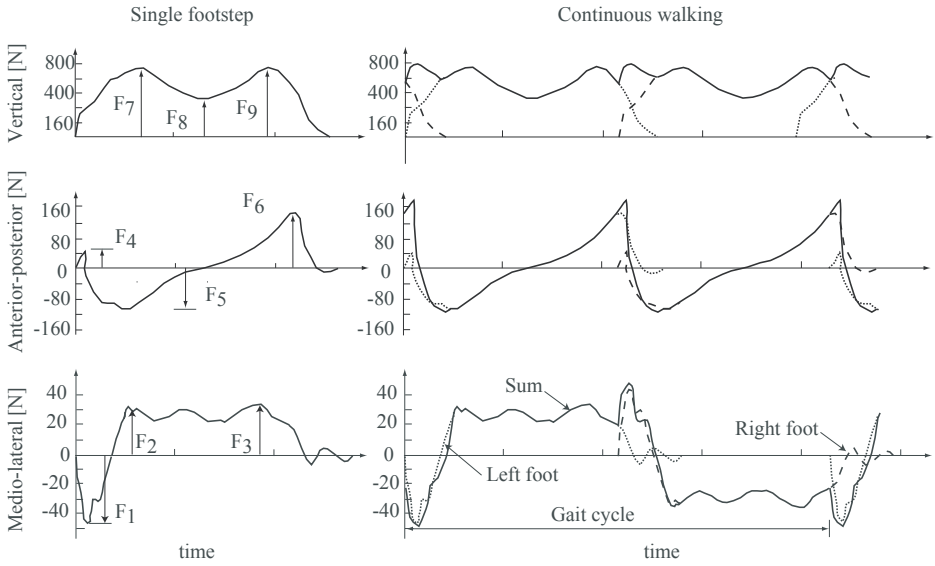

Figure 2.2: *Typical shape of the ground reaction forces projected onto vertical, anterior-posterior and medio-lateral directions for (left) a single footstep and (right) for consecutive footsteps (reproduced from Živanović et al. (2005a)).*

It should be mentioned that for civil engineering applications, the GRFs are usually quantified in the frequency domain through the body-weight normalised Fourier amplitudes, known as Dynamic Load Factors (or simply DLFs) (Rainer and Pernica, 1986; Rainer et al., 1988; Bachmann and Ammann, 1987; Bachmann et al., 1996b; Kerr, 1998; Sahnaci and Kasperski, 2005) or through the Power Spectral Density (PSD) (Eriksson, 1993, 1994; Brownjohn et al., 2004b; Ricciardelli and Pizzimenti, 2007). The reason for this is that low-frequency structures are primarily excited by repetitive footfalls when the step frequency is close to a structural resonance frequency. Therefore, an accurate description of the spectral properties of the loading process is more important than an accurate representation of the temporal shape of each footfall. Different methods of modelling the medio-lateral loads are presented by Ingólfsson et al. (2010a), but for the treatment of the vertical component of the GRF, reference is made to the literature review by Živanović et al. (2005a) or that of Racic et al. (2009).

2.1.2 Variability in gait parameters

According to Racic et al. (2009), the gait parameters are typically defined through three spatial quantities (the stride length, step length and step width) and two temporal quantities (walking speed and step frequency). The step length is defined as the linear distance (in the walking direction) from the heel strike of one foot to the heel strike of the other foot, whereas the stride length is the distance between two consecutive heel strikes of the same foot. The step frequency is also denoted pacing frequency or pacing rate. There is a geometric relationship between the step length (l_s), step frequency (f_s) and forward walking speed (v_s), written as:

$$v_s = f_s l_s \tag{2.1}$$

The relationship between the three gait parameters (v_s, f_s and l_s) is complicated as pedestrians vary most of their temporo-spatial and kinetic gait parameters, (including both the step length and frequency) when changing their walking velocity (Bejek et al., 2006). Yamasaki et al. (1991) found that female subjects tend to walk with a shorter step length and higher step frequency than their male counterparts at the same speed, but that both parameters increased with increasing walking speed. Milner and Quanbury (1970) showed that for natural walking at different forward velocities, both the step frequency and step length are approximately proportional to the square-root of the velocity. More generally, the relationship can be written as a power law of the type: $f_s = a v_s^b$, where the exponent b, has been reported in the range 0.5 to 0.58 (Yamasaki et al., 1991; Kuo, 2001). The selection of step length and frequency is governed by the strategy of humans to minimise the metabolic energy consumption at a given walking speed (Kuo, 2001). Bertram and Ruina (2001) investigated the relationship between the walking speed and step frequency at different types of constraints during treadmill walking. At various walking speeds, people were instructed to walk either freely, at a fixed step frequency or fixed step length. It was shown that the shape of the (f_s, v_s)-curve varied considerably depending on the particular constraint. In Fig. 2.3, the variation in the pacing frequency (step frequency) and the step length are shown as functions of the walking speed from two different studies.

Gait variations may be classified into two different groups; *intra-subject variability* and *inter-subject variability*. Intra-subject variability is related to gait variability of the same person in different situations. This counts random fluctuations in the gait parameters during continuous walking (Hausdorff et al., 2001) as well as day-to-day variability (Terrier and Schutz, 2003; Terrier et al., 2005) illuminated in scatter in measured gait parameters of the same person in two or more nominally identical situations. On the other hand inter-subject variability is related to the variability in the gait parameters between different people.

Human locomotion is not a static quantity, but changes throughout the lifetime. For instance, the biomechanical strategy of young children taking their first steps is to minimise their risk of falling, which for adults changes to minimising the metabolic energy expenditure (Vaughan, 2003). This change in locomotion causes a natural variation in the gait parameters with age. In Fig. 2.4, the free (unrestricted) walking speed is shown as a function of age, illustrating this variability. In a long time scale, this change in walking

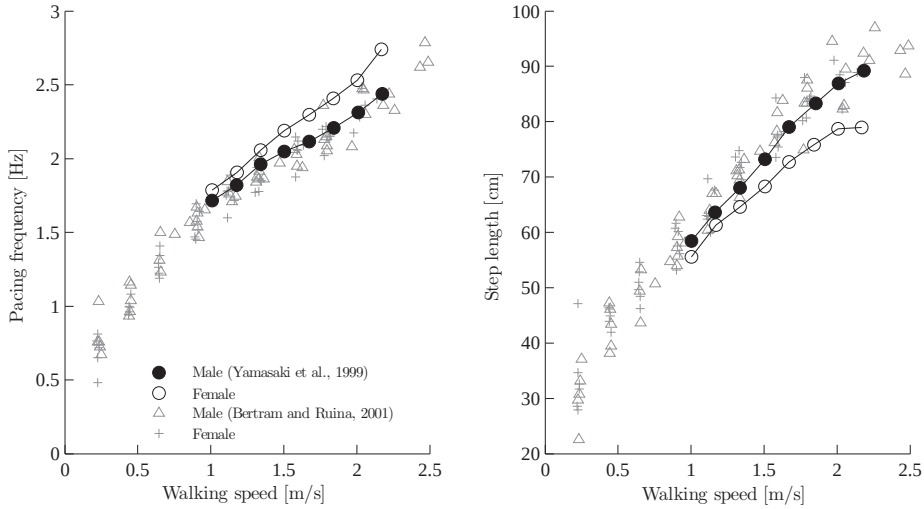

Figure 2.3: *Variation in (left) the pacing frequency and (right) the step length as function of the walking speed (Figure based on data from Yamasaki et al. (1991) and Bertram and Ruina (2001)).*

speed as function of age can be viewed as an intra-subject variability as the free walking speed of the same person changes in time. On the other hand, in a group of people at different ages, inter-subject variability is a reason for the distribution of free walking velocities.

Kasperski (2007) noted that several factors, physical, physiological and environmental, influence the free walking speed. In a study by Bornstein and Bornstein (1976), on the so-called *Pace of Life* in 20 different cities, it was shown that the mean walking speed ($\overline{v}_s$) increases with the population size (N_{pop}), following a logarithmic law: $\overline{v}_s = 0.26 \log N_{\text{pop}} + 0.015\,[\text{m/s}]$. Bornstein (1979), points out that the population size is not the sole contributor to difference in the walking speed, but ergonomical, cognitive, social and economic factors which are different between large and small cities may be the determinants of a faster pace of life in larger cities. In a similar study by Wirtz and Ries (1992), the observations of Bornstein and Bornstein (1976) and Bornstein (1979) were confirmed, but it was argued that the population composition influenced the average walking speed. This is supported by the observation that larger cities tended to have higher proportion of young males (20-30 year-old) and lower proportions of elderly people (larger than 60 years). In a recent study by Finnis and Walton (2007), the mean walking speed from 51 different cities (including the data from Bornstein and Bornstein (1976) and Bornstein (1979)) did not show the same significant correlation with the population size. Factors such as climate, cultural values, travel purpose, general life-style and body size may contribute to different walking speeds between different cities (Wirtz and Ries, 1992; Levine, 1999). In relation to dynamic loading of footbridges, the step frequency (and thereby walking speed and step lengths) are important modelling parameters and several

field studies as well as laboratory investigations have been carried out within the civil engineering community to determine these quantities. Ingólfsson et al. (2010a) presents a summary of relevant studies and further references.

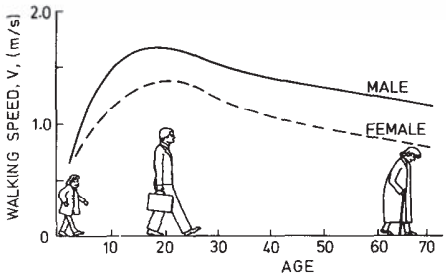

Figure 2.4: *Relationship between the preferred walking speed as a function of age for men and women (Figure from Smith (1995)).*

2.2 Crowd-induced lateral bridge vibrations

Until the beginning of the new millennium, engineering consultants and scientists were only concerned with vertical response of footbridges subject to pedestrian crowds. In The British Standard, BS 5400 (BS 5400, 1978), which was the first code to deal specifically with serviceability of pedestrian structures due to walking excitation, did not have any provisions for checking lateral responses and to the author's knowledge, neither did any other international codes of practice.

Therefore, it drew great attention when two high profile footbridges, pont de Solférino in Paris and the London Millennium Bridge, suffered from excessive lateral vibrations and had to be closed for public shortly after their inauguration in 1999 and 2000 respectively.

These bridges are far from being the first or the only bridges that have experienced this phenomenon, with the first reported incidents dated back to the late fifties (Sun and Yuan, 2008; Blekherman, 2005). Probably the first scientific assessment of the potential negative effect of pedestrian crowds on low frequency footbridges was offered by Peterson (1972) (as reviewed by Bachmann and Ammann (1987)), who explained that when the lateral movement of the centre of gravity of the body has a frequency which matches the natural frequency of the footbridge, resonant vibrations occur and people synchronise their walking to the movement of the structure (Bachmann, 1992). This explanation was based on observation made on a steel footbridge in Germany (Fig. 2.5) which experienced strong lateral vibrations during an crowd event.

An often cited incident of lateral footbridge vibrations is related to the Toda Park Bridge in Japan (Fig. 2.5). The bridge, which connects a boat race stadium with a railway station, experienced strong lateral vibrations when large crowds of people would leave the stadium to cross the bridge. Fujino et al. (1993) concluded that these vibrations were an order of magnitude larger than what could be calculated when assuming resonant walking frequency of all pedestrians and mutually independent (random) phases. Video analysis was used to track the head movement of randomly selected pedestrians and it

was found that up to 20 % synchronised their walking to the movement of the bridge. The phenomenon was described in a similar way to that of Bachmann (1992), i.e. small oscillations in the bridge cause some pedestrians to synchronise their walking, which in turn increases the oscillations and the number of synchronised pedestrians (Fujino et al., 1993). However, they also pointed out that at very large vibration amplitudes, people will not be able to continue walking and thereby the vibrations become self-limited.

Figure 2.5: *Toda Park Bridge in Toda City, Japan (top) (Pictures from Nakamura and Kawasaki (2006, 2009)) and a steel arch footbridge across Main at Erlach, Germany (bottom).*

In the appended literature review (Ingólfsson et al., 2010a), several other reports of bridges with similar problems are summarised with references to relevant scientific publications.

2.2.1 Results from full-scale measurements

After the incidents in Paris and London, engineers became more focused on avoiding the possibility of what had become known as *Synchronous Lateral Excitation* (SLE). Several full-scale measurements have been carried out on different bridges, both as an integrated part of their design (Brownjohn et al., 2004a; Mistler and Heiland, 2007; Hoorpah et al., 2008; Caetano et al., 2010a,b) and for the purpose of understanding the behaviour of existing bridges that have experienced strong lateral vibrations (Dziuba et al., 2001; Dallard et al., 2001a; Nakamura, 2003; Rönnquist et al., 2008; Macdonald, 2008). In Ingólfsson et al. (2010a), an in-depth presentation of these tests is provided and herewith only some main conclusions are summarised.

On the London Millennium Bridge, controlled pedestrian crowd tests were carried out to verify and understand the observations made on the opening day. It was observed that for a certain number of pedestrians, the bridge response was limited, whereas a small

increase in the number of pedestrians (beyond a critical number) often resulted in diverging lateral response (Dallard et al., 2001a). Based on back-calculations of the measured acceleration response, the important finding was made that the pedestrian force had a component strongly correlated with the lateral velocity of the structure, in the form of *negative damping*. This suggested that the pedestrians input a velocity proportional load $F(t) = c_p\dot{u}$, where c_p is a pedestrian damping constant (found as $c_p = 300\,\mathrm{Ns/m}$), $u(t)$ is the bridge displacement and dot represents differentiation with respect to time. This lead to the development of *Arup's stability criterion*, written in terms of the number of pedestrians needed to cancel the inherent structural damping, and thereby cause instability. For uniformly distributed pedestrians, the stability criterion takes a particularly simple form (Dallard et al., 2001a):

$$N_{cr} = \frac{4\pi f M \zeta}{c_p \frac{1}{L}\int_0^L [\Phi(x)]^2\,\mathrm{d}x}. \tag{2.2}$$

The critical number of pedestrians thereby depends on the modal properties of the structure where M, ζ, f and $\Phi(x)$ are the modal mass, damping, frequency and mode shape of the particular mode in question and L is the bridge length.

In fact, the ability of the stability criterion in Eq. (2.2) to provide a reasonable prediction the critical number of pedestrians has been verified on other bridges. Full-scale pedestrian tests on the Mezzanine Bridge at Singapore's Changi Airport, verified that excessive lateral vibrations could be triggered with 150 people occupying the structure, whilst Arup's stability criterion predicted only a slightly lowe critical number of pedestrians (Brownjohn et al., 2004c).

On the Coimbra footbridge in Portugal, a rapid increase in the lateral vibration amplitude of the bridge was observed for small increase in the number of people beyond the theoretically determined critical number of pedestrians (Caetano et al., 2010a). This observation was made during controlled crowd tests on the structure, prior to its opening and prior to the installation of laterally active tuned mass dampers.

On the Cliffton Suspension Bridge in UK (Macdonald, 2008), the velocity proportional coefficient, c_p, was determined in a similar way to that of the Millennium Bridge. Measured acceleration response during crowd induced vibrations was used to show that the pedestrian-induced loading could reasonably be modelled as being velocity proportional with parameter c_p in the range $160 - 210\,\mathrm{Ns/m}$.

This suggests that models which rely on the development of negative damping caused by pedestrians can be used for prediction of pedestrian-induced vibrations. The challenge seems, first of all, to determine what the negative damping depends on and then to quantify how it varies with frequency and to determine its sensitivity to pedestrian-specific parameters (inter- and intra-subject variability). This aspect is treated in more detail in Chapter 4 and Chapter 5.

2.2.2 Lessons learned from full scale testings

In new long span footbridges, the possibility of excessive lateral vibrations is a serious threat to the design and the role of full scale measurements of bridges prior to their

opening is increasingly becoming an integrated part of the design process. In particular, for bridges that are deemed susceptible to human induced vibrations, full scale testing is vital for several reasons.

- The structural response (and critical number of pedestrians) depends on the inherent structural damping, which cannot accurately be predicted without testing.
- External damping devices, such as tuned mass dampers, depend on an accurate tuning to the structural properties (Butz et al., 2008), which is usually only possible through experimental modal identification.
- Due to uncertainties in the phenomenon governing SLE and the general lack of experimental data from different bridges, controlled crowd tests are needed for 1) investigating the possibility of SLE and finding its trigger (e.g. critical crowd density) and 2) for the purpose of verifying the selected solution strategy.

2.3 Interaction mechanisms

As highlighted before, the development of large lateral vibrations is related to an interaction between the pedestrian and the movement of the underlying surface, also denoted *Human-Structure Interaction*. Another type of interaction occurs amongst pedestrians when each individual is spatially or visually restricted by the presence of other pedestrians, denoted *Human-Human Interaction*. In this section, both types of interaction mechanisms will be discussed.

2.3.1 Human-human interaction

When the pedestrian walking is completely unrestricted (spatially and visually), their walking characteristics may be determined from the free walking speed and normal gait parameters as discussed in Section 2.1. Footbridges are bounded physically (e.g by the handrails) and often constitute a narrow passage between two points subject to bi-directional pedestrian traffic. Thereby, the walking may become spatially restricted. Depending on the particular crowd density, different levels of interaction may occur amongst the pedestrians, which may cause deviations in their walking pattern from that of the unrestricted walk. In Fig. 2.6, different crowd densities are illustrated, indicating that even at the lowest densities an interaction between the walker could be expected. As postulated by Ricciardelli and Pizzimenti (2007), the most extreme type of human-human interaction occurs in large density regions where the pedestrians will synchronise and walk a common frequency and phase. However, in everyday situations, this extreme form of human-human interaction is not expected to occur. Therefore, an understanding of the real correlation amongst pedestrians in a crowd is vital for the understanding and quantification of the total crowd induced loading of footbridges.

A considerable amaount of research has been carried out in the past to understand and quantify the interaction amongst human beings in crowds, both in the fields of urban design and planning of pedestrian facilities (Tanaboriboon et al., 1986; Lam et al., 2002; Ishaque and Noland, 2008; Papadimitriou et al., 2009) and in relation to crowd dynamics

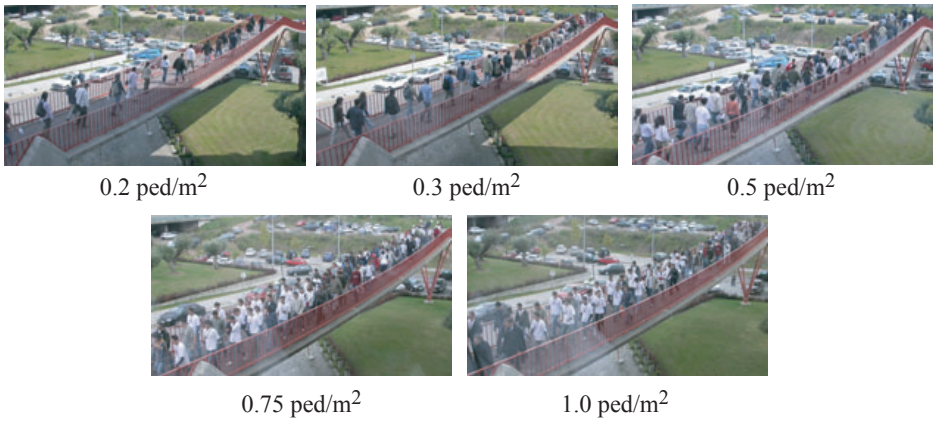

Figure 2.6: *Examples of different crowd densities on a stress ribbon footbridge in Portugal (Pictures from Cunha et al. (2008)).*

for evacuation during catastrophic events (Stanton and Wanless, 1995; Lee and Hughes, 2007; Kuang, 2008).

In an early study on the dynamic behaviour of footbridges, Wheeler (1981, 1982) addressed the modelling of pedestrian streams. He noted that a consequence of increasing the number people on the bridge is a *regimentation into a common forward speed and pace frequency* and that the pacing frequency drops due to slower walking speeds, but without people falling in step. Although several studies exists to support the former statement (Andersen, 2009; Venuti and Bruno, 2007; Bruno and Venuti, 2008), very little is know about the variation of the gait parameters and degree of synchronisation amongst pedestrians as a result of an increase in the crowd density. In recent years some preliminary studies have been carried out and some tentative conclusions are summarised below (as reviewed by Ingólfsson et al. (2010a)):

- Mean pedestrian step frequency (as well as speed and step length) decreases with an increase in the crowd density.
- The inter-subject variability measured as the standard deviation of individual step frequencies within the group decreased with an increase in the crowd density (except in one study that showed constant inter-subject variability).
- The intra-subject variability measured as individual gait variations increase with the crowd density.
- Collective phase synchronisation between individuals does not occur. Occasionally phase synchronisation between pairs of individual walkers can occur.

Based on these conclusions, it seems that human-human interaction is mainly governed by a modulation of the walking velocity of the group dictated by the forward movement of the crowd. As the crowd density increases, the distribution of step frequencies within the crowd decreases (i.e. a more narrow distribution is obtained). In response to the

change in walking speed, the pedestrians modulate their step length and step frequency (as shown in Fig. 2.3, Section 2.1.2) and both the resulting average step frequency and the standard deviation decrease with increasing crowd densities. This effect is shown qualitatively in Fig. 2.7 and more or less corresponds to the initial description of human-human interaction as provided by Wheeler (1981). In Fig. 2.7, the parameters f_{Free} and ρ_{Free} correspond to the free and unrestricted average step frequency and crowd density respectively, whereas ρ_M represents the jam density, i.e. the density for which people cannot continue to walk.

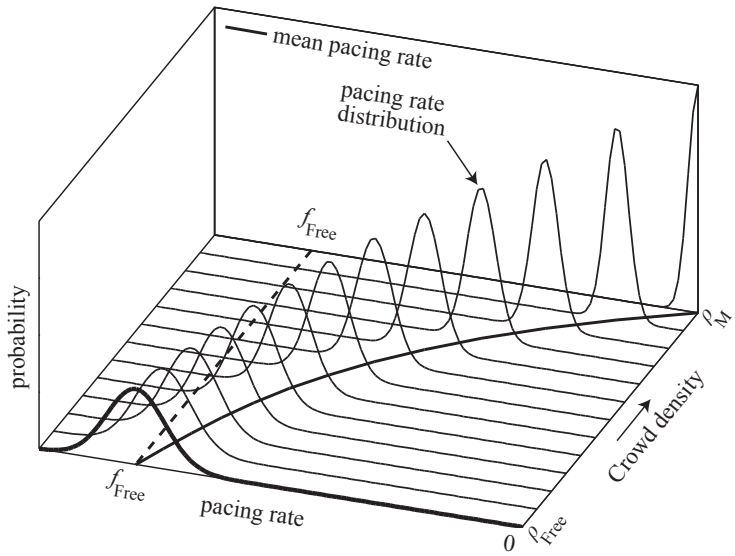

Figure 2.7: *Schematic view of the relationship between the average crowd density and step frequency distribution.*

2.3.2 Human-structure interaction

The human body is a complex mechanical system with inherent mass, stiffness and damping properties (Griffin, 2004). When a human-being occupies a structure, a combined human-structure system is formed. The term human-structure interaction covers the two-way feedback within the human-structure system. It is well-known and generally accepted that in low-frequency vertical vibrations, the presence of passive occupants add to the overall structural damping and mass (Sachse et al., 2003). Few studies exist on the effect of walking pedestrians on the human-structure system, but early studies (Ohlsson, 1982; Pimentel and Waldron, 1997) noted a drop in the dynamic load on flexible floors during walking as compared to measurements on a rigid floor (see Živanović et al. (2005a)). This is well in line with the results from recent studies which indicate that walking people add to the overall mass and damping of vertically vibrating structures (Živanović et al., 2005b, 2009; Jørgensen, 2009).

The problem of human-structure interaction has two aspects; one is the modifications to the apparent structural (dynamic) properties such as mass, damping and stiffness (human-to-structure) and the other is related to the changes in the pedestrian walking pattern as a result of the structural movements (structure-to-human). Although these two aspects cannot be treated entirely independently, it is a convenient discretisation of the problem. This also highlights the need for coupling between biomechanicists who are mainly concerned with adjustments in gait parameters in different circumstances and civil engineers who have mostly focused the research into quantification of changes of the forces or the additional mass and damping from the occupants.

For crowds walking on a laterally flexible bridge, excessive bridge vibrations are a consequence of human-structure interaction, but the nature of this interaction is not fully understood. Based on the experimental observations made by Fujino et al. (1993) and later Yoshida et al. (2002) it was concluded that the head movement of a large proportion of the crowd was synchronised with the movement of the underlying pavement and thereby the development of large pedestrian forces was attributed to synchronisation. This has become a commonly accepted view, i.e. that synchronisation of the pedestrians walking to the lateral oscillation of a bridge is a necessary condition for the development of SLE and that pedestrians tend to spread their legs further apart and change their walking frequency and phase to match that of the floor (McRobie et al., 2003).

In the field of biomechanics, few studies exist on the effect of lateral surface movement on the walking characteristics. Kay and Warren Jr (2001) used a visual stimulation to study the temporal correlation between lateral sinusoidal oscillations of the visual field (at frequencies between 0.075 - 1.025 Hz) and the lateral movement of the test person's neck. They concluded that the pedestrian pacing frequency locked to the driving frequency in a large range of frequencies (0.65 - 0.925 Hz). It should be pointed out that the visual stimulus was a narrow hallway which vibrated at a very large (fictive) amplitude of around 0.32 m. Recently, McAndrew et al. (2010) presented studies of both visual stimulation as well as physical perturbations of a treadmill during walking. The treadmill was driven into lateral oscillations at combinations of four distinct frequencies (0.16, 0.21, 0.24 and 0.49 Hz), each with different amplitudes (50, 40, 70 and 25 mm). Interestingly, the step width increased considerably, the pacing frequency increased and step length decreased during the lateral vibrations. Furthermore, the lateral movement of the neck (C7 vertebral) was monitored and its power spectral density featured peaks at each of the vibration frequencies as well as at half the pacing frequency. This shows that forces are generated at these frequencies but without synchronisation between the walker and the treadmill.

For walking on a laterally oscillating surface, Brady et al. (2009) introduced the terms *Fixed to Base* and *Fixed in Space* to discriminate between pedestrians that translate laterally with the base and those who hold a fixed position in space and allow the treadmill to move beneath them. Experiments carried out at low frequency (0.2-0.3 Hz) and large amplitude (127 mm) lateral vibrations showed that the step width generally increased as a consequence of the vibrations. Pedestrians who were fixed in space had a tendency to step wider with the left foot when the base was moving to the right and narrower when it was moving to the left. For pedestrians fixed to the base, the opposite tendency was true. This asymmetry in the gait and the ability of pedestrians to input energy into (or extract energy from) the structure thereby depends on whether they are fixed in space or

fixed to base.

Erlicher et al. (2010) suggested that the lateral pedestrian-induced force can be modelled as the restoring force of a modified hybrid Van der Pol/Rayleigh oscillator. By tuning the parameters of the oscillator, lateral GRFs as measured on a rigid surface were reproduced with a good accuracy. The model can be applied on a laterally moving floor where initial analysis shows that the load amplitude of the fundamental harmonic increases with the vibration amplitude and that the frequency of the oscillator is entrained by the frequency of the moving floor (Trovato et al., 2009). As reviewed by Ingólfsson et al. (2010a, 2011), several other existing models rely on the assumption that pedestrians synchronise with the moving structure (Strogatz et al., 2005; Butz, 2006; Venuti et al., 2007; Nakamura et al., 2008; Bruno and Venuti, 2009; Bodgi, 2008) and neglect the possibility of the development of large vibrations at lateral frequencies away from the mean excitation frequency (i.e. at half the step frequency).

Recently, Macdonald (2008) argues that synchronisation is not a necessary trigger of SLE. This conclusion is based on the initial work by Barker (2002) and three important observations made during crowd-induced lateral vibrations of the Cliffton Suspension bridge in Bristol (UK):

1. The natural frequency of the dominant lateral vibration mode (0.53 Hz) was well outside the range of normal walking (0.9-1.0 Hz).

2. Large amplitude vibrations were observed simultaneously in two vibration modes (at 0.53 Hz and 0.76 Hz).

3. The measured vertical response did show signs of excitation at twice the modal frequencies as expected if the pedestrians walked in synchrony.

According to Brownjohn et al. (2004a) and Dallard et al. (2001a), the lack of correlated vertical forces at twice the frequency of the lateral motion question the necessity of synchronisation to trigger SLE. Subsequently, Macdonald (2009) presented a simplified mechanical model (inverted pendulum) of the human body combined with lateral balance control from biomechanical studies. The model was used to verify the Millennium Bridge observation that velocity proportional load can be generated such that pedestrians act as negative dampers on a structure. The surprising issue was that the pedestrians' walking frequencies remained unaffected, and the model does therefore not rely on human-structure phase synchronisation.

2.4 Critical number of pedestrians

As reviewed by Ingólfsson et al. (2010a), many analytical models of pedestrian-induced lateral loads exist which differ considerably both in complexity as well as in the basic assumptions upon which they rely. Probably the most simple model to date is that of Dallard et al. (2001a) in which the critical number of pedestrians needed to trigger instability can be obtained in closed form (see Eq. (2.2)). Alternatively, still relying on linear dynamics, an equivalent pedestrian-induced load can be defined as a harmonic load (point or uniformly distributed) applied at the resonance frequency. The load intensity

is defined through an equivalent number of pedestrians which may depend on random vibration theory (Sétra, 2006), the number of synchronised pedestrians (Danbon and Grillaud, 2005; Fujino et al., 1993) or through fitting of experimental data (Rönnquist, 2005).

As mentioned in the previous section (Section 2.3.2), several models rely on the assumption of human-structure synchronisation. The most pronounced example of this is the model of Strogatz et al. (2005) which is formulated in the framework of coupled oscillators known from nonlinear sciences (Strogatz and Stewart, 1993). The model assumes that the pedestrians react to a small stimulus from the bridge, either through acceleration (Strogatz et al., 2005) or displacement (Eckhardt et al., 2007), and modify their instantaneous phase depending on the motion of the bridge. The equations of motion become nonlinear as the development of the pedestrian phase depends on the vibration response. Simplified expressions for the development of instability have been obtained in closed form for these models and are summarised in Table 2.1. According to the French Road Directorate (Sétra, 2006), human-structure synchronisation occurs when the lateral acceleration of the bridge exceeds a certain threshold (0.10 – $0.20\,\mathrm{m/s^2}$), but until then, the pedestrian walking remains random. Lateral vibrations have frequently occurred at vibrations lower than the average walking frequency[1], e.g. the first mode of the Millennium Bridge at 0.5 Hz. According to Piccardo and Tubino (2008), this situation can occur if the DLF of the first load harmonic is displacement proportional. Thereby, lower frequency modes are parametrically excited by the pedestrian load, provided that the relationship between the modal frequency (f_0) and the walking frequency ($f_w = f_s/2$) is 2:1 (i.e. $f_w = 2f_0$). Based on the model, a stability criterion was derived, written in terms of a critical number of pedestrians. A more elaborate review of each load model is presented by Ingólfsson et al. (2010a). In Fig. 2.9, a graphical comparison between the formulas in Table 2.1 are shown. The calculation is based on a half-sine mode shape, uniform distribution of pedestrians on the bridge, modal mass 150 tons, damping 1 % of critical and model specific parameters as listed in Table 2.1 and shown in Fig. 2.8. In Fig. 2.9, the average walking frequency, $\bar{f}_w$, is taken in the range 0.9 – 1.0 Hz and the minimum critical number of pedestrians used in the figure.

2.5 Human response to lateral vibrations

Human beings are very sensitive to vibrations and vibrations in structures occupied by humans are therefore mostly a matter of serviceability rather than structural strength or integrity. Several factors, mechanical, physiological and psychological strongly affect the human perception of vibrations. The mechanical factors are such as the type of vibration (e.g. sine, random, etc.), magnitude, frequency, direction, duration of vibration etc. (Tamura et al., 2006). The physiological parameters that may affect the vibration perception are weight, age, gender, race, posture, activity during vibration etc. (Kanda et al., 1994). The psychological parameters count visual and acoustical effects, persons earlier experience with vibrations, mood, etc. (ISO 10137, 2007; Duarte and de Brito Pereira,

[1]Here the term walking frequency (f_w) is introduced as half the step frequency ($f_s = 2f_w$), referring to the excitation frequency of the pedestrian-induced lateral load. The walking frequency is also denoted the gait cycle frequency.

Table 2.1: *Comparison between different expressions for the critical number of pedestrians needed to trigger excessive lateral bridge vibrations.*

Model	N_{cr}	Parameters
Dallard et al. (2001a)	$\frac{2\omega_0\zeta M}{c_p\bar{\Psi}}$	$c_p = 300\,\mathrm{Ns/m}$
Newland (2003, 2004)	$\frac{2\zeta M}{m_p\alpha\beta\bar{\Psi}}$	$\alpha = 2/3$ $\beta = 0.2$ $m_p = 70\,\mathrm{kg}$
Roberts (2005a,b)	$\frac{(1+\tilde{\alpha}^2)}{2}\frac{Mr^2}{m_p\Psi H_{n,av}}$	$\tilde{\alpha} \in [0;1]$ (here $\tilde{\alpha} = 1$) $r = f_0/\bar{f}_w$
Eckhardt et al. (2007)	$\frac{16\sqrt{2\pi}\zeta M\kappa\sigma_{f_w}}{G_1}$	$\kappa = 0.57\,\mathrm{m/s}$ $\sigma_{f_w} \in [0.05; 0.10\,\mathrm{Hz}]$ (here $\sigma_{f_w} = 0.075\,\mathrm{Hz}$) $G_1 = 25\,\mathrm{N}$
Strogatz et al. (2005)	$\frac{8\sqrt{2\pi}\zeta M\omega_0^2\sigma_{f_w}}{G_1\tilde{\kappa}}$	$\tilde{\kappa} = 16\,\mathrm{m^{-1}s^{-1}}$
Sétra (2006)[1]	$\frac{0.0086\zeta\,(a_{\mathrm{Lim}}M)^2}{\tilde{\Upsilon}\,(f_0)\,\tilde{\Psi}G_1^2}$	$a_{\mathrm{Lim}} \in [0.10; 0.20\,\mathrm{m/s^2}]$ (here $a_{\mathrm{Lim}} = 0.15\,\mathrm{m/s^2}$) $\tilde{\Upsilon}\,(f_0)$: Fig. 2.8
Sétra (2006)[2]	$\frac{0.292\,(a_{\mathrm{Lim}}M\zeta)^2}{\tilde{\Upsilon}\,(f_0)\,\tilde{\Psi}G_1^2}$	
Piccardo and Tubino (2008)	$\frac{4M\pi f_w}{m_p g\beta\mathrm{DLF}_{in}\Psi}\sqrt{\left[r^2-1/4\right]^2+r^2\zeta^2}$	$f_w \in [0.80; 1.05\,\mathrm{Hz}]$ $\mathrm{DLF}_{in} = 2\,\mathrm{m^{-1}}$ $g = 9.82\,\mathrm{m/s^2}$

[1] Sparse and dense crowds

[2] Very dense crowd

$$\Psi = \frac{1}{L}\int_0^L \left[\Phi(x)\right]^2 \mathrm{d}x$$

$$\tilde{\Psi} = \left[\frac{1}{L}\int_0^L \Phi(x)\mathrm{d}x\right]^2$$

$$H_{n,av} = \int_{1-\Delta r}^{1+\Delta r} r\left[\left(1-r^2\right)^2 + \left(2\zeta r\right)^2\right]^{-1/2}\mathrm{d}r, \text{ here } \Delta r = 0.1$$

$\bar{f}_w$: average walking frequency of the crowd

σ_{f_w}: standard deviation of walking frequencies

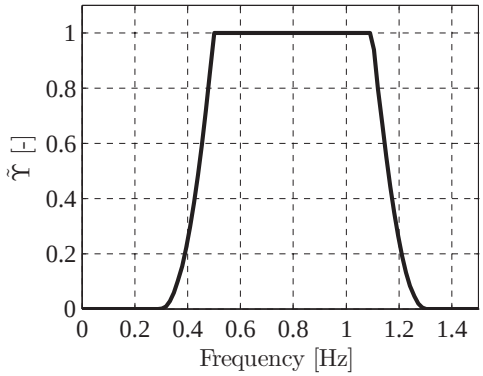

Figure 2.8: *Frequency dependent mode shape function used by Sétra (2006).*

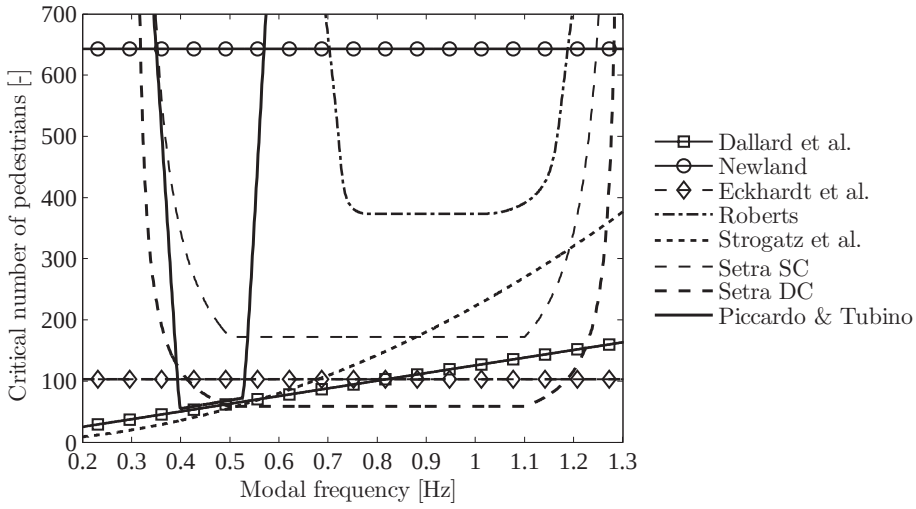

Figure 2.9: *The critical number of pedestrians shown as a function of the modal frequency for the models in Table 2.1.*

2006). As such, there is a large inter-subject variability in the vibration felt by different people. Furthermore, the same person is likely to react differently to the same vibration, causing a considerable intra-subject variability (Griffin, 2004).

The vibration felt by a pedestrian crossing a footbridge is generally non-stationary and the exposure time may be small compared to the overall duration of the crowd event. Živanović and Pavic (2007) introduced the concept of conditional probability for subjective evaluation of footbridge vibrations. The conditional probability $P(U|A)$ is defined as the probability of discomfort (U) at a certain vibration level (A).

A great deal of work has been published on both whole body and hand transmitted vibrations, much of which is summarised in the Handbook of Human Vibration by Griffin (2004). The literature review by Živanović et al. (2005a) presents several investigations related to footbridge vibrations, most of which concern vertical vibrations and is not within the scope of this thesis. Here, the focus is solely on human response to lateral whole body vibration, with the aim to provide a brief overview of current state-of-the-art with application to footbridges.

2.5.1 Quantification of vibrations

It is customary to measure oscillatory motion through acceleration, e.g. in terms of absolute peak, peak-to-peak or some time average of the acceleration. Typically, RMS (root-mean-square) value of the acceleration response is used:

$$a_{\mathrm{RMS}} = \sqrt{\frac{1}{T}\int_0^T [a(t)]^2 \,\mathrm{d}t} \tag{2.3}$$

where $a(t)$ is the acceleration time history, and T is the averaging time. The reason for using RMS acceleration as a general way of quantifying vibrations is the convenience of measurement and analysis (Griffin, 2004).

Another measure of human exposure to vibrations is the VDV (Vibration Dose Value) which is often used for non-stationary vibrations and vibrations where the characteristics vary in time. The VDV is defined as (Griffin, 2004):

$$a_{\mathrm{VDV}} = \left(\int_0^T [a(t)]^4 \,\mathrm{d}t\right)^{\frac{1}{4}} \tag{2.4}$$

For footbridges, Barker et al. (2005) and Barker (2007) argue that VDV value of acceleration is a better means of evaluating the human comfort than the peak or the RMS value. However, it has been shown that for pedestrians crossing a footbridge vibrating dominantly in a single mode, there is a linear correlation between the perceived peak acceleration, the maximum 1 s RMS and the VDV value of the acceleration perceived during crossing. This suggests that any of these measure are equally applicable for assessment of the human response to vibration on footbridges (Živanović and Pavic, 2007).

2.5.2 Research on human response to vibration in buildings

Human response to lateral vibrations related to footbridge design has scarcely been investigated. More attention has been paid to comfort of occupants of structures such as high

rise buildings (Chen and Robertson, 1973; Irwin, 1981), control towers (Denoon et al., 1999, 2000), offshore platforms (Irwin, 1978) and during transportation in cars, ships, trains, airplanes etc.

Chang (1973) used results from the aerospace industry to create comfort criteria thresholds for maximum allowable acceleration. Different categories were defined, but the limit for perceptible vibrations was defined as $0.05\,\mathrm{m/s^2}$ over the entire frequency range relevant for tall buildings.

Goto (1983) used a motion simulator to recreate low frequency horizontal building motion and also found that the perception threshold is in the region $0.05\,\mathrm{m/s^2}$. Interestingly, it is stated that the acceleration limit for walking is $0.5\,\mathrm{m/s^2}$ to $0.7\,\mathrm{m/s^2}$. However, it is not reported how these values depend on the frequency of the motion or whether this is peak or RMS acceleration.

Hansen et al. (1973) conducted interviews with 107 users of two buildings with lateral sway frequencies in the range 0.17 Hz to 0.19 Hz and 0.24 Hz respectively, following a storm event. The limiting RMS value of the acceleration was chosen similarly to the aforementioned values as $0.05\,\mathrm{m/s^2}$ and defined such that less than 2 % of the occupants (in the top third of the building) would complain each year (Hansen et al., 1973). It is worth noticing, that in the calculation of the RMS value of the acceleration, an average time of 20 minutes was used.

Irwin (1978) collected the results from several studies to define guidelines for upper magnitudes of whole body vibrations for three categories of structures; buildings, offshore structures and bridges. For buildings, two different sub-categories were defined, one for storm induced motion and one for frequently induced motion of buildings. For storm induced vibrations, the threshold value is given in Fig. 2.10 as curve 1a, defined for the worst 10 minutes of a storm with a return period of at least 5 years. If obeyed, not more than 2 per cent of the people that experience the maximum vibration will complain. The lower threshold of perception of motion was put forward by Irwin (1978) as curve 1b in Fig. 2.10, intended for frequently induced motion of sensitive buildings, e.g. hospital operating theaters. For residential buildings, offices and workshops, Ashley (1977) proposed that the base curve (curve 1b) criteria should be multiplied with weighting factors to take into account that larger allowable acceleration is acceptable in these buildings (Irwin, 1978). Interestingly, a criterion for allowable horizontal acceleration in a footbridge due to storm is given as curve 6 in Fig. 2.10. This allowable acceleration for bridges is higher than for buildings as it takes into account the (low) probability of occurrence of the storm and the assumption that only few pedestrians will cross the bridge during such an event. This criterion is not directly applicable to vibrations induced by pedestrians, however it is interesting to note the order of magnitude proposed in the study.

Melbourne and Cheung (1988) argue that for some structures, there may be a need to investigate the serviceability for different return periods. In a later study, Melbourne (1998) proposed the following equation for the maximum allowable peak acceleration (in $\mathrm{m/s^2}$):

$$\hat{a} = \sqrt{2\ln f_0 T}\left(0.68 + \frac{\ln R}{5}\right)\exp\left(-3.65 - 0.41\ln f_0\right), \qquad f_0 \in [0.06\,\mathrm{Hz}, 1.0\,\mathrm{Hz}], \quad (2.5)$$

where f_0 is the structural frequency, T is the event duration (usually 10 minutes) and R is the return period (in years). The first term in the equation is the peak factor for a Gaussian process, the second term is scaling factor taking into account different return periods than 5 years and the final term is the analytical equation for curve 1a in Fig. 2.10.

A recently proposed approach related to human comfort on footbridges subjected to (random) wind vibrations was proposed by Flaga et al. (2008a). The criteria was based on earlier studies and standards within the field and is shown in Fig. 2.10.

The concept of base curves, representing equal human perception to vibration over the frequency range has been adopted in the ISO 2631 (ISO 2631-2, 1989, 2003) and BS 6472 (BS 6472, 1992) standards relating to human response to whole body vibrations. Similarly to Irwin's definition, the base curve represents the vibration perception threshold and different multiplication factors are applied for different types of structures. Guidelines on selecting appropriate multiplication factors are provided in ISO 10137 (ISO 10137, 2007) and BS 6472 (BS 6472, 1992).

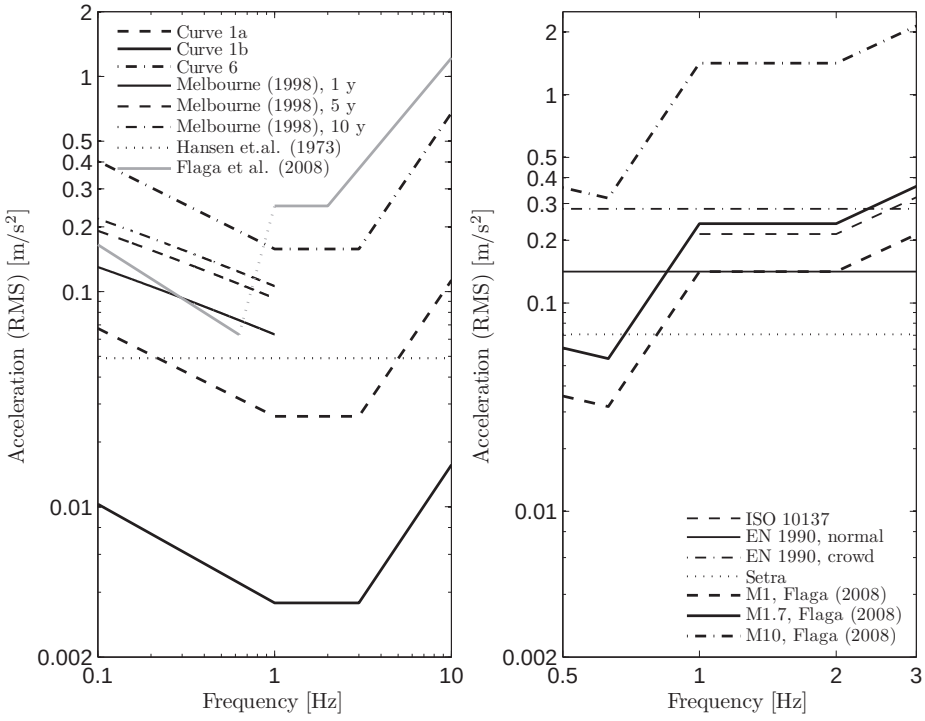

Figure 2.10: *Comparison between different studies on human response to horizontal vibrations in (left) buildings and (right) for footbridges.*

2.5.3 Human response to lateral footbridge vibrations and 'lock-in'

Apart from the studies of Flaga et al. (2008a) on comfort of pedestrians on footbridges to wind induced vibrations, they also studied the comfort requirements for men-induced vibrations of footbridges (Flaga et al., 2008b). Three different comfort criteria lines are defined, firstly a base curve (M1) not to be exceeded for frequent (daily) events, secondly a curve (M1.7) for events occurring more rarely than once per week and finally a curve (M10) for vandal loads considering only the Ultimate Limit State of the structure. All three curves are shown in Fig. 2.10. it is noted that peak acceleration has been transformed into RMS values for the sake of comparison with the results from the studies on building occupants (Fig. 2.10, left) by dividing the peak acceleration criterion with $\sqrt{2}$.

According to ISO 10137:2007 (ISO 10137, 2007), it is recommended that the lateral acceleration of walkways to pedestrian or wind induced vibration should not exceed 60 times the base curve, corresponding to RMS value of $0.21\,\mathrm{m/s^2}$ at the frequency 1.0 Hz calculated using an average time of 1 s. In Appendix A2 of EN 1990 (EN 1990, 2005), limiting values for the maximum allowable lateral acceleration of footbridges as $0.2\,\mathrm{m/s^2}$ in normal use and $0.4\,\mathrm{m/s^2}$ for exceptional crowd conditions.

These values deal only with the comfort of the pedestrians, but do not address the probability of lock-in, which may occur for vibration amplitudes lower than the comfort threshold. In a recently published guide on the design of footbridges, (*fib* (2005)), a lock-in threshold of $0.08\,\mathrm{m/s^2}$ for a vibration frequency of 1.0 Hz is provided. However, it is unclear how this value has been derived.

According to Baumann and Bachmann (1987), lock-in occurs at vibration amplitudes exceeding 2 to 3 mm (at 1.0 Hz), corresponding to an acceleration of 0.08 to $0.12\,\mathrm{m/s^2}$, resulting in a synchronisation of as many as 80 % of the pedestrians (Bachmann, 2002).

In an attempt to avoid the possibility of synchronous lateral excitation of footbridges, a limit of $0.10\,\mathrm{m/s^2}$ for the lateral peak acceleration of footbridges was proposed by the French Road Authorities (Sétra, 2006). This limiting value was based on the full-scale measurements performed on the Solferino Bridge in Paris during its closure (Charles and Bui, 2005). It is further reported, that for accelerations exceeding this threshold, the percentage of synchronised pedestrians increases and can reach values as high as 60 % for lateral peak acceleration of $0.9\,\mathrm{m/s^2}$. The percentage of synchronised pedestrians was determined from back-calculation of the measured vibration response as the equivalent number of resoant pedestrians, needed to produce the measured acceleration response. An interesting observation that was made during the crowd tests on the Solferino Bridge, is that when the vibration occurs in a torsional mode (with both horizontal and vertical motion) no lock-in was observed despite large vibration amplitudes (Sétra, 2006). The authors explain that *high horizontal acceleration levels are then noted and it seems their effects have been masked by the vertical acceleration*, (Sétra, 2006).

Also worth mentioning, is that Nakamura (2003) used the observations made during the field tests of the Nasu Shiobara Bridge (M-Bridge) in Japan to propose a serviceability criterion of $1.35\,\mathrm{m/s^2}$ for lateral bridge vibrations. This serviceability criterion was defined as the acceleration level for which the pedestrians often lose balance and stop walking. Therefore, it should probably be treated as an extreme level of vibration which can be accepted on footbridges, rather than a target serviceability critierion.

Chapter 3

Preliminary Studies

3.1 Preface

As described in Chapter 2, a significant amount of research has been undertaken in the last decade to quantify the pedestrian-induced lateral forces and the interaction of humans with a laterally moving surface. Although the general conclusion is the same, i.e. there exists a non-negligible interaction between pedestrians and a laterally moving structure, there is still a dispute regarding its origin and the conditions under which and how it develops.

The contradictory conclusions about the origin of the human-structure interaction raises the following questions, which still remain unanswered:

1. What is the load induced by pedestrians walking on a laterally oscillating surface as function of vibration frequency and amplitude?

2. Is synchronisation a necessary trigger for the development of diverging lateral vibrations?

3. How does the load depend on the walking characteristics of the pedestrian (i.e. walking speed, pacing frequency and step length).

As a first step towards answering these questions, a preliminary experimental investigation using a 17 m long laboratory platform was carried out (Section 3.3). By measuring the lateral acceleration response of the platform and monitoring the movement of the pedestrians, the effect of single pedestrians and crowds were studied. The results from the platform investigations were used as a basis for the development of a larger experimental campaign. The results from the preliminary investigations are presented in this chapter with the main emphasis of the work presented by Ingólfsson et al. (2008a) (Paper II of this thesis).

3.2 Experimental determination of human-induced forces

In this section, a very brief introduction to different measurement techniques which were considered for the experimental campaign is presented.

3.2.1 Force plate measurements

A force plate is a relatively small plate (typically around 600x600 mm), supported on a load cell to measure the GRF generated by the human body during walking or standing. Force plates are commonly used in relation to gait analysis and in biomechanics. The first attempts to measure the GRF are dated back to the late nineteenth century (Baker, 2007), and in the 1930's the first three-component mechanical force plate was developed (Elftman, 1938). Today, forces plates are standard inventories in any gait laboratory and in the last decade or so, it is increasingly being used for civil engineering purposes (Kerr, 1998; Sahnaci and Kasperski, 2005; Butz, 2006; Racic et al., 2009).

Measurements of the GRF through the use of force plates is not ideal due to their limited size. During walking, a single force plate can only measure the GRF from a single footstep, thus in order to capture a series of consecutive footsteps, an array of force plates is necessary. Therefore, this was not considered further in relation to the research presented herewith. A detailed discussion relating to technical aspects of force plates and their applicability in civil engineering is given by Racic (2009).

3.2.2 Section models and assembly structures

When dealing with serviceability of pedestrian structures, the measurement of the GRFs from a series of consecutive footsteps (ideally from continuous walking) is necessary. In particular when investigating human-structure interaction, a certain exposure time is needed to ensure a proper quantification of the phenomenon can be achieved. The best case scenario is to be able to measure the GRFs from different pedestrians while crossing a real-life footbridge under natural circumstances. However, for several reasons field tests cannot replace laboratory investigations but should rather be treated as benchmark cases to verify the models which are based on the laboratory tests.

In order to achieve realistic laboratory circumstances, several researchers have used instrumented platforms to investigate human-structure interaction, (Hobbs, 2000; McRobie et al., 2003; Butz et al., 2005; Rönnquist, 2005; Sétra, 2006; Živanović et al., 2009). This offers advantages in that the structural properties can normally be modified quite easily, the instrumentation is simple and access to the facility is more or less unlimited. The shortcomings with building platforms or other assembly structures in the laboratory is the space requirement and construction cost. Furthermore, many laboratory platforms are either too short to capture more than only few footsteps and they tend to have a very low modal mass, which means that the measured response during pedestrian tests is larger than generally observed in the field (Rönnquist, 2005).

The laboratory of Civil Engineering at DTU has been used on earlier occasions to study human-induced vertical forces using two different and custom built low frequency footbridges with span of 12 m (Ingólfsson, 2006) and 16 m (Jørgensen, 2009) respectively. Therefore, it was decided to carry out preliminary experimental investigations in the laboratory, using a 17 m long suspended platform, to represent a footbridge with a low-frequency lateral vibration mode.

3.2.3 Treadmill Ergometer Devices

The use of treadmills to study human locomotion is widely accepted in the scientific community and like the force plate, an instrumented treadmill is a standard inventory item in many gait laboratories. An instrumented treadmill is hereby referred to as one which is connected to the ground through load cells and thereby offers the possibility to measure GRFs during continuous walking.

To the author's knowledge, Brownjohn et al. (2004b) were the first researchers in civil engineering to utilise an instrumented treadmill to quantify continuous pedestrian-induced vertical forces. For the determination of pedestrian-induced lateral forces and for investigations into human-structure interaction, treadmills have been used with succes on a few occasions (McRobie et al., 2003; Pizzimenti and Ricciardelli, 2005; Sétra, 2006; Sun and Yuan, 2008). The advantage is that the treadmill does not require much space and it can be placed on top of short laboratory platforms or driven laterally by a shaking table.

The shortcoming with using a treadmill is that it may not completely resemble natural walking and by imposing a fixed forward velocity, some freedom of the test subject to vary his walking is restricted. As reviewed by Racic et al. (2009), it has been shown that analysis of gait using a treadmill is equivalent to analysis of normal (overground) walking. However, the applicability of treadmills to study human-structure interaction has not been verified in the same way, as only few such experiments have been carried out in the past. In addition, no benchmark data exists on the expected behaviour of pedestrians on a laterally moving surface, which can be used as a comparison with the the results obtained from treadmill experiments.

Having evaluated the advantages and shortcomings of different experimental procedures, it was decided to carry out an experimental campaign using a laterally driven instrumented treadmill to quantify the pedestrian-induced lateral forces from individuals. This is presented in detail in Chapter 4.

3.3 Preliminary investigations

A preliminary experimental analysis was carried out in the laboratory of DTU Civil Engineering, using an instrumented platform. The platform is made of concrete and is cast as a prestressed double T-girder with overall length of 17 m and weight 19.6 tons (Fig. 3.1).

The platform was constructed by the author to study pedestrian-induced lateral vibrations. It has frequently been used by the author as well as students under his supervision (Knudsen, 2007; Christiansen, 2008). The platform is suspended from hangers at one end and fixed onto two flexible columns at the other end. The mechanical behaviour is governed by a pendulum motion with a rotational rigidity at the end, see Fig. 3.2. The experimentally determined fundamental natural frequency of the platform is 0.87 Hz, which could also be verified theoretically (0.81 Hz) under the assumption that the shape of the vibration mode is triangular (i.e. in-plane bending of the deck is neglected) (Ingólfsson et al., 2008a). The difference in the measured frequency and the theoretical one may be attributed to inaccuracies in e.g. the estimated rotational stiffness of the support columns, the mass of the element or the assumed mode shape. At low amplitude vibra-

tion, the viscous damping ratio was determined from free-decay experiments to be around 0.79 % of critical damping.

Different pedestrian tests were carried out on the platform. In this thesis, the results from five single pedestrian tests as well as crowd tests with varying number of participants (from two to eight) are summarised.

Figure 3.1: *Suspended concrete platform at the laboratory of DTU Civil Engineering*

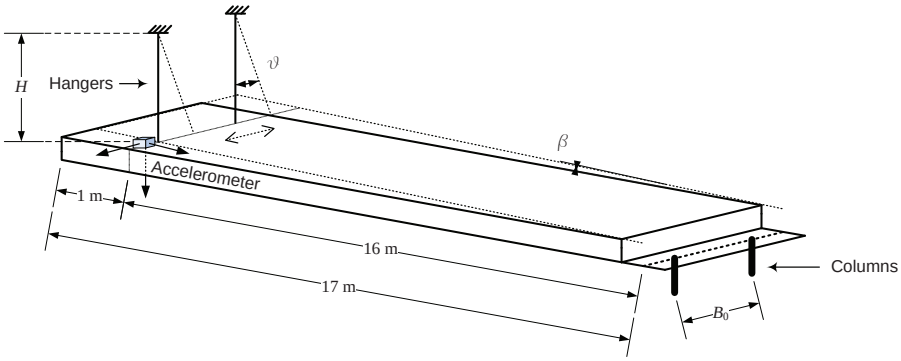

Figure 3.2: *A schematic view of the mechanical behaviour of the platform.*

3.3.1 Single pedestrian tests

In the single pedestrian tests, a metronome was used to ensure that the pedestrian walking frequency matched the natural frequency of the (empty) platform. It has been suggested that the dynamic lateral load varies with the vibration amplitude when walking on a laterally moving platform (Hobbs, 2000; McRobie et al., 2003; Rönnquist, 2005), thus the purpose of this part of the research is to test that hypothesis. The structural response of

the platform was measured[1] and compared with that obtained by assuming no interaction with the structure. For a linear structure with a triangular mode shape subject to a moving harmonic force (starting from the fixed support), the envelope of the acceleration response can be written in closed form as (Ingólfsson et al., 2008a):

$$\ddot{y}(t) = \frac{\mathrm{DLF} \cdot W}{M} \frac{1}{4\pi\zeta^2 n} \left(e^{-\omega_0 \zeta t} - 1 + \omega_0 \zeta t\right) \tag{3.1}$$

where ζ, M and ω_0 are the modal damping, mass and angular frequency of the fundamental vibration mode of the platform respectively and n is the number of steps needed by the pedestrian to cross the bridge. The weight of the pedestrian is denoted W and DLF is an unknown dynamic load factor.

The expression in Eq. (3.1) was used to fit the envelope of the measured response from the pedestrians using a numerical (nonlinear) least-square model. The parameter DLF is unknown and the least-square problem was formulated to find a value of DLF which provides the best fit. It was shown that for all five pedestrians, the model in Eq. (3.1) provided a good fit to the measured acceleration envelope, suggesting that the dynamic load factor remained (approximately) constant during the passage time of the pedestrians (Ingólfsson et al., 2008a). The conclusion to be drawn from this study is that for predicting the acceleration response of the platform, a simple linear model is sufficient, suggesting that human-structure interaction did not noticeably change the loading from the pedestrian. Furthermore, the back-calculated values of the DLF (mean value 0.055, S.D. 0.022) were in the same range as reported by earlier studies derived from fixed platforms (see Chapter 2).

During the tests, the maximum platform acceleration was lower than the lock-in threshold ($0.2\,\mathrm{m/s^2}$) as defined by Sétra (2006). As noted by Ingólfsson et al. (2008a), this, in combination with the triangular mode shape, relatively short passage time and transient effects associated with the bridge starting at rest, minimised the effect of any type of human-structure interaction. Finally, by using a metronome to control the pacing frequency, the phase of the walking is tied to that of the metronome, hence human-structure synchronisation is unlikely to occur in such circumstances.

Further investigations were carried out by Christiansen (2008), using the platform. Similar dynamic tests were carried out with up to 20 individuals crossing the platform at various metronome-controlled as well as freely selected step frequencies. An effort was put in to quantify the frequency dependent lateral DLF from back-calculation of the measured response, similarly to that presented herewith. It was found that the DLF of the fundamental harmonic depends on the relationship between the walking frequency and the modal frequency of the platform. This dependency was such that the minimum value of the DLF was obtained when walking at resonance, whereas the DLF would increase on both sides of the resonance walking frequency. However, it proved difficult to obtain reliable estimates of the DLF, particularly at walking frequencies away from the resonance frequency of the platform. Therefore, the results should be taken with some precaution and have not been used or published further. It should be noted that the DLFs of higher harmonics could not be obtained. However, in contrast to the aforementioned results,

[1]The acceleration was measured with a tri-axial accelerometer (GeoSIG, AC-63, 5000 mV/g), positioned at the hangar location ($x = 16\,\mathrm{m}$), as shown in Fig. 3.2

the results of Christiansen (2008) suggest that human-structure interaction is significant under certain conditions and needs to be taken into account.

Christiansen (2008), also measured the lateral force in the absence of bridge motion from twenty test subjects. The main conclusion was that the results were comparable to those of other researchers, both in terms of magnitude and step frequency dependency.

3.3.2 Pedestrian crowd test

In addition to the single pedestrian tests, crowd tests were carried out to investigate the possibility of developing large amplitude vibrations on the platform and to investigate the possible onset to synchronisation. A total of seven crowd tests were carried out, each with a duration of three minutes, in which the number of pedestrians was kept constant by controlling their arrival onto the bridge. The pedestrians were asked to walk freely, i.e. at their own selected pacing frequency. The number of people on the bridge was increased from two pedestrians in the first tests, to eight in the last one, with an increment of one person between each test (Ingólfsson et al., 2008a). Thereby, the forward speed of the pedestrians was, to some degree, restricted by the speed of the crowd. Since the lateral force could not be measured directly in the tests, the correlated pedestrian force, i.e. the component of load in phase with the modal velocity, could only be obtained indirectly by applying Arup's method of back calculation (Dallard et al., 2001a):

$$F_{\text{corr}} = 2\zeta M\ddot{q} + M\frac{\Delta\ddot{q}}{\pi} \tag{3.2}$$

where $\ddot{q}$ is the measured modal acceleration and $\Delta\ddot{q}$ is the change in acceleration amplitude between two consecutive vibration cycles. During the crowd tests, lateral acceleration amplitudes up to $0.28\,\text{m/s}^2$ ($0.20\,\text{m/s}^2$ for 1 s RMS) were measured. No sign of correlation between F_{corr} and the lateral velocity amplitude was observed (see Fig. 3.3), suggesting that the people did not synchronise with the lateral movement of the platform. Analysis of video recordings were carried out by Knudsen (2007), who concluded that the pedestrian pacing rates were determined by the pedestrian preferences and not the platform movement. Without excluding the possibility of synchronisation on a laterally moving platform, it was concluded that on the current setup no signs of the development of lock-in were observed. This can be attributed to the limited length of the platform (17 m) or its triangular mode shape, causing a general low level of vibrations to be felt by the pedestrians during the passage.

3.3.3 Tests on modified platform

In order to accommodate for the shortcomings associated with the triangular vibration mode, the platform was modified. It was suspended at both ends, instead of only at one end. In this setup the platform featured two natural vibration modes susceptible to pedestrian-induced lateral vibrations; a sway mode and a twist mode with natural frequencies around 0.63 Hz and 0.93 Hz respectively.

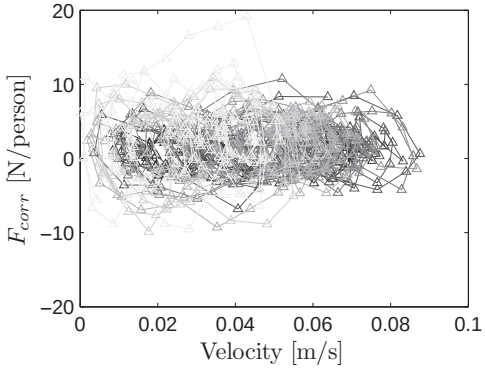

Figure 3.3: *Correlated pedestrian force per person as function of the structural velocity for all crowd tests, calculated according to Eq.* (3.2).

Modal survey

Different experimental techniques were used to determine the natural vibration characteristics of the platform, including free decays, ambient vibration measurements (i.e. in the absence of external loading) as well as forced vibrations[2]. In the forced vibration tests, the lateral excitation was generated using an electrodynamic shaker (model APS 113). The shaker was placed in one position of the deck, whilst accelerometers were moved to different locations. For each acceleration location, a pseudo-random force was created with constant spectral energy content in the frequency range 0 to 40 Hz. The force induced by the shaker was measured indirectly, by measuring the acceleration of the reaction masses and multiplying with the moving mass of the shaker.

In Fig. 3.4, the output from forced response tests, for 11 test points along the length of the bridge deck is shown. The existence of two natural frequencies are clearly illustrated in the graphs. The amplitude difference in each line in Fig. 3.4 (top-left) represents the variation in the response (per unit force input) along the bridge deck. For mode two, there is a considerable variation, which is due to the shape of the twist mode. In Fig. 3.4 (bottom), the results from the modal survey are summarised for the first two lateral vibration modes. The estimated modal masses are based on the assumption that the shape of the sway mode is uniform with constant modal ordinate along the length of the platform and that the shape of the twist mode is purely triangular. Thereby, the modal mass of the sway mode is equal to the total mass of the element, i.e. 19.6 t, whereas the modal mass of the twist mode is only one-third of the total concrete mass, i.e. 6.5 t.

In Table 3.1, the modal characteristics of the first four vibration modes are presented. It is noted that the lowest vertical vibration mode has a frequency of 4.71 Hz and due to its low damping it may be excited by vertical pedestrian-induced forces during the crowd tests. However, as the frequency falls within the range of the third harmonic of

[2]The modal identification was carried out in collaboration with Dr. Stana Živanović from the University of Sheffield (now University of Warwick), during a research visit in December 2008. Post-processing of ambient and forced vibration data were also carried out by Dr. Stana Živanović.

the vertical pedestrian-induced force, it was assumed that the influence on the lateral vibration behaviour would be minimal.

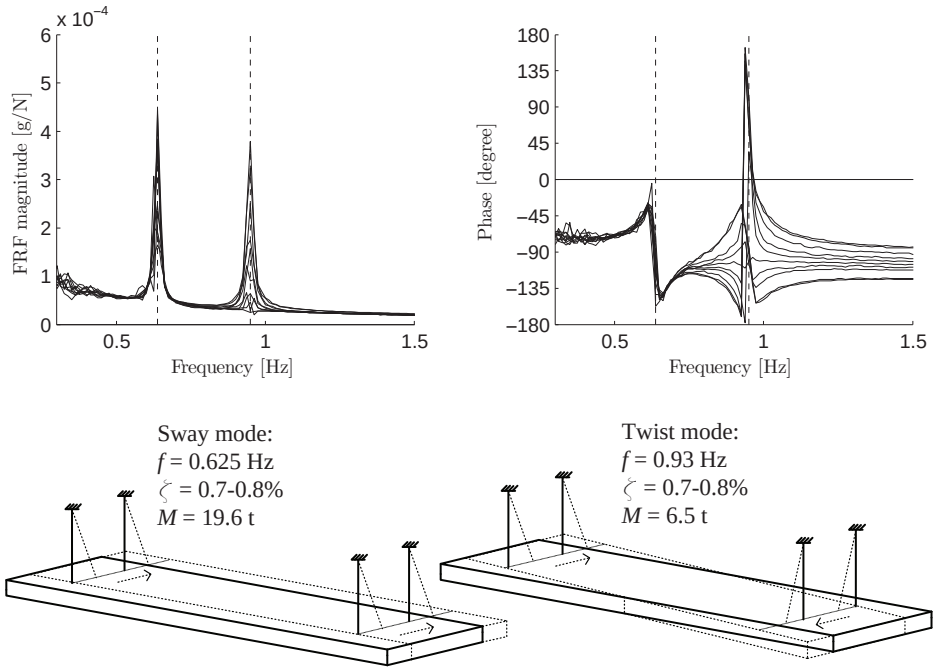

Figure 3.4: *Amplitude spectrum (cross FRF) (top-left) and phase spectrum (top-right) between shaker input and acceleration response in different test points during pseudo-white noise shaker excitation. Schematic view of the fundamental sway mode (bottom-left) and the twist mode (bottom-right).*

Table 3.1: *Modal properties of the modified platform at the laboratory of DTU Civil Engineering*

Description	Modal frequency (f_0) (Hz)	Modal damping (ζ) (%)	Modal mass (M) (tonne)
Fundamental sway mode	0.625	0.7 - 0.8	19.6
Lateral twist mode	0.93	0.7 - 0.8	6.5
Fundamental vertical mode	4.71	0.3	-
Fundamental torsional mode	6.27	0.7	-

Pedestrian crowd tests

A single set of crowd tests was carried out with a varying number of pedestrians on the bridge, Fig. 3.5. The idea of the test was to maintain a constant number of people on the bridge during a period of few minutes. A number of volunteering pedestrians were asked to form a straight line at one end of the platform (bridge entrance). The number of people present on the bridge at any time instance was varied from 1 to 10 persons during the tests. The constant number of pedestrians on the bridge was maintained such that every time a person left the bridge, a new person was instructed to enter it. The person who exited the bridge walked back to the entrance and re-entered the bridge when instructed to do so. The total number of participants was therefore larger than the number of persons on the bridge at any one time. This was the only way to maintain a constant number of people on the bridge for a longer period of time, without conducting a circulatory test on the platform itself. A circulatory test was deemed inappropriate, primarily because the turn-zone would occupy a non-negligible portion of the surface area of the platform.

Figure 3.5: *Pedestrians crossing the laboratory platform during a crowd test.*

During the tests there were no visual signs of synchronisation between the pedestrian walking and the vibration of the bridge. Vibrations in the sway mode seemed to develop more strongly than those of the twist mode despite its higher modal mass and the fact that the walking frequency of the pedestrians was closer to the natural frequency of the twist mode.

In Fig. 3.6 (top), the acceleration time history of the response, measured at the corner of the bridge deck, is shown, both for the raw unfiltered signal and a low-pass filtered signal (with cutoff frequency 10 Hz). The response amplitude seems to gradually increase with the number of people on the bridge, but no signs of instability, i.e. diverging vibration amplitudes, are present in the data. An interesting observation is made when considering the spectrogram of the acceleration response in Fig. 3.6 (middle), which confirms the initial observation that both lateral vibration modes are excited during the crowd tests. Furthermore, as shown in Fig. 3.6 (bottom), the response magnitude in the sway mode is noticeably larger than that of the twist mode. This mechanism of multi-mode response,

in which stronger vibrations are observed in the lower frequency mode was also described by Macdonald (2008), who observed a similar behaviour on the Clifton Suspension Bridge during an event with large pedestrian-induced lateral vibrations, see Section 2.3.2.

It should be noted that the acceleration level observed during the crowd test was generally lower than $0.25\,\mathrm{m/s^2}$ (filtered). This means that the vibration magnitude as felt by the pedestrians is comparable to what could be observed on as-built footbridges during pedestrian-induced lateral vibrations. Thereby, the platform provides a realistic scale-effect and is representative of real footbridge vibrations. The twist mode features a nodal point at midspan, which could resemble a short bridge section taken around midspan of a longer structure. Then the sway mode would represent a fundamental lateral vibration mode, whereas the twist mode represents the second lateral vibration mode. For such a structure, the higher mode is primarily excited away from the centre of the span as very little energy is transmitted to the mode around the nodal point. Therefore, the comparison to a real footbridge is questionable in terms of load and modal response of the twist mode.

3.3.4 Conclusions from platform tests

The concrete platform at the laboratory of DTU Civil Engineering was used in an attempt to answer the research questions posed at the beginning of this chapter. Despite a large effort, it proved difficult to determine the load from pedestrians through back-calculations of the measured response without measuring the load directly. Back-calculations rely on the response measurements as well as an accurate representation of the dynamic characteristics of the structure in terms of natural frequencies, modal mass and damping. All these quantities are known to be subject to variations and amplitude dependencies (Racic et al., 2010). In its initial configuration, the fundamental vibration mode of the platform was triangular. As discussed by Ingólfsson et al. (2008a), this configuration was found inappropriate for studying human-structure interaction due to the triangular mode shape. The modified platform proved more appropriate, but as already stated, the presence of a twist mode is problematic as it is not a representative vibration mode of a real footbridge.

The platform tests have proven more successful in answering the research question regarding the importance of human-structure synchronisation for the onset of large lateral vibrations. The results from the tests provided valuable insight into the mechanism of human-structure interaction as it was found that synchronisation does not occur instantaneously when walking on a laterally vibrating surface (Ingólfsson et al., 2008a). On the modified platform, it was shown that large vibrations could be developed in the low-frequency sway mode during the pedestrian crowd tests. Visual observations made during the tests and the simultaneous vibrations in the sway mode, question the importance of human-structure synchronisation for the development of excessive vibrations.

However, without a direct measurement of the lateral forces it is difficult to make a robust method for quantification of the pedestrian-induced loads. Therefore, further instrumentation of the platform was considered. This involved applying an actuator with load cells between the laboratory floor and the structure. This way, the structure could be exited into vibrations at different amplitudes and frequencies during the passage of pedestrians. The method was used successfully on a different assembly structure in the

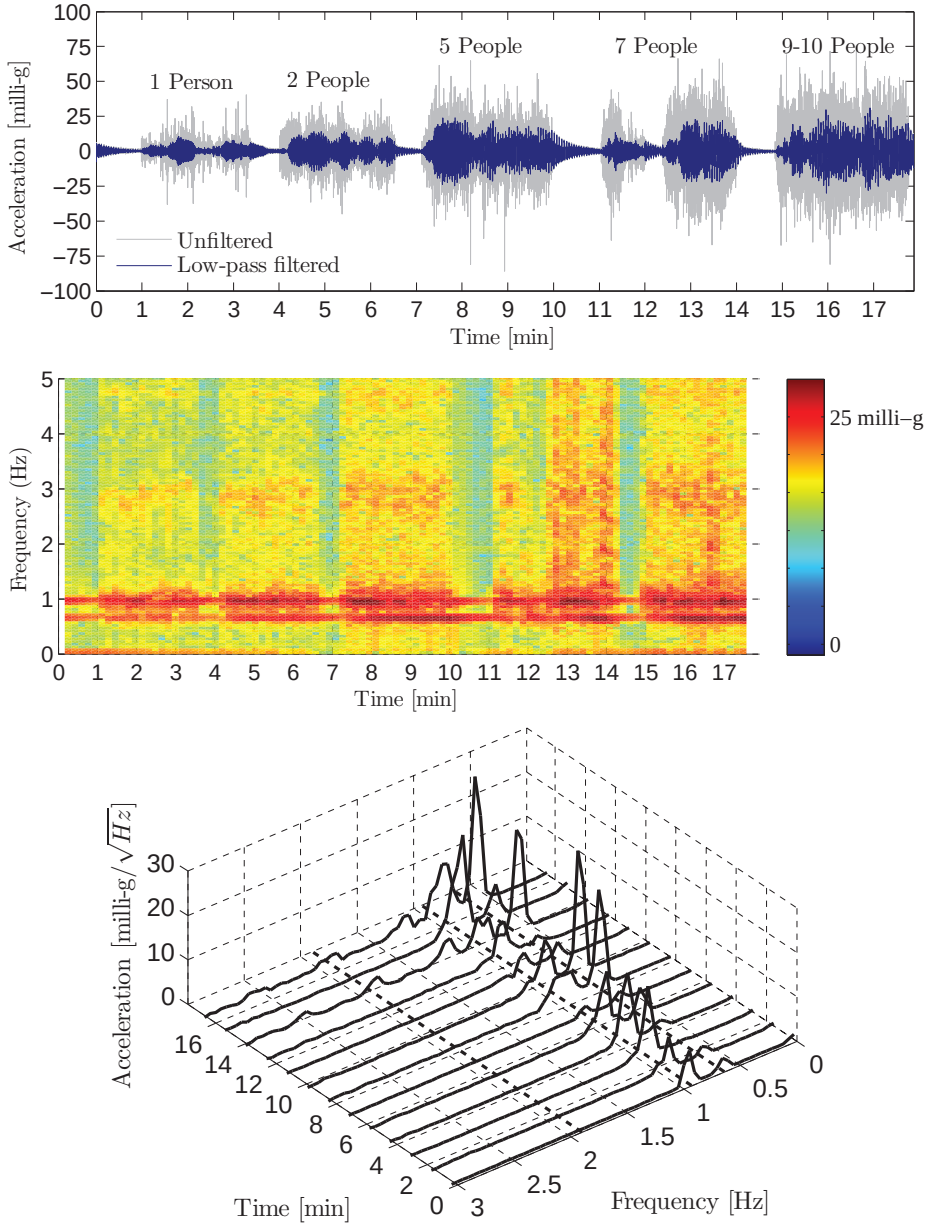

Figure 3.6: *Time history (top) and spectrogram (middle) and a waterfall plot (bottom) of the acceleration response during the pedestrian crowd tests.*

laboratory, where the vertical forces from single pedestrians and groups were measured (Jørgensen, 2009). However, due to its weight, the inertia force of the platform is much higher than the variation in the pedestrian-induced lateral force and due to its length, only a limited number of steps could be measured. Therefore, it was decided not to carry out further tests on the platform, but instead focus on the experimental campaign presented in Chapter 4.

Chapter 4

Experimental Campaign

As already mentioned, the laboratory platform proved insufficient for the purpose of this research, as the lateral pedestrian-induced forces could not readily be measured and the estimation of the forces relied on back-calculations of the measured response (Knudsen, 2007; Christiansen, 2008; Ingólfsson et al., 2008a).

Based on the conclusions of previous studies, a statistical characterisation of the lateral GRFs over a range of frequencies and amplitudes is necessary for understanding the development of large amplitude bridge vibrations. Since the driving mechanisms do not seem to depend on an instantaneous synchronisation between the pedestrian walking and the movement of the bridge, this characterisation should be based on a considerable number of repetitive footsteps.

Therefore, an instrumented treadmill, driven in a lateral sinusoidal motion, was used to measure directly the forces induced by pedestrians during continuous walking. A detailed description of the experimental campaign and the main results are presented by Ingólfsson et al. (2011, 2010b) (Papers II and III of this thesis).

The chapter is structured into seven sections. In the first four sections, an extended summary of the experiments is given. In Section 4.5, the results from the static tests are summarised together with some supplementary Fourier analysis of the measured forces. In Section 4.6, the main results from the dynamic pedestrian tests are briefly summarised and in the final two sections the conclusions from the experimental campaign are presented.

4.1 Background

The instrumented treadmill used in this study was constructed by Pizzimenti and Ricciardelli at the University of Reggio Calabria as a part of the PhD thesis of Pizzimenti (2004). In his thesis, a detailed description of the treadmill, its design and construction is provided. In addition a comprehensive study on the ground reaction force from pedestrians walking on a fixed surface was carried out and presented, both in the thesis (Pizzimenti, 2004) and later in a joint publications of the two researchers (Ricciardelli and Pizzimenti, 2007). As reviewed by Ingólfsson et al. (2010a) (paper I of this thesis), a frequency-domain procedure was used to quantify the pedestrian-induced load and in particular, a Gaussian shaped PSD was introduced to fit the experimentally determined PSD around each of the first five harmonics.

For the case with treadmill motion, a pilot study was carried out by Pizzimenti (2004), where the load from five test subjects were obtained at three different vibration amplitudes (15 mm, 30 mm and 45 mm) ant at five different lateral vibration frequencies in the range 0.60 to 0.92 Hz. Pizzimenti (2004) identified two different mechanisms, the first one being centred around half the pacing frequency and its higher harmonics and the second one which occurs at the frequency of the lateral vibration. This component is caused by the interaction between the treadmill motion and the movement of the pedestrian and was denoted "the self-excited force". The self-excited portion of the load was further subdivided into two components, one in-phase with the displacement and one in-phase with the velocity of the treadmill, written in terms of body-weight normalised dynamic load factors (DLF_{in} and DLF_{out} respectively):

$$F(t) = F_{st}(t) + \underbrace{\mathrm{DLF_{In}} \cdot W \sin(2\pi f_L t)}_{\text{In-phase load}} + \underbrace{\mathrm{DLF_{Out}} \cdot W \cos(2\pi f_L t)}_{\text{Out-of-phase load}} \tag{4.1}$$

For the five test subjects used in the pilot study, the contribution of the pedestrian to the overall modal mass and damping of the structure, could be obtained directly from the DLF of the self-excited force coefficients. The results from the pilot studies were published by Pizzimenti (2004) and in a joint publication by Pizzimenti and Ricciardelli (2005). It was shown that the in-phase component of the pedestrian load was generally negative, meaning that the pedestrians add stiffness to the structure (or alternatively decrease mass). For the out-of-phase component of the load, pedestrians act as negative dampers at one combination of frequency and amplitude. The average DLFs found in the tests, are shown in Fig. 4.1.

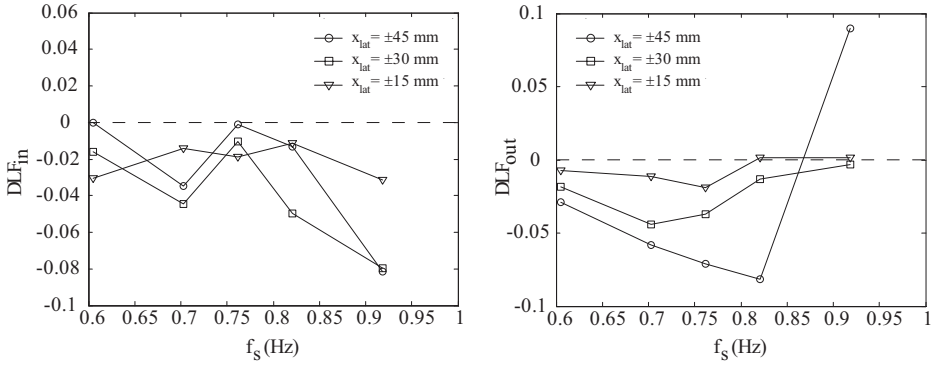

Figure 4.1: *Average DLF for the in-phase (a) and out-of-phase (b) components of the self-excited pedestrian force (Figure reproduced from Pizzimenti and Ricciardelli (2005)).*

During the experimental work presented in this thesis, the treadmill was situated in the laboratory of the Inter University Research Centre for Building Aerodynamics and Wind Engineering (CRIACIV) in Prato. It was moved from the University of Reggio Calabria in 2006 and subject to minor modifications prior to the work described in this thesis. The modifications include a substitution of the hangers, from S-shaped bars to low-friction

hinges (see Fig. 4.2). In addition, the inverters used to control the motors were substituted and the gearing between the forward velocity of the treadmill and the motor rotation was modified to allow for larger walking speeds. Finally, the accelerometers, displacement measures and data acquisition is different from that used by Pizzimenti (2004). These are described in Section 4.2. For a more detailed description of the mechanical modifications, see Bonanni (2007).

4.2 Description of the Treadmill Ergometer Device

In brief, the treadmill ergometer device (Fig. 4.2) consists of three separate parts, stages 1 to 3. Stage 1 is a steel frame which is fixed onto the laboratory floor and stages 2 and 3 are connected to the base through low-friction guided rails. Stage 2 is a steel frame which is driven in a lateral motion by an asynchronous motor (1.1 kW and 1.5 HP), through a shank. The shank is mounted eccentrically on a rotating steel disc, allowing for various vibration amplitudes (4.5 mm, 10.0 mm, 19.4 mm, 28.7 mm, 31.0, 38.3 and 48.0 mm). Stage 3 consists of the walking surface (dimension 100x180 cm), made of a steel frame system covered with plywood and a rubber belt. The connection between stages 2 and 3 consists of a suspension system using four low friction hangers as well as four flexural load cells (3.7711 mV/N) for measuring the lateral force between the two stages. The forward motion of the belt is driven by an asynchronous motor (1.1 kW and 1.5 HP) which is supported at stage 2. The separation of stages 2 and 3 is made to minimise the weight (and thereby the inertia force) of the walking surface. Both motors are controlled using Variable Speed Drive inverters allowing for variable walking speeds and lateral vibration frequencies respectively.

The lateral motion of the treadmill is monitored with two high-sensitivity accelerometers (PCB Piezotronics,type 393N12, 10 V/g) connected to a 4-channel signal conditioner (PCB Piezotronics, type 441A42) as well as a displacement laser (100 mV/mm). The accelerometers are placed at the two hanger locations (on one side of the treadmill) and the displacement laser is located at the middle of the treadmill. The forward walking speed is determined using an encoder mounted onto one of the cylinders which drive the treadmill belt. All signals were acquired with ±5 V 24-Bit data acquisition modules (National Instruments, cDAQ-9172+BNC 9234) with a sampling rate of 2048 Hz.

The accuracy of the measured pedestrian-induced forces relies on an accurate calibration of the treadmill, in particular the contribution of the weight of stage 3 on the resulting forces is of importance. For an empty treadmill, the measured force between stage 2 and 3 equals the inertia force of stage 3. Therefore, the total mass of stage 3 (100.38 kg) was carefully measured by Bonanni (2007), who rebuilt the treadmill at CRIACIV. Prior to the pedestrian tests, an extensive calibration scheme was undertaken, to establish the exact relationship between the output voltage of the load cell and the expected inertia force in the treadmill at all relevant combinations of vibration frequencies and amplitudes. In each test, the calibration constant, $\hat{k}_i$, was defined as (Ingólfsson et al., 2011):

$$\hat{k}_i = M_{\text{Stage 3}} \frac{\sigma_{\ddot{x},i}}{\sigma_{V,i}} \tag{4.2}$$

where $M_{\text{Stage 3}}$ is the mass of stage 3, $\sigma_{\ddot{x},i}$ and $\sigma_{V,i}$ are the standard deviations of the treadmill acceleration and voltage output from the load cells respectively. A clear linear trend

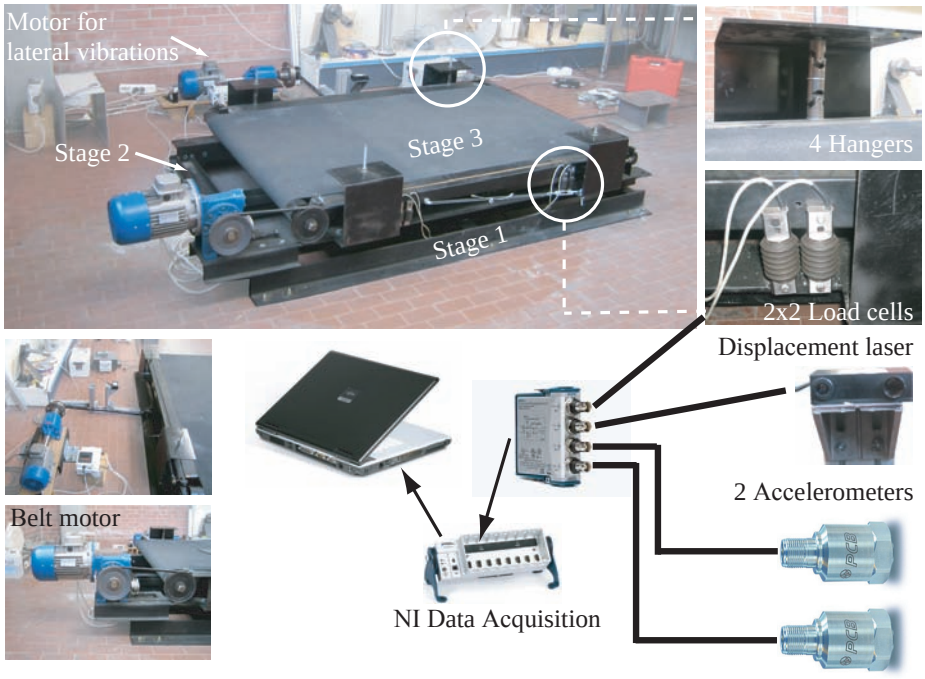

Figure 4.2: *Treadmill ergometer device.*

was observed with a linear correlation coefficient close to unity (ρ =0.99997). By applying the calibration constant to transfer voltage into force, the error in the measurements can be calculated as the difference between the calculated inertia force of the treadmill and the measured force in the load cell. With an empty treadmill, the resulting lateral force was measured for all relevant combinations of frequencies and amplitudes. The mean value of the error, defined as the RMS value of the measured force ($\hat{k}\sigma_{V,i}$) minus the RMS value of the calculated inertia force ($\sigma_{\ddot{x},i}M_{\text{Stage 3}}$), was found as 1.2 N (S.D. 0.2 N). This error is considered acceptable for most practical purposes.

4.3 Description of the experiments

During the summer 2009, an extensive experimental campaign was undertaken, which involved three fundamentally different tests on the treadmill (Ingólfsson et al., 2011, 2010b):

- Normal walking without lateral movement of the treadmill (static tests).
- Normal walking with a sinusoidal lateral movement of the treadmill at different frequencies and amplitudes (dynamic tests).
- Walking with and without lateral movement of the treadmill at slower forward velocities.

Generally, a large range of walking speeds should be investigated, both normal walk, faster and slower walking speeds. At each walking speed, a number of vibration frequencies and amplitudes should be tested. However, this calls for a very large number of tests that is required for each test person. Therefore, it was decided to carry out a large number of tests at normal walking speeds and focus primarily on the investigation of the frequency and amplitude dependency of the measured force. However, few benchmark tests were carried out with pedestrians walking at a slower forward speed, in order to obtain a qualitative insight into the walking speed dependency on the measured forces.

Normal walk is herewith defined as walking on the treadmill at a forward speed selected by the pedestrian in the absence of any lateral movement. After having selected a comfortable walking speed, the test person carried out the static tests, with a total duration of 2 min. Directly following the static tests, a number of dynamic tests were carried out. The vibration amplitude was randomly selected and the pedestrian was asked to walk continuously on the treadmill at a constant forward speed (the same as in the static tests). During walking, the vibration frequency was increased in steps, from the lowest frequency tested to the highest one. Each step lasted 30 s plus a transition interval in which time the frequency was changed. Each person spent between one and two hours in the laboratory, depending on their availability, which also dictated the number of amplitudes tested by each pedestrian. Most of the test series were recorded with a digital video camera. The entire experimental campaign comprised a total of seventy-one individuals (45 male and 26 female), with characteristics as summarised in Table 4.1. The total test matrix features combinations of various displacement amplitudes (4.5 to 48.0 mm) and vibration frequencies (0.33 to 1.07 Hz). In Fig. 4.3, a graphical representation of the test matrix is shown which indicates the number of individual tests carried out at each

particular combination of frequency and amplitude. The test persons were obtained with assistance from students and faculty members of the University of Firenze in Prato and consisted of friends, family and colleagues of the author and his assistants. The volunteers thereby represented a diverse group of people of different nationality, age, education and occupation. All the tests were carried out in the period between May and August, 2009.

Table 4.1: *Mean values and standard deviation (in brackets) of some characteristics quantities of the test subjects.*

	Body mass [kg]	Age [years]	Height [cm]	Leg [cm]	Ankle [cm]	Wrist [cm]	Speed [m/s]	Frequency [Hz]
Male	82.3 (11.15)	33.9 (19.63)	178.2 (5.24)	103.1 (4.81)	23.6 (1.60)	17.2 (1.05)	1.30 (0.20)	0.85 (0.07)
Female	61.4 (11.32)	32.1 (10.03)	164.4 (5.37)	95.4 (4.00)	21.9 (2.08)	15.2 (1.05)	1.27 (0.23)	0.87 (0.09)
Total	74.6 (15.1)	33.2 (10.4)	173.0 (8.5)	100.2 (5.8)	23.0 (2.0)	16.4 (1.4)	1.29 (0.21)	0.86 (0.08)

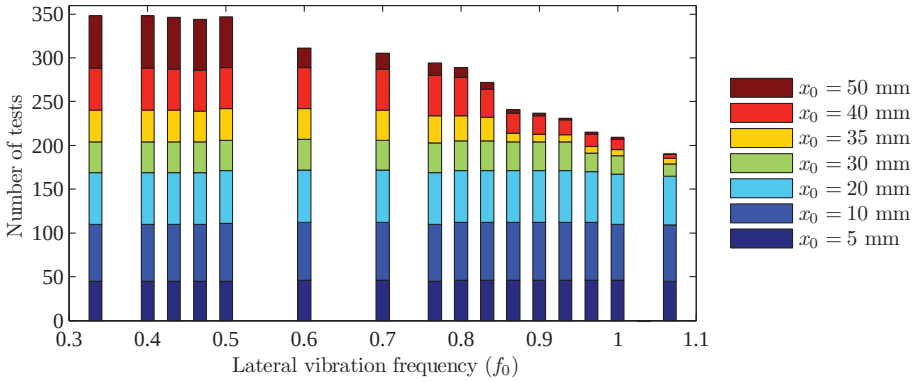

Figure 4.3: *Test matrix from experimental campaign.*

In addition to the tests performed at user selected walking speeds, nine persons were asked to repeat their experiments at three different walking speeds determined as 90 %, 75 % and 60 % of the original normal walking speed. This was done to investigate intra-subject variability in the loading and the effect of imposed slower walking speed on the resulting GRFs. This has particular interest when modelling pedestrian crowds where the walking speed is determined by the common forward velocity of the crowd, rather than individual preferences.

To the author's knowledge, the experimental campaign presented herewith, is the most comprehensive set of tests on lateral pedestrian-induced forces which has been carried out

to date, with more than 4800 individual tests covering the total walking distance of more than 55 km.

4.4 Human-body accelerometers

As discussed in Chapter 2, it has often been postulated that human-structure synchronisation is necessary for the development of SLE. However, visual observations during the initial treadmill tests suggested that synchronisation was not as pronounced as generally believed. Although the vibrations were clearly noticeable by the test subjects and even annoying, no systematic form of synchronisation was observed. To verify this observation, further analysis was carried out using tri-axial body-mounted accelerometers.

The accelerometers, which are wireless and time-synchronised, were originally developed at the Technical University of Denmark (Christensen and Dyekjær, 2007) and later modified by Andersen (2009) for the specific purpose of studying the interaction amongst individual pedestrians within a crowd. Due to their compact design, one body accelerometer could be attached to the waist of the test subject whilst the other one could be placed on the treadmill (see Fig. 4.4). A total of ten test subjects were monitored using the body accelerometers to allow for simultaneous measurement of the body acceleration whilst measuring directly the force transmitted to the structure. This part of the test campaign is described in detail by Ingólfsson et al. (2010b).

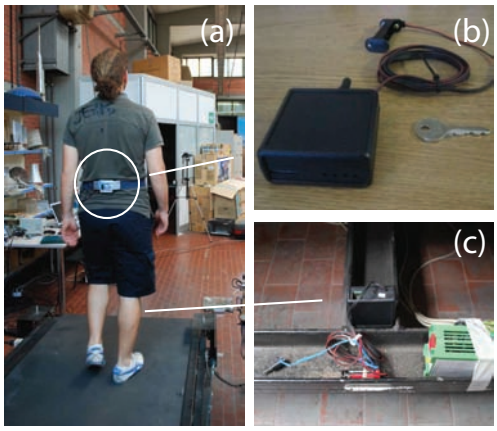

Figure 4.4: *Tri-axial accelerometer attached to the waist of the test person and onto stage 2 of the treadmill.*

4.5 Lateral forces without treadmill motion

The equivalent static pedestrian force refers to the lateral load transmitted to the ground by pedestrians in the absence of lateral motion. As discussed in section Section 2.1.1, the ground reaction forces are caused by the acceleration and deceleration of the human body's centre of mass. On a rigid surface this movement generates a narrow-band load

with energy concentrations around half of the average step frequency (also defined as the walking frequency, $f_w = f_s/2$) and its integer harmonics. A total of seventy-one different test subjects participated in the experimental campaign, where each pedestrian walked for two minutes on the treadmill without lateral motion at his/her own preferred forward velocity. As discussed in Section 2.1.2, during walking the gait parameters are subject to random fluctuations, which cause variations in the GRFs between each step. This intra-subject variability causes a spread of spectral energy away from the main harmonics to adjacent frequencies making the overall loading process a narrow-band random process rather than perfectly periodic. In Fig. 4.5 three examples of measured force time-histories and their associated square-root PSD[1] are shown, indicating variations in people's ability to maintain constant gait parameters during continuous walking. It is also worth noting that the distinct presence of even harmonics suggest that the gait is asymmetric with a systematic difference between the left foot and the right foot.

4.5.1 Fourier series analysis of the measured force

The equivalent static force (i.e. in the absence of treadmill motion) may be quantified in different ways depending on the application. In the time domain, the force is often simplified as a truncated Fourier series with fundamental frequency, f_w, equal the pedestrian walking frequency (Bachmann et al., 1996b; Živanović et al., 2005a; Ingólfsson et al., 2010a).

From basic Fourier analysis it is recalled that any periodic function with fundamental frequency f (or period of repetition $T = 1/f$) can be written as an infinite trigonometric series (Sólnes, 1997):

$$F(t) = \frac{a_0}{2} + \sum_{j=1}^{\infty} c_j \cos\left(2\pi j f t - \phi_j\right) \tag{4.3}$$

$$c_j = \sqrt{a_j^2 + b_j^2} \qquad \tan\phi_j = \frac{a_j}{b_j} \tag{4.4}$$

$$a_j = \frac{2}{T}\int_0^T F(t)\cos\left(2\pi j f t\right)\mathrm{d}t \qquad j \geq 0 \tag{4.5}$$

$$b_j = \frac{2}{T}\int_0^T F(t)\sin\left(2\pi j f t\right)\mathrm{d}t \qquad j \geq 1 \tag{4.6}$$

$$\tag{4.7}$$

It is further known that although not perfectly periodic, the pedestrian-induced force signal is near periodic with fundamental frequency equal to the walking frequency, $f_1 = f_w$. Therefore, in order to reduce the numerical energy leakage between spectral bins, the length of the measured time series were modified such that they contain an integer number of cycles with frequency equal the walking frequency. The original signal was sampled at rate 2048 Hz ($\Delta t \cong 4.88 \cdot 10^{-4}$) with a total of $N = 245\,760$ distinct data points, $t_n = (n-1)\,\Delta t$, $n = 1 \ldots N$. The analysis was carried out in steps:

[1]Square-root PSD is defined as the square-root of a single sided PSD, where the sum of the squares, mutliplied with the frequency resolution, equals the variance of the parent signal.

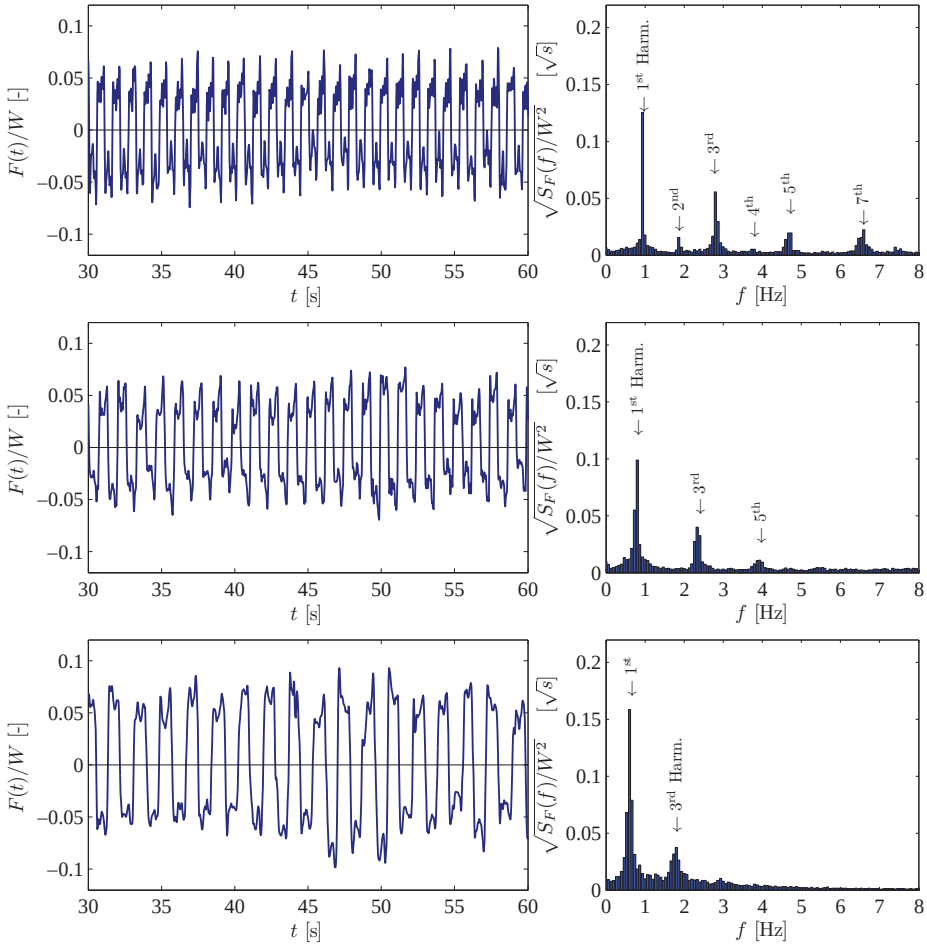

Figure 4.5: *Examples of measured body weight normalised force time-histories (low-pass filtered with cutoff at* 8.0 Hz*) and the corresponding square-root PSD (averaged over 8 non-overlapping rectangular windows) from 3 different single pedestrians walking on a stationary surface.*

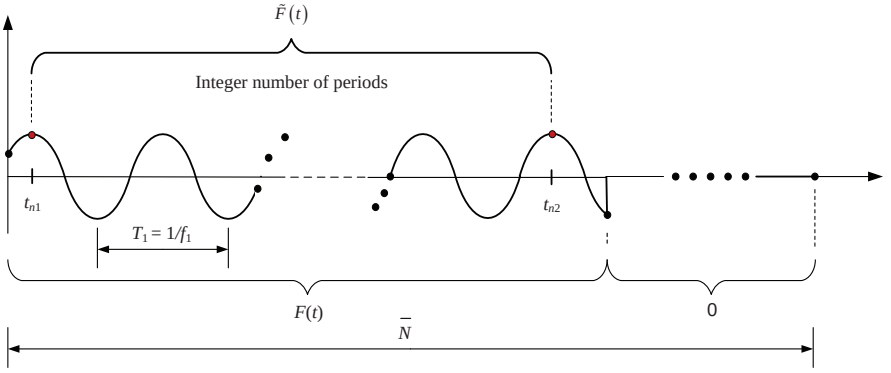

Figure 4.6: *Schematic representation of the preprocessing of the measured lateral GRF.*

1. To identify the fundamental frequency, f_1, the length of the force signal was increased to the total length $\overline{N} = 2^k$ in which all elements of $F(t_n)$ are zero for $t_n > (N-1)\,\Delta t$. The exponent k is selected such that $\overline{N} > N$ and to obtain a high frequency resolution ($\Delta f = 1/\left(\overline{N}\Delta t\right)$). The new (zero-padded) force vector is analysed with the fast Fourier transform (FFT) and the fundamental frequency f_1 is determined as the first (large) peak in the resulting Fourier spectrum.

2. Based on the fundamental frequency f_1 and the phase angle $\phi(f_1)$ a new force vector $\tilde{F}(t)$ is generated from the original force vector, $\tilde{F}(t) = \{F(t_{n_1}), \ldots, F(t_{n_2})\}$. As illustrated in Fig. 4.6, the time instances t_{n_1} and t_{n_2} are selected such that the new force vector initiates at the maximum value of the first harmonic and contains the maximum integer number of fundamental periods ($T_1 = 1/f_1$), possible within the 2 minute signal.

3. The new force signal $\tilde{F}(t)$ is now used in all subsequent data treatment. For simplicity $\{\tilde{}\}$ is omitted from now on and $F(t)$ therefore refers to the modified time series.

The Fourier transform of the new time series has a frequency resolution (Δf) which is related to the walking frequency through an integer, i.e. $f_1 = f_w = k\Delta f,\ k \in \mathbb{Z}$. The Fourier series definition in Eq. (4.3) can be used to create a perfectly periodic approximation to the walking force, $F_p(t)$ using the walking frequency as the fundamental frequency. Furthermore, since the even harmonics are generally low, only a number of odd harmonics are included:

$$F(t) \cong F_p(t) = c_1 \cos\left(2\pi f_w t\right) + \sum_{j=2}^{n_p} c_j \cos\left(2\pi(2j-1) f_w t - \phi_j\right). \tag{4.8}$$

It is noted that due to the selection of the initial time, the phase angle of the first harmonic is zero and the remaining phase angles are therefore relative to the first harmonic. The advantage of using this representation is that the DLFs (i.e. $\mathrm{DLF}_{2j-1} = c_j/W$) and the

phase angles can be extracted directly from the Fourier spectrum for the creation of a simplified model which fits reasonably to the measured data. In Fig. 4.7 a comparison between the measured pedestrian force and the use of the truncated Fourier series is shown. The reproduced force, $F_p(t)$, is generated from the first seven odd harmonics ($n_p = 7$). It is worth noting that there is an energy leakage around the main walking frequency caused by the imperfections in the walking as discussed in Section 2.1.2, being more pronounced at the higher harmonics than at the first one. The shape of the reproduced force is similar to that of the measured force, but does not contain the amplitude variations. This observation is consistent with those of Brownjohn et al. (2004b) for the vertical component of the GRF, measured during continuous walking.

The distribution of the DLFs of the first three harmonics and the associated phase angles are shown in Fig. 4.8. For the fundamental harmonic, the mean value is 0.037 (S.D. 0.012) and for the third and fifth the values are 0.009 (S.D. 0.005) and 0.002 (S.D. 0.001) respectively. It is noted that the phase angle of the third harmonic is distributed around π whereas that of the fifth harmonic is more or less uniformly distributed in the range $0 - 2\pi$.

The GRF is generated due to the inertia force produced by acceleration of the body centre of mass. The force which is transferred to the ground through the foot is counteracted by an equal but opposite force in equilibrium with the the inertia force produced by the acceleration of the centre of mass. Therefore, the acceleration of the centre of mass (projected onto the medio-lateral direction) can be obtained directly from lateral component of the GRF as:

$$\ddot{y}(t) = -\frac{1}{m_p} F(t). \tag{4.9}$$

Here $y(t)$ represents the lateral movement of the centre of mass, dot represents differentiation with respect to time, m_p is the body mass and $F(t)$ is the measured lateral force. Now, both the velocity as well as the displacement can be obtained through numerical integration of the acceleration. As proposed by Erlicher et al. (2010), the numerical integration can be carried out in the frequency domain through the Fourier transform of the lateral force. The pedestrian induced load (and acceleration) has been written as a sum of trigonometric functions therefore the derivatives are easily obtained as:

$$\dot{y}(t) \cong -\sum_{j=1}^{\infty} \frac{c_j}{2\pi(2j-1)f_w m_p} \sin\left(2\pi(2j-1)f_w t - \phi_j\right) \tag{4.10}$$

$$y(t) \cong \sum_{j=1}^{\infty} \frac{c_j}{\left(2\pi(2j-1)f_w\right)^2 m_p} \cos\left(2\pi(2j-1)f_w t - \phi_j\right) \tag{4.11}$$

where it has been assumed that $F(t)$ is a zero-mean signal. In fact, as the factors $2\pi(2j-1)f_w$ and $(2\pi(2j-1)f_w)^2$ appear in the denominator of $\dot{y}$ and $y(t)$ respectively, low frequency contributions are magnified and high-frequencies attenuated during the integration process. This means that a DC component in the force signal causes a linear drift of the integrated velocity and a parabolic drift on the displacement. Therefore, the force signal was high-pass filtered with a cutoff frequency at 0.5 Hz to avoid the aforementioned numerical problems.

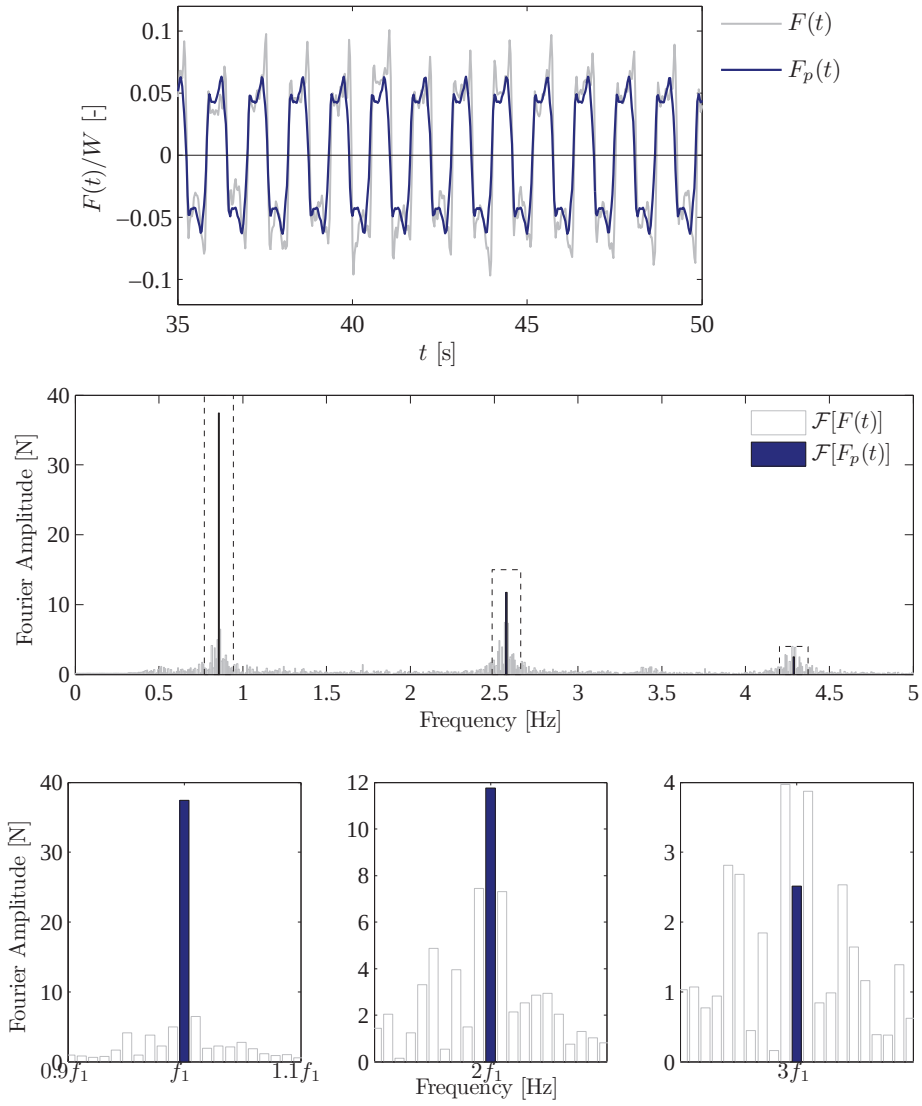

Figure 4.7: *Body weight normalised time-history of the lateral GRF (top) and the associated Fourier spectrum (middle and bottom) for a single test subject.*

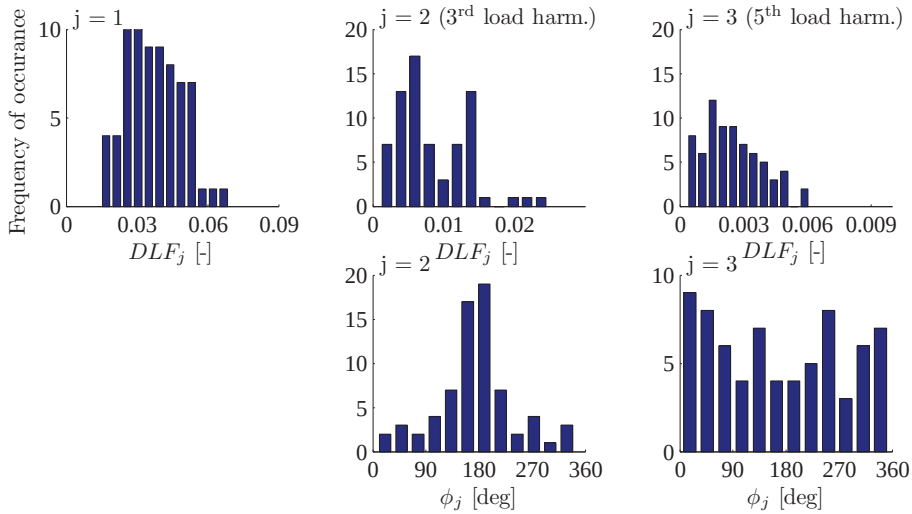

Figure 4.8: *Distribution of DLFs (top) and phase angles (bottom) for the first three odd harmonics in the perfectly periodic load model.*

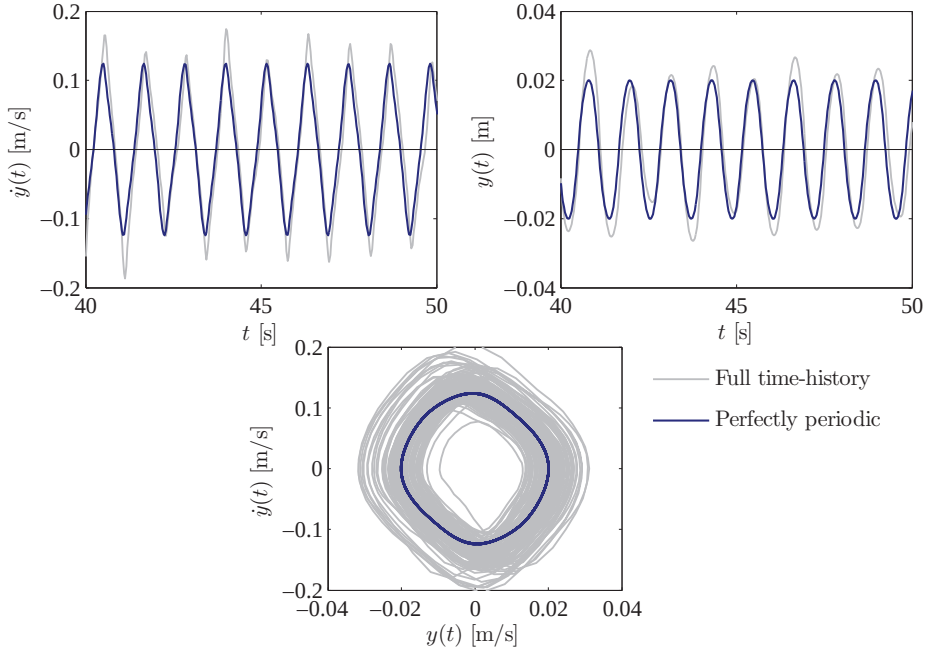

Figure 4.9: *An example of the measured lateral velocity (top-left) and displacement (top-right) time histories as well as a state-space plot (bottom) of the body centre of mass compared to that derived from the perfectly periodic model.*

By applying the numerical integration scheme presented in Eqs. (4.10) and (4.11), the lateral velocity and displacement of the pedestrians' centre of mass were determined. An example of the calculated displacement and velocity is shown in Fig. 4.9. Again it is noted that qualitatively the shape of the time-histories agree well with both the full time histories as well as earlier reports regarding the pedestrian movement (Townsend, 1985; Macdonald, 2009; Erlicher et al., 2010). However, a considerable intra-subject variability is observed. This is most clearly seen in the phase plane plot, in which the radii of the closed trajectories vary between cycles, questioning the applicability of the perfectly periodic model. The Fourier model is advantageous as it can be used to obtain simplified expressions for the load and it seems to render the temporal properties of the load fairly well, in particular for walkers with more or less constant gait parameters. On the other hand, walkers which feature a large intra-subject variability in the gait parameters, the perfectly periodic model is incapable of reproducing the load properly. One measure of the ability of the periodic model to represent the load is to compare the variance (or mean-square value) of the load in the two models, $\sigma^2_{F_p}/\sigma^2_F$. On average, only 43 % (S.D. 15 %) of the variance is represented in the periodic model and only in 5 of 71 test subjects, the variance of the perfectly periodic model exceeds 70 % of the total variance. This stresses the importance of taking into account the intra-subject variability in the load.

4.5.2 Equivalent "perfect" DLF

As shown in Fig. 4.7, the intra-subject variability makes the perfectly periodic description of the loading insufficient due to the spread in energy away from the main load harmonics. Thereby, the DLFs shown in Fig. 4.8, which are derived from the perfectly periodic model in Eq. (4.8) underestimate the load of the particular load harmonic.

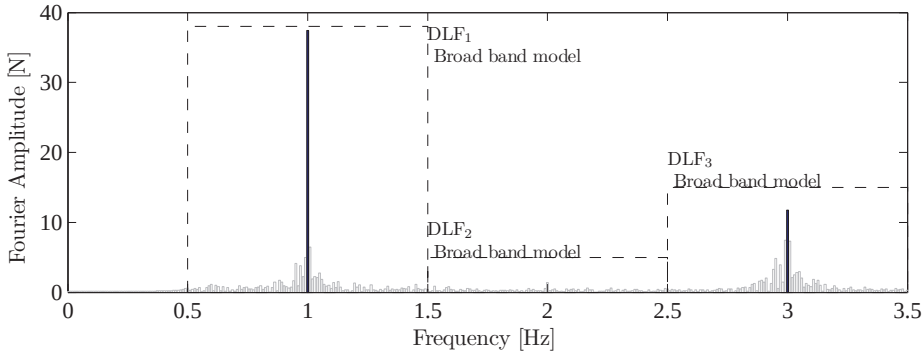

Figure 4.10: *Illustration of the perfectly periodic model used to calculate the DLF from the experimentally determined Fourier spectrum of the pedestrian-induced load.*

Due to this spread of energy around the main harmonics, the load amplitude can be quantified through an equivalent "perfect" DLF. A simple and straightforward way is to link the DLF to the overall variance of the load around the particular harmonic, such that the mean-square value of the equivalent force equals that of the measured force.

Thereby, the DLF of the jth harmonic from the broad band model is written in terms of the mean-square value of the measured force around the jth harmonic ($\tilde{\sigma}^2_{F,j}$) in the following way:

$$\mathrm{DLF}_j = \frac{\sqrt{2}\ \tilde{\sigma}_{F,j}}{W}, \qquad \text{Broad band model.} \tag{4.12}$$

where W is the pedestrian body weight. This type of model is herewith denoted the broad band model for the equivalent DLF, as it equally includes the load contributions at all frequencies between two adjacent harmonics. In Fig. 4.10, the definition of the equivalent DLF for the broad band model is illustrated. In Fig. 4.11, the equivalent DLFs from the static tests are shown as function of the individual walking frequency (normalised with the average walking frequency of the population, $\overline{f}_w$).

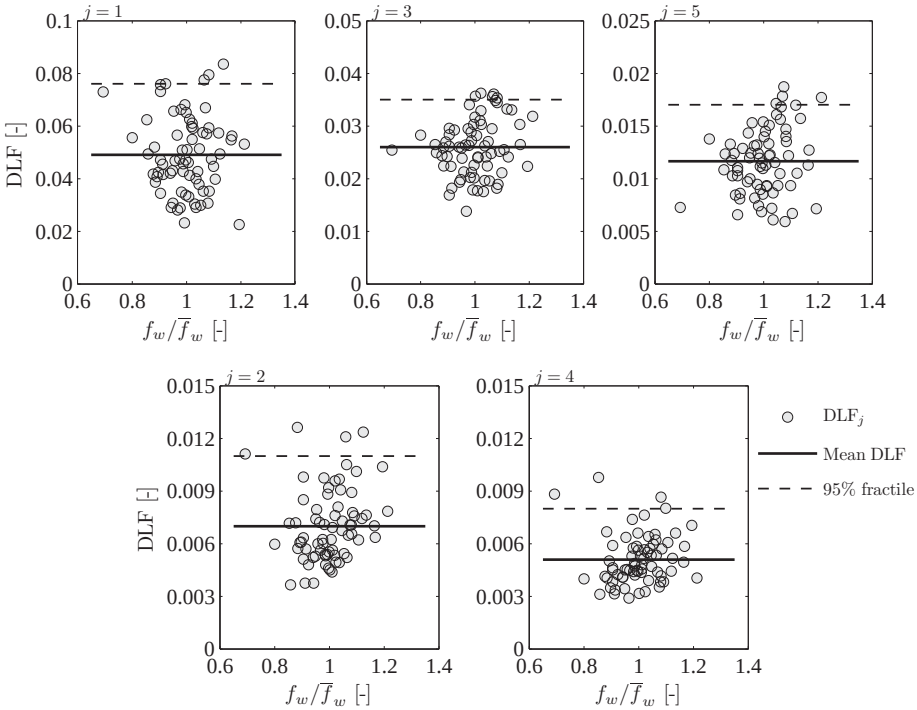

Figure 4.11: *Equivalent DLF of the first five load harmonics using the broad band model shown as function of normalised walking frequency.*

As civil engineering structure are generally lightly damped, only load contributions around the resonance frequency contribute significantly to the response. Therefore, DLFs from the broad band model, generally provide a conservative estimate of the effect the pedestrian loading on structures.

Eriksson (1994) used the so-called *white-noise approximation* to define a damping dependent band-width ($\pi\zeta j f_w$) in which load contributions should be included when calculating the DLF. The calculation of the bandwidth is based on the assumption that

the underlying load is a white-noise process (or at least constant in the frequency range which excites the structure). Even for lightly damped structures, the assumption of constant load amplitudes in the bandwidth ($\pi\zeta j f_w$) may be conservative. This is due to the narrow-band nature of the loading. This can be taken into account by using the experimentally obtained PSD to calculate the response, $\tilde{\sigma}^2_{u,j}$, of a single-degree-of-freedom (SDOF) system with unit stiffness, damping ratio ζ and natural frequency equal to the the walking frequency. The equivalent DLF is thereby obtained by requiring that $\tilde{\sigma}^2_{u,j}$ equals the mean-square response of the same SDOF system when subject to an equivalent perfectly periodic force at resonance. The body weight normalised amplitude of the perfectly periodic force becomes (Ingólfsson et al., 2011):

$$\mathrm{DLF}_j = \frac{2\sqrt{2}\zeta\ \tilde{\sigma}_{u,j}}{W}, \qquad \text{Narrow band model.} \tag{4.13}$$

In Fig. 4.12, a comparison between the broad band model and the narrow band model is shown for the DLF of the fundamental load harmonic. It is noted that as the structural damping increases, the narrow band model approaches the broad band model. However, for damping ratios usually encountered on footbridges, there is a considerable difference between the two models.

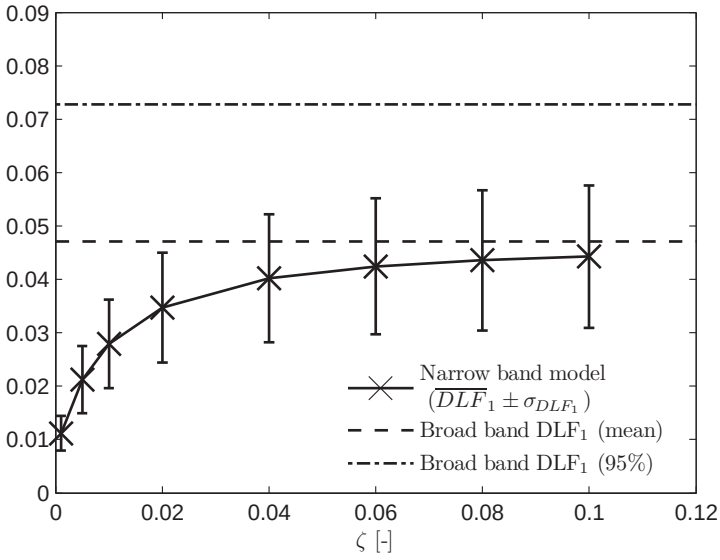

Figure 4.12: *Equivalent DLF of the fundamental load harmonic for the narrow band model as function of the damping ratio compared with the broad band model.*

4.5.3 Power Spectral Density of GRFs

Due to the near-periodic nature of the loading process, it seems appropriate to define the pedestrian load in the frequency domain in terms of its spectral properties. The PSD

features a distinct peak at the walking frequency and decays quickly to almost zero. Initially, a Lorentzian profile was used to fit the experimentally determined spectral density. This is convenient as it represents a first order auto-regressive process (Chatfield, 2004). However, it was found that a Gaussian shaped spectrum provided a better fit to the data, in particular at the higher harmonics, and was therefore chosen. The spectrum presented herewith is a slightly modified version of that presented by Ricciardelli and Pizzimenti (2007), as the constant C_1 has been introduced. This type of spectrum originates from wind engineering and was proposed by Vickery and Clark (1972) to fit the spectrum of generalised lift force in models of vortex excitation. The PSD function, $S_{F,j}(f)$, is written in a general (non-dimensional) form and represents the fitted PSD around load harmonic j:

$$\frac{S_{F,j}(f)\cdot f}{\tilde{\sigma}^2_{F,j}} = C_j + \frac{2A_j}{\sqrt{2\pi}B_j}\exp\left\{-2\left[\frac{f/(jf_w)-1}{B_j}\right]^2\right\}. \tag{4.14}$$

The parameters A_j, B_j and C_j are determined by the data fit and $\tilde{\sigma}^2_{F,j}$ is the area of the PSD (i.e. the total variance of the lateral force) around the jth harmonic. The parameters A_j, B_j and C_j are summarised in Table 4.2 both for the model in Eq. (4.14) as well as for the case where $C_j = 0$. As shown in Fig. 4.13, Eq. (4.14) provides a good fit to the average PSD, in particular at the odd harmonics. The experimental PSD is obtained as the average of seven 50 percent overlapping rectangular windows. Each window is zero-padded to obtain a better frequency resolution. The average PSD is obtained as the average spectral ordinate from all individual spectra at each distinct frequency. A considerable variation in the shape between each individual is caused by the difference in the ability of pedestrians to maintain constant gait parameters during walking. This intra-subject variability is quantified through the width of the spectrum whereas the magnitude of the load is obtained through the quantity $\tilde{\sigma}^2_{F,j}$. The mean values of $\tilde{\sigma}^2_{F,j}$ $(j = 1, \ldots, 5)$ and that with 5 percentage probability of exceedance (95% fractile) are listed in Table 4.2 for the first five load harmonics.

Table 4.2: *Summary of parameters for the Gaussian shape spectrum for representation of the pedestrian-induced lateral force. The numbers in the brackets represent the case when $C = 0$.*

	$j=1$	$j=2$	$j=3$	$j=4$	$j=5$
A_j	0.841 (0.900)	0.016 (0.020)	0.719 (0.774)	0.013 (0.0258)	0.606 (0.612)
B_j	0.041 (0.043)	0.027 (0.031)	0.025 (0.026)	0.026 (0.064)	0.026 (0.026)
C_j	0.527	0.043	0.738	0.065	0.081
$\tilde{\sigma}_{F,j}/W$ (mean value)	0.035	0.005	0.018	0.004	0.008
$\tilde{\sigma}_{F,j}/W$ (95% fractile)	0.054	0.008	0.025	0.006	0.012

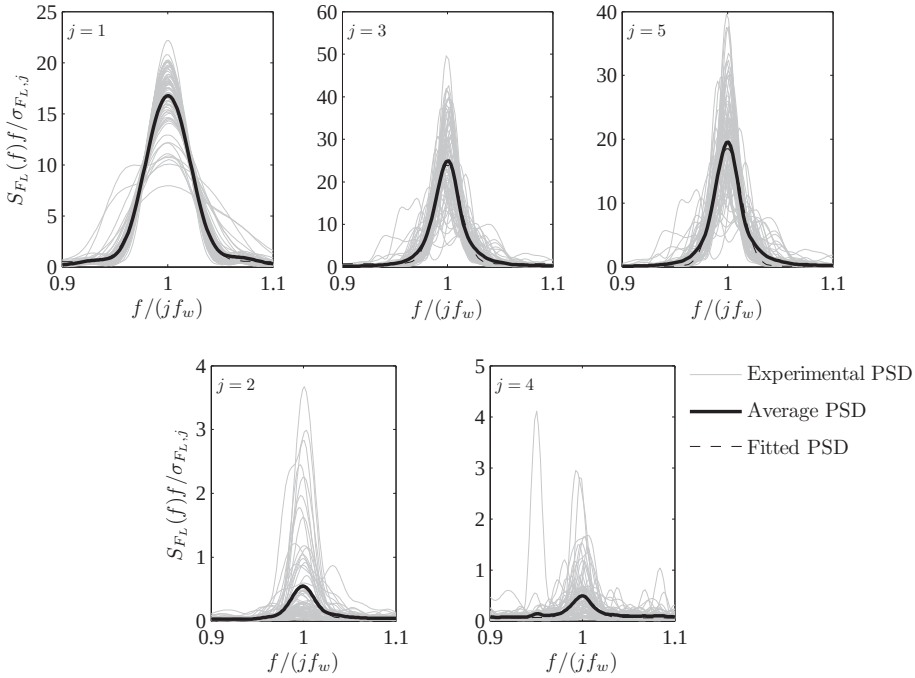

Figure 4.13: *Experimental PSD of the first five load harmonics for each pedestrian shown with the average PSD for all pedestrians and the fitted Gaussian shaped spectrum.*

4.6 Motion induced lateral forces

A variety of dynamic pedestrian tests were carried out in which the treadmill was driven in a lateral sinusoidal motion at different frequencies and amplitudes whilst the lateral GRFs from the pedestrians was measured. In the frequency domain, the load features distinct peaks at the walking frequency and its integer harmonics. Peaks also occur at the frequency of the lateral movement owing to the interaction between the motion of the platform and the motion of the body centre of mass. The existence of these contribution was shown by Pizzimenti (2004).

In Fig. 4.14, an example of the measured body weight normalised pedestrian-induced force is shown during a lateral vibration at frequency 1.03 Hz and amplitude 19.4 mm.

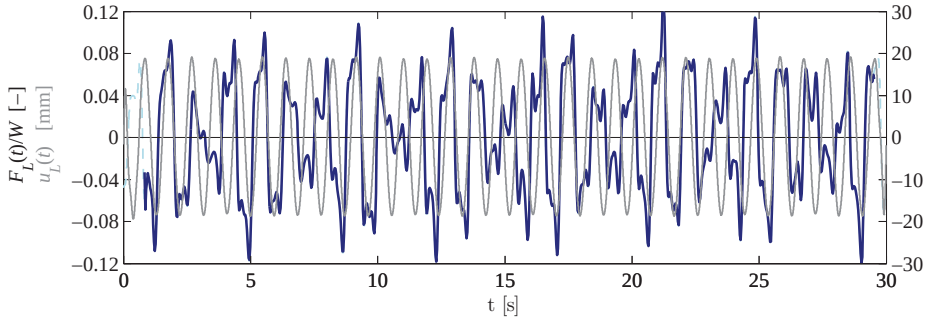

Figure 4.14: *Example of a measured weight-normalised force time-history (low-pass filtered with cutoff at* 8.0 Hz*) and the displacement time history of the treadmill during a pedestrian walking test.*

The portion of force, centred at the frequency of the lateral movement is denoted the *self-excited* pedestrian force. The self-excited portion of the force has a particular interest as it acts to modify the apparent modal properties (mass, damping or stiffness) of a given structure depending on the phase angle between the self-excited force and the structural movements. The most extreme type of human-structure interaction is the type of synchronisation (or lock-in) where the self-excited force is in phase with the structural velocity and thereby constantly inputs energy into the system. In the general case however, the movement of the centre of mass is not synchronised with the underlying platform and consists of the superposition of several harmonic signals at different frequencies. The instantaneous phase between the lateral platform movement and that of the pedestrian's centre of mass is non-constant and the term synchronisation or phase locking are inapplicable. Even in the absence of synchronisation, it is important to quantify the motion-induced portion of the load, and therefore a generic method must be used which is applicable both in the general case as well as in the special case of human-structure phase synchronisation.

With the focus being on the self-excited component of the pedestrian-induced force, the fundamental frequency of interest is the frequency of the lateral motion $f_L \in [0.3; 1.070\,\text{Hz}]$. Therefore, the length of the time series was modified such that it contains an integer number of cycles with frequency equal to the lateral oscillation frequency. The original signal was sampled at a rate of 2048 Hz ($\Delta t \cong 4.88 \cdot 10^{-4}$) with a total of $N = 61\,440$ distinct

data points ($t_n = (n-1)\,\Delta t$, $n = 1 \ldots N$), corresponding to an overall sampling time of 30 s. In Fig. 4.14, the dashed line represents the portion of the measured force which was truncated to obtain an integer number of vibration cycles. The modification made to the original time series is similar to that described in Section 4.5.1 for the equivalent static force. In Fig. 4.15, the spectral properties of the time series in Fig. 4.14 are shown, both for the original time series and the modified one. The open bars represent analysis carried out on the original (full-length) signal and the filled bars show that of the modified signal, such that it contains an integer number of lateral vibration periods. It is clear that a considerable energy leakage occurs between adjacent spectral bins of the original signal. This stresses the importance of including only an integer number of vibration periods in the signal before taking the Fourier transform.

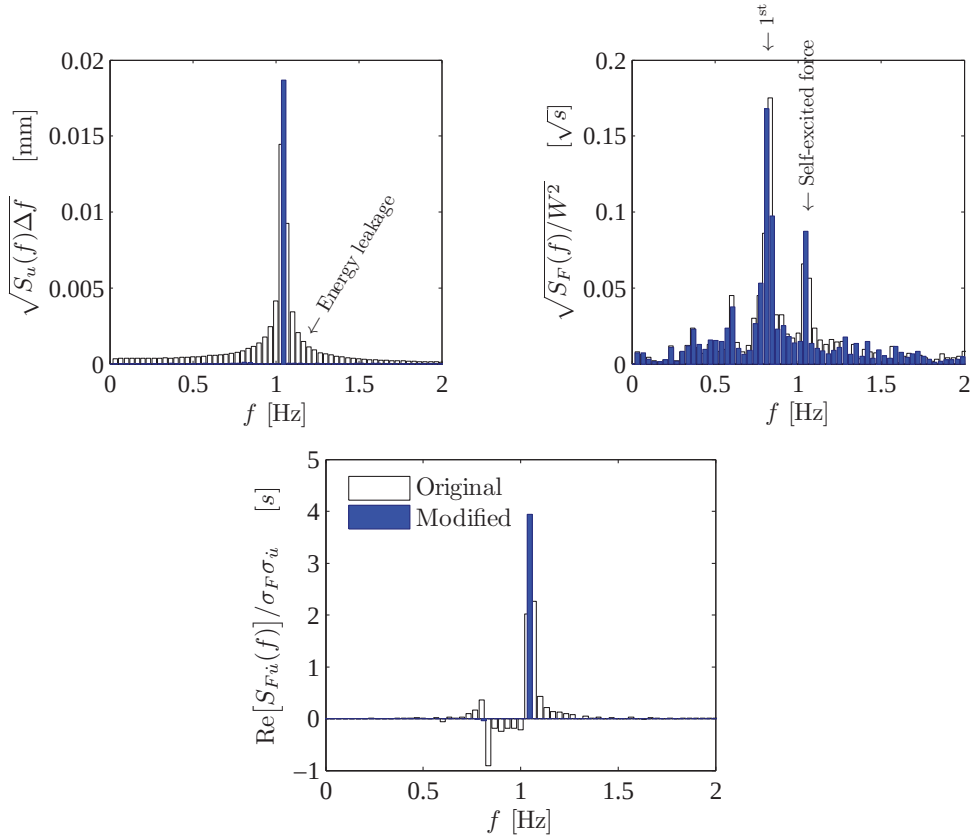

Figure 4.15: *Square-root PSD of the the lateral displacement and force (top) and the real part of their single-sided cross spectral density (bottom) from the time-histories in Fig. 4.14 (amplitude* 19.4 mm *and frequency* 1.03 Hz*).*

4.6.1 Cross spectral density between GRF and lateral displacement

The cross spectral density $\tilde{S}_{F\dot{u}}(f)$ provides a frequency domain representation of the covariance between the two quantities $F(t)$ and $\dot{u}(t)$. It is a complex quantity, defined as the Fourier transform of the cross-correlation function $R_{F\dot{u}}(\tau)$. This has a particular interest, as it can be shown that the work done by the pedestrian-induced lateral force per unit time P_F, can be obtained directly from the cross spectral density (Ingólfsson et al., 2011):

$$P_F = \lim_{T\to\infty} \frac{1}{T_{\text{tot}}} \int_0^{T_{\text{tot}}} F(t)\dot{u}\mathrm{d}t = \int_{-\infty}^{\infty} \tilde{S}_{F\dot{u}}(f)\mathrm{d}f \tag{4.15}$$

The cross spectral density, $\tilde{S}_{F\dot{u}}(f)$, is double sided where the contributions at negative frequencies are complex conjugates of those on the positive side, i.e. $\tilde{S}^*_{F\dot{u}}(f) = \tilde{S}_{F\dot{u}}(-f)$. In the evaluation of the integral in Eq. (4.15), only the real part of the cross spectrum (denoted the co-spectral density, $\text{Co}_{F\dot{u}}$) is of interest as all imaginary parts (quad-spectral density $\text{Qu}_{F\dot{u}}$) cancel out. Therefore, a single sided cross spectral density can be obtained from the double sided spectral density as (Strömmen, 2006):

$$\text{Re}\left[S_{F\dot{u}}(f)\right] = 2\text{Re}\left[\tilde{S}_{F\dot{u}}(f)\right] \qquad f \geq 0 \tag{4.16}$$

In this case, the area under the real-valued single sided spectral density equals the covariance between the processes F and $\dot{u}$.

In Fig. 4.15, the real value of the single sided cross-spectral density is shown, both for the original as well as for the truncated time series. Again, the importance of using an integer number of vibration cycles is illustrated. For the original signal, two peaks are observed around the lateral vibration frequency instead of just a single peak as observed in the modified signal. Furthermore, due to the aforementioned energy leakage, non-negligible contributions occur in the original signal at frequencies different from the vibration frequency.

For finite length records, the cross spectral density is evaluated at discrete frequencies, f_i, and when the length of the time series is adjusted to contain an integer number of oscillation periods, the only contribution of interest is that at the frequency of the lateral oscillation $f_i = f_L$. Therefore, the work done by the lateral force per unit time can be re-written as:

$$P_F = \text{Re}\left[S_{F\dot{u}}(f_i)\right]\Delta f \tag{4.17}$$

$$\Delta f = 1/\left(\overline{N}\Delta t\right) \tag{4.18}$$

where $\overline{N}$ is the length of the time series to be evaluated. In random vibration theory (Strömmen, 2006), it is customary to normalise the Co-spectrum with the auto-spectral densities of the two individual components (here F and $\dot{u}$). Here, the normalised Co-spectrum only has an interest at the frequency of the lateral motion, f_L, and therefore it is normalised with the variances $\sigma^2_{\dot{u}}$ and $\sigma^2_{F_s}$ of the treadmill velocity and the self-excited

force respectively[2]. This normalisation can be written as:

$$\tilde{C}o_{F\dot{u}}(f_L) = \frac{\mathrm{Re}\left[S_{F\dot{u}}(f_L)\right]\Delta f}{\sigma_{\dot{u}}\sigma_{F_s}} \tag{4.19}$$

$$\sigma_{F_s}^2 = S_F(f_L)\Delta f \tag{4.20}$$

The term $\sigma_{F_s}^2$ can be interpreted as the variance of the self-excited load and the normalised Co-spectrum thereby represents the cosine of the angle between the self-excited force and the treadmill velocity. The phase angle, can also be evaluated directly from the cross-spectral density, i.e.:

$$\varphi_{F\dot{u}}(f) = \arctan\frac{\mathrm{Qu}_{F\dot{u}}(f)}{\mathrm{Co}_{F\dot{u}}(f)} \tag{4.21}$$

$$\cos\varphi_{F\dot{u}}(f) = \tilde{C}o_{F\dot{u}}(f) \tag{4.22}$$

At each particular frequency, f, both F and u are simple harmonic functions, separated by the phase angle $\varphi_{Fu}(f)$. The definition of this phase angle is as shown in Fig. 4.16. The ordinate of the cross-spectral density is obtained as the covariance between F and u at the frequency f, separated by the phase $\varphi_{Fu}(f)$. This is illustrated in the following example:

$$F(t) = F_0\sin\left(2\pi ft + \varphi_{Fu}\right) \tag{4.23}$$

$$u(t) = u_0\sin\left(2\pi ft\right) \tag{4.24}$$

$$\mathrm{Re}\left[S_{Fu}(2\pi f)\right]\Delta f = \frac{1}{2}F_0u_0\cos\varphi_{Fu} \tag{4.25}$$

When the phase angle $\varphi_{Fu}(f)$ is defined in the interval $[0;\ 2\pi]$, the angle between the F and $\dot{u}$ is obtained as $\varphi_{F\dot{u}}(f) = \varphi_{Fu}(f) - \pi/2$. Similarly, $\varphi_{F\ddot{u}}(f) = \varphi_{Fu}(f) - \pi$.

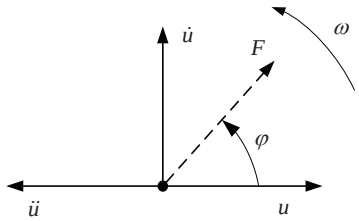

Figure 4.16: *Illustration of the phase angle between a force F and structural displacement u*

4.6.2 Equivalent pedestrian damping and inertia forces

A simple and straightforward way to interpret the results from the tests is to define an equivalent damping force, $F_{D,eq}(t)$, proportional to the lateral velocity and an equivalent

[2]Both the treadmill motion and the self-excited force only occur at the frequency of the lateral treadmill motion, hence $\sigma_{\dot{u}}^2 \cong S_{\dot{u}}(f_L)\Delta f$ and $\sigma_{F_s}^2 = S_F(f_L)\Delta f$

inertia force, $F_{I,eq}(t)$, proportional to its acceleration (Ingólfsson et al., 2011):

$$F_{D,eq}(t) = -c_p\dot{u} = -c_p\dot{u}_0 \sin(\omega_L t + \varphi) \tag{4.26}$$
$$F_{I,eq}(t) = -\varrho_p m_p\ddot{u} = -\varrho_p m_p\ddot{u}_0 \sin(\omega_L t + \varphi + \pi/2) \tag{4.27}$$

where $\omega_L = 2\pi f_L$, $\dot{u}_0$ and $\ddot{u}_0$ are the velocity and acceleration amplitudes of the lateral vibration, m_p is the pedestrian mass and φ is an arbitrary phase. The minus appears as the equivalent inertia and damping forces are treated as external loads which appear positive on the right-hand-side of the equation of motion ($c_p > 0$ and $\varrho_p > 0$ imply negative structural damping and mass respectively). By imposing the condition that the equivalent pedestrian load inputs the same energy per unit time as the measured force, Ingólfsson et al. (2011) showed that the parameters c_p and ϱ_p can be determined through the cross spectral density as follows:

$$c_p = \frac{\mathrm{Re}\left[S_{F\dot{u}}(f_L)\right]\Delta f}{\sigma_{\dot{u}}^2} = \tilde{C}o_{F\dot{u}}(f_L)\frac{\sigma_{F_s}}{\sigma_{\dot{u}}} \tag{4.28}$$
$$m_p\varrho_p = \frac{\mathrm{Re}\left[S_{F\ddot{u}}(f_L)\right]\Delta f}{\sigma_{\ddot{u}}^2} = \tilde{C}o_{F\ddot{u}}(f_L)\frac{\sigma_{F_s}}{\sigma_{\ddot{u}}}. \tag{4.29}$$

From Eqs. (4.26) and (4.27) the amplitudes of the velocity-proportional and the acceleration-proportional loads are obtained as:

$$G_{D,eq} = c_p\dot{u}_0 = \sqrt{2}\tilde{C}o_{F\dot{u}}(f_L)\sigma_{F_s} \tag{4.30}$$
$$G_{I,eq} = m_p\varrho_p\ddot{u}_0 = \sqrt{2}\tilde{C}o_{F\ddot{u}}(f_L)\sigma_{F_s}. \tag{4.31}$$

4.6.3 Results from a single pedestrian

As already mentioned, a series of single pedestrian tests was carried out. In each test the person walked at several different combinations of lateral vibration frequencies and amplitudes. In Fig. 4.17 an example of the output from a single pedestrian is shown as function of the relationship between the lateral vibration frequency (f_L) and the pedestrian walking frequency (f_w) as measured in the static test. The normalised Co-spectrum (evaluated at the frequency of the lateral motion f_L) is an indirect measure of the phase angle between the force and the displacement. Negative values of $\tilde{C}o_{F\dot{u}}(f_L)$ imply negative c_p and vice versa. For this particular test person, there is a pattern in the development of $\tilde{C}o_{F\dot{u}}(f_L)$, generally being negative at low frequencies and around the average walking frequency, but positive in other regions. The RMS value of the self-excited part of the load is generally low at low frequencies, but increases both with the frequency and amplitude of the lateral motion.

The motion-induced parameters c_p and $\varrho_p m_p$ are obtained from Eq. (4.28) and Eq. (4.29) and depend on the Co-spectrum which determines the sign and relative magnitude of the self-excited force component σ_{F_s}. However, due to the normalisation with the vibration amplitude (velocity and acceleration respectively), there is the possibility of large variations in the values of c_p and $\varrho_p m_p$. The same pedestrian force will give larger values of c_p and $\varrho_p m_p$ at low amplitude vibration than at large ones.

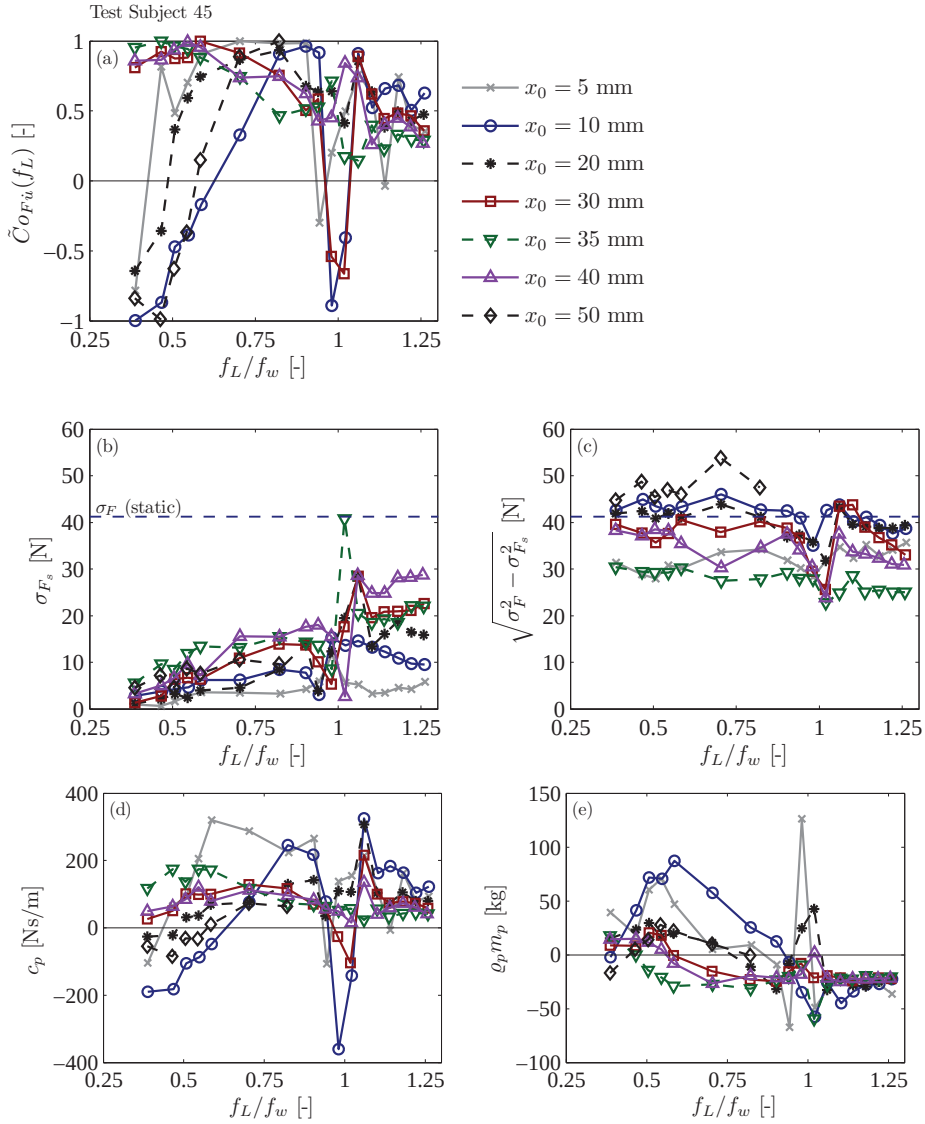

Figure 4.17: *Results from a single pedestrian test subject (Subject # 45) in the dynamic tests; (a) normalised Co-spectrum ordinate at the frequency of the lateral motion; (b) RMS value of the self-excited portion of the load; (c) RMS value of the residual of the pedestrian load; (d) the velocity and (e) the acceleration proportional load coefficients.*

There are different ways to represent the results from the dynamic tests. In Ingólfsson et al. (2011) emphasis is placed on the quantification of the velocity and acceleration proportional load coefficients. These coefficients are derived from the cross-spectrum between the lateral force and the treadmill displacement, which in turn can be represented physically as the dot product between the self-excited force and the treadmill displacement. In Fig. 4.18, the phase angle between the self-excited force and the lateral displacement is shown for the same test subject. For each dot in Fig. 4.18 (left), the distance to the centre represents the RMS magnitude of the self-excited force. In Fig. 4.18 (right) a polar histogram of the phase angle is shown, which clearly illustrates that phase angles in the range 20 to 50 deg are the most common. In the histogram, the sign convention for the resulting c_p and ϱ_p values is indicated.

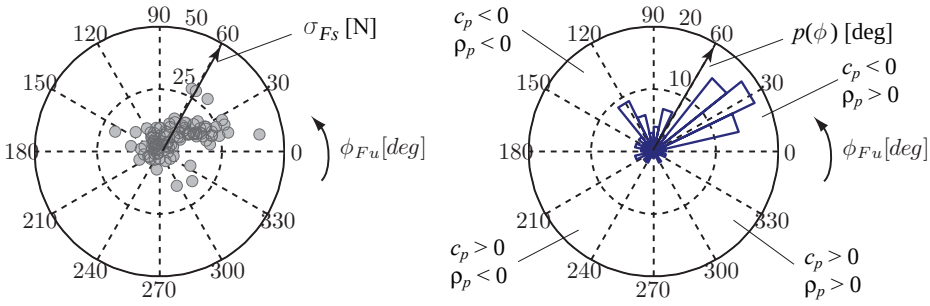

Figure 4.18: *Phase angle between the lateral displacement and the self-excited pedestrian force for a single test subject (Subject #45), shown (left) as a function of the load amplitude and (right) as a polar histogram.*

4.6.4 Results from all pedestrians

In the previous section, the results from one single pedestrian were presented, illustrating various parameters in the model and different ways to treat the data. In Ingólfsson et al. (2011), the load coefficients c_p and ϱ_p calculated from all pedestrians are presented in terms of mean values as well as their frequency and amplitude dependency. It is shown that the mean values, $\overline{c}_p$ and $\overline{\varrho}_p$, are both frequency and amplitude dependent. The amplitude dependency is seen as a near-linear drop in the numeric value of $\overline{c}_p$ and $\overline{\varrho}_p$ for increasing amplitudes (Ingólfsson et al., 2011), whereas the frequency dependency is slightly more complex. At low frequencies, $\overline{c}_p$ is generally negative but increases with increasing frequency. Each curve in Fig. 4.19 (a) is made up of a near linear segment and a near horizontal one, starting from negative values at low frequencies and becomes positive and near frequency independent at higher frequencies. The frequency axis is normalised with the mean walking frequency ($\overline{f}_w$) of the population, as measured in the static test. The slope of the curve increases with decreasing vibration amplitudes and so does the frequency at which the curve turns from positive to negative values. It is worth noting

that the mass proportional constant $\overline{\varrho}_p$ is generally positive at low frequencies, suggesting that pedestrians decrease the overall modal mass of the structure, but add to the mass at higher frequencies. This effect was explained by Pizzimenti and Ricciardelli (2005) as *added stiffness* and was observed at all frequencies (≥ 0.60 Hz) and amplitudes (15 – 45 mm). It is interesting to note, that negative mass is observed in the same frequency range, confirming the observation of Pizzimenti and Ricciardelli (2005).

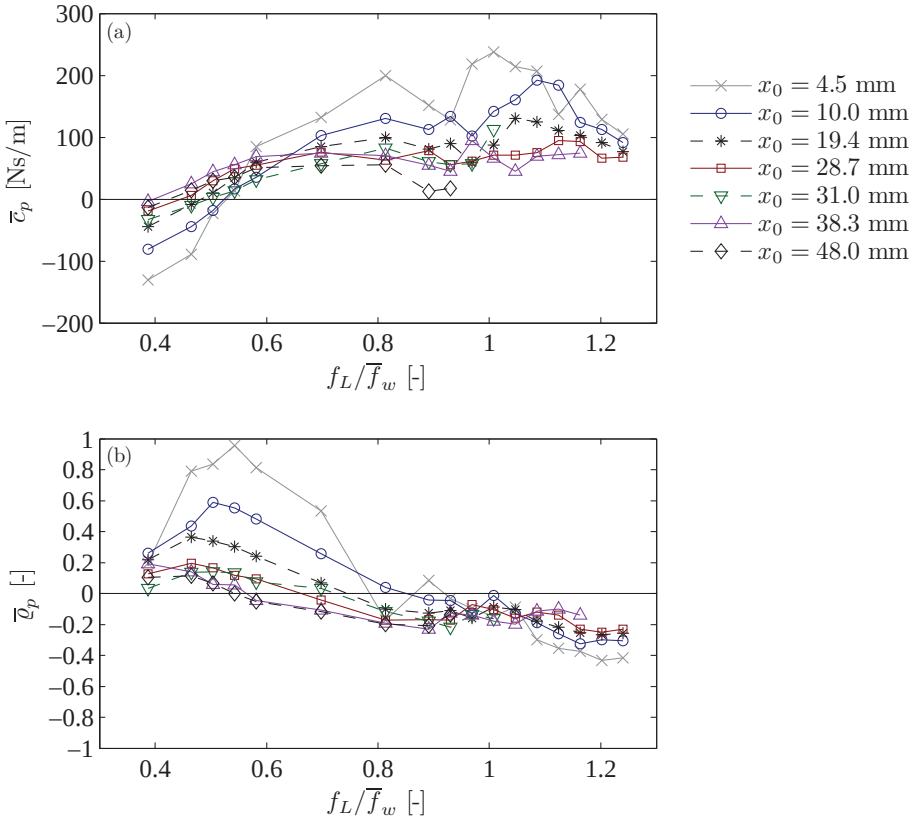

Figure 4.19: *Average value of the pedestrian load coefficient, $\overline{c}_p$ (a) and the mass proportional load coefficient $\overline{\varrho}_p$ (b) as function of the normalised frequency for different lateral displacement amplitudes.*

An alternative representation of the self-excited force is through its RMS value σ_{Fs} and the phase angle ϕ_{Fx}, see Fig. 4.20 and Fig. 4.21. In Fig. 4.20, two general phenomena can be observed; (i) for frequencies away from the natural walking frequency, there is a near linear increase in the RMS value with frequency and (ii) at frequencies close to the natural walking frequency, much larger values of σ_{Fs} are observed, matching (and even increasing) those measured in the static tests for the first load harmonic. The existence of a self-excited force at frequencies away from the natural walking frequency suggests that

there is an acceleration of the body centre of mass caused by the treadmill vibration and potentially the contra-acting balancing of the pedestrian's body. If the body engages in a rigid body movement with the treadmill, the amplitude of the self-excited equals the body mass times the lateral acceleration and phase angle equals 180 degrees. However, as shown in Fig. 4.20 and Fig. 4.21, both the magnitude of the self-excited force is lower than this and the phase angle varies with the frequency, suggesting a more complex interaction between the pedestrian and the laterally moving structure. For comparison, the mean value (solid line) and 95 percent fractile (dashed line) of the body-weight normalised RMS value of the fundamental load harmonic from the static tests are indicated in the figure.

The phase angle also shows a general frequency-dependent trend for frequencies away from the walking frequency. At low frequencies, the phase angle is generally in the upper half-plane suggesting an increased modal damping and at higher frequencies it moves to the lower half-plane suggesting negative damping. This observation is in line with the results from Fig. 4.19 (a). At frequencies close to the natural walking frequency, the phase angle is much more scattered and is probably governed by timing between the footstep and the vibration rather than a secondary movement of the centre of mass as a reaction to the lateral vibrations. Both the smooth development in the phase as function of the frequency and the linear increase in the self-excited force indicate that there is a common underlying mechanism which controls the balancing of the body centre of mass, which does not differ in nature between the individuals (although a considerable scatter in the data is observed).

4.7 Investigation into human-structure synchronisation

Human structure synchronisation can be addressed in different ways. During the experimental campaign, several observations regarding the potential for human-structure synchronisation were made. Ingólfsson et al. (2011), summarised some qualitative conclusions, which were based on visual observations, analysis of video recordings of the tests as well as testimonies from the participants:

1. Pedestrians react differently to the vibrating surface and only some of the pedestrians deliberately (or consciously) modify their walking to match a comfortable phase. This would only occur during lateral oscillations at frequencies close to the natural walking frequency.

2. The phase modification was not systematic as some pedestrians spread their legs further apart whilst other would cross their legs.

3. During large lateral vibrations, some people complained that they would prefer to walk at a slower forward velocity, in order to adjust their walking frequency to better match the lateral vibration frequency. Typically, this occurred when the lateral vibration frequency was slightly lower than the walking frequency and the phase difference between the pedestrian and the treadmill drifts slowly apart. This slow phase drift gives a feeling of alternating synchronised and non-synchronised walking.

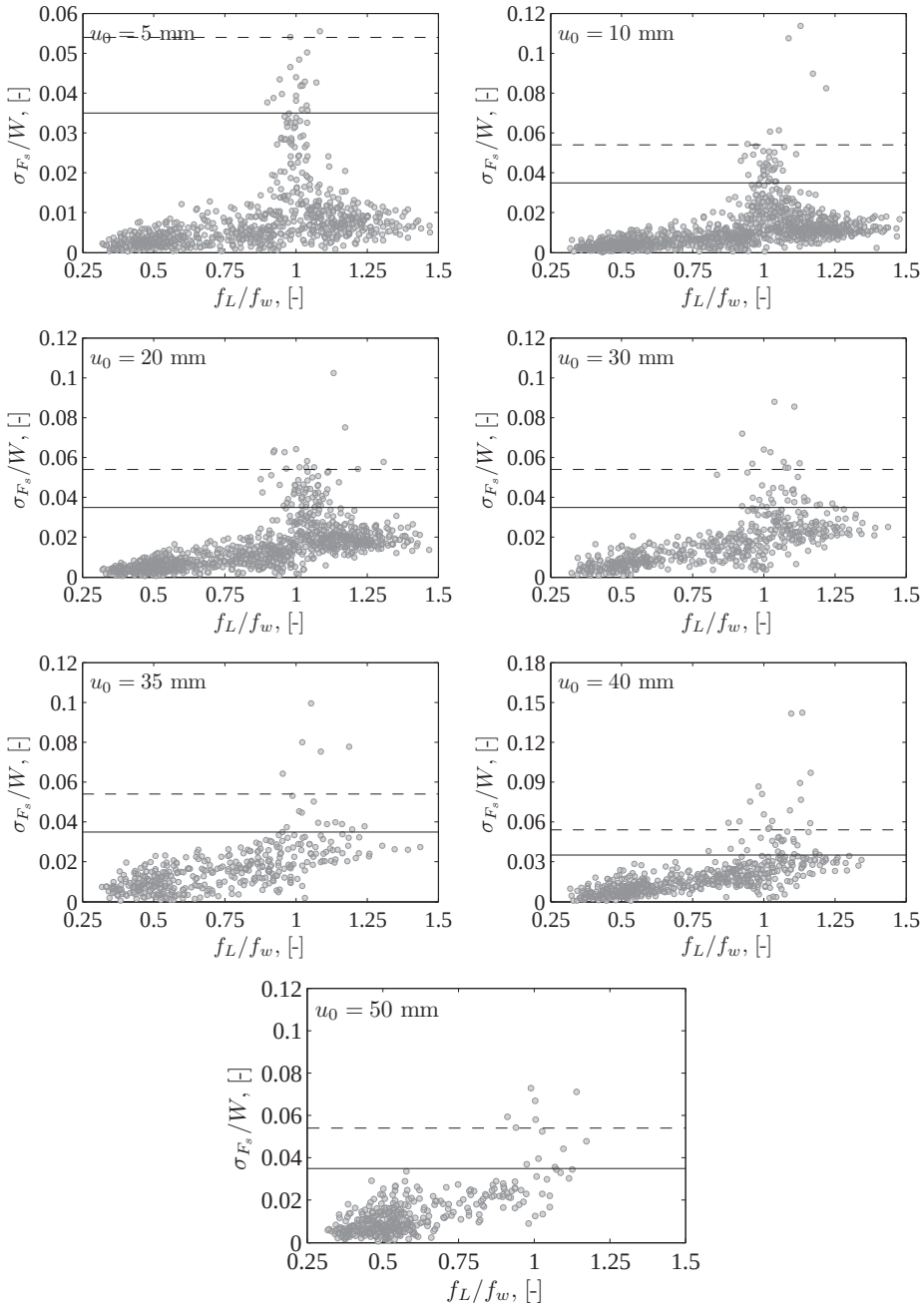

Figure 4.20: *Amplitude of the self-excited force as function of the normalised vibration frequency at different amplitudes.*

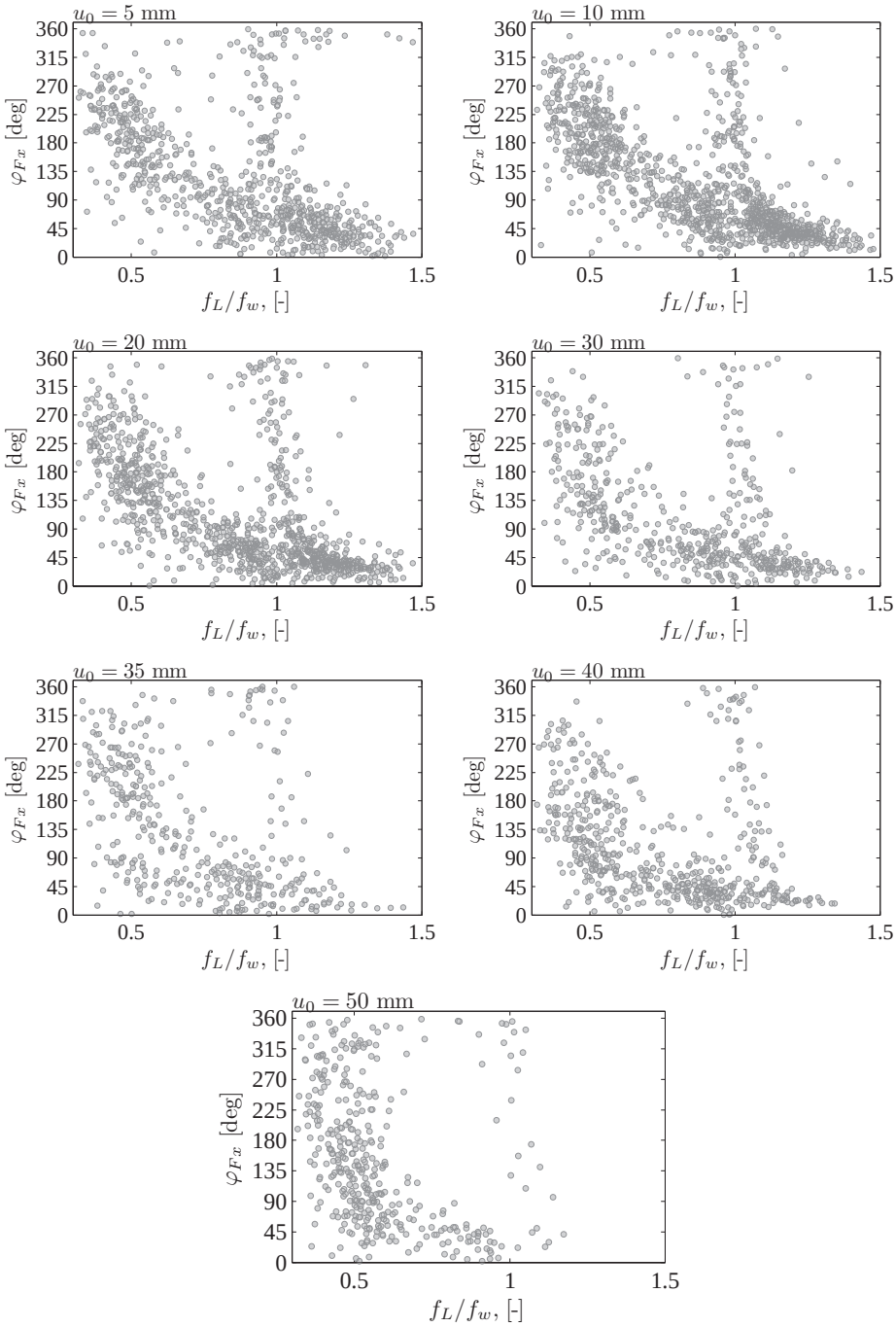

Figure 4.21: *Phase angle of the self-excited force as function of the normalised vibration frequency at different amplitudes.*

4. Human-structure phase synchronisation is to a large extent governed by randomness.

5. The importance of human-structure synchronisation in relation to the generation of self-excited forces in the form of negative damping is questionable.

Motivated by these observations, further analysis of the walking pattern of seven individuals was undertaken using the waist-mounted tri-axial human-body accelerometers described in Section 4.4. The instantaneous phase difference, $\phi_{\ddot{u},\ddot{y}}(t)$, between the lateral acceleration of the pedestrian ($\ddot{y}$) and that of the platform ($\ddot{u}$) was determined through the Hilbert transforms ($\tilde{\ddot{y}}(t)$ and $\tilde{\ddot{u}}(t)$) of the measured accelerations (Mormann et al., 2000):

$$\phi_{\ddot{u},\ddot{y}}(t) = \phi_{\ddot{u}}(t) - \phi_{\ddot{y}}(t) \tag{4.32}$$

$$\phi_{\ddot{y}}(t) = \arctan \frac{\tilde{\ddot{y}}(t)}{\ddot{y}(t)} \tag{4.33}$$

$$\phi_{\ddot{u}}(t) = \arctan \frac{\tilde{\ddot{u}}(t)}{\ddot{u}(t)} \tag{4.34}$$

If the phase difference is constant, the pedestrian walking frequency matches the frequency of the treadmill motion, whereas a drift in the instantaneous phase difference indicates a different frequency in the underlying signals suggesting a difference in the walking frequency and the lateral vibration frequency of the treadmill. If the drift is slow, the frequencies are closely spaced but for widely spaced frequencies the drift occurs more quick. By introducing the term *mean phase coherence*, the degree of synchronisation between the movement of the bridge and that of the pedestrian can be quantified. The mean phase coherence, $R_{u,y}$, defined as (Mormann et al., 2000):

$$R_{u,y} = \left| \frac{1}{N} \sum_{j=0}^{N-1} e^{i\phi_{u,y}(j\Delta t)} \right| \tag{4.35}$$

where Δt is the sampling interval, N is the number of samples and $i = \sqrt{-1}$. It is noted that the condition $R = 1$ is reached if and only if the time series are completely synchronised, i.e. for strict phase locking. The condition $R = 0$ is obtained for a uniform distribution of phases, Mormann et al. (2000). Thereby, the mean phase coherence be used to represent the instantaneous degree of synchronisation between the movement of the body and that of the treadmill.

The analysis is presented in Ingólfsson et al. (2010b) (Paper IV of this thesis), where it is shown that large mean phase coherence was only observed when the lateral vibration frequency was close to the natural walking frequency of the pedestrian. This suggests that that the walking frequency remained unchanged during the tests. However, as positive values of the velocity proportional coefficients were observed at most frequencies (i.e. negative damping), it can be concluded that pedestrian-structure phase synchronisation is not a necessary condition for the development of equivalent negative damping. This observation stresses the importance of investigating in more detail the mechanisms of human-structure interaction at all frequencies and moving beyond considering only synchronisation as the sole contributor to excessive lateral bridge vibrations.

4.8 Conclusions from experimental campaign

In the experimental campaign presented in this chapter, the lateral forces from 71 individuals have been measured, both on a fixed floor and during lateral vibration. Since various combinations of lateral vibration frequencies and amplitudes were tested, the results from the experiments create a significant and unique database of pedestrian-induced lateral forces.

The existence of self-excited pedestrian-induced loads has been verified and quantified through equivalent velocity and inertia proportional coefficients, c_p and ϱ_p. In particular, it was shown that both c_p and ϱ_p depend on the vibration frequency and amplitude (Ingólfsson et al., 2011). Alternatively, the self-excited forces may be represented through the amplitude and the phase angle between this force and the lateral displacement. This approach was introduced in Section 4.6 of this thesis.

The very large scatter in the data stresses the complexity which is related to human-induced dynamic loads and the reaction of pedestrians to a vibrating surface. Also, the limited number of steps recorded during the 30 s pedestrian tests and the fact that people may have been affected by the fictive circumstances associated with walking on a treadmill as opposed to a real footbridge, may contribute to an increased scatter. However, based on the results presented herewith, a probabilistic quantification seems necessary when modelling the aggregate effect of crowds of pedestrians on footbridges.

Another important conclusion which was drawn from the study is related to the importance of human-structure interaction (Ingólfsson et al., 2010b). It was found that negative pedestrian-damping can occur over a range of frequencies and that it does not depend on human-structure phase synchronisation. This is important, as it has become a commonly accepted view that synchronisation is necessary for the development of excessive vibrations. Therefore, load models which rely on phase synchronisation are insufficient particularly for natural frequencies away from the average walking frequency.

Chapter 5

Stochastic load model

In this chapter, a novel stochastic load model for the frequency and amplitude dependent pedestrian-induced lateral force is presented. The parameters in the load model are based directly on measured lateral forces as presented in Chapter 4. Thereby, the load model provides a statistically robust tool to predict the potential of bridges to excessive lateral vibrations. The material presented in this chapter is primarily based on the manuscript by Ingólfsson and Georgakis (2011) (Paper V of this thesis). In this chapter a brief introduction to the load model is given and some main conclusions are summarised.

5.1 Time-domain load model

The core of the load model is the experimental data presented in Chapter 4 and the philosophy adopted here is to use a simple, yet accurate representation of the loading. Having quantified the equivalent damping of the pedestrians and shown that pedestrians extract energy over a broad range of vibration frequencies, it is natural to quantify the motion-induced portion of the load through damping and acceleration proportional loads. The remaining load is centred around the walking frequency (being defined as half the step frequency) and its integer harmonics. As a simplified approximation, this force is taken as the equivalent static force, i.e. the force measured in the absence of lateral vibrations. The pedestrian-induced lateral force is therefore written as a simple sum of the equivalent static load $F_{st}(t)$, and the motion-induced loads, quantified as equivalent damping and inertia forces respectively:

$$F(t) = F_{st}(t) + \underbrace{c_p\left(f_0/f_w, u_0\right)\cdot\dot{u}}_{\text{equivalent damping}} + \underbrace{m_p\varrho_p\left(f_0/f_w, u_0\right)\cdot\ddot{u}}_{\text{equivalent inertia}} \tag{5.1}$$

The functions $c_p\left(f_0/f_w, u_0\right)$ and $\varrho_p\left(f_0/f_w, u_0\right)$ define the self-excited forces and depend on the vibration frequency, f_0, and amplitude u_0. The lateral displacement of the pavement is denoted u and f_w is the pedestrian walking frequency.

The model is simple, but due to large randomness in the experimental data, it is necessary to quantify each entity in the model using a probabilistic framework.

5.1.1 Equivalent static forces

The equivalent static force is represented as a narrow-band stochastic process through the non-dimensional Gaussian shaped PSD in Eq. (4.14), with parameters as given in Table 4.2. It is noted that the Gaussian function only contains information about the shape of the PSD, whereas the amplitude information is obtained from the standard deviation of the force around each harmonic, quantified through its log-normal shaped probability distribution (Ingólfsson and Georgakis, 2011).

With the equivalent static force presented through its PSD, a pseudo-random time history for the jth load harmonic can be generated for the purpose of numerical simulations through the following formulation (Shinozuka and Deodatis, 1991):

$$F(t) = \sum_{k=0}^{N-1} \sqrt{2S_F\left(f_k\right)\Delta f} \cdot \cos\left(2\pi f_k t + \psi_k\right) \tag{5.2}$$

$$S_F(f_k) = \sum_{j=i}^{N_{\text{Harm}}} S_{F,j}(f_k) \tag{5.3}$$

$$\Delta f = \frac{1}{N\Delta t} = \frac{2}{T_{tot}}. \tag{5.4}$$

$$S_{F,j}(f_k) = \frac{2A_j\tilde{\sigma}_{F,j}^2}{\sqrt{2\pi}B_j f_k} \exp\left\{-2\left[\frac{f_k/jf_w - 1}{B_j}\right]^2\right\}. \tag{5.5}$$

The parameters ψ_k are randomly generated phase angles, drawn from a uniform distribution, $f_k = k\Delta f$, $k = 0 \ldots N-1$ are the distinct frequency from which the power spectrum ordinates are calculated, N is the total number of data points, N_{Harm} is the total number of load harmonics (here $N_{\text{Harm}} = 5$) and T_{tot} is the total duration of the time series. The power spectral density function $S_{F,j}(f)$ depends on the shape (parameters A_j and B_j in Table 5.1) and the magnitude $\tilde{\sigma}_{F,j}^2 = W^2\text{DLF}_j^2/2$. Du to scatter in the measured DLFs, a log-normal distribution can be used to model their probability distributions (Ingólfsson et al., 2011). The probability density functions are written in terms of the parameters χ_j and ξ_j, which are listed in Table 5.1:

$$p(\text{DLF}_j) = \frac{1}{\text{DLF}_j\,\xi_j\sqrt{2\pi}} \exp\left[-\frac{\left[\ln \text{DLF}_j - \chi_j\right]^2}{2\xi_j^2}\right]. \tag{5.6}$$

By using this representation of the load, the spectral content of the time series approximates that of the measured load. However, the temporal shape of the force does not match the shape of a real footfall force since the model does not provide a relationship between the values of the phase angles and the spectral ordinates. Alternatively, a step-by-step model may be used for $F_j(t)$, where each footfall is modelled as a perfectly periodic truncated Fourier series. The fundamental frequency of this series (i.e. the walking frequency) can be varied to include an intra-subject variability in the model. This way, both the temporal shape of the time series as well as its spectral content can approximately be retained, (Živanović et al., 2007).

To the authors' knowledge, there exist no analytical time-domain models, which are capable of capturing both the temporal shape of the walking force and its frequency

Table 5.1: *Summary of parameters for the Gaussian shape spectrum for representation of the pedestrian-induced lateral force.*

	$j=1$	$j=2$	$j=3$	$j=4$	$j=5$
A_j	0.900	0.020	0.774	0.0258	0.612
B_j	0.043	0.031	0.026	0.064	0.026
χ_j	-3.061	-5.004	-3.674	-5.315	-4.492
ξ_j	0.3078	0.2876	0.2169	0.2655	0.2818

content. Therefore, emphasis is placed on an accurate representation of the frequency content, which is obtained by using the experimentally determined PSDs directly to reconstruct the load. Therefore, the simple representation in Eq. (5.2) is maintained in the load model.

5.1.2 Motion-induced forces

The motion induced forces are defined through the velocity and acceleration proportional coefficients c_p and ϱ_p respectively as obtained from the dynamic pedestrian tests, see Section 4.6. In the treatment of the raw data, Ingólfsson et al. (2011) noted that the motion induced forces showed a considerable frequency and amplitude dependency. The amplitude dependency shows a near linear decrease in the numerical value of the coefficients c_p and ϱ_p at all frequencies. The frequency dependency is slightly more complex.

In Ingólfsson and Georgakis (2011) the frequency dependency is dealt with by splitting the data into nine different frequency regions depending on the relationship between the vibration frequency of the structure and the walking frequency of the test subjects. The nine regions are defined through bands bracketed by normalised frequency pairs $\{0-0.45\}$, $\{0.45-0.55\}$, $\{0.55-0.65\}$, $\{0.65-0.75\}$, $\{0.85-0.95\}$, $\{0.95-1.05\}$, $\{1.05-1.15\}$, $\{1.15-\infty\}$. In each frequency bin, an expression of the type:

$$c_p\left(f_0/f_w, u_0\right) = \theta_0\left(f_0/f_w\right) + \theta_1\left(f_0/f_w\right)\cdot u_0 + X\cdot\theta_2\left(f_0/f_w\right)\cdot e^{\theta_3(f_0/f_w)u_0} \tag{5.7}$$

$$\varrho_p\left(f_0/f_w, u_0\right) = \underbrace{\phi_0\left(f_0/f_w\right) + \phi_1\left(f_0/f_w\right)\cdot u_0}_{\text{mean vale}} + \underbrace{X\cdot\phi_2\left(f_0/f_w\right)\cdot e^{\phi_3(f_0/f_w)u_0}}_{\text{random error}} \tag{5.8}$$

is used to model the load coefficients (Ingólfsson and Georgakis, 2011). The first two terms in Eqs. (5.7) and (5.8) represent the development of the amplitude dependent mean values, whereas the final term is the random deviation which decreases with increasing vibration amplitudes. In each bin, the parameters θ_0, θ_1, ϕ_0, ϕ_1 were determined by fitting a linear function through the mean values of the load coefficients. The parameters θ_2, θ_3, ϕ_2, ϕ_3 were similarly determined by fitting an exponential function through the standard deviation as function of the amplitude. A more detailed description of the procedure for determination of the load coefficient is presented by Ingólfsson and Georgakis (2011). The parameters of the load model, θ_j and ϕ_j, $j=0,1,2,3$ are summarised in Table 5.2. In all cases (except two), a significant linear correlation between the fitted variables was observed with mean value $\rho = 0.88$ (S.D 0.06 for c_p and 0.07 for ϱ_p).

In two of the frequency ranges, the correlation is low ($\rho < 0.5$) and therefore the amplitude independent mean values of the velocity and acceleration proportional coefficients have also been provided (in brackets). These values have been used in the load model presented herewith.

In addition, the linear functions are only used up to an amplitude of 50 mm, as this is the range for which there exists experimental data. For larger amplitudes, a constant value, corresponding to that at 50 mm amplitude is used.

Table 5.2: *Parameters of the regression models in Eq.* (5.7) *and Eq.* (5.8).

Frequency range f_0/f_w	θ_0 (Ns/m)	θ_1 (N s/m^2)	θ_2 (Ns/m)	θ_3 (m^{-1})	ϕ_0 (-)	ϕ_1 (m^{-1})	ϕ_2 (-)	ϕ_3 (m^{-1})
$0 - 0.45$	-100	2360	150.3	-21.6	0.460	-8.5	1.003	-28.1
$0.45 - 0.55$	-18	1237	143.2	-18.2	0.801	-18.1	0.662	-20.5
	(14.3)	(0)						
$0.55 - 0.65$	73	-667	150.7	-23.5	0.680	-18.2	0.773	-25.2
$0.65 - 0.75$	152	-2240	139.4	-24.7	0.270	-9.8	0.574	-24.8
$0.75 - 0.85$	162	-2643	151.4	-30.6	-0.057	-3.5	0.408	-24.3
$0.85 - 0.95$	101	-1055	342.0	-38.2	-0.158	-1.5	0.763	-44.6
					(-0.197)	(0)		
$0.95 - 1.05$	203	-5080	555.9	-42.3	0.074	-4.7	1.30	-36.9
$1.05 - 1.15$	214	-3284	195.3	-13.1	-0.324	5.6	0.832	-35.4
$1.15 - \infty$	129	-1858	166.5	-35.5	-0.362	4.3	0.309	-23.1

The parameter X is a first-order autoregressive process with an exponential autocorrelation function. In discrete time, $X_k \ , k = 1 \ldots N$ is generated from a recursive formula (Hogsberg and Krenk, 2007):

$$X_{k+1} = \exp\left[-\omega_c \Delta t\right] X_k + w_k \sqrt{1 - \exp\left[-2\omega_c \Delta t\right]}. \tag{5.9}$$

where N is the total number of time instances, Δt is the time separation and w_k are independent standard Gaussian variables. The parameter ω_c is selected such that the desired temporal correlation of the process is obtained. It is noted that the two extremes, $\omega_c = 0$ and $\omega_c \to \infty$, correspond to situations with full and no temporal correlation respectively. In the first case, the stochastic variable X remains constant for all k and when $\omega_c \to \infty$, X_k are independent standard gaussian variables. For intermediate values of ω_c an exponentially decreasing temporal correlation is introduced, which can be used to represent the intra-subject variability in the time series of the c_p and ϱ_p coefficients. Currently, the parameter ω_c, which controls the degree of intra-subject variability, can only be determined qualitatively.

5.2 Application of model

5.2.1 Basic load parameters: a single pedestrian and crowds

The pedestrian load model is based on the experimental campaign which was presented in Chapter 4. The nature of those experiments was such that lateral pedestrian-induced

forces were determined for walking on a sinusoidally moving surface with constant amplitude. Therefore, the load model deals with the response of pedestrians to a single-mode vibration of varying amplitudes. For linear structures with viscously damped modes, the modal equation of motion is written as:

$$\ddot{q}(t) + 2\zeta\omega_0\dot{q}(t) + \omega_0^2 q(t) = p(t) \tag{5.10}$$

$$u(x,t) = \sum_{j=1}^{\infty} \Phi(x) q(t) \tag{5.11}$$

where ζ, ω_0, $q(t)$ and $\Phi(x)$ are the modal damping, angular frequency, modal displacement and mode shape and $u(x,t)$ is the physical bridge displacement. If it is assumed that the mass normalised modal load, $p(t)$, of a single pedestrian crossing the footbridge with a constant forward velocity, v_p, can be written as (Ingólfsson and Georgakis, 2011):

$$p(t) = \frac{1}{M} \begin{cases} F_{st}(t)\Phi(v_p t) + (c_p\dot{q}(t) + m_p\varrho_p\ddot{q}(t))\left[\Phi(v_p t)\right]^2 & \text{for } t_0 \le t \le t_0 + t_d \\ 0 & \text{otherwise} \end{cases}. \tag{5.12}$$

The modal mass is denoted M, t_0 is the arrival time of the pedestrian onto the bridge and $t_d = L/v_p$ is the time it takes a pedestrian to cross the bridge of length L. In Fig. 5.1, a pseudo-random time series is shown for the normalised modal load at different vibration amplitudes according to Eq. (5.12). For the generation of the figure, the walking frequency was taken as $f_w = 0.85\,\text{Hz}$ and the body-weight normalised pedestrian load coefficients were taken as $c_p/W = 0.1\,\text{s/m}$ and $\varrho_p/g = 0.1\,\text{s}^2/\text{m}$, respectively and the mode shape is assumed to follow a unity-normalised half-sine. In the absence of modal displacement, the modal load is governed by the equivalent static load as generated through the use of Eq. (5.2), but as the vibration amplitude is increased (at frequency $f_0 = 1.0\,\text{Hz}$), the self-excited portion of the load becomes more pronounced.

The modal load from a crowd of N_p pedestrians can be written as a simple summation:

$$p(t) = \sum_{i=1}^{N_p} p_i(t). \tag{5.13}$$

The challenge lies in the determination of the pedestrian-specific modelling parameters and their probability distributions. In particular the distribution of pacing rates within the group is important (i.e. its mean value and standard deviation) as well as the relationship between the crowd density and the forward walking velocity. As reviewed in Chapter 2 and by Ingólfsson et al. (2010a), a large amount of information currently exists regarding the natural choice of gait parameters (i.e. the combination of walking speed, frequency and step length). This applies both for pedestrians in spatially unrestricted circumstances as well as in crowds for which human-human interaction occurs. Therefore, when modelling a particular crowd scenario, attention must be paid to a careful definition of the input parameters in the simulations and often several different conditions should be checked to ensure that the whole spectrum of possible cases has been covered.

In the benchmark simulations presented herewith, the pedestrians are modelled as independent autonomous oscillators, where the load from each pedestrian is generated

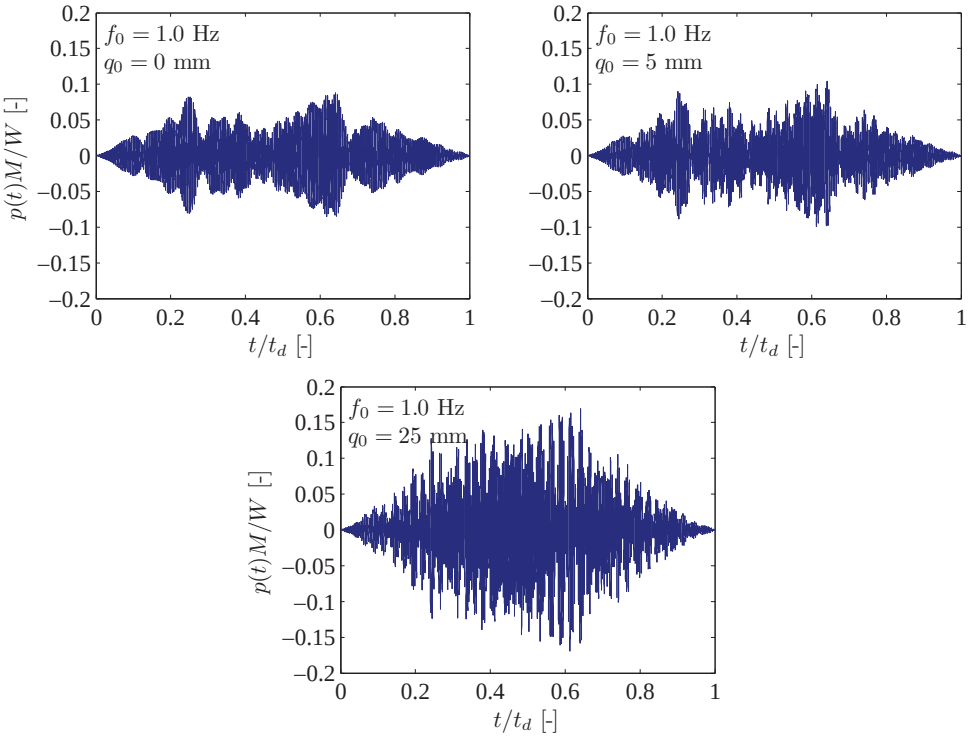

Figure 5.1: *Pseudo-random time series of the pedestrian-induced lateral force from a single pedestrian crossing a sinusoidal mode shape for different vibration amplitudes.*

according to Eq. (5.2) – Eq. (5.6) with parameters according to Table 5.1. Initially, the walking frequencies of all pedestrians are identical and they are assumed to arrive to the bridge with a constant inter-arrival time. The randomness in the simulations is introduced through variations in the pedestrian-induced loads (DLFs, c_p and ϱ_p values).

5.2.2 Numerical solution scheme

With amplitude dependent motion-induced pedestrian loads, the equation of motion becomes non-linear. Different solution techniques were tested, e.g. the fourth order Runga-Kutta method (through the in-built Matlab function ODE45), nonlinear Newmark integration (Krenk, 2009) and modified time-stepping method based on a linear interpolation of the excitation (Chopra, 2001). In a series of benchmark simulations, all methods proved sufficiently accurate and provided nearly identical results for the time-history of the response even at high acceleration levels, i.e. during periods with a large negative damping.

The final selection was to use a modified time-stepping method, in which the structural damping and modal mass was updated in each time step. When the time step and the change in damping between each time step is sufficiently small, accurate results are obtained for this method at a lower computational cost than the two other methods.

It should be noted that the mode shape of the structure is assumed to remain unchanged throughout the simulation and all response calculations are based on the mode shape as calculated for the empty bridge. Both the modal mass, damping and natural frequency are allowed to vary between time steps in the numerical solution.

5.2.3 Treatment of output

Due to the large randomness in the data, both the vibration amplitudes and the potential for excessive vibrations through the development of negative damping random. Therefore, a suitable selection of the duration of the numerical simulation and a proper statistical treatment of the data is important, such that each event (or simulation) is related to a certain probability of exceedance. The concept of using extreme value analysis for the treatment of simulated vertical response of footbridges was introduced by Ingólfsson et al. (2007) and later used by Ingólfsson et al. (2008b) and Georgakis and Ingólfsson (2008) to create a Response Spectrum design methodology. The Response Spectrum method is based on a series of numerical Monte Carlo simulations in which the expected peak response of a footbridge subject to a random crowd of a known intensity is provided as a function of its return period. This methodology can be developed and implemented in the treatment of the output from lateral load simulations to predict the critical number of pedestrians of a footbridge for various return periods.

5.3 Validation of pedestrian load model

Several numerical response simulations have been carried out to validate the pedestrian loading model and demonstrate its applicability for the prediction of pedestrian-induced lateral vibrations. In Ingólfsson and Georgakis (2011), a more detailed analysis is presented, but herewith only the main results are presented followed by a short discussion.

Table 5.3: *Modal properties of the Millennium Bridge (without any external damping) (Table reproduced with permission from Ove Arup and Partners)*

Description	Abbreviation	Frequency (Hz)	Damping (%)	Modal mass (tonne)
First lateral mode of central span	CL1	0.48 - 0.49	0.75 - 0.77	128 - 130
First lateral mode of Southern span	SL1	0.80 - 0.81	0.6 - 0.7	172
First lateral mode of northern span	NL1	1.04	0.32	113

5.3.1 Response simulations

Several preliminary response simulations were carried out based on the following simplified assumptions:

- The person's body weight is a normally distributed random variable ($\mu_W = 727\,\mathrm{N}$, $\sigma_W = 145\,\mathrm{N}$).
- All pedestrians walk at a common walking frequency ($\mu_{f_w} = 0.85\,\mathrm{Hz}$) and forward velocity ($\mu_{v_w} = 1.14\,\mathrm{m/s}$).
- The number of pedestrians on the bridge is gradually increased by 25 persons every 5 minute, until the total number of pedestrians has reached 300.
- The pedestrian inter-arrival time is constant and taken such that the total number of pedestrians on the bridge remains constant during each five-minute interval.
- Three different vibration modes are considered, CL1, SL1 and NL1 of the London Millennium Bridge (see Table 5.3).

In Fig. 5.2, the acceleration response of the first three modes (CL1, SL1 and NL1) of the Millennium Bridge are shown for three distinct crowd simulations. It is noted, that for simplicity, all three modes are assumed to follow a half-sine. The time scale in Fig. 5.2 is normalised with the passage time of a single pedestrian. It is noted that in all three cases instability is observed for less than 300 persons on the bridge (Dallard et al., 2001a). In particular it is worth noting that nominally same crowd can cause large vibrations in all three modes, despite their different natural frequencies. The results in Fig. 5.2 thereby verify the potential of the model (qualitatively) to predict excessive lateral footbridge vibrations.

5.3.2 Definition of instability

An important aspect relating to the problem of excessive pedestrian-induced vibrations is the definition of instability (or excessive vibrations). A more elaborate discussion is given by Ingólfsson and Georgakis (2011), so only a brief overview is presented here. The

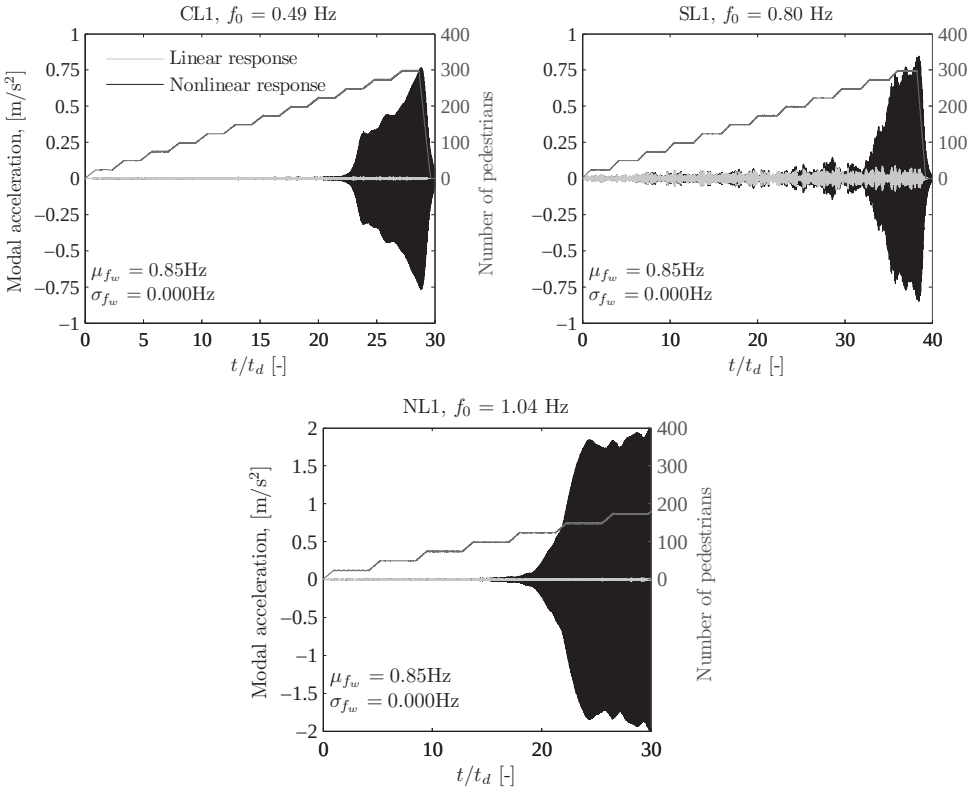

Figure 5.2: *Simulated modal response of (left) CL1, (right) SL1 and (bottom) NL1 for a gradually increasing crowd, walking at a common frequency ($\mu_{f_w} = 0.85\,\mathrm{Hz}$).*

overall modal damping of the structure is defined as the inherent structural damping plus the contribution of each pedestrian:

$$\zeta_{tot}(t) = \frac{1}{2\omega M}\left(C - \sum_{i=1}^{N_p(t)} c_{pi}(t)\left[\Phi(v_{pi}t)\right]^2\right). \tag{5.14}$$

In Fig. 5.3, the development of the overall modal damping is shown for the same simulations as presented in Fig. 5.2. Here, the term "linear response", means the response of the structure when the self-excited loads are neglected. In Eq. (5.14), $N_p(t)$ indicates the number of pedestrians present on the bridge at any given time instance, t. It is noted that the point of initial zero-crossing of the damping ($\zeta_{tot}(t) < 0$) occurs earlier than the point at which large vibration amplitudes develop. Therefore, care should be taken on how instability is defined.

According to Arup's stability criterion, instability occurs when the pedestrian damping cancels the inherent structural damping. When treating the simulated response, this may be translated to the number of pedestrians present on the bridge during the time of initial zero-crossing of the overall damping. On the other hand, people will not notice instability unless it develops into excessive vibrations and therefore an acceleration criterion may be used to quantify the critical number of pedestrians. According to Sétra (2006), a suitable comfort level for lateral footbridge vibrations is $0.1 - 0.2\,\mathrm{m/s^2}$.

By comparing the acceleration response from Fig. 5.2 to the development of the structural damping in Fig. 5.3, the difference in the two definitions and their impact on the *critical number of pedestrians* are clearly illustrated.

A single realisation can only offer a qualitative view into the nature of the bridge response and the development of the overall modal mass and damping and therefore simulations of the response of CL1 have been repeated 200 times. In Fig. 5.4 (top), the change in the modal mass is shown through the modification in the natural frequency of the system and in Fig. 5.4 (bottom) the change in the overall modal damping ratio is depicted. The figure shows the individual realisations, the mean value as well as the 5 and 95 percent quantiles. In addition, the realisation which corresponds to the response in Fig. 5.3 is also emphasised in Fig. 5.4.

It is noted that the effect of the pedestrians on the natural frequency is quite minimal, but it is worth noting that they act to decrease the apparent structural mass and thereby raise the modal frequency. In Fig. 5.4 (bottom) it is noted that the modal damping generally decreases with the number of people on the bridge but there are considerable fluctuations due to the randomness in the pedestrian load coefficients.

5.3.3 Sensitivity analysis

In Ingólfsson and Georgakis (2011), it was also shown that the response characteristics of different modes were affected by the selected pacing rate distribution (mean and standard deviation), the level of ambient (background) noise and the duration of the response simulations. All these factors influenced the number of pedestrians on the bridge when instability was triggered (either defined as a damping or an acceleration criterion).

To demonstrate both the dependency on the walking frequency distribution as well as the large difference between the two stability criteria, sixty response simulations were

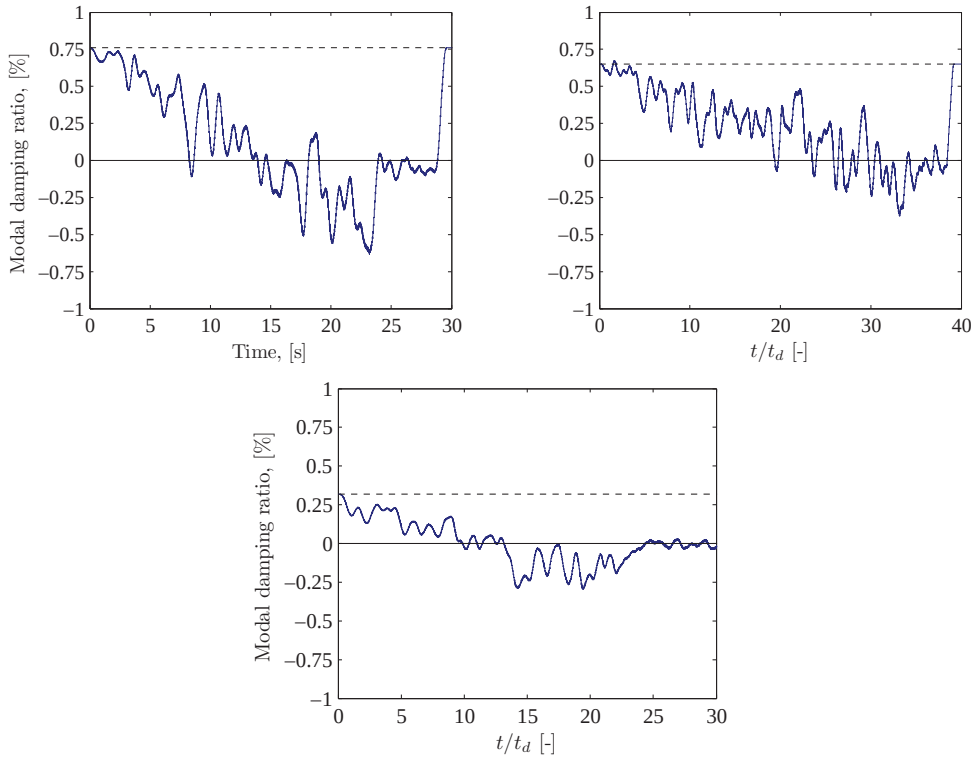

Figure 5.3: *Modal damping for (left) CL1, (right) SL1 and (bottom) NL1 subject to a gradually increasing crowd with a common step frequency ($\mu_{f_w} = 0.85\,\mathrm{Hz}$).*

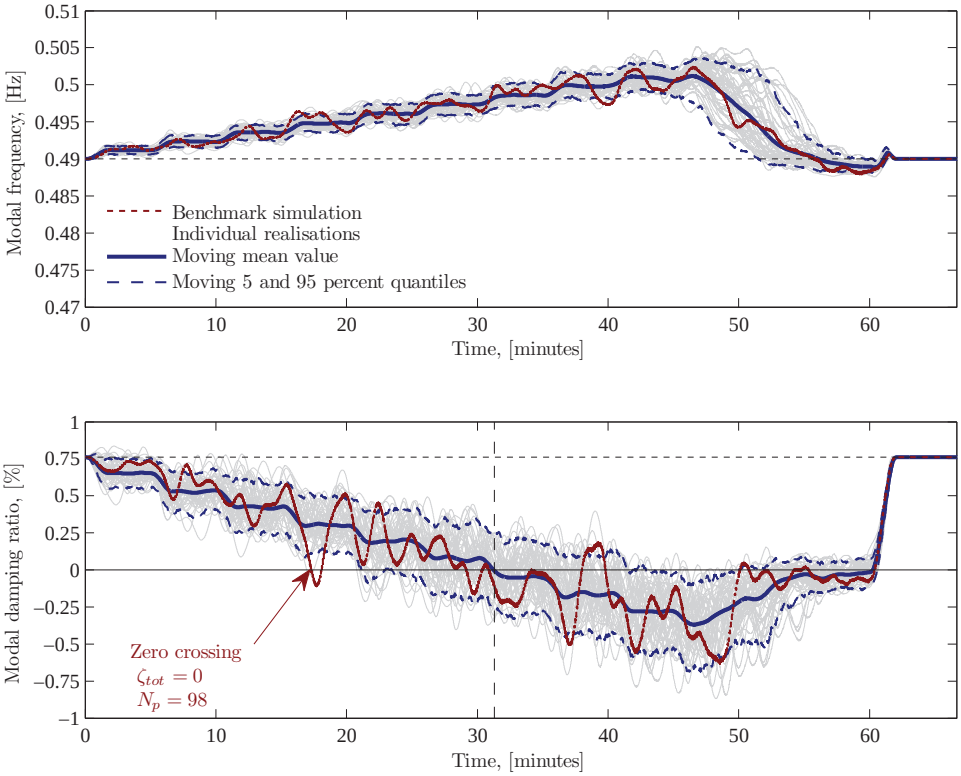

Figure 5.4: *Changes in the modal frequency and damping of CL1 subject to a gradually increasing crowd with a common step frequency ($\mu_{f_w} = 0.85\,\mathrm{Hz}$).*

carried out for each mode in which six different average walking frequencies (with S.D. 0.075 Hz) were introduced in the simulations. In each of the three modes (CL1, SL1 and NL1), the average value of the critical number of pedestrians (defined in two different ways) is shown as function of the pacing rate distribution. For NL1, the damping value $\zeta = 0.7\,\%$ was used in the simulations, which renders a more realistic estimate of the bridge damping. The value of 0.32 % (from Table 5.3) is based on poor quality data from the experimental modal ID and does not necessarily render the real damping of the mode (Ove Arup and Partners International Ltd., 2002).

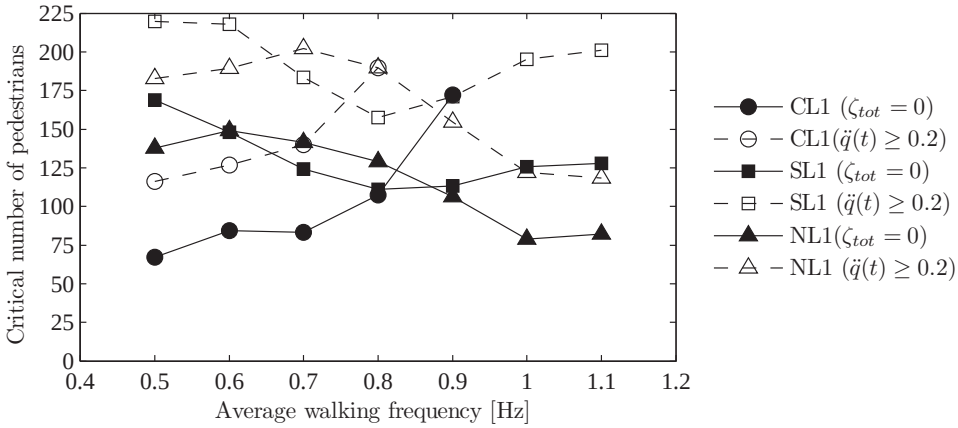

Figure 5.5: *Mean value of the critical number of pedestrians for CL1, NL1 and SL1 as function of the average walking frequency.*

In Fig. 5.5 the results are shown, which illustrates both the frequency dependency of the self-excited forces, but also the large difference in the predicted value of the critical number of pedestrians, depending on the definition of instability. Also, it should be noted that there is a random variation in the critical number of pedestrians, caused by the randomness associated with the relatively small number of simulations at each frequency. Interestingly, instability was not be triggered in the simulations when the mean walking frequency was selected higher than 0.9 Hz. This is explained by the low ratio between the vibration frequency and the pedestrian walking frequency.

It should be noted, that in its current form, the pedestrian loads depend only on the relationship between the lateral vibration frequency and the walking frequency. Thereby, any effects of changes in the walking speed are only taken indirectly into account.

5.4 Concluding remarks

The load model presented in this chapter can efficiently be used to predict the potential for excessive lateral vibrations of footbridges. Care has to be taken in the definition of the the pacing rate distribution, simulation time and the level of background noise. Variations in these parameters, cause a variation in the predicted number of pedestrians. Furthermore, it was shown by Ingólfsson and Georgakis (2011), that the definition of instability (or

excessive vibrations) affects the critical number of pedestrians. As a simplified approach, the development of the mean (or a certain quantile) negative damping (as shown in Fig. 5.4) can be used to provide an initial estimate on the potential for excessive vibrations. This requires sufficient time to obtain steady negative damping and sufficient time to build up excessive vibrations. Alternatively, a series of simulations can be undertaken for particular crowd scenario where the parameters are varied and the output is treated probabilistically.

Based on the benchmark tests, the predicted critical number of pedestrians needed to cause large lateral vibrations of the first three modes of the Millennium Bridge, are within the range as reported from the opening day. This, despite the difference in the natural frequencies of the three modes.

However, it should be noted that the load model is only applicable for lateral vibrations of a single mode. The effect of multi-modal response on the pedestrian-induced load is therefore unknown. This issue is addressed further by Ingólfsson and Georgakis (2011).

Chapter 6

Simplified stability criterion for footbridges

The capability of the stochastic load model to simulate pedestrian-induced lateral vibrations and to predict the development of instability was demonstrated in Chapter 5. However, numerical response simulations may be complicated to implement and can be extremely time demanding in execution. Therefore, engineers will benefit from a simplified stability criterion which can be used to estimate the potential of a certain bridge to instability in an easy an straight-forward way, similarly to the already known Arup formula. In this section, a simplified stability criterion is proposed, based on the experimental data presented in Chapter 5.

6.1 Condition for instability

During the temporary closure of the Millennium Bridge, full scale crowd experiments were conducted with the main conclusion that pedestrian-induced loading can be modelled as negative linear dampers, with the constant velocity proportional load coefficient $c_p = 300\,\mathrm{Ns/m}$, (Dallard et al., 2001a). This led to the classic stability criterion in Eq. (2.2) written in terms of the limiting number of pedestrians needed to initiate excessive lateral vibrations. As summarised in Table 2.1, several other simplified stability criteria have been derived. The prediction of the critical number of pedestrians using those criteria, differs considerably, see Fig. 2.9.

When comparing the susceptibility of different bridges to instability, it may be convenient to use the non-dimensional pedestrian Scruton number (Newland, 2004) defined as:

$$S_{cp} = \frac{2\zeta M}{M_p}. \tag{6.1}$$

Here ζ and M are the modal damping and mass respectively and M_p is defined as the modal mass of the pedestrians written in terms of the spatial distribution of the pedestrian mass $m_p(x)$, i.e.

$$M_p = \int_0^L m_p(x) \left[\Phi(x)\right]^2 \mathrm{d}x. \tag{6.2}$$

The Scruton number is a convenient non-dimensionalisation which allows a comparison between bridges (and modes) with different damping and modal masses. Arup's stability criterion can be re-written as a criterion for the Scruton number in the following way:

$$S_{cp} > \frac{c_p}{2\pi f_0 m_0}. \tag{6.3}$$

where m_0 is the mass of single pedestrian (here taken as 75 kg). This criterion assumes that the pedestrians are uniformly distributed along the mode shape. When $c_p = 300\,\mathrm{Ns/m}$, as proposed by Dallard et al. (2001a), the criterion is as depicted in Fig. 6.1. Also in Fig. 6.1 is the stability criterion which was developed by Newland (2004) for two different degrees of assumed synchronisation. As reviewed by Ingólfsson et al. (2010a), several bridges have experienced large lateral vibrations. In order to calculate the pedestrian Scruton number during these vibrations, information is needed about the modal mass, damping and pedestrian distribution. In few of these cases, all this information exists. These cases count the Coimbre footbridge in Portugal, the Clifton Suspension Bridge in the UK (two modes), Changi Mezzanine Bridge in Singapore and the Lardal footbridge in Norway (Ingólfsson et al., 2010a). In Fig. 6.1, the filled markers represent the pedestrian Scruton number for the above mentioned cases. The open markers represent less reliable estimates from the Solferino Bridge in Paris and the Tri-Country Footbridge in Germany. All the data points have been estimated from published cases of excessive vibrations, based on the literature review by (Ingólfsson et al., 2010a) (Paper I of this thesis). As shown in Fig. 6.1, the number of data points is not sufficient for a proper comparison with the theoretical curves. However, it seems that Arup's criterion is conservative, as none of the observations are outside of the region defined as stable.

6.2 Experimental data

6.2.1 Simplified stability criterion

Based on the measured pedestrian load coefficient, the most simple stability criterion can be obtained by neglecting the amplitude dependency and considering only the constant value θ_0 from Table 5.2, corresponding to the initial pedestrian damping coefficient. An average stability criterion can be obtained by assuming either constant values of c_p in each frequency bin, or through some interpolation. The simplest interpolation is a piecewise linear function which passes through each data point. Alternatively, a second order polynomial fit has been used. The polynomial which provides the best fit is mathematically expressed as:

$$\bar{c}_{p0}(r) = -794r^2 + 1558r - 580; \mathrm{Ns/m} \qquad 0.4 \leq r \leq 1.2 \tag{6.4}$$

$$r = f_0/f_w. \tag{6.5}$$

If this expression is substituted into Eq. (6.3) and all pedestrians are assumed to walk at a common frequency $\bar{f}_w$, a criterion for the pedestrian Scruton can be obtained:

$$S_{cp}(f_0) > \frac{-794\left(f_0/\bar{f}_w\right)^2 + 1558\left(f_0/\bar{f}_w\right) - 580}{2\pi f_0 m_0}. \tag{6.6}$$

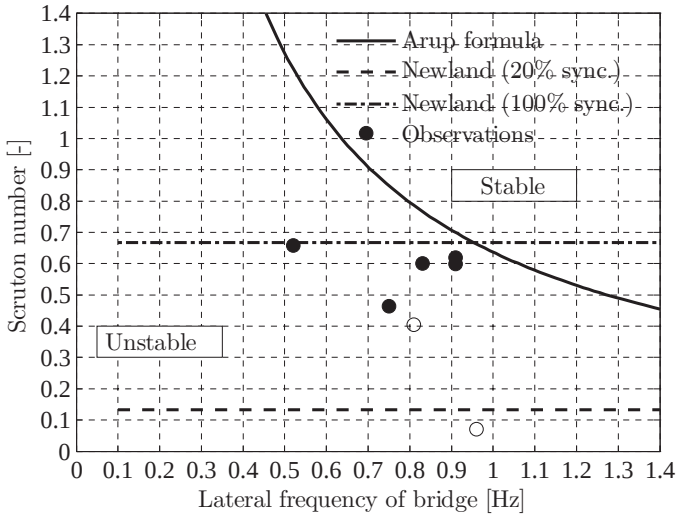

Figure 6.1: *Existing criteria for the minimum Scruton number for stability shown together with experimental observations as reported during events with excessive vibrations on actual footbridges.*

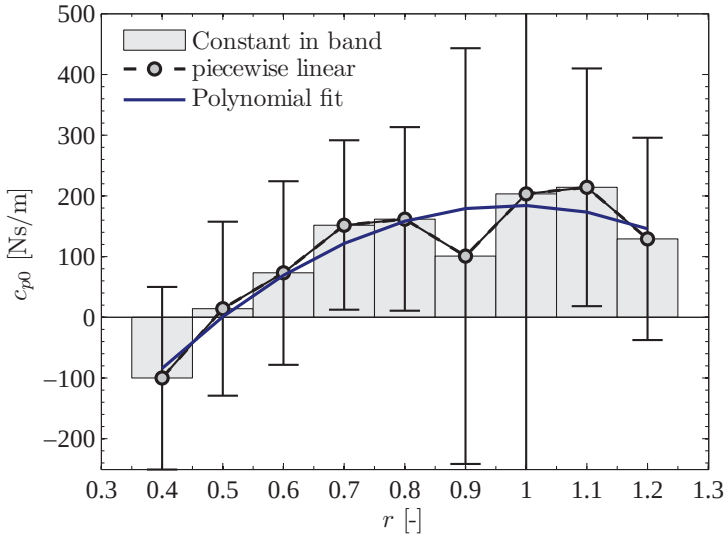

Figure 6.2: *Average value and standard deviation of the velocity proportional pedestrian load coefficient as function of the non-dimensional frequency.*

where unit of m_0 is [kg] (here $m_0 = 75\,\text{kg}$ is used) and the unit of f_0 is [Hz]. If further, a distribution of walking frequencies is assumed, the criteria for the necessary Scruton number is rewritten as:

$$S_{cp}(f_0) > \int_{-\infty}^{\infty} \frac{-794\,(f_0/f)^2 + 1558\,(f_0/f) - 580}{2\pi f_0 m_0} p_{f_w}(f)\,\mathrm{d}f \tag{6.7}$$

$$p_{f_w}(f) = \frac{1}{\sqrt{2\pi}\sigma_{f_w}} \exp\left[\frac{-(f-\mu_{f_w})^2}{2\sigma_{f_w}^2}\right] \tag{6.8}$$

where μ_{f_w} is the average walking frequency and σ_{f_w} its standard deviation. For most practical values of σ_{f_w}, the difference between Eq. (6.7) and Eq. (6.3) is small and for simplicity, that in Eq. (6.3) is used in the following.

Although the distribution of the walking frequencies is less important, the mean walking frequency changes the stability criterion considerably. This effect is illustrated in Fig. 6.3, which shows the critical Scruton number as a function of the lateral bridge frequency for various different selections of μ_{f_w}.

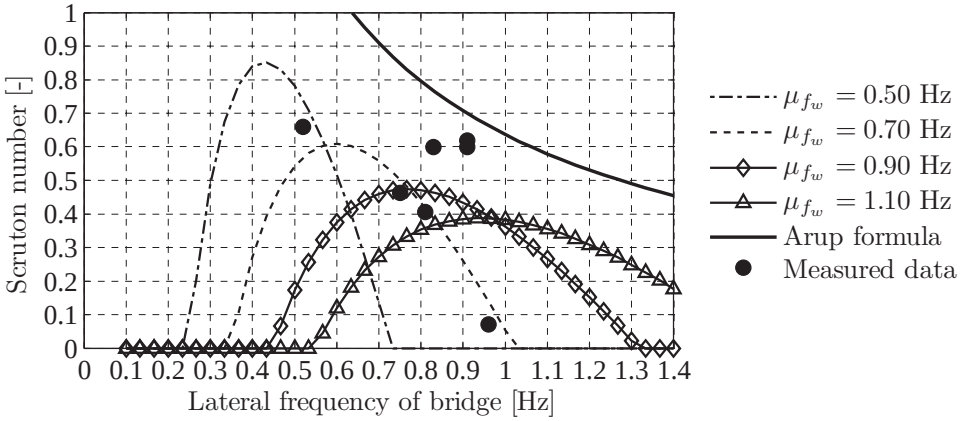

Figure 6.3: *Criteria for the minimum Scruton number based on the average value of the measured pedestrian load coefficients, shown for various values of the average walking frequency.*

6.2.2 Probability-based stability criterion

There is considerable amount of randomness present in the experimental data. This is clearly seen from Fig. 6.2 in which the average pedestrian load coefficient is shown together with single standard deviation error bars. It is further seen that the standard deviation is almost constant ($\sigma_{c_p} \cong 150\,\text{Ns/m}$) in the first five frequency bins and the last one, whereas it increases considerably around $0.9 \leq r \leq 1.0$ to the values in the range $340\,\text{Ns/m} - 550\,\text{Ns/m}$.

A conservative model for the frequency dependent standard deviation (for a single person) can be written as:

$$\sigma_{c_p}(r) = \sigma_{c_p,0}\left(1 + \Delta\sigma_{c_p}\Psi(r)\right) \tag{6.9}$$

where $\Delta\sigma_{c_p,0} = 150\,\mathrm{Ns/m}$, $\sigma_{c_p} = 375\,\mathrm{Ns/m}$ and $\Psi(r)$ is a piecewise linear function taken from Fig. 6.4.

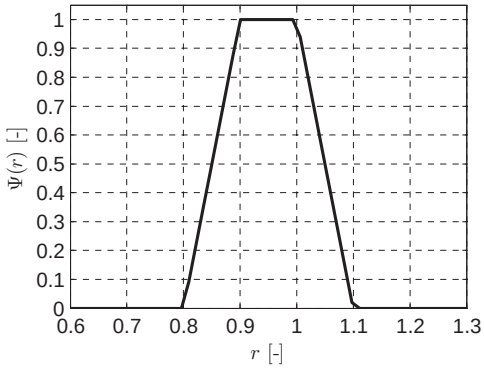

Figure 6.4: *Function for the determination of the frequency dependent standard deviation $\sigma_{c_p}(r)$ of the velocity proportional pedestrian load coefficient.*

If the distribution of the load coefficients around the mean value are assumed to follow a Gaussian distribution, the 95% fractile for a group of N_p pedestrians can be obtained as:

$$c_{p,95\%} = c_{p0} + 1.65\sigma_{c_p,\mathrm{Group}}. \tag{6.10}$$

where $\sigma_{c_p,\mathrm{Group}}$ is the total standard deviation of the overall pedestrian damping for the total group. If it is further assumed, that the values of c_p for each pedestrian are independent identically distributed random variables (IID), a simplified expression for the standard deviation for a group of N_p pedestrians can be obtained as:

$$\sigma_{c_p,\mathrm{Group}} = \sqrt{N_p}\sigma_{c_p} \tag{6.11}$$

It is noted, that in the calculation of the aggregate effect of the group, it has been assumed that all pedestrians contribute equally to the overall damping. Thereby, the effect of the mode shape has been neglected (i.e. a uniform mode has been assumed). In the case on non-uniform mode, the overall standard deviation takes a different form.

Based on the model in Eq. (6.11), a new stability criterion can be created, corresponding to a Scruton number with 95% probability of bridge stability if not exceeded, see Fig. 6.5. The criterion is generated for $N_p = 250$ assuming an average pedestrian walking frequency of 1.0 Hz.

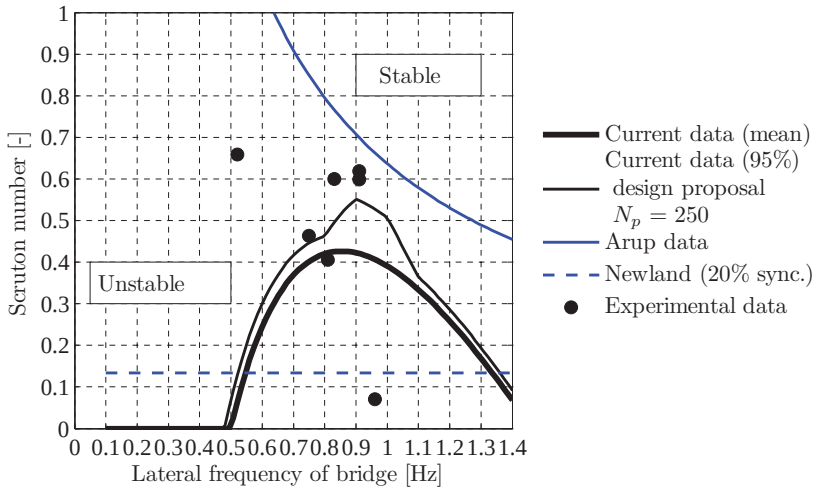

Figure 6.5: *Example of the criteria for the minimum Scruton number subject to a pedestrian crowd of 250 persons with mean walking frequency* 1.0 Hz.

Chapter 7

Conclusions

In the past decade, a large amount of research has been carried out to understand the phenomenon of human-structure interaction in the development of excessive crowd-induced lateral vibrations on long-span footbridges.

As reviewed in Chapter 2, research in the field can broadly be split into three categories (i) full scale measurements of crowd-induced vibrations on actual footbridges, (ii) experimental laboratory investigations with single pedestrians and (iii) mathematical modelling. Research in each of the three categories has been beneficial in increasing the understanding of the underlying mechanisms that govern human-structure interaction. This research has also increased the capability of predicting the onset to excessive vibrations. However, there has been a gap between the mathematical modelling on one hand and empirical observations on the other. In particular the commonly accepted view that synchronisation is a necessary trigger for the development of excessive lateral vibrations, is often used as a basis in load models, despite a lack of clear experimental data to support such an hypothesis. Published experimental data from several laterally vibrating footbridges suggest that synchronisation of the pedestrian walking to the lateral movement is not a necessary trigger for the development of large oscillations. In fact, to the author's knowledge, there exist no studies that explicitly show that pedestrian synchronise (or lock-in) their step frequency to the lateral movement of a footbridge. Furthermore, only a limited amount of data exists on lateral forces induced by pedestrians when walking on a laterally flexible surface.

Therefore, the main objectives of this thesis was to (i) determine whether synchronisation of pedestrians to the structural movement is a necessary trigger for development of large lateral bridge vibrations and (ii) provide statistically reliable experimental data for the lateral pedestrian-induced forces for a variety of different lateral vibration frequencies and amplitudes.

In Chapter 3 the results from a series of preliminary laboratory studies are presented. A 17 m long suspended concrete platform was used in various pedestrian tests, in which the measured acceleration response was used in an attempt to back-calculate the load from the pedestrians. It was concluded that the laboratory platform could only be used to study human-structure interaction from a qualitative point of view, since it was not possible to measure the pedestrian-induced forces directly. The initial suspicion that synchronisation is not as important as commonly believed were confirmed during the platform tests, but

not further quantified.

The main body of work in this thesis is presented in Chapters 4 and 5, which deal with the experimental campaign and the development and verification of a novel stochastic load model.

The data gathered in the experimental campaign is based on measured forces from 71 pedestrians, walking on both a laterally fixed and oscillating surface at various amplitudes and frequencies. Particular attention was paid on quantification of the self-excited component of the pedestrian load through damping and mass proportional coefficients, respectively. Analysis of the self-excited pedestrian load reveals that pedestrians (on average) input energy into the structure over a large frequency range. It is further shown that the component in phase with the structural velocity can be modelled as a velocity proportional force. The component in phase with the acceleration is also found to depend on the frequency of the structure. It is observed that for low frequencies, pedestrians subtract from the overall modal mass and add to the mass at higher frequency motion, with an amplitude dependent transition. In addition to the frequency dependency, it is also shown that the motion-induced forces are amplitude dependent. This amplitude dependency is such that the negative pedestrian damping decreases with increasing amplitudes. This means that the vibrations of any given footbridge may become self-limiting.

The very large scatter in the data, suggests that a probabilistic approach is necessary for an accurate estimation of the susceptibility of a footbridge to excessive vibrations. In particular, the critical number of pedestrian needed to trigger SLE may vary considerably depending on the particular crowd occupying the bridge.

In Chapter 5 a stochastic load model is presented for modelling of the frequency and amplitude dependent pedestrian-induced lateral forces. The model is shown to successfully predict excessive lateral vibrations in a number of benchmark tests. Furthermore, the self-excited pedestrian force has been quantified through an extensive experimental campaign and is represented in a stochastic framework. It is shown that several parameters influence the response characteristics, in particular the distribution of walking frequencies in the group, duration of the load event, definition of instability and the level of background noise.

Finally, a simplified probabilistic stability criterion is presented in Chapter 6 which can be used for design purposes for providing a first estimate on the susceptibility of a bridge to crowd induced lateral vibrations.

7.1 Recommendations for future work

7.1.1 Effect of walking speed

Currently, the models presented herewith are only applicable to normal free walking, and the motion-dependent forces (or the self-excited forces) depend only on the relationship between the frequency of the lateral movement and the walking frequency. However, as a part of the experimental campaign, the load pedestrian-induced load at various (imposed) walking speeds were also investigated for a limited number of people. A further processing of the data should provide an indication of the effect of imposed walking speed. This may prove important, in particular for the modelling of large crowds of people, where free and

unrestricted walking is nearly impossible.

7.1.2 Refined load model and stability criterion

Herewith, the load model and the stability criterion is based on a the most simple representation of the amplitude dependency of the pedestrian damping coefficient; a linear function. An improvement to the load model can be made, by introducing functions that can capture both the amplitude dependency as well as the frequency dependency of the pedestrian load coefficients, whilst allowing for a reliable extrapolation to zero-amplitude. The extrapolation to zero amplitude is important for the stability criterion and the choice of mathematical function to fit the experimental data affects the predicted value of c_p at zero amplitudes.

7.1.3 Full-scale testing

There is a general lack of experimental data from full-scale observation of crowd-induced lateral vibrations. Therefore, engineering consultants and researchers are strongly encouraged to carry out tests and monitor the vibration behaviour of any bridge that is susceptible to excessive lateral vibrations. This is crucial for obtaining a better comparison between laboratory circumstances and the real behaviour of actual footbridges. In particular, excitation of low-frequency modes seems under-estimated in the procedure presented here.

It has been suggested that nonlinear phenomena such as parametric excitation or autoparametric resonance are responsible for excessive bridge vibrations (Ingólfsson et al., 2010a). This could participate to a quicker development of instability than found in the work presented herewith. However, further analysis of the current experimental data is necessary for investigating this phenomenon. To investigate the case where vertical loads may excite lateral modes, different experimental setup has to be used, allowing for the necessary geometrical coupling between the vertical and lateral modes. This has not been covered within the scope of this thesis.

7.1.4 Combined vibrations

Both the London Millennium Bridge and the Clifton Suspension Bridge featured large modal response in two vibration modes simultaneously. The load model presented in this thesis is based on experimentally obtained forces during walking when exposed to a single harmonic excitation. Therefore, investigating the effect of multiple modes on the self-excited pedestrian forces is a natural continuation of the work presented in this thesis. This could involve pedestrian tests where the base motion is a sum of one or more harmonic components. Furthermore, little is know about the combined effect of vertical and lateral vibration on the GRFs.

As the number of possible tests increases dramatically when including more vibration frequencies in the signal or vertical vibrations, a more practical approach is to develop a mathematical which describes the movement of the pedestrian body and thereby the forces generated during walking on a laterally oscillating surface. If this model can successfully

predict, or replicate the main results of the study presented in this thesis, it can be used to model the combined effect of multiple vibration modes or directions.

Bibliography

AASHTO. *Guide Specifications for Design of Pedestrian Bridges*. American Association of State, Highway and Transportation Officials, August 1997.

R.K. Andersen. Pedestrian-induced vibrations: Human-human interaction. MSc Thesis, Department of Civil Engineering, Technical University of Denmark, 2009.

T.P. Andriacchi and E.J. Alexander. Studies of human locomotion: past, present and future. *Journal of Biomechanics*, 33:1217–1224, 2000.

T.P. Andriacchi, J.A. Ogle, and J.O. Galante. Walking speed as a basis for normal and abnormal gait measurements. *Journal of Biomechanics*, 10(4):261–268, 1977.

Aristotle. *On the Gait of Animals*. 350 B.C.

C. Ashley. Proposed international standards for concerning vibration in buildings. In *Proceedings Symposium on Instrumentation for Ground Vibration and Earthquakes*, UK, 1977. Institution of Civil Engineers.

H. Bachmann. Case studies of structures with man-induced vibrations. *Journal of Structural Engineering*, 118(3):631–647, 1992.

H. Bachmann. "lively" footbridges – a real challenge. In *Proceedings of Footbridge 2002, First International Conference*, Paris, November 2002.

H. Bachmann and W.J. Ammann. *Vibrations in Structures. Induced by Man and Machine*. Structural Engineering Documents. International Association for Bridge and Structural Engineering (IABSE), Zürich, Switzerland, 3rd edition, 1987.

H. Bachmann, W.J. Ammann, and et.al. *Vibration Problems in Structures. Practical Guidelines*. Birkhauser, 2nd edition, 1996a.

H. Bachmann, A.J. Pretlov, and H. Rainer. *Vibration Problems in Structures: Practical Guidelines*, chapter Appendix G: dynamic forces from rhythmical human body motions. Birkhäuser, 1996b.

R. Baker. The history of gait analysis before the advent of modern computers. *Gait & Posture*, 27:331–342, 2007.

C. Barker. Some observations on the nature of the mechanism that drives the self-excited lateral response of footbridges. In *Proceedings of Footbridge 2002, First International Conference*, Paris, November 2002.

C. Barker. Footbridge pedestrian vibration limits background to response calculation. *International Journal of Space Structures*, 22(1):35–43, 2007.

C. Barker, S. DeNeumann, D. Mackenzie, and R. Ko. Footbridge pedestrian vibration limits. part 1: Pedestrian input. In *Proceedings of Footbridge 2005, Second International Conference*, Venice, December 2005.

K. Baumann and H. Bachmann. Durch Menschen verursachte dynamische Lasten und deren Auswirkungen auf Balkentragwerke (dynamic loading induced by persons and its effect on beam structures). report 7501-3, Institute of Structural Engineering, Swiss Fed. Inst. of Tech. (ETH), 1987. (in German).

Z. Bejek, R. Paróczai, Á Illyés, and R.M. Kiss. The influence of walking speed on gait parameters in healthy people and in patients with osteoarthritis. *Knee Surgery, Sports Traumatology, Arthroscopy*, 14:612–622, 2006.

J.E.A. Bertram and A. Ruina. Multiple walking speed-frequency relations are predicted by constrained optimization. *Journal of Theoretical Biology*, 209(4):445–453, 2001.

J. Blanchard, B.L. Davies, and J.W. Smith. Design criteria and analysis for dynamic loading of footbridges. In *TRRL Suppl Rep and Symp on Dyn Behav of Bridges*, number 275, pages 90–106. Transp and Road Res Lab, 1977.

A.N. Blekherman. Swaying of pedestrian bridges. *Journal of Bridge Engineering*, 10(2): 142–150, 2005.

J. Bodgi. *Synchronization piétons-structure: Application aux vibration des passerelles souples (Pedestrian-structure synchronization: Application to vibration of flexible bridges).* PhD thesis, Ecole Nationale des Ponts - ParisTech, September 2008. (in French).

N. Bonanni. Valutazione sperimentale dell'azione antropica sulle passerelle pedonali (experimental evaluation of the human activity on a footbridge). BSc thesis, University of Florence, 2007. (In Italian).

M.H. Bornstein. The pace of life: revisted. *International Journal of Psychology*, 14:83–90, 1979.

M.H. Bornstein and H.G. Bornstein. The pace of life. *Nature*, 259:557–559, 1976.

R.A. Brady, B.T. Peters, and J.J. Bloomberg. Strategies of healthy adults walking on a laterally oscillating treadmill. *Gait & Posture*, 29:645–649, 2009.

Bro 2004. *Vägverkets allmänna tekniska beskrivning för nybyggande och forbättring av broar (SRA's general technical description for new construction and improvement of bridges).* Svensk Byggtjänst, Stockholm, Sverige, 2004. (In Swedish).

J. Brownjohn, S. Zivanovic, and A. Pavic. Crowd dynamic loading on footbridges. In *Proceedings of Footbridge 2008, Third International Conference*, Porto, 2-4 July 2008.

J. Brownjohn, E. Caetano, X. Cespedes, P. Charles, A. Cunha, P. Duflot, M. Feldmann, O. Flamand, C. Heinemeyer, W. Hoorpah, A. Low, F. Magalhaes, C. Meinhardt, C. Moutinho, A. Pavic, D. Taylor, S. Zivanovic, T. Zoli, and K. Zoltowski. *Footbridge Vibration Design*. Taylor and Francis, 2009.

J.M.W. Brownjohn, P. Fok, M. Roche, and P. Omenzetter. Long span steel pedestrian bridge at Singapore Changi airport - part 2: Crowd loading tests and vibration mitigation measures. *The Structural Engineer*, 82(16):28–34, 2004a.

J.M.W. Brownjohn, A. Pavic, and P. Omenzetter. A spectral density approach for modelling continuous vertical forces on pedestrian structures due to walking. *Canadian Journal of Civil Engineering*, 31(1):65–77, 2004b.

J.M.W. Brownjohn, A. Pavic, and P. Omenzetter. Modeling and measuring dynamic crowd loading on a long span footbridge. In *Proceedings of the 2004 International Conference on Noise and Vibration Engineering, ISMA*, pages 751–765, 2004c.

L. Bruno and F. Venuti. The pedestrian speed-density relation: modelling and application. In *Proceedings of Footbridge 2008, Third International Conference*, Porto, 2-4 July 2008.

L. Bruno and F. Venuti. Crowd-structure interaction in footbridges: Modelling, application to a real case-study and sensitivity analyses. *Journal of Sound and Vibration*, 323 (1-2):475–493, 2009.

BS 5400. *Steel, Concrete and compostite Bridges, Part 2: Specifications for Loads; Appendix C: Vibration Serviceability Requirements for Foot and Cycle Track Bridges.* British Standards Institute, London, UK, 1978.

BS 6472. *BS 6472:1992 Guide to Evaluation of human exposure to vibration in buildings (1 Hz to 80 Hz).* British Standards Institute, 1992.

C. Butz. *Beitrag zur Berechnung fußgängerinduzierter Brückenschwingungen (On the calculation of pedestrian-induced vibration of bridges).* PhD thesis, RWTH Aachen, 2006. (In German).

C. Butz. A probabilistic engineering load model for pedestrian streams. In *Proceedings of Footbridge 2008, Third International Conference*, Porto, 2-4 July 2008.

C. Butz, F. Magalhaes, A. Cunha, E. Caetano, and A. Goldack. Experimental characterization of the dynamic behaviour of lively footbridges. In *Proceedings of Footbridge 2005, Second International Conference*, Venice, 6-8 December 2005.

C. Butz, C. Heinemeyer, A. Keil, M. Schlaich, A. Goldack, S. Trometer, M. Lukić, B. Chabrolin, A. Lemaire, P.O. Martin, A. Cunha, and E. Caetano. *Design of Footbridges - Guidelines and background document.* HIVOSS, 2007. RFS2-CT-2007-00033.

C. Butz, J. Dist, and P. Huber. Effectiveness of horizontal tuned mass damper exemplified at the footbridge in Coimbre. In *Proceedings of Footbridge 2008, Third International Conference*, Porto, 2-4 July 2008.

E. Caetano, Á. Cunha, F. Magalhães, and C. Moutinho. Studies for controlling human-induced vibration of the Pedro e Inês footbridge, Portugal. part 1: Assessment of dynamic behaviour. *Engineering Structures*, 32:1069–1081, 2010a.

E. Caetano, Á. Cunha, F. Magalhães, and C. Moutinho. Studies for controlling human-induced vibration of the Pedro e Inês footbridge, Portugal. part 2: Implementation of tuned mass dampers. *Engineering Structures*, 32:1082–1091, 2010b.

F.K. Chang. Human response to motions in tall buildings. *ASCE Journal of the Structural Division*, 99(ST6):1259–1272, 1973.

P. Charles and V. Bui. Transversal dynamic actions of pedestrians. synchronization. In *Proceedings of Footbridge 2005, Second International Conference*, Venice, 6-8 December 2005.

C. Chatfield. *The Analysis of Time Series. An Introduction.* Texts in Statistical Science. Chapman & Hall / CRC, 6th edition, 2004.

P.W. Chen and L.E. Robertson. Human perception threshold of horizontal motion. *ASCE Journal of Structural Division*, 98:1681–1695, 1973.

A.K. Chopra. *Dynamics of Structures. Theory and Applications to Earthquake Engineering.* Civil Engineering and Engineering Mechanics. Prentice Hall International Series, 2nd edition, 2001.

T. Christensen and L. Dyekjær. 3-aksial accelerationslogger med μsd-hukommelseskort (3-axial acceleration loggers with μsd-memory card). Project report at DTU Civil Engineering (in Danish), June 2007.

M. Christiansen. Fodgængerinducerede svingninger i gangbroer (pedestrian-induced vibrations of footbridges). MSc thesis, Department of Civil Engineering, Technical University of Denmark, 2008. (in Danish).

A. Cunha, E. Caetano, C. Moutinho, and F. Magalhaes. The role of dynamic testing in design, construction and long-term monitoring of lively footbridges. In *Proceedings of Footbridge 2008, Third International Conference*, Porto, 2-4 July 2008.

J.G.S. da Silva, P.C.G. Vellasco, S.A.L. de Andrea, L.R.O. de Lima, and F.P. Figueiredo. Vibration analysis of footbridges due to vertical human loads. *Computers and Structures*, 85:1693–1703, 2007.

P. Dallard, A.J. Fitzpatrick, A. Flint, S.Le. Bourva, A. Low, R.M.R. Smith, and M. Willford. The London Millennium Footbridge. *The Structural Engineer*, 79(22):17–33, 2001a.

P. Dallard, T. Fitzpatrick, A. Flint, A. Low, R.R. Smith, M. Willford, and M. Roche. London Millennium Bridge: Pedestrian-induced lateral vibration. *Journal of Bridge Engineering*, 6(6):412–417, 2001b.

F. Danbon and G. Grillaud. Dynamic behaviour of a steel footbridge. Characterisation and modelling of the dynamic loading induced by a moving crowd on the Solferino footbridge in Paris. In *Proceedings of Footbridge 2005, Second International Conference*, Venice, 6-8 December 2005.

R.O. Denoon, C.W. Letchford, K.C.S. Kwok, and D.L. Morrison. Field measurements of human reaction to wind-induced building motion. In *Wind Engineering into the 21st Century*, Rotterdam, 1999.

R.O. Denoon, R.D. Roberts, C.W. Letchford, and K.C.S. Kwok. Field experiments to investigate occupant perception and tolerance of wind-induced building motion. Research Report No 803, Department of Civil Engineering, the University of Sidney, September 2000.

DRD. *Belastnings- og beregningsregler for vej- og stibroer (Load and design specifications for road- and footbridges).* Danish Road Directorate, November 2002. In Danish.

M.L.M. Duarte and M. de Brito Pereira. Vision influence on whole-body human vibration comfort levels. *Shock and Vibration*, 13:367–377, 2006.

P. Dziuba, G. Grillaud, O. Flamand, S. Sanquier, and Y. Tétard. La passerelle Solférino comportement dynamique (dynamic behaviour of the Solférino bridge). *Bulletin Ouvrages Métalliques*, 1:34–57, 2001. (in French).

B. Eckhardt, E. Ott, S.H. Strogatz, D.M. Abrams, and A. McRobie. Modeling walker synchronization on the Millennium Bridge. *Physical Review E*, 75:21110–1–10, 2007.

H. Elftman. The measurement of the external force in walking. *Science*, 88(2276):152–153, 1938.

EN 1990. *EN 1990/A1:2002. Eurocode - Basis of structural design.* CEN, European Committee for Standardization, December 2005.

ENV 1995-2. *ENV 1995-2:1997. Eurocode 5: Design of Timber Structures Part 2. Bridges.* CEN, European Committee for Standardization, Brussels, Belgium, 1997.

P.E. Eriksson. Low-frequency forces caused by people: Design force models. *IABSE International Colloquium*, 69:149–156, 1993.

P.E. Eriksson. *Vibration of Low-Frequency Floors - Dynamic Forces and Response Prediction.* PhD thesis, Chalmers University of Technology, Department of Structural Engineering, Göteborg, March 1994.

S. Erlicher, A. Trovato, and P. Argoul. Modeling the lateral pedestrian force on a rigid floor by a self-sustained oscillator. *Mechanical Systems and Signal Processing*, 24(5): 1579–1604, 2010.

FIB. *Guidelines for the design of footbridges, bulletin 32*. Fédération international du béton (*fib*), November 2005.

K.K. Finnis and D. Walton. Field observations of factors influencing walking speeds. In *2nd International Conference on Sustainability Engineering and Science*, 2007.

A. Flaga, M. Pantak, and T. Michalowski. Examination of own human comfort criteria for footbridges in case of wind-induced vibrations. In *Proceedings of Footbridge 2008, Third International Conference*, Porto, 2-4 July 2008a.

A. Flaga, M. Pantak, and T. Michalowski. Vibration comfort criteria for footbridges for pedestrians on footbridges. In *Proceedings of Footbridge 2008, Third International Conference*, Porto, 2-4 July 2008b.

Y. Fujino, B.M. Pacheco, S.I. Nakamura, and P. Warnitchai. Synchronization of human walking observed during lateral vibration of a congested pedestrian bridge. *Earthquake Engineering & Structural Dynamics*, 22(9):741–758, 1993.

C.T. Georgakis and E.T. Ingólfsson. Vertical footbridge vibrations: the response spectrum methodology. In *Proceedings of Footbridge 2008, Third International Conference*, Porto, 2-4 July 2008.

T. Goto. Studies of wind-induces motion of tall buildings based on occupants' reactions. *Journal of Wind Engineering and Industrial Aerodynamics*, 13:241–252, 1983.

M.J. Griffin. *Handbook of human vibration*. Elsevier academic press, London, U.K., 2004.

G.V. Gudmundsson, E.T. Ingólfsson, B. Einarsson, and B. Bessason. Vibration serviceability assessment of three lively bridges in Reykjavik. In *Proceedings of Footbridge 2008, Third International Conference*, Porto, 2-4 July 2008.

R.J. Hansen, J.W. Reed, and E.H. Vanmarcke. Human response to wind-induced motion of buildings. *ASCE Journal of the Structural Division*, 99(ST7):1589–1605, 1973.

J.M. Hausdorff, Y. Ashkenazy, C.-K. Peng, P.Ch. Ivanov, H.E. Stanley, and A.L. Goldberger. When human walking becomes random walking: fractal analysis and modeling of gait rhythm fluctuations. *Physica A*, 302(1-4):138–147, 2001.

R.E. Hobbs. Test on lateral forces induced by pedestrians crossing a platform driven laterally. Technical report, Civil Engineering Department, Imperial College London, London, UK, August 2000. A report for Ove Arup and Partners.

J. Hogsberg and S. Krenk. Adaptive tuning of elasto-plastic damper. *International Journal of Non-Linear Mechanics*, 42:928–940, 2007.

W. Hoorpah, O. Flamand, and X. Cespedes. The Simon de Beauvoir footbridge in Paris. Experimental verification of the dynamic behaviour under pedestrian loads and discussion of corrective modifications. In *Proceedings of Footbridge 2008, Third International Conference*, Porto, 2-4 July 2008.

E.T. Ingólfsson. Pedestrian-Induced Vibrations of Line-like Structures. MSc thesis, Department of Civil Engineering, Technical University of Denmark, June 2006.

E.T. Ingólfsson and C.T. Georgakis. A stochastic load model for pedestrian-induced lateral forces on footbridges. *Engineering Structures*, 2011. in press.

E.T. Ingólfsson, C.T. Georgakis, J. Jönsson, and F. Ricciardelli. Vertical footbridge vibrations: Towards an improved and codifiable response evaluation. In *third International Conference on Structural Engineering, Mechanics and Computation*, Cape Town, South Africa, 10-12 September 2007.

E.T. Ingólfsson, C.T. Georgakis, and A. Knudsen. A preliminary experimental investigation into lateral pedestrian-structure interaction. In *Proceedings of the 7th European Conference on Structural Dynamics*, Southampton, 7-9 July 2008a.

E.T. Ingólfsson, C.T. Georgakis, and M.N. Svendsen. Vertical footbridge vibrations: details regarding and experimental validation of the response spectrum methodology. In *Proceedings of Footbridge 2008, Third International Conference*, Porto, 2-4 July 2008b.

E.T. Ingólfsson, C.T. Georgakis, and J. Jönsson. Pedestrian-induced lateral vibrations of footbridges: Literature review. Unpublished manuscript, 2010a.

E.T. Ingólfsson, C.T. Georgakis, F. Ricciardelli, and L. Procino. Lateral human-structure interaction on footbridges. In *Tenth International Conference on Recent Advances in Structural Dynamics*, Southampton, 12-14 July 2010b.

E.T. Ingólfsson, C.T. Georgakis, F. Ricciardelli, and J. Jönsson. Experimental identification of pedestrian-induced lateral forces on footbridges. *Journal of Sound and Vibration*, 330:1265–1284, 2011.

A.W. Irwin. Human response to dynamic motion of structures. *Struct Eng Part A*, 56A (9):237–244, 1978.

A.W. Irwin. Perception, comfort and performance criteria for human beings exposed to whole body pure yaw vibration and vibration containing yaw and translation components. *Journal of Sound and Vibration*, 76(4):481–497, 1981.

M.M. Ishaque and R.B. Noland. Behavioural issues in pedestrian speed choice and street crossing behaviour: a review. *Transport Reviews*, 28:61–85, 2008.

ISO 10137. *ISO 10137:2007 Bases for design of structures - Serviceability of buildings and walkways against vibration*. International Organization for Standardization, 2007.

ISO 2631-2. *ISO 2631-2:1989 Evaluation of human exposure to whole-body vibration - Part 2: Continuous and shock-induced vibration in buildings (1 to 80 Hz)*. International Organization for Standardization, 1989.

ISO 2631-2. *ISO 2631-2:2003 Evaluation of human exposure to whole-body vibration - Part 2: Continuous and shock-induced vibration in buildings (1 to 80 Hz)*. International Organization for Standardization, 2003.

T. Ji and B.R. Ellis. Floor vibration. floor vibration induced by dance-type loads. Theory. *The Structural Engineer*, 72(3):37–44, 1994.

N. Jørgensen. Human structure interaction: Influence of walking pedestrians on the dynamic properties of footbridge structures they occupy. MSc Thesis, Department of Civil Engineering, Technical University of Denmark, August 2009.

J. Kanda, Y. Tamura, K. Fujii, T. Ohtsuki, K. Shioya, and S. Nakata. Probabilistic evaluation of human perception threshold of horizontal vibration of buildings (0.125 Hz to 6.0 Hz). In *Proceedings of the Structures Congress '94*, pages 648–653. Published by ASCE, 1994.

M. Kasperski. Actual problems with stand structures due to spectatorinduced vibrations. In *Proceedings of the 4th European conference on structural dynamics*, Florence, 5-8 June 1996.

M. Kasperski. Vibration serviceability for pedestrain bridges. *Proceedings of the ICE: Structures and Buildings*, 159(5):273–282, 2006.

M. Kasperski. Serviceability of pedestrian structures. In *Proceedings of the 25th IMAC Conference*, Orlando, Florida, 19-22 February 2007.

B.A. Kay and W.H. Warren Jr. Coupling of posture and gait: mode locking and parametric excitation. *Biological Cybernetics*, 85:89–106, 2001.

S.C. Kerr. *Human Induced Loading on Staircases*. PhD thesis, Mechanical Engineering Department, University College London, London, UK, 1998.

A. Knudsen. Pedestrian-induced lateral vibrations of bridges. MSc thesis, Department of Civil Engineering, Technical University of Denmark, 2007.

S. Krenk. *Non-linear Modeling and Analysis of Solids and Structures*. Cambridge University Press, 2009.

H. Kuang. Analysis of pedestrian dynamics in counter flow via an extended lattice gas model. *Physical Review E*, 78(6), 2008.

A.D. Kuo. A simple model of the bipedal walking predicts the preferred speed – step length relationship. *Journal of Biomechanical Engineering*, 123:264–269, 2001.

W.H.K. Lam, J.Y.S. Lee, and C.Y. Cheung. A study of the bi-directional pedestrian flow characteristics at Hong Kong signalized crosswalk facilities. *Transportation*, 29: 169–192, 2002.

R.S.C. Lee and R.L. Hughes. Minimisation of the risk of trampling in a crowd. *Mathematical and Computers in Simulation*, 74:29–37, 2007.

R.V. Levine. The pace of life in 31 countries. *Journal of Cross-Cultural Psychology*, 30: 178–205, 1999.

Q. Li, J. Fan, J. Nie, Q. Li, and Y. Chen. Crowd-induced random vibration of footbridges and vibration control using multiple tuned mass dampers. *Journal of Sound and Vibration*, 329:4068–4092, 2010.

J.H.G. Macdonald. Pedestrian-induced vibrations of the Clifton Suspension Bridge, UK. *Proceedings of the ICE: Bridge Engineering*, 161(BE2):69–77, 2008.

J.H.G. Macdonald. Lateral excitation of bridges by balancing pedestrians. *Proceedings of the Royal Society A*, 465:1055–1073, 2009.

Y. Matsumoto, T. Nishioka, H. Shiojiri, and K. Matsuzaki. Dynamic design of footbridges. In *IABSE Proceedings*, volume P-17/78, pages 1–15, 1978.

P.M. McAndrew, J.B. Dingwell, and J.M. Wilken. Walking variability during continuous pseudo-random oscillations of the support surface and visual field. *Journal of Biomechanics*, 43:1470–1475, 2010.

A. McRobie, G. Morgenthal, J. Lasenby, and M. Ringer. Section model tests on human-structure lock-in. *Proceedings of the ICE: Bridge Engineering*, 156(BE2):71–79, 2003.

W.H. Melbourne. Comfort criteria for wind-induced motion in structures. *Structural Engineering International*, 1:40–44, 1998.

W.H. Melbourne and J.C.K.C. Cheung. Designing for serviceability accelerations in tall buildings. In *4th International Conference On Tall Buildings*, Hong Kong and Shanghai, 1988.

M. Milner and A.O. Quanbury. Facets of control in human walking. *Nature*, 227:734–735, 1970.

M Mistler and D. Heiland. Lock-in-Effekt beings Brücken infolge Fußgängeranregung - Schwingungstest der weltlängsten Fußgänger- und Velobrücke (lock-in effect due to pedestrian excitation of bridges - vibration test of the world's longest pedestrian and bicycle bridge). In *D-A-CH Tagung*, Vienna, 27-28 September 2007. (in German).

F. Mormann, K. Lehnertz, P. David, and C.E. Elger. Mean phase coherence as a measure for phase synchronization and its application to the EEG of epilepsy patients. *Physica D*, 144:358–369, 2000.

NA to BS EN 1991-2 UK. *National Annex to Eurocode 1: Actions on structure - Part 2: Traffic loads on bridges*. CEN, European Committee for Standardization, May 2008.

S. Nakamura and T. Kawasaki. A method for predicting the lateral girder response of footbridges induced by pedestrians. *Journal of Constructional Steel Research*, 65:1705–1711, 2009.

S.I. Nakamura. Field measurements of lateral vibration on a pedestrian bridge. *The Structural Engineer*, 81(22):22–26, 2003.

S.I. Nakamura and T. Kawasaki. Lateral vibration of footbridges by synchronous walking. *Journal of Constructional Steel Research*, 62(11):1148–1160, 2006.

S.I. Nakamura, T. Kawasaki, H. Katsuura, and K. Yokoyama. Experimental studies on lateral forces induced by pedestrians. *Journal of Constructional Steel Research*, 64: 247–252, 2008.

D.E. Newland. Pedestrian excitation of bridges - recent results. In *Proceedings of the Tenth International Congress on Sound and Vibration*, pages 533–547, 2003.

D.E. Newland. Pedestrian excitation of bridges. In *Proceedings of the Institution of Mechanical Engineers, Part C: Journal of Mechanical Engineering Science*, volume 218, pages 477–492, 2004.

OHBDC. *Ontario Highway Bridge Design Code*. Highway Engineering Division, Ministry of Transportation and Communication, Ontario, Canada, 1983.

S.V. Ohlsson. *Floor vibration and human discomfort*. PhD thesis, Chalmers University of Technology, Göteborg, 1982.

Ove Arup and Partners International Ltd. London Borough of Southwalk Millennium Bridge. Prototype test report 2: Damping test results. (Unpublished internal report), February 2002.

E. Papadimitriou, G. Yannis, and J. Golias. A critical assessment of pedestrian behaviour models. *Transportation Research Part F*, 12(3):242–255, 2009.

A. Pavic and P. Reynolds. Vibration serviceability of long-span concrete building floors. Part 1: review of background information. *The Shock and Vibration Digest*, 34(3): 191–211, 2002a.

A. Pavic and P. Reynolds. Vibration serviceability of long-span concrete building floors. Part 2: review of mathematical modelling approaches. *The Shock and Vibration Digest*, 34(4):279–297, 2002b.

L. Pedersen and C. Frier. Sensitivity of footbridge vibrations to stochastic walking parameters. *Journal of Sound and Vibration*, 329:2683–2701, 2010.

J. Perry. *Gait Analysis. Normal and Pathological Function*. SLACK Incorporate, 1992.

C. Peterson. Theorie der Zufallsschwingungen und Anwendungen (theory of random vibrations and applications). Work Report 2/72, Structural Engineering Laboratory, Technical University of Munich, 1972. In German.

G. Piccardo and F. Tubino. Parametric resonance of flexible footbridges under crowd-induced lateral excitation. *Journal of Sound and Vibration*, 311:353–371, 2008.

R.L. Pimentel and P. Waldron. Validation of the pedestrian load model through the modal testing of a composite footbridge. In *Proceedings of the 15th IMAC Conference*, volume 1, pages 286–292. SEM, 1997.

A.D. Pizzimenti. *Analisi sperimentale dei meccanismi di eccitazione laterale delle passerelle ad opera dei pedoni (experimental analysis of the lateral pedestrian-induced mechanism of excitation of footbridges).* PhD thesis, Department of Civil and Environmental Engineering, University of Catania, 2004. (in Italian).

A.D. Pizzimenti and F. Ricciardelli. Experimental evaluation of the dynamic lateral loading of footbridges by walking pedestrians. In *Proceedings of the 6th International Conference on Structural Dynamics*, Paris, 4-7 September 2005.

V. Racic. *Experimental measurement and mathematical modelling of near-periodic human-induced dynamic force signals.* PhD Thesis, Department of Civil & Structural Engineering, The University of Sheffield, November 2009.

V. Racic, A. Pavic, and J.M.W. Brownjohn. Experimental identification and analytical modelling of walking forces: Literature review. *Journal of Sound and Vibration*, 326: 1–49, 2009.

V. Racic, J.M.W. Brownjohn, and A. Pavic. Reproduction and application of human bouncing and jumping forces from visual marker data. *Journal of Sound and Vibration*, 329:3397–3416, 2010.

J.H. Rainer and G. Pernica. Vertical dynamic forces from footsteps. *Canadian Acoustics*, 14(2):12–21, 1986.

J.H. Rainer, G. Pernica, and D.E. Allen. Dynamic loading and response of footbridges. *Canadian Journal of Civil Engineering*, 15(1):66–71, 1988.

F. Ricciardelli and A.D. Pizzimenti. Lateral walking-induced forces on footbridges. *Journal of Bridge Engineering*, 12(6):677–688, 2007.

T.M. Roberts. Lateral pedestrian excitation of footbridges. *Journal of Bridge Engineering*, 10(1):107–112, 2005a.

T.M. Roberts. Synchronised pedestrian lateral excitation of footbridges. In *Proceedings of the 6th International Conference on Structural Dynamics*, Paris, 4-7 September 2005b.

A. Rönnquist. *Pedestrian induced vibrations of slender footbridges.* PhD thesis, Norwegian University of Science and Technology, 2005.

A. Rönnquist, Strømmen, and L. Wollebæk. Dynamic properties from full scale recordings and FE-modelling of a slender footbridge with flexible connections. *Structural Engineering International*, 4:421–426, 2008.

G.K. Rose. Clinical gait assessment: a personal view. *Journal of Medical Engineering and Technology*, 7:273–279, 1983.

R. Sachse, A. Pavic, and P. Reynolds. Human-structure dynamic interaction in civil engineering dynamics: A literature review. *The Shock and Vibration Digest*, 35(1): 3–18, January 2003.

C. Sahnaci and M. Kasperski. Random loads induced by walking. In *Proceedings of the 6th European Conference on Structural Dynamics*, Southampton, 7-9 July 2005.

Sétra. *Footbridges, Assessment of vibrational behaviour of footbridges under pedestrian loading*. The Technical Department for Transport, Roads and Bridges Engineering and Road Safety, November 2006.

M. Shinozuka and G. Deodatis. Simulation of stochastic processes by spectral representation. *Applied Mechanics Review*, 44(4):191–204, 1991.

R.A. Smith. Density, velocity and flow relationship for closely packed crowds. *Safety Science*, 18:321–327, 1995.

J.Th. Snæbjörnsson and R. Sigbjörnsson. Footbridge dynamics and pedestrian induced vibrations - a case study. In *Proceedings of the Third International Conference on Structural Dynamcis*, Prague, June 1999.

J. Sólnes. *Stochastic processes and random vibrations, Theory and practice*. John Wiley & Sons, Chichester, England, 1997.

R.J.C. Stanton and G.K. Wanless. Pedestrian movement. *Safety Science*, 18:291–300, 1995.

S.H. Strogatz and I. Stewart. Coupled oscillators and biological synchronisation. *Scientific American*, 269:68–73, 1993.

S.H. Strogatz, D.M. Abrams, A. McRobie, B. Eckhardt, and E. Ott. Crowd synchrony on the millennium bridge. *Nature*, 438(7064):43–44, 2005.

E.N. Strömmen. *Theory of bridge aerodynamics*. Springer, 2006.

L. Sun and X. Yuan. Study on pedestrian-induced vibration of footbridge. In *Proceedings of Footbridge 2008, Third International Conference*, Porto, 6-8 July 2008.

Y. Tamura, S. Kawana, O. Nakamura, J. Kanada, and S. Nakata. Evaluation perception of wind-induced vibration in buildings. *Structures & Buildings*, 159(SB5):283–293, 2006.

Y. Tanaboriboon, S. S. Hwa, and C. Hoong. Pedestrian characteristics study in Singapore. *Journal of Transportation Engineering*, 112(3):229–235, 1986.

P. Terrier and Y. Schutz. Variability of gait patterns during unconstrained walking assessed by satellite positioning (GPS). *European Journal of Applied Physiology*, 90(5-6): 554–561, 2003.

P. Terrier, V. Turner, and Y. Schutz. GPS analysis of human locomotion: further evidence for long-range correlations in stride-to-stride fluctuations of gait parameters. *Human Movement Science*, 24(1):97–115, 2005.

M.A. Townsend. Biped gait stabilisation via foot placement. *Journal of Biomechanics*, 18:21–38, 1985.

A. Trovato, S. Erlicher, and P. Argoul. Modeling the lateral pedestrian force on rigid and moving floors by a self-sustained oscillator. In *ECCOMAS Thematic Conference on Computational Methods in Structural Dynamics and Earthquake Engineering*, Rhodes, Greece, 22-24 June 2009.

F. Tubino and G. Piccardo. Determinstic and stochastic approaches in the vibration serviceability assessment of pedestrain bridges. In *Proceedings of the 7th European Conference on Structural Dynamics*, Southampton, 7-9 July 2008.

H. Uustal and E. Baerga. *Physical Medicine and Rehabilitation Board Review*, chapter Prosthetics and orthotics. Demos Medical Publishing, 2004.

C.L. Vaughan. Theories of bipedal walking: an odyssey. *Journal of Biomechanics*, 36(4): 513–523, 2003.

F. Venuti and L. Bruno. An interpretative model of the pedestrian fundamental relation. *C.R. Mecanique*, 335:194–200, 2007.

F. Venuti, L. Bruno, and P. Napoli. Pedestrian lateral action on lively footbridges: A new load model. *Structural Engineering International*, 17:236–241, 2007.

B.J. Vickery and A.W. Clark. Lift of across-wind response of tapered stacks. *ASCE Journal of the Structural Division*, 98:1–20, 1972.

S. Živanović. *Probability-based Estimation of Vibration for Pedestrian Structures due to Walking*. PhD thesis, Department of Civil & Structural Engineering, University of Sheffield, February 2006.

S. Živanović and A. Pavic. Probabilistic approach to subjective assessment of footbridge vibration. In *42nd United Kingdom Conference on Human Response to Vibration*, Southampton, UK, 10 - 12 September 2007.

S. Živanović, A. Pavic, and P. Reynolds. Vibration serviceability of footbridges under human-induced excitation: a literature review. *Journal of Sound and Vibration*, 279 (1-2):1–74, 2005a.

S. Živanović, A. Pavic, and P. Reynolds. Human-structure dynamic interaction in footbridges. *Proceedings of the ICE: Bridge Engineering*, 158(4):165–177, 2005b.

S. Živanović, A. Pavic, P. Reynolds, and P. Vujovic. Dynamic analysis of lively footbridge under everyday pedestrian traffic. In *Proceedings of the sixth European conference on structural dynamics*, 2005c.

S. Živanović, A. Pavic, and P. Reynolds. Probability-based prediction of multi-mode vibration response to walking excitation. *Engineering Structures*, 29:942–954, 2007.

S. Živanović, I.M. Díaz, and A. Pavić. Influence of walking and standing crowds on structural dynamic performance. In *Proceedings of the 27th IMAC Conference*, Orlando, USA, 9-12 February 2009.

S. Živanović, A. Pavić, and E.T. Ingólfsson. Modelling spatially unrestricted pedestrian traffic on footbridges. *ASCE Journal of Strucutral Engineering*, 136(10):1296–1308, 2010.

J. E. Wheeler. Prediction and control of pedestrian-induced vibration in footbridges. *ASCE Journal of the Structural Division*, 108:2045–2065, 1982.

J.E. Wheeler. Crowd loading of footbridges. Technical report, Technical Report No. 23, Main Roads Department, Western Australia, 1981.

M.R. Willford and P. Young. Improved methodologies for the prediction of footfall-induced vibration. In *Proceedings of the 6th European Conference on Structural Dynamics*, 2005.

M.R. Willford and P. Young. A design guide for footfall induced vibration of structures. Technical guide CCIP-016, The Concrete Centre, November 2006.

P. Wirtz and G. Ries. The pace of life - reanalysed: Why does walking speed of pedestrians correlate with city size? *Behaviour*, 123:77–83, 1992.

B. Wolmuth and J. Surtees. Crowd-related failure of bridges. *Proceedings of the ICE: Civil Engineering*, 156(3):116–123, 2003.

M. Yamasaki, T. Sasaki, and M. Torii. Sex difference in the pattern of lower limb movement during treadmill walking. *European Journal of Applied Physiology*, 62:99–103, 1991.

J. Yoshida, M. Abe, Y. Fujino, and K. Higashiuwatoko. Image analysis of human induced lateral vibration of a pedestrian bridge. In *Proceedings of Footbridge 2002, First International Conference*, 10-12 November 2002.

Part II

Appended papers

Paper I (Ingólfsson et al., 2010a)

"Pedestrian-induced lateral vibrations of footbridges: Literature review"

E.T. Ingólfsson, C.T. Georgakis & J. Jönsson

Unpublished manuscript

Pedestrian-induced lateral vibrations of footbridges: Literature review

E.T. Ingólfsson[a,*], C.T. Georgakis[a], J. Jönsson[a,]

[a]*Deparment of Civil Engineering, Technical University of Denmark, Building 118, Brovej, 2800 Kgs. Lyngby, Denmark*

Abstract

The earliest scientific descriptions of excessive pedestrian-induced lateral vibrations are dated back to the 1970s, but it was not until the beginning of the new millennium that bridge engineers fully comprehended the potential negative effect of pedestrian crowds on long-span footbridges. Following the unexpected serviceability failures of Paris' Solferino and London's Millennium footbridges in 1999 and 2000, a new tract of research initiated, focused on understanding the phenomenon which has become known as Synchronous Lateral Excitation (SLE).

In this paper, a comprehensive review of studies related to pedestrian-induced lateral vibrations of footbridges is provided and is primarily based on studies published within the last decade.

Research in this field can generally be split into three categories; (i) full-scale testing of existing bridges subject to crowd loading, (ii) laboratory studies on human-structure interaction between single pedestrians and laterally moving platforms and (iii) mathematical modelling of the pedestrian-induced load. It is shown herein, that a significant amount of research has been carried out within each of the three categories, but there is only a limited interconnection, particularly between the mathematical models on one side and the empirical observations on the other. The main purpose of this review is to provide this link, through a detailed and critical review of publications within each of the three categories.

Key words: Pedestrian-induced lateral vibrations, Footbridges, Synchronisation, Full-scale testing, load models, laboratory platforms, Ground Reaction Forces

Contents

*Corresponding author

Email addresses: eti@byg.dtu.dk (E.T. Ingólfsson)

1. Introduction

With the promise of extensive urban regeneration, isolated segments of the landscape are being increasingly connected by architecturally novel and challenging footbridges [1–3]. This has led to a boom in footbridge design and construction, allowing recent examples to easily match road bridges in terms of cost and span. The challenges in footbridge design lie in the fulfillment of the architectural demands for long, light and slender structures. And whilst the architects and engineering consultants are constantly improving material usage and cost, many new footbridges are experiencing excessive vibrations for which extensive retrofit costs are being incurred. The temporary closures of both pont de Solférino in Paris in 1999 and then the London Millennium Bridge in 2000, following excessive pedestrian-induced lateral vibrations during their inauguration, [4, 5], are probably the most famous and publicised cases of this. Subsequent research revealed that the potential negative effect of pedestrian-induced lateral forces on footbridges was not limited to the innovative design of the two bridges, but had been observed on several other bridges of different shapes, sizes and function in the past.

In fact, any bridge with sufficiently low natural frequency subject to a sufficiently large number of pedestrians can suffer from similar excessive vibrations.

Therefore, an international conference devoted to the design and dynamic behaviour of footbridges (also known as "Footbridge 2002") was established in Paris in 2002 and with 69 paper contributions it attracted researchers, engineers and architects from all around the world. Several work groups were created in the beginning of this century to define design guidelines for footbridges [6]. The first international guide was published in 2005 by *fib* (federation internationale du beton) dealing with general design of footbridges, including design from dynamics loads, [7]. The French Association of Civil Engineers and the French road authority Sétra published in 2006 a comprehensive guide for dynamic design of footbridges [5]. A European research project SYNPEX was established in 2003 for developing advanced load models for synchronous pedestrian excitation and optimised design guidelines for steel footbridges. In 2007 and 2008, the results from their work were published as a guideline, [8–11]. A simultaneous effort commissioned by the UK Highway Agency was undertaken by TRL Limited and Flint & Neill Partnership to define design guidelines in the Highway Agency's Design Manual for Roads and Bridges, [12–16]. The methodology has further been adopted in the UK National Annex to Eurocode 1991-2:2003, [17, 18]. During the third international conference ("Footbridge 2008") a workshop entitled "Footbridges vibration design: worldwide experience" was held, featuring ten invited contributions with focus on design recommendations, guidelines and case studies on human induced vibration and vibration mitigation. The contributions have ben published in slightly modified versions as a book entitled "Footbridge Vibration Design" [19].

Following the extensive recent research effort, an increasing number of engineers now put an effort in the design stage to accommodate the potential threat of pedestrian induced lateral vibrations, [20–23]. Typical countermeasures involve the design of a vibration mitigation device such as a Tuned Mass Damper (TMD) with subsequent experimental modal analysis and pedestrian response tests for tuning and verification purposes [24–27].

Despite this tremendous research effort, several questions relating to lateral pedestrian induced vibrations still remain unanswered. Many examples of bridges have been reported as 'lively' and an increasing number of full scale pedestrian crowd tests have been perform to verify the existence of "synchronous lateral excitation" (SLE) and to determine the critical number of pedestrians needed to trigger SLE. However, there is a general dispute about the basic mechanism of pedestrian-induced lateral forces and several different hypotheses and pedestrian load models exist with origin from different corners of the scientific community.

Pedestrian induced lateral vibrations is a sub-branch of a large research area within vibration serviceability of structures and is mainly a concern for footbridges with natural frequencies of lateral vibration modes below approximately 1.3 Hz. In recent years several papers have been published within the field of vibration serviceability of structures. Especially it is worth mentioning the review devoted to footbridge structures by Zivanovic et.al. [28], in which a comprehensive overview of the entire field of vibration serviceability is given. Also worth mentioning is the review by Racic et al. [29] focused on modelling of human induced walking forces, largely seen from a bio-mechanical point of view and that of Venuti and Bruno [30] which is primarily focused on crowd modelling for footbridge applications.

The purpose of this paper is to provide a comprehensive review of the state-of-the-art, with emphasis on published cases of pedestrian-induced lateral bridge vibrations, the results from experimental studies and the recent development in modelling of pedestrian loading and its effect on structures. The content of this review is presented (nearly) chronologically and can be divided into five parts. Following an introduction to early cases of lateral vibrations and lateral ground reaction forces from pedestrians on a fixed floor, a thorough presentation of the work made during the retrofit period of the Solférino Bridge in Paris and the London Millennium Bridge is given. Since 2002, more researchers have been devoted to the determination of pedestrian loads on flexible footbridges and several attempts have been made to quantify the interaction between a pedestrian and a laterally moving structure. The main results from experimental studies on lateral loads on a moving structure are summarized in Section 5 and results from reported full scale measurements of lively pedestrian bridges are presented in some detail in Section 6. In the final section, a detailed description of the state-of-the-art in the development of pedestrian load models and response evaluation techniques is given.

2. Early cases of excessive lateral bridge vibrations

To the authors' knowledge, the earliest reported incidents of excessive lateral vibrations induced by crowds are dated back to the late 1950's, one involving a road/railway bridge in China (the Wuhan Yangtze Bridge) in 1957 [31] and another one involving a pedestrian suspension bridge in Kiev following its opening in 1958 [32].

This shows that the problem of crowd-induced lateral vibrations is not limited to footbridges. In fact, several large road bridges around the world have suffered from this problem during exceptional crowd events, such as opening day events [33], public demonstrations or festive events [4, 34]. Even the 120 year old Brooklyn Bridge in New York City swayed remarkably when traversed by crowds of pedestrians

during a power black out, leading to several complaints from concerned citizens [35, 36]. Characteristic for these cases is that there are no reports on how or whether these issues were assessed any further or if they have been observed on other occasions.

The first assessment of lateral crowd induced excitation was offered by Petersen [37] (as reviewed by Bachmann and Ammann [38]), who observed strong lateral vibrations of a steel arch footbridge at Erlach in Germany, during crossing of about 300-400 pedestrians. The vibration occurred on the 110 m main span of the bridge at frequency around 1.1 Hz and were explained as a consequence of a lateral sway of the centre of gravity of the human body occurring at half the pacing frequency, resulting in resonant vibrations and a synchronisation of the step with the oscillation of the bridge, [39]. In this particular case, the vibration problem was solved by installing a horizontal Tuned Mass Damper (TMD).

Figure 1: Toda Park Bridge in Toda City, Japan (T-Bridge). (Figures from [40] (left) and [41] (right))

One of the most cited incidents of excessive lateral vibrations occurring in the last century is related to the Toda Park Bridge in Toda City, Japan (T-bridge) [42, 43]. The bridge is a cable-stayed bridge with the overall length of 179 m divided into a main span (134 m) and a side span (45 m), see Fig. 1. The frequency of the fundamental vibration mode was reported 1.0 Hz but would drop to 0.91 Hz when fully congested with people. The bridge that connects a stadium and a bus terminal was traversed by around 20 000 pedestrians following a boat race with up to 2000 people simultaneously on the bridge (corresponding to a crowd density of 2.1 ped/m^2). During this event, the lateral acceleration of the bridge girder was an order of magnitude larger than predicted when assuming resonance pacing rate of all pedestrians and mutually independent (random) phases. Video analysis was used to track the head movement of randomly selected pedestrians and it was found that up to 20 % synchronised their walking to the movement of the bridge. This observation was used to describe the phenomenon of human-structure phase synchronisation (or "lock-in" as follows, [42]: "First a small lateral motion is induced by the random lateral human walking forces, and walking of some pedestrians is synchronised to the girder motion. Then resonant force acts on the girder, consequently the girder motion is increased. Walking of more pedestrians are synchronised, increasing the lateral girder motion. In this sense, this vibration has a self-excited nature. Of course, because of adaptive nature of human being, the girder amplitude will not go to infinity and will reach a steady-state". It is worth noting that this description, although more detailed, is essentially similar to that of Petersen [37], from 1972.

Finally two 3D steel truss footbridges designed by the world renown architect and structural engineer

Santiago Calatrava, for the 1998 World Exposition in Lisbon exhibited strong lateral vibrations when traversed by only few pedestrians. The bridges that connect the Orient Railway Station to the Vasca da Gama Shopping Centre are now closed to the public, partly due to their poor dynamic performance [44].

3. Lateral footstep forces on a rigid surface

During walking, the ground reaction force (GRF) occurs due to acceleration (and deceleration) of the centre of mass (CoM) of the body. In general the GRF is a three dimensional vector which varies in time and space due to the forward movement of the person [29].

As reviewed by Zivanovic et al. [28], early studies on the lateral component of the GRFs were carried out by Harper et al. [45], which revealed that the horizontal component of the force was generally very small and that its lateral component is caused by balancing of the body during walking. Andriacchi et al. [46] measured single footstep forces using a force plate and report that the peak force amplitudes (vertical and lateral) increase numerically with an increase in the walking speed. Similar observations were made more recently by Masani et al. [47]. Chao et al. [48] measured single footstep forces from several persons and found that the peak lateral forces (F_1 to F_3 in Fig. 2) are around 4 to 5 % of the body weight for men and little less for women, but with a considerable difference between individuals. It was further found that the sex-related variation in the GRF was more significant than the age-related variation.

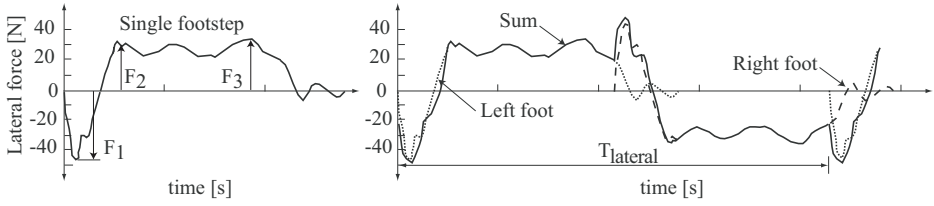

Figure 2: Typical shape of a walking force from two footsteps (Figure reproduced from [28])

Several parameters influence the shape of the GRFs which is governed by large intra and inter-subject variability. The intra-subject variability is related to changes in the GRF from the same person, measured at two different time instances, whereas the inter-subject variability refers to the variability between different people [28, 29]. Variations in the gait parameters during continuous walking is a form of intra-subject variability which causes random fluctuations in the shape of the GRF from each footstep. However, perfect periodicity in the walking is often assumed as it implies that the force time history of a series of consecutive steps can be modelled as a Fourier series with fundamental harmonic equal the duration of two consecutive steps (Fig. 2):

$$F_L(t) = \sum_{j=1}^{n} G_j \sin\left(2\pi j f_w t - \phi_j\right). \tag{1}$$

The fundamental frequency, f_w, of the Fourier series therefore equals the walking frequency (defined as half the pacing rate f_p) and G_j and ϕ_j represent the load amplitude and phase angle of load harmonic

j, respectively. Often the load amplitude is defined through the body weight normalised dynamic load factor (DLF), $\mathrm{DLF}_j = G_j/W$. According to Bachmann and Ammann [38] the value of the first five DLFs are $\mathrm{DLF}_j = \{0.039,\ 0.01,\ 0.042,\ 0.012,\ 0.015\}$, $j = 1 \ldots 5$. In a later publication by same authors, the values $\mathrm{DLF}_1 = \mathrm{DLF}_3 = 0.1$ are suggested for design purposes [49].

Other researchers have similarly determined the DLFs from measured GRFs using instrumented force plates [50, 51]. Butz [50] reports that the mean value for the fundamental DLF is 0.038, which is based on measurement from 98 persons at various age crossing an outdoor catwalk with integrated force plates. Crowe et al. [52] measured DLFs for both the first and the second load harmonics and the mean values were reported as $\mathrm{DLF}_1 = 0.046$ and $\mathrm{DLF}_2 = 0.003$.

Non-zero load harmonic at even integer harmonics implies that the walking is imperfect. As already indicated, this intra-subject variability is caused by small variations in the load pattern for each step during the walking, e.g. due to difference between GRF from strong and weak leg [53]. In a load modelling perspective, this was initially addressed by Brownjohn et al. [54] who measured continuous vertical loads using an instrumented treadmill and subsequently suggested that the load could be treated as a narrow-band random process.

Later, Pizzimenti [55] used an instrumented treadmill to measure the lateral component of the GRFs from 66 individuals and Ricciardelli and Pizzimenti [56] defined DLFs for an average (perfectly periodic) footprint as the sum of the contributions in the Fourier spectra of the measured force in a narrow band around the frequency of the respective harmonic. The characteristic values (with 95 % probability of non-exeedance) of the first five DLFs were reported as $\mathrm{DLF}_{j,k} = \{0.04,\ 0.0077,\ 0.023,\ 0.0043,\ 0.011\}$, $j = 1 \ldots 5$. In their model, the band width was taken as $\Delta f_j = \pi \zeta_j j f_w$ (jf_w: frequency of jth load harmonic, ζ_j: a structural damping, assumed 1 %) following the approach of Ohlsson [57] and Eriksson [58].

Due to the non-deterministic nature of the loading, a frequency-domain representation was offered by Pizzimenti and Ricciardelli [59] through a characteristic Power Spectral Density (PSD) for the first five load harmonics. The general (non-dimensional) form was given as:

$$\frac{S_{F_L}(f) \cdot f}{\tilde{F}_{Lj}^2} = \frac{2A_j}{\sqrt{2\pi} B_j} \exp\left\{ -2 \left[\frac{f/jf_w - 1}{B_j} \right]^2 \right\} \tag{2}$$

where A_j and B_j are parameters determined by the data fit and $\tilde{F}_{Lj}^2$ is the area of the PSD around the jth harmonic, see Table 1.

Studies have shown that there is a variability between overground and treadmill locomotion and in particular an increase in the cadence and a decrease in the stance period have been observed for walking on treadmills [60, 61]. According to Sahnaci and Kasperski [62], force plate measurements only capable of measuring single footsteps introduce a bias in the GRF opposed to natural walking because the test subjects have to adjust their walking speed and step length when approaching the force plate. For this reason they used a platform supported on load cells, allowing measurements of GRFs for several consecutive footsteps. The fundamental DLF from 251 (195 male and 56 female) test subjects is shown in Fig. 3. It is noted that the fundamental load amplitudes (with characteristic value $\mathrm{DLF}_{1,k} = 0.04$) as

Table 1: Parameters for PSD in Eq. (2) according to Pizzimenti and Ricciardelli [59]

	$j=1$	$j=2$	$j=3$	$j=4$	$j=5$
A_j	0.96	0.73	0.879	0.55	0.74
B_j	0.0616	0.039	0.0288	0.037	0.025
$\left(\tilde{F}_{Lj}^2/\tilde{F}_L^2\right)_k$	0.81	0.050	0.277	0.047	0.072
$\tilde{F}_L^2$ (mean)			$0.0012W^2$		
$\tilde{F}_L^2$ (characteristic)			$0.0020W^2$		

reported by Ricciardelli and Pizzimenti [56] are generally lower than those in Fig. 3. According to Sahnaci and Kasperski [51] this difference may be attributed to a general difference between GRFs as measured on a treadmill compared to overground walking. However, since this value represents an equivalent DLF which takes into account imperfections during walking and the narrow band of the structure, a direct comparison between the DLFs from the two studies is not possible. A further discussion on the difference between treadmill and overground walking is presented by Racic et al. [29].

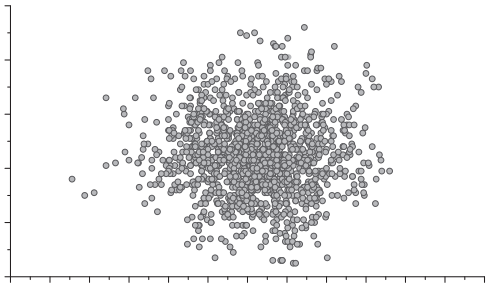

Figure 3: Measured DLFs for the first load harmonic. (Figure from [53])

A promising method to overcome the trade-off between short duration measurements on platforms of limited length and the subjectivism associated with treadmill walking is to use pressure insoles to measure the GRF from walking. Fong et al. [63] describes a system capable of measuring all components of the GRF, but to the authors' knowledge GRFs from continuous walking have not yet been published.

The investigations presented in this section are related to the lateral GRFs measured on rigid surfaces such as single footprint force plate fixed to the ground, a treadmill or laterally restrained platforms. However, for bridges with low natural frequencies, the effect of the lateral motion on the GRF and the change in the crowd dynamics due to human-structure interaction must be accounted for. Until the beginning of this millennium, only few studies existed about the effect of a laterally moving surface on the GRFs. However, with the serviceability failures of pont de Solférino in Paris and the Millennium

Bridge in London a new tract of research was established, devoted to the understanding of the interaction between pedestrian walking and a laterally moving surface and in particular its effect on the lateral GRF. Therefore, the remaining part of this review is based on research carried out in the period between 2000 and 2010.

4. Paris pont de Solférino and London Millennium Bridge

On December 15, 1999, pont de Solférino footbridge (now called Passarelle Léopold-Sédar-Senghor) across the Seine in Paris, linking the Musee d'Orsay to the Tuileries Gardens was opened to the public for crossing. On the opening day of this 140 m long steel arch footbridge, unexpected lateral oscillations developed and the bridge was subsequently closed to the public. A comprehensive test program was undertaken which involved modal testing of the structure, pedestrian crowd tests and installation of 14 TMDs with subsequent testing and monitoring of the bridge. In November 2000, the bridge was reopened after almost a year of temporary closure.

An almost identical scenario played out in London, which involved the Millennium Bridge, designed by a team of architect Lord Norman Foster (Foster and Partners), sculptor Sir Anthony Caro and engineering consultants Ove Arup Partnership. The London Millennium Bridge, which connects St. Paul's Cathedral with the Tate Modern Gallery was the first entirely new bridge across the Thames in London for over a century, or since Tower Bridge was completed in 1894 [64]. The bridge is an extremely shallow suspension bridge in three spans; a south span of 108 m, a central span of 144 m and a north span of 81 m. The bridge deck has a width of 4 m and consists of aluminium box sections creating a very light superstructure (2 t/m) [4]. In the design competition submission, the bridge was described as a "'thin' blade of stainless steel and cables, whilst at night it will appear as a 'blade of light'" [65].

Figure 4: Pont de Solférino in Paris (left)(Picture from `http://www.mimram.com/`) and the London Millennium Bridge (right).

On the opening day, 10 June 2000, large lateral vibrations occurred when between 80 000 and 100 000 people crossed the bridge, with up to 2000 people on the deck at any one time [4, 34]. Large amplitude vibrations in four different vibration modes were reported; on the Southern span at frequency around 0.8 Hz, at the central span in the first and second lateral vibration modes at 0.48 Hz and 0.95 Hz respec-

tively and more rarely on the Northern span at frequency around 1 Hz. On 12 June 2000, it was decided to close the bridge for pedestrian traffic, while a retrofit solution could be developed and implemented. During the next 18 months an extensive test program, similar to that in Paris was undertaken. One of the main observations made on the opening day was that the bridge exhibited a stability-like behaviour. The bridge vibrated excessively when congested by a large crowd of people, but if the number of pedestrians was reduced or if they stopped walking, the bridge vibration would reduce substantially [4, 66].

On 14 June, an interesting attempt to explain the cause of the excessive vibrations was provided by Professor Josephson, in a letter to The Guardian [67], stating that "the problem has little to do with crowds walking in step: it is connected with what people do as they try to maintain balance if the surface on which they are walking starts to move".

4.1. Full scale testing of pont de Solférino

The full scale testing of the bridge involved a modal identification of the empty structure which revealed ten vibration modes with frequencies lower than 5 Hz, three of which were identified as critical; a horizontal (lateral) mode with coupled torsional movement at frequency 0.81 Hz and two torsional modes at 1.94 Hz and 2.22 Hz respectively. The generalised mass of the first vibration mode was reported as approximately 400 t [68]. The damping ratios (of the empty structure) were extremely small, but increased considerable with the presence of stationary pedestrians (in total 116 people) [69]. This human-structure interaction for passive (standing) people is well known [70], whereas the effect of walking on the apparent modal damping is less researched. However, recent research suggests that also walking pedestrians add damping to perceptibly vibrating structures in the vertical direction [71–74]. The characteristics of the first six vibration modes are shown in Table 2.

Table 2: Modal properties of pont de Solférino without added damping

Description	Frequency (Hz)	Damping (empty) (%)	Damping (with 116 people) (%)	Modal mass (tonne)
Symmetric horisontal mode	0.81 (0.70)[1]	0.38 (3.5)[1]	1.6	400
First anti-symmetric vertical mode	1.22	-	-	not reported
First anti-symmetric torsional mode	1.59	0.2 - 0.5	-	not reported
First symmetric vertical mode	1.69	0.49	-	not reported
First symmetric torsional mode	1.94	0.50	1.36	not reported
Second symmetric torsional mode	2.22	0.28	1.60	not reported

[1] After installation of 6 horizontal TMDs.

The first series of crowd tests was performed on the bridge in February 2000 using up to 122 pedestrians test subjects performing different types of rhythmic activities. Dziuba et al. [69] report that a large number of pedestrian could produce excessive lateral response of the first mode with acceleration

amplitudes up to $0.6\,\mathrm{m/s^2}$ (displacement 24 mm). A total of 14 TMDs (weight 2500 kg) was installed on the bridge, 6 of which were designed to suppress horizontal vibrations. As such, the modal frequency of the fundamental lateral mode dropped to around 0.7 Hz and damping increased to 3.5 %.

In 2002, another test campaign was arranged, which involved up to 386 volunteering pedestrians. In the main crowd tests (with inactive TMDs), the number of pedestrians on the bridge was gradually increased to a maximum of 207 to 229 people and the walking speed of the pedestrians was varied between very slow and slow walk in an attempt to match the natural frequency of the first mode without enforcing a controlled walking frequency. In each of the three tests and for each walking speed the group circled the bridge for about 15 minutes. The equivalent number of resonance pedestrians was defined by Charles and Bui [75] as:

$$N_{eq} = \frac{\pi}{2}\sqrt{\frac{2}{T}}\frac{\int_t^{t+T} F(\tau)\dot{q}(\tau)\mathrm{d}\tau}{F_{1p}\sqrt{\int_t^{t+T}\left[\dot{q}(\tau)\right]^2\mathrm{d}\tau}} \tag{3}$$

where T is the modal period, $F(t)$ is the lateral modal force and F_{1p} is the amplitude of the first load harmonic of an equivalent single resonant pedestrian walking at a frequency that matches the modal frequency. The modal displacement is denoted $q(t)$ and the dot represents a differentiation with respect to time. The physical interpretation of N_{eq} is the number of uniformly distributed and synchronised equivalent pedestrians, which input the same amount of energy into the mode per oscillation period as that of the entire group [75]. The dynamic modal pedestrian force was derived from back-analysis of the measured acceleration response.

In Fig. 5, an acceleration time history is shown from one of the crowd tests together with the equivalent degree of synchronisation defined as N_{eq}/N. Charles and Bui [75] note that the three peaks in the response are due to uneven distribution of the pedestrians during the tests. Based on the circulating tests as well as the transient tests with a large number of people crossing the bridge in one group, it was concluded that excessive lateral vibrations could be initiated and that synchronisation of the pedestrian movement to that of the bridge occurred when the acceleration reaches a threshold of about 0.1 to $0.15\,\mathrm{m/s^2}$. It was further found that around 140 pedestrians were needed to obtain acceleration response exceeding $0.1\,\mathrm{m/s^2}$.

4.2. Full scale testing of the London Millennium Bridge

In July 2000, some initial full-scale tests were carried out on the bridge with around 100 employees from Arup. According to Dallard et al. [4], these tests were made to refine the load models for the pedestrians. To the authors knowledge, no results from these tests have been published.

The retrofit solution adopted on the Millennium Bridge consisted of 37 viscous dampers and 29 pairs of vertical TMDs. Prior to their installation, a modal identification of the structure was performed to validate the theoretical models and to test the effect of three prototype dampers. A custom made horizontal actuator with a moving mass of 1000 kg was used to identify the lateral vibration modes,

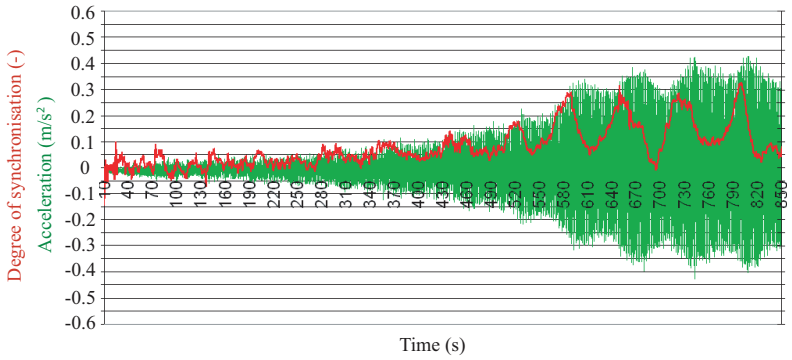

Figure 5: Lateral acceleration response and degree of synchronisation during circulations of an increasing number of pedestrians walking randomly at slow speed (Figure reproduced after [75]).

Table 3: Modal properties of the Millennium Bridge without added damping (Table reproduced with permission from Arup Partnership [76])

Description	Frequency (Hz)	Damping (%)	Modal mass (tonne)
First lateral mode of central span (CL1)	0.48 - 0.49	0.75 - 0.77	128 - 130
First lateral mode of Southern span (SL1)	0.80 - 0.81	0.6 - 0.7	172
Second lateral mode of central span (CL2)	0.95 - 0.99	1.3	145 - 148
First lateral mode of northern span (NL1)	1.04	0.32	113*
Third vertical mode of central span (CV3)	1.15 - 1.16	0.80	155
Fourth vertical mode of central span (CV4)	1.54 - 1.55	0.55	140
Fifth vertical mode of central span (CV5)	1.89 - 1.91	0.58 - 0.65	135
Sixth vertical mode of central span (CV6)	2.32 - 2.33	0.95	135

* Estimated from FE analysis due to poor quality measurements

Figure 6: Crowd tests on the London Millennium Bridge (Shown with permission from Arup Partnership).

whereas a counter-rotating eccentric mass shaker was used for the vertical ones. Four lateral and four vertical vibration modes were identified for the empty structure, see Table 3, [76–78].

On 19th December 2000, 275 Arup employees were used for crowd tests on the structure, (Fig. 6) with the primary purpose to validate the pedestrian loading model and to verify the stability like behaviour as observed during the opening days. In total, 14 different pedestrian crowd tests were made, most in which the number of pedestrians on the bridge was gradually increased. In Fig. 7 two different lateral acceleration response time histories are shown (measured in two different test series); on the left the response of the northern span (NL1) is shown and on the right, the response of the central span (CL1).

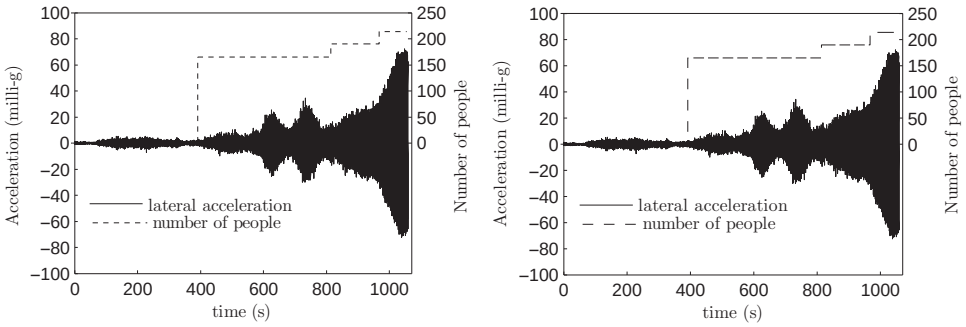

Figure 7: Lateral accelerations measured on the Millennium Bridge during different crowd tests. Left: Vibrations of the northern span at frequency 1.0 Hz (Figure from [34]). Right: Vibrations of the centre span at frequency 0.48 Hz (Reproduced with permission from Arup Partnership).

The test verified the initial observations that for a certain number of pedestrians, the response was limited, but a small increase beyond a critical number resulted in diverging response amplitudes. From simple energy considerations, it could be shown that the magnitude of the correlated (modal) pedestrian

force, F_{corr}, being the component in phase with the modal velocity could be written as [4]:

$$F_{corr} = F_D + 2M\frac{1}{\omega_0}\frac{\mathrm{d}\ddot{q}_0}{\mathrm{d}t} \tag{4}$$

where F_D is the damper force ($c\dot{q}_0$ for linear viscous damping), M is the modal mass, ω_0 is the angular modal frequency and $\dot{q}_0$ and $\ddot{q}_0$ are the amplitudes of the velocity and acceleration respectively. An important finding from the pedestrian tests is that the correlated pedestrian force was strongly related to the velocity of the structure, which suggests that pedestrians act as negative dampers on the structure, Fig. 8. However, an equally important observation was that the vertical response of the structure at twice the modal frequency did not show any disproportional increase in the response which would be expected as a consequence of synchronisation of the stepping frequencies. In January 2002 final pedestrian tests were made after installation of the damping devices and since its reopening no excessive vibrations have been reported on the bridge.

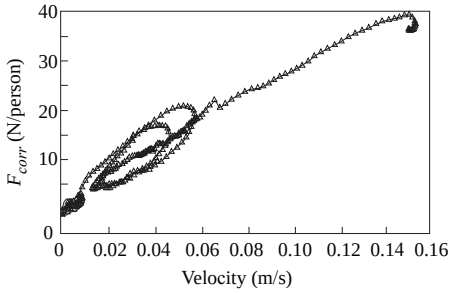

Figure 8: Correlated pedestrian force per person as function of the local velocity of the structure, derived from the response in Fig. 7 (right) as observed on the Millennium Bridge (Figure reproduced from [4]).

4.3. Laboratory tests

In addition to the full-scale testing of the London Millennium Bridge, a series of laboratory tests were undertaken during the eighteen month retrofit period. The experimental campaign involved walking on spot on a shaking table at the University of Southampton [4] and walking across a 7.3 m laterally driven test platform at Imperial College (see Fig. 9) [79]. It was reported that the lateral DLF increases with the vibration amplitude but is vibration frequency independent. The tests also revealed that the probability of "lock-in" increases with the vibration amplitude, from between 30-40 % at 5 mm amplitudes up to around 80 % at 30 mm [80]. A summary of published test results is shown in Fig. 10. The number of people used in the tests and the statistics of the results are not presented in the papers but the results provide a useful insight into the complexity of human-structure interaction in the lateral direction.

The research project related to the Solférino bridge was initiated by the French Road Directorate and involved a suspended laboratory platform (7 m by 2 m) with a variable lateral frequency in the range 0.5 to 1.1 Hz [75]. The dynamic (modal) pedestrian force was derived from the displacement response and its derivatives, obtained through numerical differentiation. Both transient response tests and tests where a

treadmill was placed on the platform were carried out and the main conclusions from the tests were that the peak value of the pedestrian force varies from 20 to 100 N, with mean value of the first load harmonic being 35 N, but no correlation with the velocity of the structure was observed. Further, it was concluded that a synchronisation phenomenon was observed with a distinct threshold of around 0.15 m/s^2, [5, 75].

Figure 9: Platform tests commissioned by the French Road Directorate (left) and Arup (right), (Pictures from [75] and `http://www.arup.com/millenniumbridge/`.)

McRobie et.al. [81] constructed a suspended platform (weight 1.2 – 2.0 t) with a lateral frequency between 0.7 Hz and 0.9 Hz equipped with a treadmill to study human-structure interaction and the potential for lock-in. Generally, it was observed that people tend to spread their feet further apart and walk at the same frequency (with constant phase) as that of the platform. The displacement of the rig was measured and by back-analysis of the response it was reported that the load amplitude could reach 300 N with the component in phase with the platform velocity (the correlated pedestrian force) up to 100 N at 100 mm vibration amplitudes [81]. The authors further describe the load as a consequence of a sudden change in the walkers gait rather than a velocity dependent increase. They argue that the increase in the overall correlated force observed on the Millennium Bridge could be attributed to an increased probability in gait transition (more pedestrians changed gait) as the vibration amplitude increased, which is consistent with the results presented in Fig. 10.

Video analysis was used by Fujino et.al. [42] to track the lateral head motion of randomly selected pedestrians during congested periods on the T-Bridge in Japan. They found that the amplitude of the head lateral motion increased with the lateral bridge amplitude and they concluded that in order to maintain body balance, people widen their gait. According to Fujino et.al. [42], laboratory experiments using a laterally moving platform, showed that people synchronise to a lateral motion for amplitudes in the range $10 - 20$ mm. On the T-bridge, the steady-state vibration amplitude reached approximately 10 mm causing 20 % of the pedestrians to synchronise to the vibration [42]. This is slightly lower than what the results from the Imperial College tests indicate (Fig. 10), where the probability of "lock-in" is $30 - 50$ % for a vibration amplitude of 10 mm.

In more recent papers [82, 83], Yoshida et al. also used the T-bridge to investigate the synchronisation of pedestrians, through an image processing technique. The data was used to estimate the pedestrian

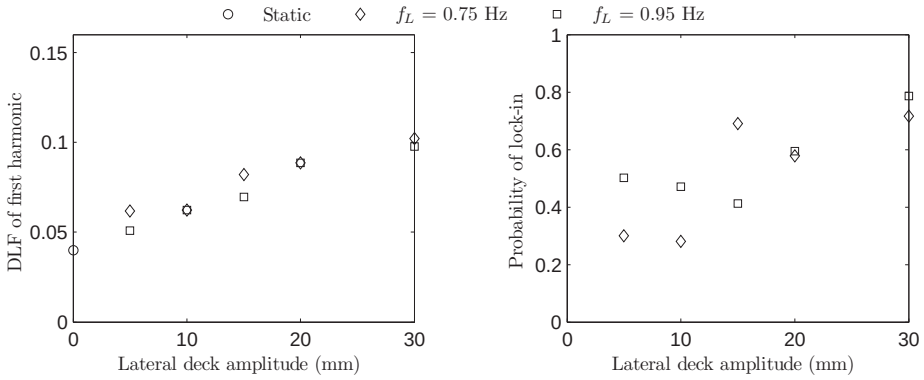

Figure 10: DLF and probability of "lock-in" for pedestrians walking on a vibrating surface. (Figure reproduced after [4])

forces and they report that during vibration amplitudes of 9 mm the average correlated pedestrian force amplitude is around 3.3 N [82], which is considerably lower than the forces reported from the Millennium Bridge (Fig. 8).

In a later publication by Yoshida et.al. [83] it was concluded that on average 60 % of the pedestrians had synchronised their pacing frequency to the lateral vibration frequency of the bridge during an event with large lateral response. Here the term "synchronisation" was attributed to pedestrians walking at a frequency ± 0.1 Hz the vibration frequency of the bridge (approximately 0.9 Hz), but not necessarily at constant or equal mutual phases. Bearing in mind that the typical standard deviation on pacing rate is 0.05 to 0.10 Hz [84], a considerable number of pedestrians will fall within the group of being synchronised, simply because their natural choice of footfall rate falls within the above mentioned boundaries.

4.4. Early analytical approaches

Arup's hypothesis, supported by the pedestrian crowd tests, is that the lateral pedestrian force has a component in phase with (correlated pedestrian force) and proportional to the velocity of the bridge during "lock-in", see Fig. 8. In this case, the correlated pedestrian force can be expressed as [4]:

$$F_{corr}(t) = c_p \dot{u}(t) \tag{5}$$

where $c_p = 300$ Ns/m is the velocity proportional lateral force coefficient and $\dot{u}(t)$ is the lateral velocity of the bridge. This finding led to Arup's stability criterion which can be expressed in terms of a critical number of pedestrians that will cancel the inherent structural damping and eventually lead to excessive vibrations, [4]:

$$N_{\mathrm{cr}} = \frac{4\pi\zeta f_0 M}{c_p \frac{1}{L}\int_0^L [\Phi(x)]^2 \mathrm{d}x}. \tag{6}$$

The quantities, ζ, M, f_0, $\Phi(x)$ represent the modal damping ratio, mass, frequency and shape of the lateral mode in question and L is the overall bridge length. This formula is also referred to as Arup's formula or Arup's stability criterion.

A different interpretation was given by Danbon and Grillaud [68], who define the load of the correlated (or synchronised) portion of the pedestrians as:

$$F(x,t) = Gb\rho\phi(u)\cos\omega t \tag{7}$$

where $G = 23\,\mathrm{N}$ is an average value of the amplitude of the first load harmonic from a pedestrian walking on a stationary surface, b is the width of the footbridge, ρ is the crowd density (persons/m^2) and $\phi(u)$ is the portion of the pedestrians who are synchronised with the lateral movement of the bridge. The parameters in the model were determined from fitting the model to the measured response on the Solférino bridge. The synchronisation function $\phi(u)$ was chosen as a bi-linear function, such that the synchronisation increases linearly from 5 % (at $u = 1$ – 2 mm) to maximum ($\phi = 0.80$ – 1.0) when $u = 5$ – 6 mm.

Based on the results of the laboratory experiments at Imperial College, Newland [85, 86] presented a feedback model of synchronous lateral excitation in which the feedback force is proportional to the displacement of the structure rather then the velocity. Mathematically, the feedback model was expressed in terms of the Fourier transforms $X(i\omega)$ and $Y(i\omega)$ of the modal excitation force and the modal displacement respectively:

$$Y(i\omega) = H(i\omega)\left\{X(i\omega) + \alpha(i\omega)Y(i\omega)\right\}. \tag{8}$$

The complex frequency response function and the modal force exerted by the pedestrians per unit modal displacement are denoted $H(i\omega)$ and $\alpha(i\omega)$ respectively. Furthermore, he assumes that the nature of the synchronisation is such that people will naturally fall into step with each other and adjust their phases such as to increase the motion of the bridge to a maximum. This assumption leads to a stability criterion similar to the one in Eq. (6). The justification for assuming that people will adjust their phases such that the maximum response is based on a description of pedestrian behaviour given by Dallard et.al. [34].

In a later paper, Newland [87] proposed a simplified load model in which the load transferred to the pavement by the walker is modelled as two inertia force terms: "The first arises from the natural displacement of a person's centre of mass while walking on a stationary pavement, and the second from the additional displacement that occurs as a consequence of movement of the pavement", [87]. The model takes the following form:

$$F(t) = m_0\beta\ddot{y}(t) + m_0\alpha\beta\ddot{u}(t-\Delta) \tag{9}$$

where $y(t)$ is the natural movement of the pedestrian's centre of mass, $u(t)$ is the movement of the pavement, m_0 is the mass of a single pedestrian and Δ is a time lag. The coefficient $\alpha = 2/3$ was derived based on the platform test at Imperial College presented in Fig. 10 and β is a synchronisation factor.

Based on this model, the damping ratio required for the bridge to be stable was derived as function of the modal mass of the bridge, M and that of the pedestrians, M_p, as $\zeta > \frac{1}{2}\alpha\beta M_p/M$.

It is worth mentioning an interesting analogy to wind engineering presented by McRobie and Morgenthal [88] where the non-dimensional "Pedestrian Scruton Number" was proposed as a measure for the susceptibility of a pedestrian bridge to excessive vertical vibrations. Newland [85] used this analogy to define the pedestrian Scruton number for lateral vibrations as:

$$S_{cp} = \frac{2\zeta M}{M_p} \tag{10}$$

where S_{cp} is the pedestrian Scruton number, M is the modal mass of the bridge and M_p is the modal mass of pedestrians. Now Arup's stability criterion in Eq. (6) can be rewritten in terms of a minimum Scruton number as:

$$S_{cp} > \frac{c_p}{2\pi f_0 m_0}. \tag{11}$$

Newland's stability criterion can also be written this way, to yield $S_{cp} > \alpha\beta$ as a criterion for stable bridge behaviour, [87].

5. Lateral footstep forces on a moving surface

The importance of human-structure interaction was highlighted with the the problems associated with the Solférino Bridge in Paris and the London Millennium Bridge. As such, several researchers have investigated the behaviour of pedestrians walking on various forms of laterally moving surfaces.

5.1. Walking on instrumented platforms

Rönnquist [89] measured lateral GRFs during crossing of a 4 m long suspended platform with adjustable lateral frequencies which varied between 0.75 Hz, 0.84 Hz, 0.95 Hz and 1.14 Hz. For each platform frequency, three different pacing rates were selected and the total of 1087 footsteps were recorded, but using only four different test persons. The study revealed that the lateral load increases with the lateral acceleration of the platform and also as the walking frequency approaches the natural frequency of the platform, [89]. Rönnquist and Strømmen [90] defined an equivalent DLF, calculated such that a single waveform with weight normalised amplitude DLF_{eq} contains the same impulse as the overall weight normalised measured footstep force. An expression for the DLF as a function of the pedestrian detuning away from the resonance frequency $(f_w - f_n)$ and the structural acceleration was given in [90] as:

$$\mathrm{DLF}_{eq} = 0.145 - 0.1\exp\left\{-\left(0.45 + 1.5\exp\left[-\frac{1}{2}\left(\frac{f_w - f_n}{0.07}\right)^2\right]\right)\ddot{u}_0^{1.35}\right\} \tag{12}$$

where $\ddot{u}_0$ is the amplitude of the structural acceleration and $f_w - f_n$ is the pedestrian de-tuning from the natural frequency of the structure. Ronnquist [89] also defined the first four DLFs of the lateral force obtained from a Fourier analysis of two consecutive footsteps. The DLF of the first harmonic was almost identical to that in Eq. (12) and is not repeated here. The DLF for the higher harmonics were

$\mathrm{DLF}_2 = 0.010 + 0.008\,\ddot{u}$ and $\mathrm{DLF}_3 = 0.015$ and $\mathrm{DLF}_4 = 0.005$. No information was provided regarding the phase of the load harmonics, thus no distinction is made between added mass or added damping (positive or negative). Furthermore, the platform used in the study was light and the measured footstep forces are applicable to accelerations in excess (up to $2\,\mathrm{m/s^2}$) of what is normally considered acceptable on a footbridge. However, Rönnquist and Strømmen state that for this reason their results provide a conservative estimate to the load induced by pedestrians on a laterally moving surface [89].

Butz [50] used a laterally driven platform equipped with four integrated force plates (see Fig. 11) to measure GRFs from 98 different persons and to quantify their degree of synchronisation. The platform (length 12 m) was driven in a sinusoidal lateral motion at frequencies ranging from 0.6 to 1.5 Hz with displacement amplitudes in the range 3 to 40 mm. The lateral GRFs were measured for slow, normal and fast walking speed. Three different degrees of synchronisation were reported; 1) crossing is completely synchronised, 2) crossing is not completely synchronised, but the pedestrian changes to synchronised walking during a passage, and 3) not synchronised or negatively synchronised (i.e. adds damping to structure). It was found that persons with natural walking frequency (i.e. as measured on a fixed floor) within ± 0.1 Hz from the lateral vibration frequency, will potentially synchronise to the structural motion and those with a lower initial walking frequency have a larger probability to synchronise than those with a higher one. Butz [50] further reports that the measured DLFs tend to increase (slightly) with the lateral platform acceleration amplitude, but due to large scatter in the data, the following values were suggested for design:

$$\mathrm{DLF}_1 = \begin{cases} 0.04, & \text{unsychronised pedestrians or fixed floor;} \\ 0.055, & \ddot{u}_0 \leq 0.5\,\mathrm{m/s^2}; \\ 0.075, & \ddot{u}_0 > 0.5\,\mathrm{m/s^2}. \end{cases} \tag{13}$$

Figure 11: left: Laterally driven platform at RWTH Aachen (Picture from [8]). Middle: Laterally driven treadmill at the University of Reggio Calabria (Picture from [55]). Right: Instrumented treadmill on a shaking table at Tongji University (Picture from [31]).

A different approach than those described earlier was taken by Nakamura et al. [91], who used an instrumented shaking table to investigate walking on the spot when subject to lateral vibrations with frequencies ranging from 0.75 to 1.25 Hz at displacement amplitudes 10 to 70 mm. Five tests subjects, equipped with accelerometers on their waist, were asked to walk on the spot while a simultaneous

measurement of the GRF was made. It was found that the weight-normalised force increased almost linearly with the vibration amplitude at all frequencies from around 0.10 at 10 mm amplitude to around 0.16 at 70 mm. It is a bit unclear how this force is defined, i.e. if it is a peak value, RMS or DLF of first load harmonic, therefore the two values can only be treated qualitatively. A synchronised pedestrian was defined as one walking with the same frequency as that of the shaking table and the tests revealed that only at the frequencies 0.87 Hz and 1.00 Hz the pedestrian tended to synchronise, the probability for this being 20 % and 40 to 50 % in the two cases respectively. This observation is generally in agreement with those of Butz [50], as described earlier. However, due to the limited number of pedestrians used in the tests and the unnatural circumstances for the walking, the results should be taken with some precaution.

5.2. Walking on laterally moving treadmills

The utilisation of instrumented treadmills for the determination of pedestrian-induced forces offers some advantages opposed to platforms of limited length where only a single or few consecutive footsteps can be recorded. In particular, the possibility to measure continuous time-histories of the pedestrian-induced forces has attracted some researchers.

Sun and Yuan [31] fixed an instrumented treadmill on a force plate which in turn was fixed onto a shaking table, Fig. 11. Seven different pedestrians were asked to walk (freely) on a treadmill at two different walking speeds 1.0 m/s (3.6 km/h) and 0.83 m/s (2.99 km/h) subjected to different combinations of lateral vibration frequencies (0.65 to 1.2 Hz) and amplitudes (4 to 50 mm). A simple equation was proposed for the DLF of the first load harmonic as function of the vibration amplitude, u_0 (in [m]) of the structure:

$$\mathrm{DLF}(u_0) = 1.18u_0 + 0.05 \qquad \text{for} u_0 < 0.05\,\mathrm{m} \tag{14}$$

It was observed during the tests that when $u_0 > 0.05$ m, people could not continue to walk steadily and had to hold the handrail to maintain their balance, hence the limit in Eq. (14). Sun and Yuan [31] report that for small vibration amplitude, the relative pedestrian phase is variable (non-constant), but as the amplitude increases the phase becomes (almost) constant and the walking frequency changes to the vibration frequency. Further, they find that on average the pedestrian load is 140.8 deg ahead of the bridge motion with standard deviation 17.9 deg. Based on their studies a qualitative equation for the probability of synchronisation as function of the vibration amplitude (u_0) and vibration frequency (f_s) was proposed [31]:

$$\rho_s(u_0, f_s) = \frac{u_0}{u_0 + c_1} e^{-c_2(f_s-1)^2} \tag{15}$$

with c_1 and c_2 as unknown parameters.

Pizzimenti [55] constructed an instrumented treadmill which could be driven in a sinusoidal lateral motion at predefined combinations of frequency and amplitude (see Fig. 11). In a pilot study, the loads from five different test subjects were obtained at three different vibration amplitudes (15 mm, 30 mm and 45 mm) and at five different lateral frequencies in the range 0.60 to 0.92 Hz. From the PSD of the load,

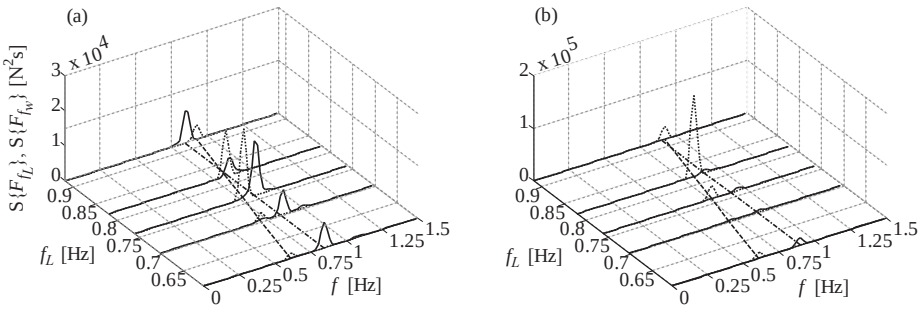

Figure 12: Examples of the PSDs of the lateral pedestrian force as a function of the lateral vibration frequency (f_L) where the solid line represents F_{f_w} and the dashed line F_{f_L} for fixed vibration amplitudes of 15 mm (a) and 30 mm (b), respectively (Figure reproduced from [59]).

two different force components were observed, the first one is centred around the walking frequency and its higher harmonics and the second one occurs at a frequency equal the vibration frequency and was denoted "the self-excited force", [59]. The pedestrian-induced lateral force was therefore written as the sum of these two components:

$$F(t) = F_{f_w}(t) + F_{f_L}(t) \tag{16}$$

where f_w is the frequency of the first load harmonic (i.e. the walking frequency) and f_L is the lateral vibration frequency. In Fig. 12 the PSD of the total lateral force for one test subject is shown for two different vibration amplitudes, 15 mm and 30 mm. The self-excited force was further subdivided into an in-phase (with displacement) and out-of-phase lateral pedestrian load components as:

$$F_{f_L}(t) = \mathrm{DLF_{in}} W \sin(2\pi f_L t) + \mathrm{DLF_{out}} W \cos(2\pi f_L t) \tag{17}$$

The DLFs ($\mathrm{DLF_{in}}$ and $\mathrm{DLF_{out}}$) were determined by using a nonlinear least-square-fit where the function in Eq. (17) was fitted to the measured force, [55]. The mean value of the measured DLFs from the five test subjects are shown in Fig. 13. According to the definition of the pedestrian-induced load in Eqs. (16) and (17), $\mathrm{DLF_{in}} > 0$ implies that the pedestrian adds to the modal mass, whereas $\mathrm{DLF_{in}} < 0$ was explained as added stiffness [59]. Similarly, $\mathrm{DLF_{out}} > 0$ corresponds to negative damping. Two interesting phenomenon were observed, firstly pedestrians seem to act as negative mass on the structure (or positive stiffness) over the entire frequency range, which is contradictory to common belief that a pedestrian adds to the modal mass of the structure. Furthermore, only for one combination of frequency and amplitude, the pedestrians act as negative dampers.

Motivated by the need of statistically reliable data for the pedestrian-induced lateral forces, Ingólfsson et al. [92] carried out an extensive experimental campaign using the instrumented treadmill from Pizzimenti's work [59]. The campaign focused on studying the lateral forces generated by single pedestrians during continuous walking on both fixed as well as laterally driven treadmill. The lateral forces were measured from seventy-one individuals at varying combinations of vibration frequencies (0.33 – 1.07 Hz)

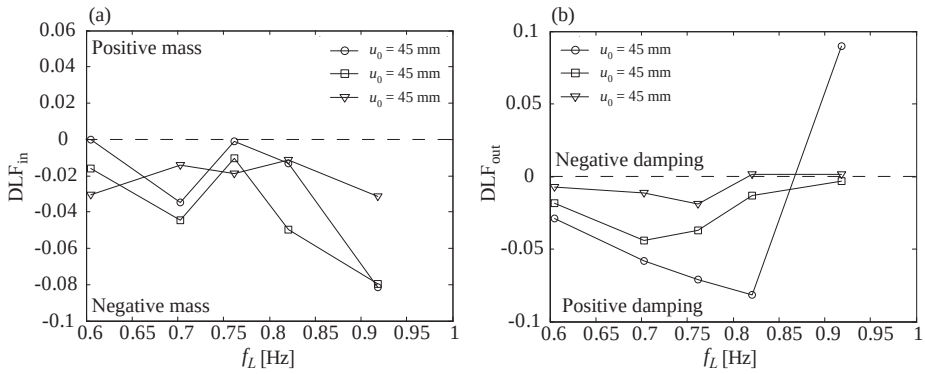

Figure 13: Average DLF for the in-phase (a) and out-of-phase (b) components of the self-excited pedestrian force. (Figure reproduced from [59])

and amplitudes (4.5 – 48 mm). By covering more than 55 km of walking distributed over almost 5000 individual tests, the data comprises the largest database of pedestrian-induced lateral forces that has been published to date. The results from the pedestrian tests were presented in terms of the velocity and acceleration proportional pedestrian load coefficients c_p and ϱ_p respectively. The velocity proportional coefficient (or pedestrian negative damping constant) was determined such that the work done by the real (measured) pedestrian force on the lateral displacement of the treadmill should equal the work done by an equivalent linear viscous damper with coefficient $-c_p$ (due to the selected sign convention). The following expressions were derived for c_p and ϱ_p [92]:

$$c_p = \frac{2}{\dot{u}_0^2}\frac{1}{T_{tot}}\int_0^{T_{tot}} F(t)\dot{u}(t)\,\mathrm{d}t = \frac{2\mathrm{Cov}\left[F(t),\dot{u}(t)\right]}{\dot{u}_0^2} \tag{18}$$

$$\varrho_p m_p = \frac{2}{\ddot{u}_0^2}\frac{1}{T_{tot}}\int_0^{T_{tot}} F(t)\ddot{u}(t)\,\mathrm{d}t = \frac{2\mathrm{Cov}\left[F(t),\ddot{u}(t)\right]}{\ddot{x}_0^2} \tag{19}$$

where Cov[ ] is a covariance operator and T_{tot} is the total duration of the load process. In Fig. 14, the results from the experimental campaign are shown (a)-(b) as probability distributions and as frequency dependent mean values taken across all test subjects and vibration amplitudes. The frequency axis is normalised with the mean walking frequency of the pedestrian test subjects. It should be noted that positive values of c_p and ϱ_p indicate an overall decrease in the modal damping and mass of the structure occupied by the pedestrian. The following main conclusions could be deduced from the study [92]:

1. Pedestrians extract energy from the structure (act as negative dampers) at most of the frequencies that were tested.
2. At lower frequencies pedestrians decrease the overall modal mass, but add to it at higher frequencies.
3. The load coefficients generally decrease (numerically) with increasing vibration amplitude, suggesting a certain self-limiting effect of the load.

4. Large scatter in the data makes a deterministic description of the experimental data impossible. Instead the load coefficients must be quantified through their probability distributions.

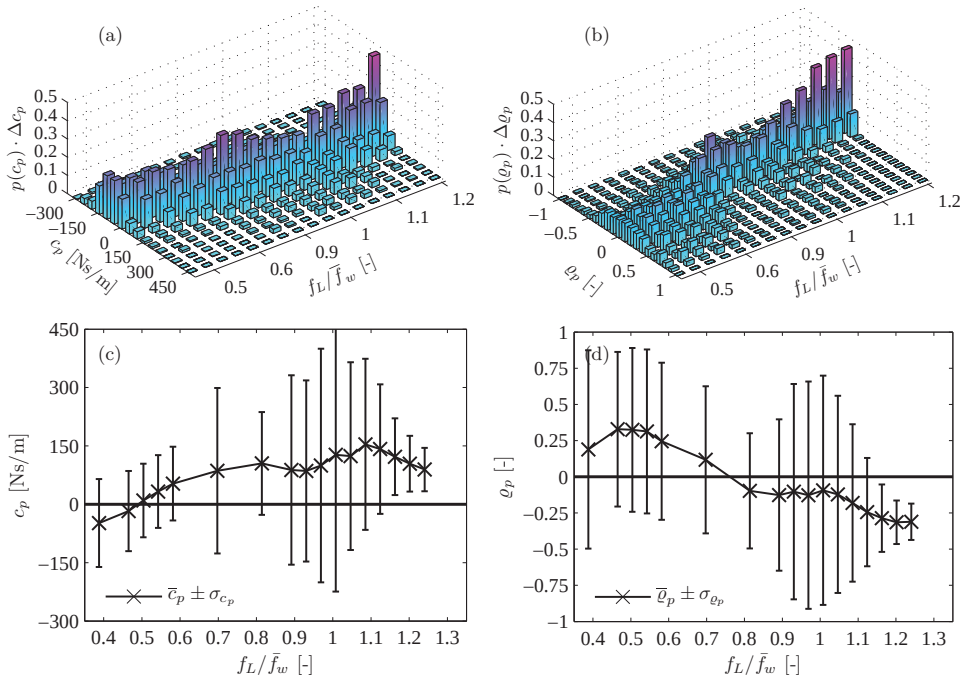

Figure 14: Probability distributions of (a) damping proportional coefficient, c_p, and (b) inertia proportional coefficient, ϱ_p, at different frequencies shown as functions of the normalised frequency and mean value ± one standard deviation of (c) c_p and (d) ϱ_p.

In a complimentary study, Ingólfsson et al. [93] studied the walking pattern of few test subjects that were instrumented with a waist-mounted accelerometer. By analysing the relative phase between the pedestrian movement and the movement of the underlying surface, it was shown that human-structure synchronisation is not a pre-condition for the development of positive values of the velocity proportional load coefficients, c_p, (i.e. negative damping) which may lead to excessive lateral vibrations.

5.3. Concluding remarks

Experimental studies on human walking on laterally moving platforms have generally been used to determine the pedestrian-induced lateral loads, their dependency on the vibration characteristics and to investigate the type of human-structure interaction, in which pedestrians possibly synchronise their walking to the movement of the underlying surface through alterations in their gait. As illustrated in the previous sections, several different experimental studies have been carried out which have provided a useful insight into the problem. For instance, there seems to exist a general agreement that the amplitude

of the pedestrian-induced lateral load increases with the vibration amplitude. A comparison between the DLF of the first lateral load harmonic as reported in different studies are summarised in Table 4.

Table 4: Comparison between fundamental DLFs from different studies.

Reference	General expression	Amplitude range
Bachmann and Ammann, [38]	0.039	fixed surface
Bachmann et.al., [49]	0.10	fixed surface
Kasperski, [53]	Fig. 3	fixed surface
Ricciardelli et.al., [94] (Mean value)	$0.05 f_w - 0.011$	fixed surface
Ricciardelli et.al. [94] (95 %)	$0.05 f_w + 0.001$	fixed surface
Pizzimenti and Ricciardelli [59] (Mean value)	Fig. 13	0 - 45 mm
Butz, [50]	0.038	fixed surface
	0.055	$\ddot{u}_0 < 0.5\,\mathrm{m/s^2}$
	0.075	$\ddot{u}_0 > 0.5\,\mathrm{m/s^2}$
Rönnquist and Strømmen, [89]	Eq. (12)	0 - 2 $\mathrm{m/s^2}$
Dallard et.al., [4]	Fig. 10	0 - 30 mm
Sun and Yuan, [31]	$1.18\,u_0 + 0.05$	$u_0 < 0.05$ m

Furthermore, many investigators have shown that human-structure synchronisation can only occur when the normal (or freely selected) walking frequency is close to the lateral vibration frequency. The large vibrations observed in the fundamental lateral mode of the Millennium Bridge at frequencies well below the normal walking frequency (0.5 Hz) render the importance of phase synchronisation for the development of excessive vibrations questionable. As presented in this review, there is a general dispute regarding the fundamental nature of human-structure interaction and the importance of synchronisation. However, synchronisation should be regarded as the most extreme form of pedestrian loading, but not a necessary onset for excessive vibrations.

6. Full scale measurements of other footbridges

As modal identification techniques are increasingly improving and both the hardware and software for vibration measurements is becoming more compact and user friendly, full scale testing of footbridges is an increasingly important tool in the assessment of pedestrian-induced vibrations of footbridges. This includes both the determination of modal properties, [95–97] and measurements of the response to large pedestrian crowds.

Even in the newest version of the Eurocode (Annex A2 of EN 1990:2002 [98]) it is stated that if the comfort criteria (defined as 0.2 - 0.4 $\mathrm{m/s^2}$ for lateral vibrations) is not satisfied with a significant margin, provisions for installation of dampers may be necessary and that "in such cases the designer should consider and identify any requirements for commissioning tests".

In this section an extensive summary of various full scale measurements of bridges susceptible to human induced lateral vibrations have been collected and are presented in a chronological order.

6.1. Changi Mezzanine Bridge

The Changi Mezzanine Bridge, Fig. 15 is a shallow arch steel bridge of welded hollow circular and rectangular sections, with a 140 m main span (between the arch supports) and two 30 m side spans. The bridge is situated at Changi International Airport in Singapore connecting two passenger terminals through the Rail Terminal, [99]. The bridge was designed by Skidmore, Owings & Merrill LLP architects and Arup (New York) and construction began in June 2000.

As a consequence of the problems with the opening of the Millennium Bridge in London, a study on the vibration serviceability under human induced loading was commissioned, including modal testing of the structure and response measurements to pedestrian crowd loading. Two critical vibration modes were identified, a symmetrical lateral vibration mode (LS1) at frequency 0.9 Hz with damping ratio 0.4 % of critical and modal mass around 453 000 kg (estimated from FE model) and a symmetric torsional mode (TS1) with frequency 1.64 Hz, damping 0.4 % of critical and an estimated modal mass around 147 000 kg [99]. It was estimated using Arup's formula for the critical number of pedestrians Eq. (6), that around 140 people were enough to cause divergent lateral vibration amplitudes [100].

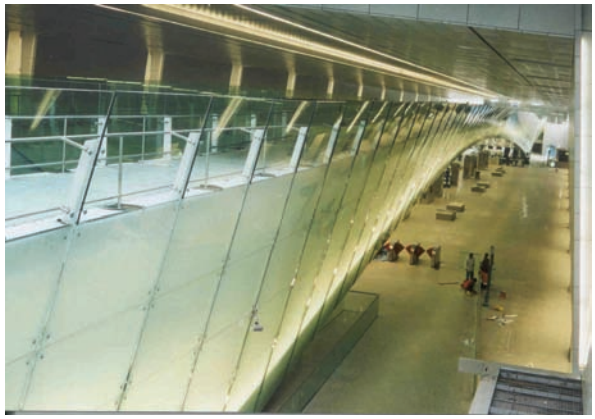

Figure 15: The Changi Mezzanine bridge at Singapore's Changi Airport (Curtesy of J.M.W. Brownjohn).

The pedestrian crowd tests were performed in February 2002 and involved up to 150 volunteers in six different tests. In the main test the number of pedestrians was gradually increased until all 150 pedestrians circled the bridge, walking at their own comfortable speed [101]. The results from these tests revealed that a disproportional increase in the amplitude of the LS1 occurred as the the number of pedestrians increased at a vibration frequency slightly lower than that of the empty structure (0.88 Hz, attributed to the added mass of the pedestrians). During the circulatory tests (with 150 pedestrians on the bridge), the amplitude of the lateral vibrations seemed to continue growing until the pedestrians were asked to stop. At that point the lateral vibration amplitude was 0.17 m/s^2 (or 5.5 mm). A similar

disproportional increase of the vertical response was not found and in fact no distinct peak in the vertical response at twice the frequency of the lateral mode was observed as expected if the pedestrian footfall was synchronised. Brownjohn et al. [101] further notes that for a reduced crowd size of 100 people, large excessive vibrations initiated only during some of the subsequent tests. This indicates that the critical number of pedestrians is not a constant, but rather a random variable with an unknown distribution.

Following the results from the dynamic analysis and the experimentally observed instability, two lateral TMDs (500 kg each) were installed to increase the damping of LS1 to 1.65 % and thereby the (theoretical) critical number of pedestrians to 560 people, [101, 102].

6.2. Nasu Shiobara Bridge (M-Bridge)

In Japan, a very light (0.4 t/m^2) suspension bridge across the Maple Valley in Nasu Shiobara (M-bridge), built in 1999 with a main span of 320 m (see Fig. 16) is situated in an area which attracts many tourists and has been known to vibrate excessively when crowded by pedestrians. The vibration occur primarily in modes with frequencies 0.88 Hz (third asymmetric mode) and 1.02 Hz (fourth symmetric mode) dependent on the position of people on the bridge [41, 103].

Figure 16: The Nasu Shiobara suspension footbridge in Japan (Picture from [41]).

In November 2002, field measurements were performed where accelerometers were mounted, both on the waist of few test persons and on the bridge. The pedestrians were asked to cross the bridge during a period with normal traffic and therefore varying vibration amplitudes. The estimated crowd density during the tests was between 0.7 and 1.3 persons/m^2, but generally with a non-uniform spatial distribution [103].

In Fig. 17, a record of pedestrian and bridge movement is shown at two different bridge locations. According to Nakamura [103] the pedestrian walking frequency was synchronised to the girder vibration and the pedestrian phase was around 120 to 160 deg ahead of the bridge motion. Nakamura further explains that in some of the tests, pedestrians lost balanced and stopped walking, causing a "detuning" of the pedestrian phase, but when the pedestrian started walking again, he/she would synchronise to the girder movement again. An example of this detuning and subsequent tuning is shown in Fig. 17. At (peak) vibration amplitudes about 10 mm (or 0.30 m/s^2 at frequency 0.88 Hz) the pedestrians could feel the vibrations and some characterised them as uncomfortable, without it affecting their normal way of

walking. At vibration amplitudes of 0.75 m/s^2 (25 mm), some pedestrians had difficulties with walking and occasionally touched the handrail. At 1.35 m/s^2 (45 mm) people often lost balance and some even stopped walking.

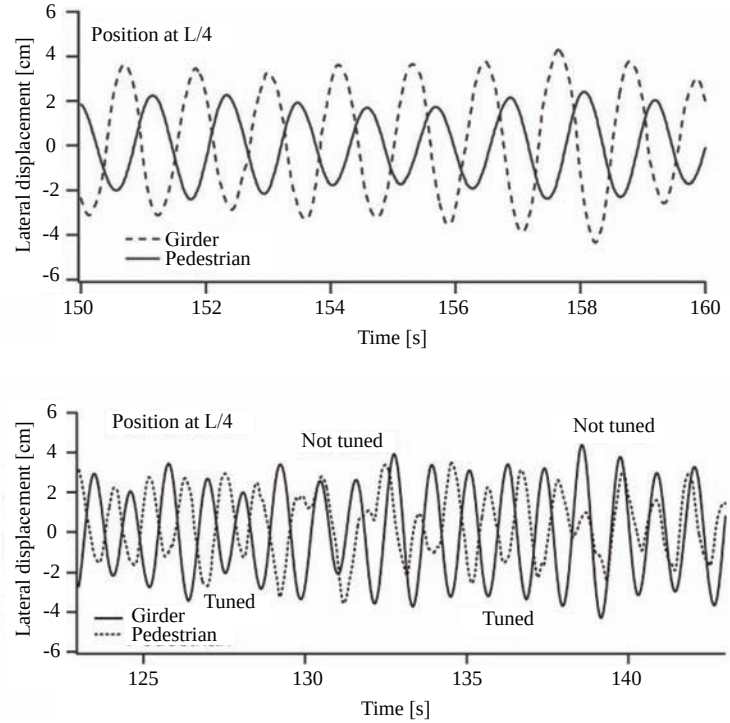

Figure 17: Lateral displacement of the M-Bridge at quarter-span shown with the lateral displacement of the pedestrian (Figure reproduce from [41]).

6.3. Lardal footbridge

The Lardal footbridge is situated in a recreational area and crosses the River Numedalsågen in Norway, Fig. 18. When inaugurated in 2001 it gained some publicity when considerable vibrations developed in the first lateral mode at 0.83 Hz when traversed by a group of pedestrians larger then a certain threshold, [104].

The bridge is a shallow arch glue-laminated timber bridge with steel cable reinforcement in certain parts of the main span. The distance between the arch supports is 91 m with two 13 m long approach spans. It was found that the first vibration mode has a damping ratio 2.5 %, modal mass 18 000 kg and a mode shape that could reasonable be approximated by a half sine with wavelength of 80 m. However, it was also observed, that the first lateral mode had a strong vertical and torsional component, with the centre of rotation underneath the bridge deck, such that the motion can be described similarly to that of an inverted pendulum [89].

Figure 18: The Lardal timber footbridge in Norway (Picture from [90])

During on-site measurements of the bridge vibrations it was found to be extremely lively, with horizontal acceleration response exceeding $1\,\mathrm{m/s^2}$ for as few as 40 pedestrians, see Fig. 19. Based on the measured acceleration response a simple linear trend between the number of pedestrians on the bridge and the peak acceleration was observed [90]:

$$\ddot{u}_{0,\max} = 0.024 N_{\mathrm{ped}} \tag{20}$$

Ronnquist et al. [105] report that as the lateral movements increase, more people tend to synchronise but a direct quantification of the number of phase synchronised pedestrians is not provided.

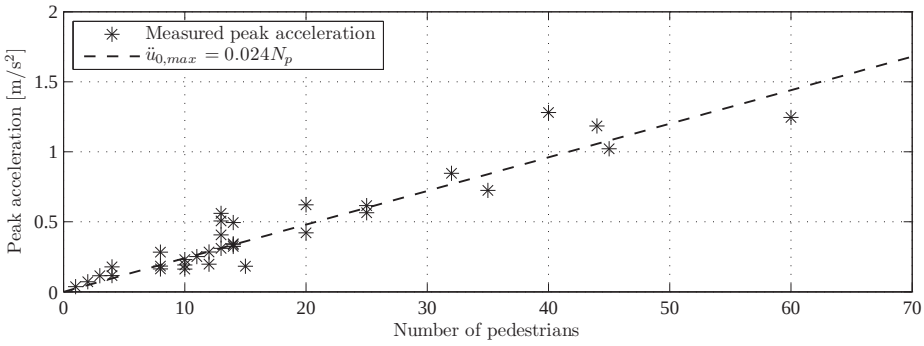

Figure 19: Measured peak acceleration as function of the number of pedestrians on the Lardal footbridge (Figure based on [89])

6.4. Coimbre Footbridge

The Coimbre Footbridge (also known as the Pedro and Inês footbridge), across the river Mondego in the city of Coimbre, Porgtugal, was built in the period 2005 to 2006 and inaugurated in November 2006. The bridge was designed by AFAssociados and Ove Arup Partnership, [106, 107] and is shown in Fig. 21. The bridge is a shallow arch bridge with a total length of 274.5 m divided into a main span (110 m), two approach spans (64 m) and shorter spans at each end connecting the river bank to the bridge. The

bridge deck is constructed as a steel-concrete composite box girder (width 4 m) and the arches are made of steel box girders. The bridge is peculiar in that it is anti-symmetric about a longitudinal axis which does not follow a straight line, but each half of the bridge consists of two half-arches that are offset 4 m from each other and meet to form a 8 by 8 m square at midspan [106].

Figure 20: Coimbre Footbridge (a) and pedestrian crowd tests (b) (Pictures from [108])

At the design stage the bridge was found susceptible to both lateral and vertical pedestrian induced loading and a comprehensive study on its serviceability was commissioned and undertaken by the Laboratory of Vibration and Monitoring from the University of Porto [25]. The analysis identified one lateral vibration mode prone to excessive lateral vibrations, at frequency between 0.7 and 0.78 Hz.

The critical number of pedestrians calculated according to Arup's formula Eq. (6) predicted that 145 pedestrians (crowd density of 0.2 person/m^2) were required to trigger SLE[1]. The formula was also used inversely, to determine the required amount of damping (5 %) to avoid SLE for a crowd density of 1 person/m^2. A total of eight TMDs were designed to control pedestrian induced vibrations, one for the firsts lateral vibration mode (weight 4920 kg) and seven for vertical modes in the frequency range 1.55 Hz to 3.06 Hz [25].

In April 2006, both ambient and free vibration tests were performed on the structure prior to installation of the glass in the handrails and the timber deck. These tests revealed that the natural frequency of the first lateral vibration mode is around 0.91 Hz with damping as low as 0.5 to 0.6 % and modal mass around 205 t (determined from an updated FE model), [109]. The ambient vibration test showed a large variation in the estimated damping and the free vibration tests were used to provide a more narrow band of estimates [110]. During controlled pedestrian crowd tests, it was found that when the number of pedestrians exceeded about 70 people, the vibration response showed a divergent behaviour. The peak midspan acceleration was around 0.2 m/s^2 for 70 pedestrians but rose to about 1.2 m/s^2 for 145 pedestrians, see Fig. 21, [108, 111]. This observation matches the critical number of pedestrians ($N_{cr} = 73$) as predicted by Arup's formula, when using the measured modal characteristics and the

[1]Synchronous Lateral Excitation (SLE) is common denominator for excessive pedestrian-induced lateral vibrations, exhibiting a disproportional (or diverging) vibration amplitudes for a small increase in the load

updated FE model as input parameters. A redesign of the dampers was performed and the final solution involved 6 individual lateral TMDs with a total weight 14.8 t to provide a theoretical damping of 7.8 %. However, this value of the theoretical damping was never reached, and subsequent forced vibration tests of the structure showed an effective damping of only 4 %, [108].

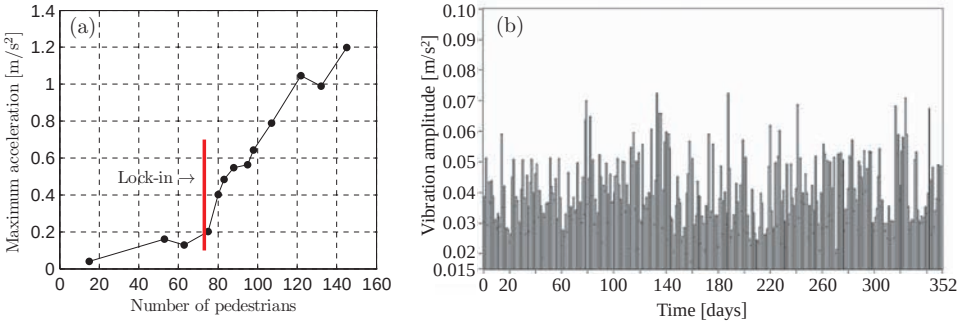

Figure 21: Results from pedestrians crowd tests (a), reproduced after [111] and maximum daily acceleration of mode 1 during the first year of service (b), from [97].

A long-term monitoring of the bridge vibrations was subsequently implemented [24], and during the first twelve months the acceleration response of lateral vibration modes has never reached amplitudes higher than the comfort threshold, defined as 0.1 m/s^2 [97]. The measured daily maximum acceleration is shown in Fig. 21.

6.5. Passarelle Simone de Beauvoir

This 304 m long footbridge in Paris is the 39th bridge across the River Seine, Fig. 22. It was designed by Feichtinger Architects and RFR Inénieurs and inaugurated on July 13, 2006. It features a 190 m main span which is a combined shallow arch and a stress ribbon with a walkway on both levels that join approximately at quarter spans, [21]. During design nine modes were deemed to be susceptible to human induced loadings, three of which were predominantly lateral. The frequencies of these lateral modes were 0.46 Hz (mode 1), 0.96 Hz(mode 3) and 1.12 Hz (mode 5) respectively, with mode 3 being localised to one of the approach spans of the bridge.

An extensive series of tests and damping provisions were commissioned in order to secure the serviceability of the structure. The test involved modal identification prior to and after the final design and implementation of TMDs respectively. The existence of the two lateral modes (number 1 and 5) was verified using a dynamic exciter. The experimentally determined frequencies and damping ratios were 0.56 Hz and 0.56 % and 1.12 Hz and 0.53 % for mode 1 and 5 respectively. No information regarding the modal masses has been provided. Viscous dampers were installed near the bridge supports to suppress the vibrations of the lateral vibration modes, but subsequent modal identification revealed that the damping in mode 1 and 5 only rose to 0.77 % and 0.58 % respectively [26].

The pedestrian crowd tests were performed on 10 July 2006 with 120 volunteering participants. The

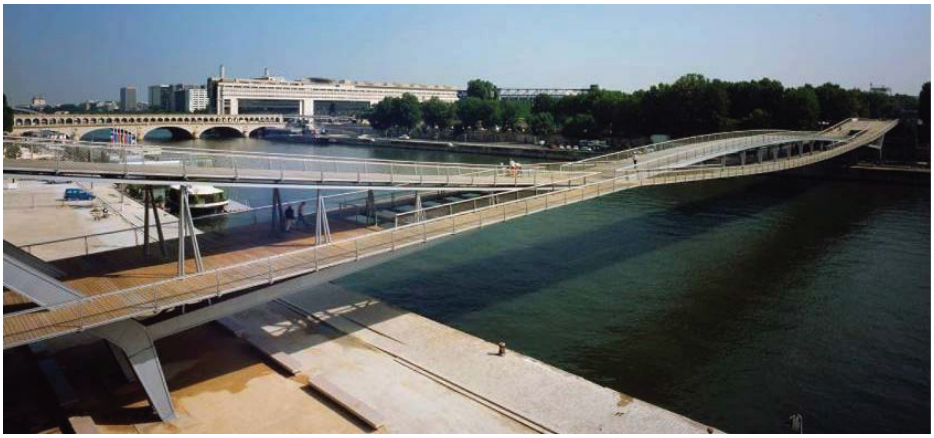

Figure 22: Passarelle Simone de Beavoir (during design known as Passarelle Bercy-Tolbiac) across River Seine in Paris (Picture from [112]).

Figure 23: Random walking of 120 pedestrians during crowd tests on 10 July 2006, (Picture from [26])

tests involved groups of varying sizes circulating the bridge, ranging from 20 to 120 people, Fig. 23. Both modes 1 and 5 were excited during the crowd tests with maximum displacement of 30 mm in mode 1 ($0.37\,\mathrm{m/s^2}$) for a crowd of 80-100 people walking randomly. Hoorpah et al. [26] report that twice this amplitude was reached when a group of 60 people walked in step using a metronome to control the pacing rate. Although large vibration amplitudes can be reached during controlled walking tests, these levels were not observed on the opening day where about 400 people occupied the structure simultaneously. Furthermore, a great amplitude dependency of the damping was observed in mode 1, increasing from less than 1 % at low vibration amplitudes < 5 mm to values around 2.5 % at amplitude around 30 mm. Also, an increase in damping has been observed over time, so the owners have not made further measures to dampen the lateral vibration modes. Instead a long-term vibration monitoring system has been installed and will provide valuable data for future assessment of the bridge vibratory behaviour.

6.6. Clifton Suspension Bridge

The Clifton Suspension Bridge in Bristol was designed by I. K. Brunel and completed in 1864, Fig. 24. The bridge has a main span of 214 m and the width of the bridge deck is 9.5 m. The Clifton Suspension Bridge is a one-lane road bridge with pedestrian walkways on either side of it [113].

Figure 24: The Clifton Suspension Bridge in Bristol, UK (Courtesy of John Macdonald).

Ambient vibration measurements revealed 27 vibration modes in the range 0.2 to 3.0 Hz, four of which were predominantly lateral. In particular, two lateral vibration modes that react strongly to pedestrian induced vibrations were identified, L2 with natural frequency of 0.524 Hz and damping 0.58 % and L3 at 0.746 Hz with damping 0.68 %. The other two lateral modes had natural frequencies and damping 0.240 Hz and 3.68 % (L1) and 0.965 Hz and 3.51 % (L4) respectively.

During a two week monitoring of the bridge in the summer of 2003, two occasions were particularly of interest, both events occurred during the annual Bristol International Balloon Fiesta, where the bridge was traversed by large crowds of pedestrians. Based on videos from a security camera monitoring the

entrance of the bridge, it was estimated that during an approximately two hour period, between 150 and 450 people were constantly on the bridge causing large vibrations in the aforementioned lateral modes (L2 and L3) with L2 being the dominant one. The maximum measured accelerations were $0.13\,\mathrm{m/s^2}$ (11.3 mm) in mode L2 and $0.11\,\mathrm{m/s^2}$ (4.5 mm) in mode L3 respectively. The lateral vibrations of the bridge experienced a stability like behaviour. Small vibration amplitudes were recorded until the number of pedestrians reached about 200 people. In a short period of time the number of people on the bridge doubled, whereas the displacement amplitude in the low frequency mode L2 increased by an order of magnitude. Subsequently, large response of mode L3 was initiated and for a while both vibration modes reacted strongly to the pedestrian induced loading, Fig. 25.

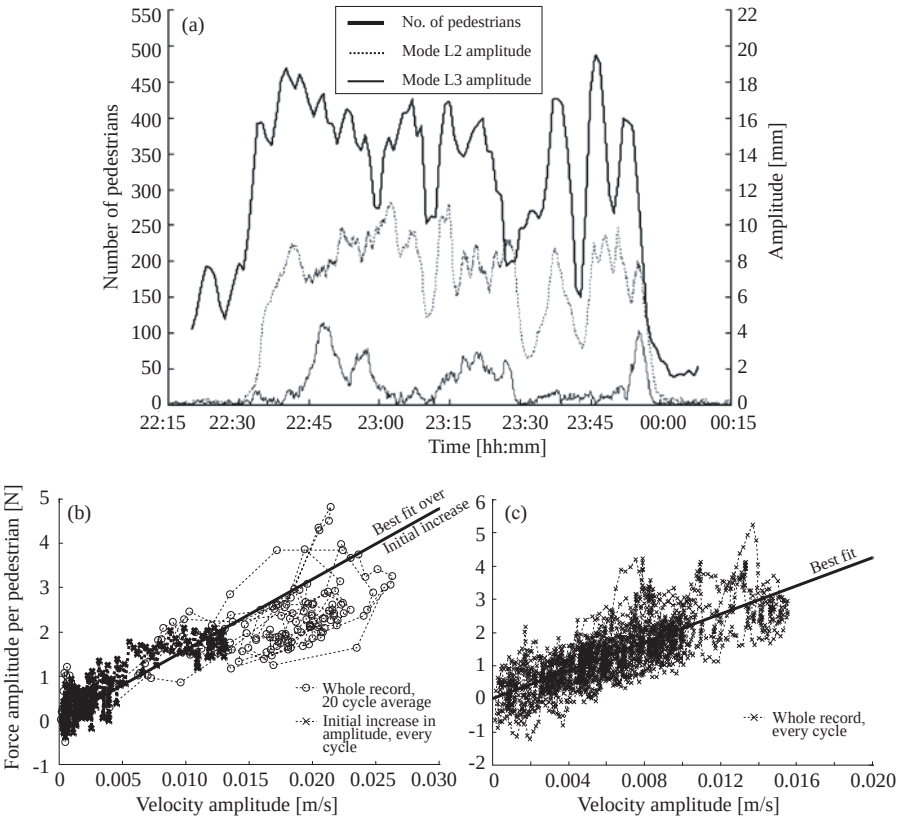

Figure 25: Results from full-scale measurements on the Clifton Suspension Bridge showing (a) the lateral displacement amplitudes of mode L2 and L3 as well as the correlated pedestrian force as function of lateral bridge velocity for mode L2 (b) and mode L3 (c) (Figures reproduced from [113]).

It was noteworthy that vibration mode L4 with a natural frequency of 0.965 Hz did not react (strongly)

to the pedestrian induced loading, which according to Macdonald [113] is attributed to its high level of damping.

Macdonald used a similar methodology to that of Dallard et al. [34] to determine the correlated pedestrian force (or in-phase force) and, as shown in Fig. 25 (b)-(c), a near linear relationship between the force and the bridge velocity was observed. The calculated critical number of pedestrians (270 people for mode L2 and 350 for mode L3) was consistent with the observations made on the bridge, Fig. 25 (a). However, the value of the velocity proportional load coefficient, c_p, (from Eq. (5)) was found lower than the value 300 Ns/m as reported from the Millennium Bridge. Macdonald noted that this difference is partially caused by inaccuracies in the modal mass and damping estimates.

The observation made on the Clifton Suspension Bridge was used to argue that, although the response behaviour of the bridge fits the assumption of negative damping, the mechanism does not necessarily involve synchronisation of step frequencies to the natural frequencies of the bridge. The fact that the vibrations occurred simultaneously in two vibration modes (L2 and L3) and initiated in the lower frequency mode with frequency further away from comfortable pacing rates, suggests that a different mechanism than synchronisation is responsible for these vibrations. Furthermore, the measured vertical bridge response did not show any frequency peaks at twice the frequency of the lateral modes, which would be a consequence of phase synchronisation.

6.7. Weil-am-Rhein footbridge

The Weil-am-Rhein footbridge, also known as the "Dreiländerbrücke" (Tri country bridge), connects the German town Weil-am-Rhein to the town Huningue in France at the border to Basel in Switzerland, Fig. 26. It is a steel-arch bridge with a suspended walkway which features a record breaking clear span of 230 m. The bridge, designed by Feichtinger Architects and Leonhardt, Andrä und Partner (LAP) engineering bureau, was opened in the summer of 2007. It consists of two steel arches, a main arch which spans the river in a vertical plane and second arch with a smaller cross section that inclines to almost meet the main arch at midspan, [114].

Figure 26: Weil-am-Rhein footbridge (Picture from [112])

The bridge designers identified three vibration modes susceptible to pedestrian induced lateral loading, all featuring symmetrical bending of the bridge deck (mode 3, 4 and 5). A subsequent modal identification

of the bridge revealed the frequencies of these modes as 0.90 Hz, 0.95 Hz and 1.00 Hz, about 10 % higher than predicted by the designers [115]. The damping is reported low (i.e. $< 1\,\%$) but no information is given about the modal mass. Franck [116] estimated the modal mass of mode 5 to around 105 t.

Strobl et al. [114] used a value $c_p = 94\,\mathrm{Ns/m}$ to calculate the critical number of pedestrians, corresponding to a correlated lateral force of 5 N per pedestrian at approximately $0.3\,\mathrm{m/s^2}$ (i.e. 20 % of the load amplitude from pedestrians walking on a rigid surface 25 N). The reason for selecting 5 N is based on the observations on the Toda Park Bridge in Japan [42] where 20 % of the pedestrians were reported in synchrony with the bridge vibrations. The estimated number of pedestrians needed to trigger SLE was reported as 500 people (density of $0.24\,\mathrm{pedestrians/m^2}$), [114]. Conversely, the damping needed to secure stability for a crowd density of $2.0\,\mathrm{pedestrians/m^2}$ was calculated as 16.5 % of critical, which would call for a 10 t TMD [114].

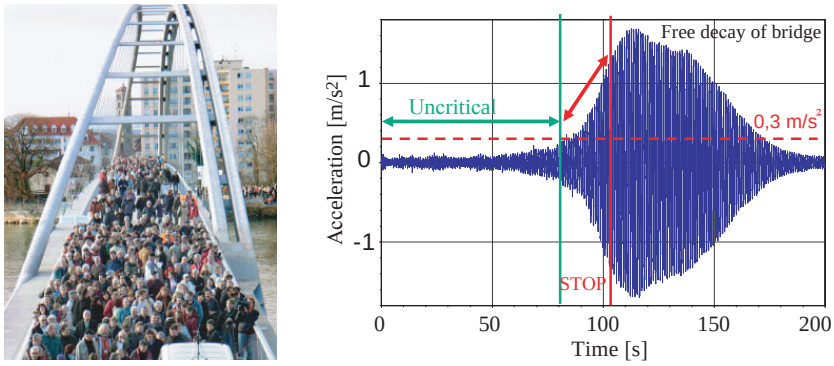

Figure 27: Crowd tests on 13 January 2007 (Picture from [114]) (left) and measured midspan acceleration during a crowd test (Figure reproduced from [115]), (right).

On 13 January 2007, prior to the opening of the bridge, pedestrian crowd tests were carried out with more than 800 volunteers. In the first test, the crowd was asked to cross the bridge (from one side) at their own normal walking pace. In this scenario, lateral acceleration amplitudes between 0.19 and $0.45\,\mathrm{m/s^2}$ were recorded without any evidence of diverging vibration amplitudes. Mistler et al. [115] attributes this to the general slow walk of people. In the second test, the group was asked to cross the bridge at a slightly higher pace and to avoid pausing during the crossing of the bridge. In this case, excessive lateral vibrations were observed in mode 5 at 0.96 Hz with amplitudes up to $1.7\,\mathrm{m/s^2}$ and peak-to-peak displacement around 80 mm, see Fig. 27. It was further pointed out that for safety reasons the walking tests were stopped prematurely. This happened while the vibration amplitude was constantly increasing, thus much larger vibration amplitude may have developed if people were allowed to continue walking. According to Mistler et al. [115], normal walking became impossible for vibration amplitudes exceeding $1.0\,\mathrm{m/s^2}$ and many people started to sway, increased their gait width and held on to each other or the hand rail during this crowd test.

Although the bridge clearly reacts strongly to pedestrian induced lateral loading, no dampers have

been installed on the bridge. One reason is that under normal walking conditions, as observed in the first tests, SLE was not be triggered, but only when people were instructed to increase their walking speed. Further, the owners believe that the crowd size needed to trigger SLE is a rare event and that lateral vibrations will therefore not be a problem on a daily basis, [27, 114, 116].

6.8. Summary of full-scale measurements

In new long span footbridges, the possibility of excessive lateral vibrations is a serious threat to the design and the role of full scale measurements of the real dynamic behaviour of the bridge prior to its inauguration is increasingly becoming an integrated part of the design process. In particular, for bridges that are deemed susceptible to human induced vibrations, full scale testing is vital for several reasons.

Firstly, the structural response (and critical number of pedestrians) depends on the inherent structural damping, which cannot accurately be predicted without testing. Secondly, external damping devices, such as TMDs, depend on an accurate tuning to the structural properties [117], which is usually only possible through experimental modal identification. Finally, due to uncertainties in the phenomenon governing SLE, and the general lack of experimental data from existing bridges, controlled crowd tests are needed for 1) investigating the possibility of SLE and finding its trigger (e.g. critical crowd density) and 2) for the purpose of verifying the selected solution strategy.

A well engineered and successfully completed test program, cannot only further the understanding of the problem with lateral footbridge vibrations, but also contribute to a more safe and economic design, which is based on the actual dynamic properties of the bridge instead of those estimated during the design. The Coimbre footbridge (Section 6.4) is a prime example of the importance of full-scale measurements, as the total damper mass installed on the bridge to suppress SLE, was much larger than anticipated during the design process. This was a consequence of wrongly assumed damping during the design and partly because of a desire to provide extra damping to take into account different uncertainties related to the dynamic behaviour of the structure [108].

Provided that pedestrians generally act as negative dampers on low-frequency lateral vibration modes then all bridges with frequencies in the range 0.4 to 1.3 Hz, with or without externally added damping have a potential to suffer from SLE if just the critical number of pedestrians is reached. The main concern of the designers will then be to determine the probability of occurrence of the critical crowd density such that an informed decision about the amount of external damping needed can be taken or even avoided altogether as was done with the Weil-am-Rhein bridge. Before this can be done with any certainty, more crowd tests are needed to establish a statistical description of the correlated pedestrian force. To date only few reports have been made where the correlated pedestrians force has been determined based on full scale measurements of crowd induced vibrations. More information is needed about the effect of bridge frequency, crowd morphology, structural parameters (damping, mass, Scruton number), event duration etc.

Furthermore, controlled laboratory experiments should be carried out to understand and quantify the governing mechanism of the interaction between a pedestrian and a laterally moving platform. A

successful link between laboratory experiments, mathematical modelling and full scale crowd tests must be established in order to fully comprehend and eventually predict the onset of SLE in future bridge design.

7. Recent development modelling of pedestrian induced lateral excitation

In recent years, several new load models and response evaluation techniques have been published relating to pedestrian-induced lateral vibrations of footbridges. These models originate from a variety of different scientific disciplines and thereby differ considerably. A critical review of the models proposed for crowd-induced lateral loading of footbridges is presented, classified according to their nature, i.e. firstly linear load and response models are presented (Section 7.1). These models are based on linear dynamics and direct resonance excitation and the group effect is taken into account through random distribution of one or more of the input parameters, typically pacing rate and phase. Next, nonlinear models characterised by either a nonlinear loading caused by human-structure interaction or by nonlinear modal coupling of vibration modes characterised by an integer relationship between their natural frequencies are presented. In the third part of this section, a more comprehensive modelling approach is reviewed in which the dynamics of the moving crowd is taken into account through a macroscopic modelling of the crowd-structure system. This section also provides a brief introduction to the dynamics of moving crowds with emphasis on quantifying human-human interaction.

7.1. Linear response models

Linear response models are here classified as those where the lateral vibrations are caused by direct resonance, i.e. by pedestrians walking at frequencies close the natural frequency of one or more lateral vibration modes.

7.1.1. Equivalent number of 'perfect' pedestrians

The term 'perfect' pedestrian, refers to the assumption that the lateral (or vertical) load time history from series of consecutive footsteps can be represented as a truncated Fourier series with fundamental period equal to the duration of two steps (or single footstep for vertical loading). As discussed in Section 3, this assumption implies that the load from each footstep is perfectly replicated and thereby intra-subject variability in the loading is neglected. The response from a group of pedestrians can be calculated as a multiplication of the response from single perfect pedestrian walking with a frequency that matches the natural frequency of the mode in question. This method is particularly preferred in codes of practice and design guidelines for evaluation of the vertical response of footbridges due to its simplicity. The effect of the group is taken into account through an effective number of pedestrians, that produces the same response as that of the entire group:

$$F(t) = n_e G_1 \sin(2\pi f_n t) \tag{21}$$

where f_n is the frequency of the mode in question. The effective number of pedestrians depends primarily on several crowd specific and structural parameters. For lateral human-induced vibrations, the effective number of resonance pedestrians has been deduced from video recordings of the motion of pedestrians walking on an actual footbridge, see Section 2, or through energy considerations as on pont de Solférino, see Eq. (3) in Section 4.1. The idea of an effective number of pedestrians has been implemented in the Sétra guideline [5] as $10.8\sqrt{N\zeta}$ for a sparse or dense crowd and $1.85\sqrt{N}$ for a very dense crowd. These results are based on stochastic response simulations for vertical footbridge response and do not take into account synchronisation of pedestrians with the movement of the bridge. The movement of the bridge, u, was accounted for by Danbon and Grillaud [68] who defined the effective number of pedestrians through a bilinear synchronisation coefficient $\phi(u)$ as described in Section 4.4. Ronnquist [89] determined an equation for the equivalent number of pedestrians, which was obtained by fitting a mathematical expression to the ratio between measured (peak) response from a group of N people to the simulated response of a single pedestrian crossing at resonance:

$$n_e = 35 - 34 \exp\left(- \left[\frac{N}{60} \right]^{1.6} \right). \tag{22}$$

In Fig. 28 a comparison between different definitions of the effective number of pedestrians is shown.

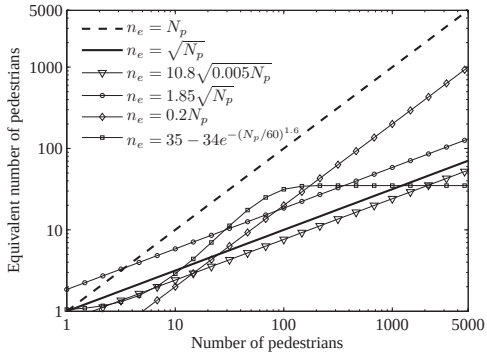

Figure 28: Comparison between different definitions of the effective number of resonance pedestrians.

7.1.2. Critical number of pedestrians

Roberts [118, 119] used linear dynamics to create a stability criterion for susceptibility of bridges towards SLE. He argued that the lateral acceleration of the body CoM is in equilibrium with the lateral force induced by the pedestrians, which for N_p equally distributed pedestrians over the bridge length L becomes:

$$\frac{N_p m_p}{L} \frac{\partial^2 u_p(x,t)}{\partial t^2} = -F(x,t) \tag{23}$$

where m_p is the average pedestrian weight and $u_p(x,t)$ is the lateral displacement of the CoM. By assuming that the movement of the CoM is sinusoidal, Eq. (23) was solved together with the equation

of motion governing the bridge vibration. A stability criterion was obtained for the condition where the amplitude of the bridge vibration exceeds that of the body CoM:

$$N_{cr} = \frac{1+\alpha^2}{2\alpha} \frac{M_n}{\frac{m_p}{\alpha L}\int_0^L \left[\Phi_n(x)\right]^2 \mathrm{d}x} \frac{\omega_n^2}{\omega_w^2 H_{n,av}} \tag{24}$$

In Eq. (24), M_n and Φ_n are the modal mass and mode shape of mode n and $H_{n,av}$ is an averaged value of the dynamic amplification, accounting for variations in the pacing rate amongst pedestrians and L is the bridge length. The proposed value of $H_{n,av}$ to be used in design is tabulated in [119]. Further, in Eq. (24) account is taken for the possibility of non-uniform pedestrian distribution, through the factor $\alpha \in [0;1]$, such that αL is the portion of the bridge occupied by pedestrians. The average angular walking frequency is denoted $\omega_w = 2\pi f_w$.

In another paper by the same author, [120], a method to calculate the steady-state response of a bridge subject to loading from a group of partially synchronised pedestrians is presented. The model is based on the assumption that the pedestrians are uniformly distributed along the span and that they can be treated as stationary oscillators. The model includes a qualitatively defined non-dimensional function, β, as the proportion of pedestrians whose motion is synchronised with the bridge motion (both in frequency and phase). The function β depends on the crowd density ρ, the bridge displacement u and a threshold value u_m which is the maximum bridge amplitude at which pedestrians are able to continue walking:

$$\beta = (1 - 0.4\rho)\left[1 - \left(\frac{u}{u_m}\right)^2\right] \tag{25}$$

It is noted that contrary to common belief, the degree of synchronisation decreases with an increase in vibration amplitude and the density.

7.1.3. Stationary response due to random incoherent crowds

Due to inter- and intra-subject variability, the response evaluation is often done in a probabilistic sense. One of the earliest attempts is that of Matsumoto et al. [121] who showed that for a flow of identical pedestrians arriving randomly to a bridge with flow intensity λ (pedestrians/second) the RMS value of the vertical acceleration response is $\sqrt{\lambda T_0}$ that of the single pedestrian, with T_0 being the passage time of the pedestrian. An often used interpretation of his results is that the response of a group of N pedestrians is $\sqrt{N}$ times that of a single pedestrian. This applies only for the RMS value of the response, whereas the peak response depends on the observation time, or return period of event, and cannot be predicted this way [84]. Furthermore, the model of Matsumoto et al. [121] assumes identical pedestrians and the distribution of walking frequencies in a real crowd is not accounted for, which for lightly damped structures may lead to overly conservative estimates of the response [84]. It is also worth noting that N follows the Poisson distribution and represents an average number of pedestrians on the bridge.

The distribution of pacing frequencies within the crowd were taken into account by Dallard et al. [4], who proposed the following approximate formula for the standard deviation of the vertical footbridge

response for a sinusoidal vibration mode:

$$\sigma_{\ddot{q}_n} = \frac{G(f_n)}{4M_n}\sqrt{\frac{\pi N f_n}{\zeta_n} p_{f_w}(f_n)} \tag{26}$$

where $G(f_n)$ is the load amplitude at the natural frequency f_n, and $p_{f_w}(f_n)$ is the probability density function for the walking frequency (with mean μ_{f_w} and standard deviation σ_{f_w}), evaluated at the modal frequency f_n. The method was derived for predicting vertical response of footbridges, but can equally well be applied for lateral vibrations in the absence of human-structure interaction.

In fact, Roberts [120] presented a similar probabilistic response evaluation technique for predicting the lateral pedestrian-induced vibrations, where the load is modelled as N stationary and uniformly distributed harmonic oscillators, each with amplitude G_1. Under the assumption that the instantaneous phase of the response is randomly distributed with a constant probability density the standard deviation of the modal acceleration response, valid for a group of unsynchronised pedestrians, is obtained as:

$$\sigma_{\ddot{q}_n} = \sqrt{\frac{N}{2L}}\frac{G_1 H_{n,av}}{M_n}\sqrt{\int_0^L \Phi_n^2(x)\mathrm{d}x}. \tag{27}$$

The intra-subject variability in the load can be accounted for, by representing the pedestrian load through its PSD. Ricciardelli et al. [122] proposed that for laterally stiff footbridges with uniformly distributed pedestrians and crowd density low enough for avoiding human-human interaction, the stationary RMS value of the modal acceleration could be calculated using the well-known white-noise approximation [123]:

$$\sigma_{\ddot{q}_n} = \frac{1}{2M_n}\sqrt{\frac{\pi N f_n}{\zeta_n} S_{Fe}(f_n)\frac{1}{L}\int_0^L \left[\Phi(x)\right]^2 \mathrm{d}x} \tag{28}$$

$$f_n S_{Fe}(f_n) = \int_0^\infty f_n S_F(f_n/f_w) p(f_w)\mathrm{d}f_w \tag{29}$$

where $S_{Fe}(f_n)$ represents the PSD of the equivalent load of one pedestrian and $S_F(f_n/f_w)$ is the PSD of a single pedestrian from Eq. (2). It is easily shown that Eq. (26) and Eq. (28) are identical when the excitation is perfectly harmonic and the mode shape is sinusoidal. In this case the PSD of a single person $S_F(f_n) = \frac{1}{2}G^2(f_n)\,\delta(f_n - f_w)$ is substituted into Eq. (29) to yield the approximation in Eq. (26).

7.1.4. Stationary response due to coherent crowds

Brownjohn et al. [99] pointed out that synchronisation amongst humans happens in clusters where small groups of pedestrians walk in step and that the correlation decreases with the distance between the pedestrians. With analogy to turbulent buffeting wind load, they define a coherence function $\mathrm{coh}(f, x_1, x_2) \in [0, 1]$ was defined to take into account the correlation amongst pedestrians as function of their spatial separation. However, no suggestion for the shape of the coherence function is given and only the two extremes, no correlation ($\mathrm{coh}(f, x_1, x_2) = \delta(x_1 - x_2)$) and full correlation ($\mathrm{coh}(f, x_1, x_2) = 1$) are analysed. An expression for the PSD of the acceleration response at point x along the bridge deck is

derived as:

$$S_{\ddot{U}}(f,x) = \Phi(x)^2 \left|H(f)\right|^2 S_P(f) \int_0^L \int_0^L \Phi(x_1)\Phi(x_2)\mathrm{coh}(f,x_1,x_2)\mathrm{d}x_1\mathrm{d}x_2 \tag{30}$$

$$S_P(f) = \left[\frac{N}{L}\right]^2 \frac{G^2(f)}{2} p_{f_w}(f) \tag{31}$$

where $H(f)$ is the frequency response function (FRF) for acceleration, $S_P(f)$ is the PSD of walking loads per unit length, N is the number of people on the bridge, L is the bridge length, $G(f)$ is the amplitude of the relevant load harmonic and W is the weight of one pedestrian [99]. The RMS acceleration response is obtained from the PSD through integration over the frequency domain $\sigma^2_{\ddot{u}_n}(x) = \int_0^\infty S_{\ddot{U}}(f,x)\mathrm{d}t$. Although Eq. (30) was derived for estimation of vertical response to footbridges, it may also be applicable to lateral vibrations in the absence of human-structure interaction.

7.1.5. Peak response due to random crowds

Frequency domain procedures assume that the load process is a stationary stochastic process and provide only information about the stationary response variance (and RMS). In an attempt to distinguish between peak and RMS accelerations, a spectral load model was created using Monte Carlo response simulations [50, 124]. The 95 % fractile of the lateral peak modal acceleration amplitude is given as:

$$\ddot{q}_{0,max} = k_{\ddot{q},95\%}\ \sigma_{\ddot{q}} \tag{32}$$

where $k_{\ddot{q},95\%}$ is the peak factor which depends on the crowd density, but is given in the range 3.63 to 3.77 . The variance of the acceleration response, $\sigma^2_{\ddot{q}}$, of modes with sinusoidal shape is given as:

$$\sigma^2_{\ddot{q}} = \frac{C k_{\mathrm{F}}\ N}{M_n^2} k_1(f_n)\zeta^{k_2(f_n)} \tag{33}$$

where C is a constant and $k_1(f_n)$ and $k_2(f_n)$ are both polynomial functions with parameters determined from Monte Carlo response simulations, see [124]. It is worth noting that this spectral load model is only valid when the average walking frequency within the crowd coincides with the natural frequency of the mode in question. In other cases, Butz [125] proposes a reduction factor to reduce the peak acceleration:

$$k_{red} = \exp\left\{-\frac{1}{2}\left(\frac{f_{w,m} - f_n}{B_{red}}\right)\right\} \tag{34}$$

where B_{red} is a constant determined from simulations, $f_{w,m}$ is the average walking frequency and f_n is the natural frequency of the relevant bridge mode.

7.1.6. Summary of linear load and response models

Due to their simplicity, linear models are generally preferred for design guidelines and codes of practice. Often, as illustrated in the proceeding sections, closed form solutions can be obtained for either the expected response amplitude or the critical number of pedestrians needed to trigger SLE and thereby time consuming response calculations can be avoided. However, linear models are based on idealised assumptions about the pedestrian-induced load, the structural behaviour, the interaction amongst pedestrians and interaction between pedestrians and the laterally vibrating structure.

7.2. Nonlinear dynamic models

Dynamic models are nonlinear if the governing equations contain nonlinear terms. A typical non-linearity in civil engineering is inelastic material behaviour, large displacements, nonlinear damping or response dependent loading. For vibration serviceability of footbridges, the materials are usually in their elastic range and the damping is typically assumed viscous (or equivalent viscous), but in the presence of human-structure interaction the loading becomes non-linear. A special type of dynamic non-linearity is modal coupling, which exists in structures with a certain geometric coupling between two (or more) vibration modes when the relationship between their natural frequencies are integers (or near integers).

7.2.1. Modified Arup models

Based on the observed pedestrian behaviour on the T-Bridge during an event with large lateral vibrations, Nakamura [126] proposed modifications to the Arup model in Eq. (5) (described in Section 4.4). The modification is based on the assumption that pedestrians will reduce their walking speed, or completely stop, when the lateral velocity of the bridge deck becomes large. Therefore, the response of the bridge will not reach infinity but is limited to a certain level. The following equation for the modal pedestrian load was proposed:

$$F_P = k_1 k_2 H[\dot{q}(t)] G(f_0) M_P g \tag{35}$$

$$H[\dot{q}(t)] = \frac{\dot{q}(t)}{k_3 + |\dot{q}(t)|} \tag{36}$$

$$G(f_0) = 1.0 \tag{37}$$

where $\dot{q}(t)$ is the modal velocity of the bridge, $M_P g$ is the modal self weight of the pedestrians and f_0 is the frequency of the lateral vibration mode under consideration. The coefficient $k_1 = 0.04$ is the fundamental DLF of the pedestrian (according to [38]) and k_2 is the percentage of pedestrians which are synchronised to the bridge vibration. The function $H[\dot{q}(t)]$ describes the nature of the synchronisation where k_3 should be determined by trial and error such that it corresponds to measured data, [126]. The synchronisation coefficient, $k_2 = 0.20$, was used, based on the observations made on the T-bridge and those established from laboratory platform tests, [40]. By matching the measured steady-state girder response to the response predicted by the load model, the value $k_3 = 0.01\,\mathrm{m/s}$ was obtained. It is worth noting that with these coefficients, the load amplitude predicted by the Arup model in Eq. (5) is 48 N for a bridge velocity of $\dot{x} = 0.16\,\mathrm{m/s}$ whereas the modified model in Eq. (35) only predicts modal loads around 5 N for the same velocity. The parameter $k_3 = 0.01$ was estimated from back-analysis of the measured response of two different bridges (T-Bridge and the M-Bridge) under different crowd conditions [40], but its determination is sensitive to the accuracy of k_1 and k_2, thus more data is needed before conclusive evidence regarding the probability of synchronisation and thereby the coefficient k_3 can be made.

Another model, which is based on the assumption that the pedestrian load can be related to the bridge velocity is that of Ingólfsson and Georgakis [127]. By treating the motion-induced portion of the load

as velocity and inertia proportional loads, the total pedestrian-induced lateral load, $F(t)$, was written as the equivalent static force plus the additional equivalent damping and inertia forces respectively:

$$F(t) = F_{st}(t) + \underbrace{c_p\left(f_0/f_w, u_0\right)\cdot\dot{u}}_{\text{equivalent damping}} + \underbrace{m_p\varrho_p\left(f_0/f_w, u_0\right)\cdot\ddot{u}}_{\text{equivalent inertia}}. \tag{38}$$

The equivalent static force, $F_{st}(t)$, was defined through its averaged Gaussian shaped PSD (see Eq. (2)). The functions $c_p\left(f_0/f_w, u_0\right)$ and $\varrho_p\left(f_0/f_w, u_0\right)$ define the self-excited forces and its dependency on the vibration frequency, f_0, and amplitude u_0. The model is based on measured forces from sixty-six pedestrian test subjects walking on a laterally driven treadmill at a range of lateral vibration frequencies and amplitudes (see Section 5) [92]. Apart from this frequency and amplitude dependency, the results from the campaign were governed by a large randomness, thus the pedestrian load coefficients were presented in a probabilistic framework [127]:

$$c_p\left(f_0/f_w, u_0\right) = \theta_0\left(f_0/f_w\right) + \theta_1\left(f_0/f_w\right)u_0 + X\cdot\theta_2\left(f_0/f_w\right)e^{\theta_3(f_0/f_w)u_0} \tag{39}$$

$$\varrho_p\left(f_0/f_w, u_0\right) = \phi_0\left(f_0/f_w\right) + \phi_1\left(f_0/f_w\right)u_0 + X\cdot\phi_2\left(f_0/f_w\right)e^{\phi_3(f_0/f_w)u_0} \tag{40}$$

The parameters θ_0, ϕ_0, θ_1 and ϕ_1 describe the development of the mean load coefficient as functions of the lateral frequency and amplitude and were determined by fitting a linear equation to the measured mean values of c_p and ϱ_p. The parameters θ_2, ϕ_2, θ_3 and ϕ_3 were determined by fitting an exponentially function to the standard deviations of the measured values of c_p and ϱ_p. The stochastic variable X was introduced as a discrete-time Gaussian Markov process. The main strength of the model is that the self-excited force components are based on an extensive experimental campaign and thereby represent a statistical reliability. Ingólfsson and Georgakis [127] demonstrated the applicability of the model to predict excessive lateral vibrations of both low frequency modes, i.e. around 0.5 Hz and modes with frequencies closer to the natural walking frequencies. Due to the randomness in the load and the frequency dependency of the load coefficients, a single response simulation is not sufficient when predicting the susceptibility of a bridge to SLE, but instead a range of different conditions must be investigated and the probability of occurrence of these events should be evaluated.

7.2.2. Amplitude dependent DLF

Based on the experimental work of Sun and Yuan [31] (see Section 5), an expression for the total load from a group of N pedestrians was given as:

$$F(t) = \frac{N\cdot\rho_s(u_0)\cdot\mathrm{DLF}(u_0)\cdot W}{u_0}\left(u\cos\left(\varphi\right) + \frac{\dot{u}}{\omega}\sin\left(\varphi\right)\right) \tag{41}$$

where $\mathrm{DLF}(u_0)$ is displacement dependent (Eq. (14)) and $\rho_s(u_0)$ is the probability of synchronisation according to Eq. (15), ω is the angular frequency of the mode in question, φ is the phase angle between pedestrian loading and displacement $u(t)$ of the structure and W is the pedestrian weight. This equation is nonlinear, since the DLF is proportional to the displacement amplitude, however also the probability of synchronisation depends on u_0. Based on the load model, Sun and Yuan [31] derive an analytical stability criterion, consisting of three coupled equations, which must be solved numerically in order to determine the possibility of SLE.

7.2.3. Modal coupling (autoparametric resonance)

In linear dynamics, the structural response only occurs at the natural frequencies of the structure (from transient loads) and at frequencies equal to the excitation frequency. However, non-linearities may cause steady-state structural vibrations at frequencies different from those of the input [128]. Two important nonlinear phenomena are parametric excitation and modal interaction. Parametric excitation occurs if the load acts through a parameter of the system and modal interaction is especially pronounced if two modes have natural frequencies that are related by an integer or near-integer relationship (e.g. $f_1 \cong 2f_2$) [129]. In both cases large vibrations can occur at frequencies different from the excitation frequency, even when the excitation is weak.

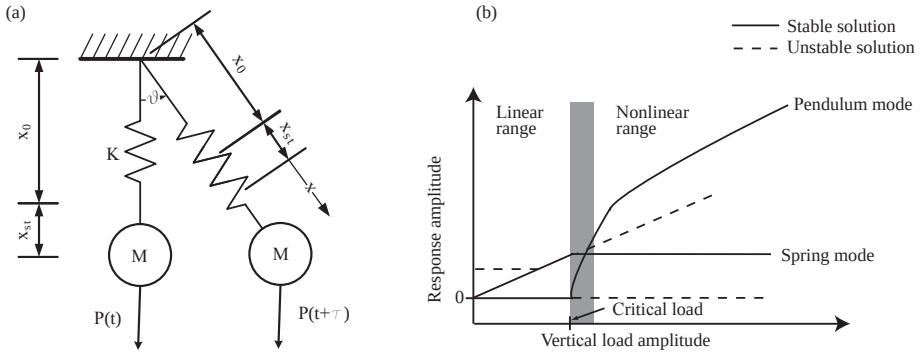

Figure 29: (a) Vertically loaded elastic pendulum with a linear spring and (b) response characteristics of the pendulum for $\omega_s = 2\Omega = 2\omega_p$.

Blekherman [32] investigated an elastic pendulum with a linear spring subject to vertical forcing, see Fig. 29. The equations of motions governing the movement (x and ϑ) of the system were obtained using Lagrange's equation:

$$\ddot{x} + \omega_s^2 x = -2\zeta_s\omega_s\dot{x} + (1+x)\,\dot{\vartheta}^2 + \omega_p^2\cos\vartheta + \frac{P_0}{Ml}\cos\,(\Omega t)\cos\vartheta - \omega_p^2 \tag{42}$$

$$(1+x)\,\ddot{\vartheta} + \left[\omega_p^2 + \frac{P_0}{Ml}\cos\,(\Omega t)\cos\vartheta\right] = -2\dot{\vartheta}\dot{x} - 2\zeta_p\omega_p\dot{\vartheta} \tag{43}$$

where ω_s, ω_p, ζ_s, ζ_p are the angular frequencies and damping ratio of the spring mode and pendulum modes respectively, $P(t) = P_0\cos(\Omega t)$ is the external load, l is the pendulum length and M is the pendulum mass. The system of equations (42) and (43) present two coupled nonlinear second order differential equations. The loading term in Eq. (43) is proportional to $\cos\vartheta$, thus there is a risk of parametric excitation for certain values of Ω. Furthermore, the coupling between the modes also present a risk of internal resonance [129]. Blekherman [130] derived the steady-state response for the pendulum and the spring motion respectively and found that in the case $\omega_s = 2\Omega = 2\omega_p$ there are two regions of interest, a linear and a nonlinear region, see Fig. 29. In the linear region the amplitude of the spring mode increases linearly with the applied load whereas the amplitude of the pendulum mode is zero. When the force amplitude reaches the bifurcation point, the amplitude of the vertical vibrations is limited (and

independent of the forcing applied) and the vibration of the pendulum mode experience a rapid increase (jump).

According to Blekherman [32], the vibrations on the London Millennium Bridge could be explained by autoparametric resonance between the second lateral mode at 0.95 Hz and the third vertical mode 1.89 Hz on the central span. The main argument is that there is a 2:1 ratio between the modal frequencies and the amplitude of the lateral load experienced a jump for a small increase in the vertical load (due to a small increase in the number of pedestrians on the bridge). Also mentioned are the vibration problems of the T-Bridge in Japan, were a relationship of 1:1:2 between the natural frequency of the stay cables (1.0 Hz), the frequency of first lateral mode (0.9 -1.0 Hz) and the third vertical mode (2.0 Hz) was observed. Fujino et al. [131] used a scaled 3-degree-of-freedom (3DOF) model of a cantilever beam supported by a taut string where the same relationship between the natural frequencies of the beam modes and the fundamental string mode were created. It was found that autoparametric resonance could be obtained in this system for a load acting at the natural frequency of the vertical beam mode, causing lateral vibrations in both the cable stays and the beam at half the excitation frequency, similarly to the pendulum investigated by Blekherman. However, Fujino et al. [42] argue that parametric excitation was not the cause for large amplitude vibrations on the T-Bridge. First of all, the vertical vibration levels in the girder which are needed to trigger the autoparametric resonance were not observed on the bridge. By investigating the relative phases of the response measurements, they concluded that the lateral cable vibrations were triggered by lateral vibrations of the bridge deck, but not parametrically by the vertical girder motion as anticipated according the experiments reported by Fujino et al. [131].

In a later paper, Blekherman [130] used a double pendulum model to represent the first anti-symmetric torsional mode at frequency 1.59 Hz and the first lateral modes at frequency 0.81 Hz of Pont de Solférino. Because of the near 2:1 relationship between the modal frequencies, it was claimed that the bridge could have a similar behaviour to that of the elastic pendulum (see Fig. 29). Furthermore, Blekherman used the results from the full scale measurements of the Pont de Solférino to support this observation. For a small group of 16 pedestrians marching in step at the natural frequency of the torsional mode, the dominant frequency in the response was the same as the step frequency. When the group size was increased to 61 pedestrians, large vibrations developed in the lateral mode at half the pacing frequency and the response was governed by vibrations of both modes with the lateral one dominating. This suggests that there exists a critical load parameter (e.g. number of resonance pedestrians) that cause divergent lateral vibration amplitudes, similar to what is predicted for the double pendulum. However, since the lateral load occurs at half the pacing frequency, the large response can be caused by direct resonance of the lateral mode, where the force is non-linearly dependent on the vibration amplitude causing the rapid jump in the observed response. In Table 5, the natural frequencies of several footbridges which have suffered from large lateral pedestrian induced vibrations are listed. Table 5 can be used as a basis for judging the susceptibility towards autoparametric resonance between vertical (or torsional) and lateral modes.

Table 5: Comparison of the characteristics of different bridges subject to excessive lateral pedestrian induced vibrations

Bridge description	Bridge type	Span [m]	f_L [Hz]	f_V [Hz]
Park Bridge, Kiev (UA) [32]	Suspension	400[1]	1	2
Bridge over Main, Erlach (DE) [38]	Steel arch	110	1.1	-
Bosporus bridge, TR [33]	Suspension	1074	-	-
Auckland Harbour, NZ [4]	Suspension	244	0.67	-
Queen's park bridge, UK [4]	Suspension	-	-	-
T-Bridge, JP [42]	Cable stay	134	0.9-1.0	0.7, 1.4, 2.0
M-Bridge, JP [41, 103]	Suspension	320	0.88, 1.02	-
Alexandra Bridge, CA [4]	Steel truss	172	-	
NEC Bridge, Birmingham (UK) [4]	Steel truss	-	0.7	-
Pont de Solférino, Paris (FR) [5, 68]	Steel arch	140	0.81	1.22, 1.59[2], 1.69
LMB Southern span, UK [4]	Shallow susp.	108	0.8	
LMB Central span, UK [78]		144	0.48, 0.95	1.15, 1.54, 1.89, 2.32
LMB Northern span, UK [4]		81	1.0	
Changi Mezzanine Bridge, SG [101]	Steel arch	140	0.9	1.6
Lardal Bridge, NO [105]	Timber arch	91	0.83	1.45, 2.85
Coimbre Bridge, PT [108, 111]	Steel arch	110	0.91	1.54, 1.88, 1.95, 2.54
Simone de Beauvoir, Paris (FR) [26]	Steel arch	190	0.56, 1.15[3]	0.72, 1.04, 1.15[3], 1.53
				1.64, 1.78, 2.2, 2.3
CSB, Bristol (UK)	Suspension	194	0.52, 0.75	0.9, 1.15, 1.38, 1.65
Weil-am-Rhein, (DE) [115]	Steel arch	230	0.96	1.62[4], 1.90[4], 2.18[4]

[1] Total bridge length.

[2] Torsional mode.

[3] This mode has both lateral and vertical components.

[4] Unclear if these frequencies are vertical, lateral or torsional.

7.2.4. Parametric resonance excitation

In the previous section, the potential threat that vertical loads may excite lateral vibration modes through nonlinear modal coupling was discussed. Another possibility is that if the lateral force is nonlinear, e.g. through a displacement dependency, lateral vibration modes with natural frequencies equal half the walking frequency, may be excited into parametric resonance. It has been shown that the pedestrian-induced load is amplitude dependent [31, 79, 90]. Newland [87] related the Fourier transform of the modal pedestrian force to that of the lateral bridge displacement, based on the results of the platform tests carried out at Imperial College in 2000 [79].

Piccardo and Tubino [132] defined an equivalent time-domain model, in which the lateral pedestrian-induced force is proportional to the displacement:

$$F(x,t) = \lambda \left[\mathrm{DLF}_1 + \mathrm{DLF}_{in} u(x,t)\right] g m_p(x) \cos \omega_w t. \tag{44}$$

The parameter λ defines the percentage of synchronised pedestrians, DLF_1 equals the load amplitude in the absence of lateral motion, DLF_{in} is the proportion of the body weight in phase with the bridge

displacement, g is the acceleration of gravity, $m_p(x)$ is the pedestrian mass distribution, $u(x,t)$ is the displacement of the bridge and ω_w is the forcing frequency (angular walking frequency). Following the approach of Piccardo and Tubino [132], using non-dimensional parameters, the equation of motion of a single mode is written as:

$$\ddot{y} + 2\eta\dot{y} + \left[\delta - 2\varepsilon\cos 2\tilde{t}\right] y = \kappa\cos 2\tilde{t} \tag{45}$$

where the non-dimensional space and time variables are $y = q_j/L$ and $\tilde{t} = \frac{1}{2}\omega_w t$ respectively with q_j being the modal displacement of mode j and L the bridge length. The remaining parameters in Eq. (45) are non-dimensional variants of the modal parameters of the bridge.

Equation (45) is a non-homogeneous damped Mathieu equation, which is characterised by the parametric excitation in y [129]. Piccardo and Tubino [132] analyse the characteristics of this equation using a perturbation technique and find that the susceptibility to instability depends on the damping ζ_j, frequency ratio ω_j/ω_w between the natural modal frequency and the forcing frequency and the mass of synchronised pedestrians λM_{pj} to the modal mass M_j. The stability criterion is given as:

$$\frac{M_{pj}}{M_j} < \frac{\omega_w^2}{2g\lambda\mathrm{DLF}_{in}}\sqrt{\left[4\frac{\omega_j^2}{\omega_w^2} - 1\right]^2 + 16\frac{\omega_j^2}{\omega_w^2}\zeta_j^2} \tag{46}$$

The minimum number of people needed to cause instability is obtained in the case $\omega_w = 2\omega_j$. The stability criterion assumes that the fraction λ of the pedestrians synchronise their pacing rate (and phase) to the frequency ω_w. Piccardo and Tubino [132] used the London Millennium Bridge as a benchmark test to verify the applicability of the procedure and find that when assuming that 30 % of the pedestrians synchronise at a walking frequency $\omega_w/(2\pi) = 0.96\,\mathrm{Hz}$ (pacing rate 1.92 Hz), which is exactly twice the frequency of the first central span lateral mode (0.48 Hz), the stability criterion in Eq. (46) compares well with the observations made on the bridge.

The stability criterion is very sensitive to the relationship between the pacing rate and the modal frequency and a very rapid increase in the critical number of pedestrians is observed when ω_w deviates from $2\omega_j$. In order to verify this model, it is necessary to know the actual distribution of pedestrian pacing rates. Furthermore, the methodology does not explain the excessive vibrations observed at frequencies around 1 Hz, but only those in the lower frequency range. It is also worth noting that the expression in (44) states that the pedestrian load has a sinusoidal component ($\mathrm{DLF}_{in} g m_p(x)\cos\omega_w t$) which is multiplied by the displacement time history $u(x,t)$. This assumption has not been verified as the platform tests at Imperial College only showed a correlation between the amplitudes of the pedestrian-induced lateral load and the platform motion. Therefore, further experimental verification of the basic load assumption in (44) is needed.

7.2.5. Pedestrian phase synchronisation

Phase synchronisation originates from the theory of coupled oscillators, primarily known from large biological and chemical systems [133]. In particular the phenomenon of collective synchronisation, described as "... an enormous system of oscillators spontaneously locks to a common frequency, despite

the inevitable difference in the natural frequencies of the individual oscillators" [134] has caught the attention of researchers working with pedestrian-induced vibrations. The first attempt to describe the lateral vibrations of the London Millennium Bridge within the framework of coupled oscillators was given by Strogatz et al. [135] who state that "wobbling and synchrony are inseparable". Their model is based on a set of coupled nonlinear ordinary differential equations which 1) describe the modal response of the structure and 2) the development of the phase of each pedestrian in relation to that of the bridge [135]:

$$\ddot{q}(t) + 2\zeta\omega_0\dot{q}(t) + \omega_0^2 q(t) = \frac{G}{M}\sum_{j=1}^{N}\sin\Theta_j(t) \tag{47}$$

$$\dot{\Theta}_j(t) = \omega_{wj} + cq_0(t)\sin\left(\Psi(t) - \Theta_j(t) + \alpha\right) \tag{48}$$

The modal mass, damping and angular frequency are denoted M, ζ and ω_0 respectively, $q(t)$ is the modal response, $G = 30\,\mathrm{N}$ is the pedestrian force amplitude, ω_{wj} is the angular walking frequency in the absence of bridge motion and $\Theta_j(t)$ is the phase, both for pedestrian j. The parameter α, denotes the initial phase between the pedestrian-induced load and the bridge displacement. The change in phase is governed by the parameter c which denotes the sensitivity of the pedestrian to bridge motion, the bridge amplitude $q_0(t)$ and total phase $\Psi(t) + \alpha$, defined such that:

$$q(t) = q_0(t)\sin\Psi(t) \tag{49}$$

$$\dot{q}(t) = \omega_0 q_0(t)\sin\Psi(t). \tag{50}$$

Strogatz et al. derived a closed form solution for the critical number of pedestrians that cause instantaneous synchronisation in the simple case where $\alpha = \pi/2$ and the (initial) distribution $p_{\omega_w}(\omega)$ of walking frequencies is symmetric about the modal frequency ω_0 [135]:

$$N_{\mathrm{cr}} = \frac{4\zeta}{\pi}\frac{K}{G\,c\,p_{\omega_w}(\omega_0)} \tag{51}$$

The only unknown in this equation is the coefficient c which was calibrated against the data from the Millennium Bridge to the value of $16\,\mathrm{m^{-1}s^{-1}}$. The assumption $\alpha = \pi/2$ is similar to that of Newland [87], which is a worst-case scenario for the input force, i.e. being in phase with the modal velocity. If the pedestrian walking frequencies are normally distributed, (with standard deviation σ_{ω_w} mean frequency equal the modal frequency) the critical number of pedestrians becomes:

$$N_{\mathrm{cr}} = \sqrt{\frac{2}{\pi}}\frac{4\zeta K}{G\,c}\sigma_{\omega_w} \tag{52}$$

The basic idea in this type of load model, is that the walking frequencies of the pedestrians (which initially are randomly distributed), lock-in to the frequency of the bridge if the external stimulus (the vibration amplitude) is strong enough and/or if the initial pacing rate is close to the vibration frequency. According to Abrams [65], the model described above will be valid for modes with natural frequencies in the range 0.75 to 1.25 Hz.

In later publications by the same authors [136, 137], the expression for the phase development Eq. (48) was modified such that the pedestrians react to the acceleration of the bridge rather than its displacement,

i.e. the modified expression reads:

$$\dot{\Theta}_j(t) = \omega_{w_j} - c\ddot{q}(t) \sin\Big(\Psi(t) - \Theta_j(t) + \alpha\Big). \tag{53}$$

It was shown that the critical number of pedestrians could be obtained under similar simplified assumptions as described above and that the parameters of the model could be calibrated against the results from the Millennium Bridge. Abdulrehem and Ott [138] analysed the modified model by Eckhardt et al. [136] in Eq. (53) and showed that the critical number of pedestrians increases quadratically with the average pacing rate and the modal frequency.

As stressed by the authors [65, 135, 136], the modelling framework is meant as a qualitative description of the coupled pedestrian bridge system and experimental justification for the choice of load model is needed together with a statistical description of the involved parameters. Although capable of explaining excessive lateral vibrations for bridge modes with frequencies around 1 Hz, in its present form the model cannot capture the excitation of lower frequency modes such as that on the Clifton Suspension Bridge or the London Millennium Bridge.

7.2.6. Pendulum walking models

At the first international footbridge conference in Paris 2002, Chris Barker [139] proposed a very simple load model for the lateral load induced by a walking pedestrian:

$$F(t) = \frac{W}{2L_{leg}} \begin{cases} -s + 2\left(u(t) - u(0)\right) & \text{for } 0 \le t \le \pi/\omega_w \\ s + 2\left(u(t) - u(0)\right) & \text{for } \pi/\omega_w \le t \le 2\pi/\omega_w \end{cases} \tag{54}$$

where W is the pedestrian weight, s is the gait width, L_{leg} is the length of the leg, $\omega_w = 2\pi f_w$ is the angular walking frequency and $u(t)$ is the lateral motion of the bridge deck (assumed simple harmonic). The basic assumption in the load model is that the maximum lateral force can be determined by resolving the 'static' vertical body force into a lateral force through the leg inclination. It is further assumed that centre of mass of the body moves in a straight line along the longitudinal axis of the bridge. In the absence of lateral bridge movement, this assumption means that the lateral force is constant during one step cycle.

According to the model, large lateral response may be expected for uncorrelated crowd of pedestrians, walking at frequencies away from the natural frequency of the lateral mode. The author argues that this is, in fact, what was observed on the Millennium Bridge in London and that a dramatic review of current load models may be necessary, somewhat in line with the statement of Professor Josephson [67] as discussed in Section 4. It should be noted however, that the main assumption that the centre of mass of the body moves in a straight line, violates the equilibrium condition, which states that a lateral GRF is caused by the inertia associated with a lateral acceleration of the body.

Inspired by the work of Barker [139], Macdonald [140] developed a load model that accounts for the lateral movement of the pedestrian's centre of mass and he further developed a control scheme for controlling the gait, based on research related to human balance. The basic assumption is that the lateral

force exerted by the pedestrian is obtained as the overall inertia force associated with the movement of the body centre of mass. The governing differential equation for the movement of the pedestrians becomes:

$$\ddot{y} + \omega_w^2 (s - y) = -\ddot{u} \tag{55}$$

where y is the movement of the centre of mass, s is the lateral position of the centre of pressure, u is the lateral bridge displacement and ω_w is the angular walking frequency. The force exerted by a pedestrian on laterally moving surface is thereby obtained as:

$$F = -m_p (\ddot{u} + \ddot{y}) = -m_p \omega_w^2 (s - y) \tag{56}$$

Based on this model, it was shown that the lateral movement of the centre of mass, in the absence of bridge motion, is approximately sinusoidal. The acceleration however, is not sinusoidal and the resulting lateral forces compare well in shape and magnitude to measured lateral force time histories.

Interestingly, Macdonald [140] argues that the lateral foot placement is the most efficient means of maintaining balance rather than the timing of the footstep, as studied by Johnson [141]. In other words, pedestrian need not to synchronise with the movement of the bridge to walk comfortably on a vibrating footbridge. The balancing strategy from Hof et al. [142] involves only control of the lateral position of the centre of pressure, i.e. s, which ensures that the centre of mass does not pass the centre of pressure with a certain margin of safety.

Through numerical simulations, Macdonald showed that by using this model, a lateral force component at the natural frequency of the bridge occurs, despite that the pedestrians walks with a constant walking frequency away from that frequency. Further, it was shown that the force components in phase with the velocity and acceleration of the bridge respectively are proportional to displacement amplitude, suggesting that pedestrians can be treated as added mass and damping. The amplitude (and sign) of these force components, depend on the natural frequency of the bridge, see Fig. 30. In the frequency interval 0.7 - 1.7 Hz, the pedestrians act as negative dampers and in the interval 0.3 - 1.2 Hz the equivalent added mass per pedestrian is negative with up to 61 % of the body mass [140]. This observation is in line with findings of other researchers [59, 113], however a further experimental verification of this observation is needed. Macdonald's load model has obtained a considerable amount of attention in the UK since it was first published, illuminated through a BBC radio interview and a Nature News article [143] entitled "Millennium Bridge wobble explained". However, results of the model show a high sensitivity to the selected control scheme, complimentary experimental data is needed to determine the correct scheme and to calibrate the model.

7.3. Comprehensive modelling of human-structure dynamic system

In this section, a review of a more comprehensive modelling approach is given which is based on a macroscopic treatment of the pedestrian crowd. Ricciardelli and Pizzimenti [56] argue that uncorrelated pedestrians enter a bridge and if the crowd density ρ is lower than a certain critical value, the crowd can be treated as a non-synchronised group. If the response of the bridge due to the non-synchronised

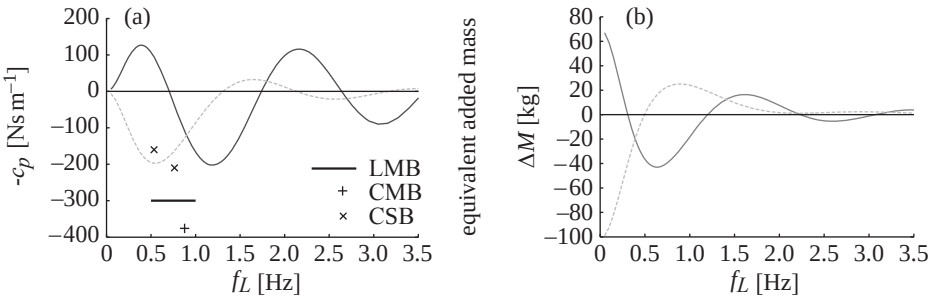

Figure 30: Simulated equivalent damping coefficient (a) and added mass (b) per pedestrian shown with estimated values from full scale measurements. LMB: London Millennium Bridge [4], CMB: Changi Mezzanine Bridge [101], CSB: Clifton Suspension Bridge, [113], Solid curve: Control law based on relative velocity of the centre of mass, Dashed curve: Control law based on absolute velocity of the centre of mass (Figure reproduced from [140]).

group (or due to another external source) exceeds a critical threshold the pedestrians synchronise with the structure which must be accounted for in the modelling. If the vibration amplitude is limited or if the pedestrian mass is lower than a critical value needed to maintain amplitudes larger than the critical threshold, the crowd remains uncorrelated and the response can be calculated without accounting for the structural movement. If the pedestrian density somewhere on the bridge is larger than a critical value this portion of the pedestrians tend to synchronise their step as a consequence of human-human interaction. If the portion of pedestrians in step produce response exceeding the lock-in threshold, human-structure interaction also occurs. Otherwise, the pedestrian loading remains independent of the movement of the structure. Although simplified, this idea touches upon two important effects that must be accounted for when modelling human induced vibrations; (i) the human-human interaction and (ii) human-structure interaction. Human-structure interaction is the potential change in the walking pattern of an individual (e.g. walking speed, frequency, phase or step length or width) due to the movement of the structure and human-human interaction is the change due to the surrounding people.

7.3.1. Dynamics of a moving crowd and human-human interaction

Dynamic pedestrian-induced lateral loading is generally narrow-banded and is concentrated around the average walking frequency of the pedestrians or its multiple harmonics. For lightly damped structures, like most footbridges, a precise description of the frequency content of the loading is vital in order to accurately predict the response. This is a difficult task since it is governed by the walking characteristics of the pedestrians within the crowd. A crowd of pedestrians is an extremely complex system and a complete description of the walking pattern of each individual is only possible in a probabilistic sense.

Several studies on the walking characteristics of crowds have been undertaken in the past, often in relation to urban design and planning of pedestrian facilities [144, 145] and in studies related to evacuation of structures during catastrophic events [146–148]. Modelling of pedestrian flow can be made

on a microscopic level where each pedestrian is modelled uniquely or macroscopically where the crowd is modeled through its average characteristics [145]. A widely used approach to the modelling of macroscopic pedestrian flow is the continuum approach where the governing parameters are the crowd intensity density, ρ (expressed in persons/m^2), the (mean) crowd velocity, v, and the pedestrian flux, $\rho \cdot v$, (persons/m/s) [149, 150].

The relationship between the density and the flux may be expressed using the mass conservation equation in its Eulerian form either in 2D [149] or 1D (which is more relevant for pedestrian bridges) as follows, [151]:

$$\frac{\partial \rho}{\partial t} + \frac{\partial}{\partial x}(\rho \cdot v) = 0 \tag{57}$$

This continuity equation is interpreted as the change in density over time in an interval dx equals the flux through the boundary. In order to solve this partial differential equation, a characterisation of the pedestrian walking speed is necessary.

7.3.2. Spatially unrestricted pedestrian behaviour

The walking speed determines the time spent by each pedestrian on the footbridge and the importance of this parameter is further illuminated through the geometric relationship between the walking speed, the step length and the pacing rate, $v_p = l_p f_p$. In relation to design of footbridges, walking speed of pedestrians has been reported in the range from 0.75 m/s for slow walking to 1.75 m/s for fast walking, [152]. In recent years other researchers have investigated the walking characteristics of individuals in order to map their natural choice of walking speed and pacing rate [30]. A summary of different studies related to the average unrestrained walking characteristics of pedestrians is shown in Table 6. Typically researchers report a relationship between the pacing rate of a person as a function of the freely selected (unrestricted) walking velocity. A linear relationship of the type:

$$f_p = a v_p + b \tag{58}$$

is often used, e.g. by Pachi and Ji [153] who report $b = 0$ and $a = 1.33\,\mathrm{m}^{-1}$ for men and $a = 1.49\,\mathrm{m}^{-1}$ for women. Zivanovic et al. [154] uses a similar expression with $b = 0.355\,\mathrm{Hz}$ and $a = 1.075\,\mathrm{m}^{-1}$. Their observations are based on data obtained from 939 different pedestrians during a 6.5 hour monitoring of an indoor footbridge. Based on the freely selected walking characteristics of 116 pedestrians walking along a 72 m corridor, a linear fit of the above-mentioned type to the data yielded $b \cong 0$ and $a = 1.326\,\mathrm{m}^{-1}$ [94]. Ingólfsson et al. [84] used the results from different studies [155–157] to formulate a power law for the relationship between pacing rate, velocity and step length:

$$f_p = 1.62 v_p^{0.35}. \tag{59}$$

This model is advantageous as it fulfills the boundary condition that $f_p(0) = 0$ whilst it allows non constant values for the stride length, opposed to the linear law from (58).

Kasperski [53] points out that both physical, psychological and environmental parameters determine the walking velocity of a person and the average walking velocity measured in 20 different cities in Ger-

many is in the range 1.41 m/s to 1.55 m/s for men and 1.36 m/s to 1.46 m/s for women. The observations were made for people walking freely in the respective city centres, [158] (reviewed in [53]).

Table 6: Comparison between unrestraint average walking characteristics according to different studies.

	N	Walking speed (m/s)			Pacing rate (Hz)		
Study		Men	Women	Total	Men	Women	Total
Matsumoto et al. [121]	505	-	-	-	-	-	1.99
Zivanovic et al. [159]	1976	-	-	-	-	-	1.87
Morgenroth [158] (after [53])	6000	1.49	1.41	1.45	-	-	-
Ricciardelli and Pizzimenti [56]	116	1.44	1.37	1.41	1.81	1.86	1.84
Sahnaci and Kasperski [62]	251	1.37	1.36	1.37	1.80	1.91	1.82
Pachi and Ji [153] [1]	400	1.35	1.25	1.30	1.80	1.86	1.83
Pachi and Ji [153] [2]	400	1.46	1.37	1.42	1.97	2.03	2.00
Zivanovic et al. [154]	939	1.51	1.45	1.47	1.89	1.98	1.94
Butz [50]	98	-	-	-	1.80	1.89	1.84
Venuti and Bruno [160] [3]	-		$1.34\,\alpha_G\alpha_T$		-	-	-

[1] Measured on two different footbridges

[2] Measured on floors in two different shopping malls

[3] The coefficient α_G depends on the geographic location (1.05 for Europe, 1.01 for USA and 0.92 for Asia) and the coefficient α_T depends on the travel purpose, (1.20 for Rush hour/Business, 1.11 for Commuters/Events and 0.84 for Leisure/Shopping).

7.3.3. Human-human dynamic interaction

As the crowd density increases, the possibility of free movement becomes restricted and people will need to adjust their walking speed to the speed of the surrounding crowd, [30, 161].

Bertram and Ruina [162] used twelve test subjects to investigated the change in the pacing rate for an imposed change in the walking velocity. The results from their study were used by Bruno and Venuti [163] to formulate the following law for the lateral forcing frequency as a function of the walking speed:

$$f_w = \left(0.35v_p^3 - 1.59v_p^2 + 2.93v_p\right)/2 \tag{60}$$

Human-human interaction denotes the interaction (and possibly synchronisation) that occurs within a crowd of pedestrians and the change in walking pattern as a consequence of the presence of other pedestrians on the bridge. Probably the most pronounced type of human-human interaction occurs when the pedestrian density increases not allowing each pedestrian to walk freely according to his/her own preferences. Tentative values in the range 0.2 to 0.5 ped/m^2 have been suggested as a limit value for free unrestrained walking [7, 11, 161]. However, Butz et al. [164] reported that during a harbour fair in Duisburg a pedestrian stream with density of 0.3 ped/m^2 occupied a footbridge and the average pacing rate in the group was about 1.5 Hz, considerably lower than what is usually reported for unconstrained

walking. This observation is confirmed by the tests performed on the London Millennium Bridge where a near linear decrease in walking velocity for increasing crowd density was observed, even at very low crowd densities [165].

Experimental investigations relating to human-human interaction were performed by Zoltowski [166] who found that the pedestrian pacing rate decreases with decreasing crowd densities. Butz [50] used a group of 18 persons who were asked to walk in one group with density varying from 1.2 to 3.0 $\mathrm{ped/m^2}$ to show a linear relationship between the forward velocity of the group and the average pacing rate. Further, the standard deviation of the pacing rates within the group generally increased with the velocity and decreased with the density of the group [50]. Similar experiments were conducted by Andersen [167] who used up to 80 volunteers walking in six different conditions (free walk to 1 $\mathrm{ped/m^2}$) to reveal that the average pacing rate, walking velocity and stride length decreased for increasing crowd density. However, the standard deviation of pacing rate remained nearly constant. The same study also showed that the distribution of individual phases was random with a near-uniform distribution at all tested crowd densities, suggesting limited phase synchronisation as a result of human-human interaction. This agrees with observations of 1200 pedestrians walking normally over different footbridges as reported by Barker [16]. In a recent study devoted to human-human interaction it was shown that the inter-subject variability, measured as the standard deviation of individual walking frequencies within the group, tends to decrease with an increase in the crowd density, [168]. In the same study, it was also shown that as the crowd density increases, intra-subject variation in the walking frequency of each individual tends to increase.

An excellent review of the interdisciplinary studies relating to human-human interaction, was given by Venuti and Bruno [30, 160] and Bruno and Venuti [163], where a general form of the Kladek formula from vehicular traffic to represent the average walking speed of the crowd as a function of the crowd density was proposed:

$$v = v_M \left\{ 1 - \exp\left[-\gamma \left(\frac{1}{\rho} - \frac{1}{\rho_M} \right) \right] \right\}. \tag{61}$$

Here v_M is the mean maximum velocity, ρ_M is the the maximum density causing the crowd to stop which depends on the travel purpose and the geographic location [160]. The parameter $\gamma = \beta \rho_M$ is a fitting parameter determined by the type of pedestrian activity (leisure $\beta = 0.245$, commuter $\beta = 0.214$ and rush hour $\beta = 0.273$). Other pedestrian speed-density relations are given in the review by Ishaque and Nolan [169] or Venuti and Bruno [30].

The general lesson learned from studies of human-human interaction is that the main effect of an increase in the crowd density is the change in the walking speed of the pedestrians. As the crowd density increases, the ability of people to walk at their own preferred speed decreases, thus the distribution of individual walking speeds (and thereby walking frequencies) becomes more narrow (i.e. the inter-subject variability decreases). To the authors' knowledge, there is no experimental evidence to support the assumption that pedestrians tend to fall into collective synchronisation when the crowd density increases. This is probably because the step length of each pedestrian remains variable (random) although the

forward velocity is the same for all pedestrians.

7.3.4. Continuous crowd modelling approach

With analogy to fluid dynamics, Venuti et.al. [151, 170] introduced a new explanation of crowd-structure interaction on a footbridge. The footbridge is modelled as a 1D beam and the equation of motion is written in modal coordinates as:

$$M_i(\rho)\ddot{q}_i(t) + C_i\dot{q}_i(t) + K_i q_i(t) = P_i(t, \rho, \dot{q}_i, \ddot{q}_i) \tag{62}$$

$$u(x,t) = \sum_{i=1}^{\infty} \Phi_i(x) q_i(t) \tag{63}$$

where $M_i(\rho)$, C_i, K_i and $\Phi_i(x)$ are the modal mass, damping, stiffness and mode shape respectively of mode i, $q_i(t)$ is the modal coordinate, $u(x,t)$ is the physical displacement and dot denotes differentiation with respect to time. For simplicity the index i will be omitted from now on. The modal pedestrian load, $P(t, \rho, \dot{q}, \ddot{q})$, is a function of the crowd mass density, ρ and of the modal coordinate q, making the equation of motion non-linear. Furthermore, The modal mass is the sum of a contribution from the structural mass M_s and that of the pedestrian crowd M_p.

The physical pedestrian force, $F(x,t)$, is modelled as the sum of three contributions, F_s due to uncorrelated pedestrians, F_{ps} due to human structure synchronisation and F_{pp} due to synchronisation amongst pedestrians (human-human synchronisation) [171].

The average walking frequency of the crowd is determined as function the crowd velocity v according to Eq. (60), [172]. The total number of pedestrians is denoted n and n_{ps} is the number of pedestrians synchronised with the movement of the structure and thereby induce a force at the structural frequency f_0. Following the studies reported by Pizzimenti [59], the force is divided into a part in phase with the velocity of the structure and one in phase with the acceleration, both of which are assumed to increase with an increase in the bridge oscillation [172]. The remaining pedestrians, $n - n_{ps}$, are assumed to walk at the average pacing rate determined from Eq. (60) where a total number n_{pp} walk in phase due to human-human interaction and the rest walk at a random phase, [171]. The number of synchronised pedestrians is determined through the synchronisation coefficients S_{ps} and S_{pp}, defined as:

$$S_{ps}(\ddot{u}_0, f_r) = \left[1 - e^{-b(\ddot{u}_0 - \ddot{u}_c)}\right]\left[e^{-50(f_r-1)^2 e^{-20\ddot{u}_0/\pi}}\right] \tag{64}$$

$$S_{pp}(\rho) = \frac{1}{2}\left[1 + \mathrm{erf}\left(a\rho_M\left[\rho - \frac{\rho_{\mathrm{sync}} + \rho_c}{2}\right]\right)\right] \tag{65}$$

where $a = 3.14$, $b = 2.68$, $f_r = f_w/f_0$, $\ddot{u}_0$ is the envelope of the acceleration time history, ρ_{sync} is the crowd density that corresponds to total synchronisation (proposed as $1.8\,\mathrm{ped/m^2}$) of the pedestrians and ρ_c is the upper limit for unconstrained free walk, proposed as $0.3\,\mathrm{ped/m^2}$, [171].

In this load model, the modelling of the pedestrian crowd is governed by Eq. (57) where the free walking speed, determined from Eq. (61) is multiplied with a correction function $g(\ddot{u}_0)$, which lowers the walking speed as the platform vibration increases, [171]. To the authors' knowledge, no studies have been performed to determine the effect of structural vibrations on the walking speed of pedestrians and only

limited experimental evidence exists for the synchronisation coefficients. However, the authors of the load model performed a thorough comparison between simulated response and the measured response on the T-Bridge in Japan which showed a good agreement, both in terms of vibration amplitude and degree of synchronisation [171, 173].

Bodgi et al. [174, 175] used the same framework, i.e. a macroscopic modelling of the pedestrian flow assuming that the crowd behaves like a compressible fluid. The governing equations for the structure and crowd respectively are Eqs. (62), (63) and (57). The 'closure' equation, which defines the relationship between the crowd density and velocity is adopted from Venuti et al. [170], whereas the pedestrian load is assumed slightly differently [175]:

$$F(x,t) = G_1 \sin(2\pi f_0 t)\, \rho b S(\dot{u}, \rho) \tag{66}$$

$$S(\dot{u}, \rho) = \begin{cases} S_p(\rho) & \ddot{u}(x,t) \leq \ddot{u}_{\min} \\ S_{ps}(\dot{u}) & \text{otherwise} \end{cases} \tag{67}$$

$$S_p(\rho) = \begin{cases} 8.6\sqrt{\zeta}/\sqrt{\rho b L} & \rho \leq \rho_c \\ 1.75/\sqrt{\rho b L} & \text{otherwise} \end{cases} \tag{68}$$

where b is the width of the bridge deck, L is its length, f_0 is the lateral frequency of the relevant mode, $\ddot{u}_{\min} = 0.1\,\mathrm{m/s^2}$ is defined as a vibration perception threshold and $S_{ps}(\dot{u})$ is a velocity dependent synchronisation function of a similar form to that in Eq. (65). The load amplitude is taken as a function of the walking speed, $G_1 = 0.6191\,\mathrm{Ns/m} \times v + 35.5171\,\mathrm{N}$. According to Bodgi et al. [175], the synchronisation coefficient $S(\dot{u}, \rho)$ defines the equivalent number of pedestrians walking with the same frequency as that of the lateral mode in question producing the same load as the entire crowd and is based on the tests reported in Sétra [5].

In a later paper by Bodgi et al. [176] they propose a different load model. This time the inspiration comes from the Kuramoto equation which was discussed in Section 7.2.5, coupled with the Eulerian description of the crowd:

$$F(x,t) = \rho(x,t) b G_1 \sin\Theta(t) \tag{69}$$

$$\frac{\partial \Theta}{\partial t}(x,t) = \omega_w + \frac{\varepsilon}{2} A_u(t) \left|\Phi(x)\right| \left[\dot{\Psi}_s(t)\right]^2 \sin\left(\Psi(t) - \Theta(x,t)\right) \tag{70}$$

$$\dot{\Psi}(t) = \omega_0(t) \tag{71}$$

Here ω_w is the (initial) angular pacing frequency, A_u is the maximum displacement of the footbridge during the last two oscillations, $\Phi(x)$ is the mode shape of the relevant mode with angular frequency $\omega_s(t)$ and ε is a constant that determines the sensitivity of the phase coupling between the pedestrian and the structure. In this framework, a different closure equation has been proposed [176]:

$$v(x,t) = \frac{1}{\pi} l_p C_s(x,t) C_\rho(x,t) \frac{\partial \Theta}{\partial t}(x,t) \tag{72}$$

where l_p is the free step and the functions $C_s(x,t)$, $\in [0,1]$ and $C_\rho(x,t)$, $\in [0,1]$ reduce the pedestrian step length with an increase in structural vibrations and local crowd density respectively. The parameters

of the model were calibrated such to match approximately the critical number of pedestrians on the Millennium Bridge [176]. Further analysis of the performance of this model is presented in the PhD thesis of Bodgi [177]

References

[1] J. Eyre, Aesthetics of footbridge design, in: Proceedings of Footbridge 2002, First International Conference, Paris, 2002.

[2] J. Strasky, New structural concepts for footbridges, in: Proceedings of Footbridge 2002, First International Conference, Paris, 2002.

[3] H. Bardsley, F. Consigny, R. Menard, B. Vaudeville, The Bercy-Tolbiac footbridge in Paris, in: Proceedings of Footbridge 2002, First International Conference, Paris, 2002.

[4] P. Dallard, A. Fitzpatrick, A. Flint, S. Bourva, A. Low, R. Smith, M. Willford, The London Millennium Footbridge, The Structural Engineer 79 (22) (2001) 17–33.

[5] Sétra, Footbridges, Assessment of vibrational behaviour of footbridges under pedestrian loading, The Technical Department for Transport, Roads and Bridges Engineering and Road Safety (November 2006).

[6] W. Hoorpah, Footbridges conference: History, reason and the way forward, in: Proceedings of Footbridge 2008, Third International Conference, Porto, 2008.

[7] FIB, Guidelines for the design of footbridges, bulletin 32, Fédération international du béton (*fib*) (November 2005).

[8] C. Butz, G. Sedlacek, Bemessungskonzept für fußgängerinduzierte Brückenschwingungen, Stahlbau 76 (6) (2007) 391–400, (In German).

[9] C. Butz, C. Heinemeyer, A. Keil, M. Schlaich, A. Goldack, S. Trometer, M. Lukić, B. Chabrolin, A. Lemaire, P. Martin, A. Cunha, E. Caetano, Design of Footbridges - Guidelines and background document, HIVOSS, rFS2-CT-2007-00033 (2007).

[10] C. Heinemeyer, M. Feldmann, European design guide for footbridge vibration, in: Proceedings of Footbridge 2008, Third International Conference, Porto, 2008.

[11] C. Butz, C. Heinemeyer, G. Sedlacek, B. Chabrolin, A. Lemaire, M. Lukic, P. Martin, Advanced load models for synchronous pedestrian excitation and optimised design guidelines for steel footbridges, Project Report RFSR-CT-2003-00019, Research fund for Coal and Steel (2008).

[12] C. Barker, S. DeNeumann, D. Mackenzie, R. Ko, Footbridge pedestrian vibration limits. part 1: Pedestrian input, in: Proceedings of Footbridge 2005, Second International Conference, Venice, 2005.

[13] C. Barker, Footbridge pedestrian vibration limits. part 3: Background to response calculations, in: Proceedings of Footbridge 2005, Second International Conference, Venice, 2005.

[14] D. Mackenzie, C. Barker, N. McFadyen, B. Allison, Footbridge pedestrian vibration limits. part 2: Human sensitivity, in: Proceedings of Footbridge 2005, Second International Conference, Venice, 2005.

[15] C. Barker, A. Daly, Dynamic response properties of footbridges: Design proposals for pedestrian excitation, unpublished project report UPR/ISS/48/05 (July 2005).

[16] C. Barker, Footbridge pedestrian vibration limits background to response calculation, International Journal of Space Structures 22 (1) (2007) 35–43.

[17] NA to BS EN 1991-2 UK, National Annex to Eurocode 1: Actions on structure - Part 2: Traffic loads on bridges, CEN, European Committee for Standardization (May 2008).

[18] C. Barker, D. Mackenzie, Calibration of the UK national annex, in: Proceedings of Footbridge 2008, Third International Conference, Porto, 2008.

[19] J. Brownjohn, E. Caetano, X. Cespedes, P. Charles, A. Cunha, P. Duflot, M. Feldmann, O. Flamand, C. Heinemeyer, W. Hoorpah, A. Low, F. Magalhaes, C. Meinhardt, C. Moutinho, A. Pavic, D. Taylor, S. Zivanovic, T. Zoli, K. Zoltowski, Footbridge Vibration Design, Taylor and Francis, 2009.

[20] C. Moutinho, E. Caetano, A. Cunha, A. Adao Da Fonseca, Dynamic behaviour of a long span stainless steel arch footbridge, in: Proceedings of Footbridge 2002, First International Conference, Paris, 2002.

[21] X. Cespedes, S. Manon, Dynamic analysis of the Bercy-Tolbiac footbride, in: Proceedings of Footbridge 2005, Second International Conference, Venice, 2005.

[22] A. Fournol, F. Gerard, V. De Ville, Y. Duchene, M. Maillard, Dynamic behaviour of Ceramique footbridge (Maastricht, NL), in: Proceedings of Footbridge 2005, Second International Conference, Venice, 2005.

[23] D. Powell, A. De Donno, A. Low, Design of damping systems for footbridges. Experience from Gatwick and Jjburg, in: Proceedings of Footbridge 2005, Second International Conference, Venice, 2005.

[24] R. Alves, J. Figueiras, M. Pimentel, C. Félix, A. Dimanda, A. Cunha, E. Caetano, Instrumentation, monitoring and execution control of the footbridge over modego river in Coimbre, in: Proceedings of Footbridge 2005, Second International Conference, Venice, 2005.

[25] E. Caetano, l. Cunha, A. D. Fonseca, R. Bastos, D. D. Fonseca Jr, Assessment and control of human induced vibrations in the new coimbra footbridge, in: Proceedings of Footbridge 2005, Second International Conference, Venice, 2005.

[26] W. Hoorpah, O. Flamand, X. Cespedes, The Simon de Beauvoir footbridge in Paris. Experimental verification of the dynamic behaviour under pedestrian loads and discussion of corrective modifications, in: Proceedings of Footbridge 2008, Third International Conference, Porto, 2008.

[27] A. Low, Design for dynamic effects in long span footbridges, in: Proceedings of Footbridge 2008, Third International Conference, Porto, 2008.

[28] S. Živanović, A. Pavic, P. Reynolds, Vibration serviceability of footbridges under human-induced excitation: a literature review, Journal of Sound and Vibration 279 (1-2) (2005) 1–74.

[29] V. Racic, A. Pavic, J. Brownjohn, Experimental identification and analytical modelling of walking forces: Literature review, Journal of Sound and Vibration 326 (2009) 1–49.

[30] F. Venuti, L. Bruno, Crowd-structure interaction in lively footbridges under synchronous lateral excitation: A literature review, Physics of Life Reviews 6 (2009) 176–206.

[31] L. Sun, X. Yuan, Study on pedestrian-induced vibration of footbridge, in: Proceedings of Footbridge 2008, Third International Conference, Porto, 2008.

[32] A. Blekherman, Swaying of pedestrian bridges, Journal of Bridge Engineering 10 (2) (2005) 142–150.

[33] B. Wolmuth, J. Surtees, Crowd-related failure of bridges, Proceedings of the ICE: Civil Engineering 156 (3) (2003) 116–123.

[34] P. Dallard, T. Fitzpatrick, A. Flint, A. Low, R. Smith, M. Willford, M. Roche, London Millennium Bridge: Pedestrian-induced lateral vibration, Journal of Bridge Engineering 6 (6) (2001) 412–417.

[35] Point of collapse, The Village Voice, New York, USA.

[36] Q. Ye, G. Fanjiang, B. Yanev, Investigation of the dynamic properties of the Brooklyn Bridge, in: Sensing Issues in Civil Structural Health Monitoring, Springer Netherlands, 2005, pp. 65–72.

[37] C. Peterson, Theorie der Zufallsschwingungen und Anwendungen (theory of random vibrations and applications), Work Report 2/72, Structural Engineering Laboratory, Technical University of Munich, in German (1972).

[38] H. Bachmann, W. Ammann, Vibrations in Structures. Induced by Man and Machine, 3rd Edition, Structural Engineering Documents, International Association for Bridge and Structural Engineering (IABSE), Zürich, Switzerland, 1987.

[39] H. Bachmann, Case studies of structures with man-induced vibrations, Journal of Structural Engineering 118 (3) (1992) 631–647.

[40] S. Nakamura, T. Kawasaki, A method for predicting the lateral girder response of footbridges induced by pedestrians, Journal of Constructional Steel Research 65 (2009) 1705–1711.

[41] S. Nakamura, T. Kawasaki, Lateral vibration of footbridges by synchronous walking, Journal of Constructional Steel Research 62 (11) (2006) 1148–1160.

[42] Y. Fujino, B. Pacheco, S. Nakamura, P. Warnitchai, Synchronization of human walking observed during lateral vibration of a congested pedestrian bridge, Earthquake Engineering & Structural Dynamics 22 (9) (1993) 741–758.

[43] S. Nakamura, Y. Fujino, Lateral vibration on a pedestrian cable-stayed bridge, Structural Engineering International: Journal of the International Association for Bridge and Structural Engineering (IABSE) 12 (4) (2002) 295–300.

[44] A. Adao Da Fonseca, Footbridges in Portugal, in: Proceedings of Footbridge 2008, Third International Conference, Porto, 2008.

[45] F. Harper, W. Warlow, B. Clarke, The forces applied to the floor by the foot in walking. 1. walking on a level surface, Tech. rep., National Building Studies - Research paper 32, Department of Scientific and Industrial Research. (1961).

[46] T. Andriacchi, J. Ogle, J. Galante, Walking speed as a basis for normal and abnormal gait measurements., Journal of Biomechanics 10 (4) (1977) 261–268.

[47] K. Masani, M. Kouzaki, T. Fukunaga, Variability of ground reaction forces during treadmill walking, Journal of Applied Physiology 92 (5) (2002) 1885–1890.

[48] E. Chao, R. Laughman, E. Schneider, R. Stauffer, Normative data of knee joint motion and ground reaction forces in adult level walking, Journal of Biomechanics 16 (2) (1983) 219–233.

[49] H. Bachmann, A. Pretlov, H. Rainer, Vibration Problems in Structures: Practical Guidelines, Birkhäuser, 1996, Ch. Appendix G: dynamic forces from rhythmical human body motions.

[50] C. Butz, Beitrag zur Berechnung fußgängerinduzierter Brückenschwingungen (on the calculation of pedestrian-induced vibration of bridges), PhD thesis, RWTH Aachen, (In German) (2006).

[51] C. Sahnaci, M. Kasperski, Excitation of buildings and pedestrian structures from walking and running, in: Proceedings of Experimental Vibration Analysis for Civil Engineering Structures, Porto, 2007, pp. 209–218.

[52] A. Crowe, M. M. Samson, M. J. Hoitsma, A. A. van Ginkel, The influence of walking speed on parameters of gait symmetry determined from ground reaction forces, Human Movement Science 15 (1996) 347–367.

[53] M. Kasperski, Serviceability of pedestrian structures, in: Proceedings of the 25th IMAC Conference, Orlando, Florida, 2007.

[54] J. Brownjohn, A. Pavic, P. Omenzetter, A spectral density approach for modelling continuous vertical forces on pedestrian structures due to walking, Canadian Journal of Civil Engineering 31 (1) (2004) 65–77. doi:10.1139/L03-072.

[55] A. Pizzimenti, Analisi sperimentale dei meccanismi di eccitazione laterale delle passerelle ad opera dei pedoni (experimental analysis of the lateral pedestrian-induced mechanism of excitation of footbridges), Ph.D. thesis, Department of Civil and Environmental Engineering, University of Catania, (in Italian) (2003).

[56] F. Ricciardelli, A. Pizzimenti, Lateral walking-induced forces on footbridges, Journal of Bridge Engineering 12 (6) (2007) 677–688.

[57] S. Ohlsson, Floor vibration and human discomfort, PhD thesis, Chalmers University of Technology, Göteborg (1982).

[58] P. Eriksson, Vibration of low-frequency floors - dynamic forces and response prediction, PhD thesis, Chalmers University of Technology, Department of Structural Engineering, Göteborg (March 1994).

[59] A. Pizzimenti, F. Ricciardelli, Experimental evaluation of the dynamic lateral loading of footbridges by walking pedestrians, in: Proceedings of the 6th International Conference on Structural Dynamics, Paris, 2005.

[60] H. Stolze, C. Mondwurf, K. Johnk, M. Illert, Gait analysis during treadmill and overground locomotion in children and adults, Electroencephalography and Clinical Neurophysiology/ Electromyography and Motor Control 105 (6) (1997) 490–497.

[61] T. Warabi, M. Kato, K. Kiriyama, T. Yoshida, N. Kobayashi, Treadmill walking and overground walking of human subjects compared by recording sole-floor reaction force, Neuroscience Research 53 (2005) 343–358.

[62] C. Sahnaci, M. Kasperski, Random loads induced by walking, in: Proceedings of the 6th European Conference on Structural Dynamics, Southampton, 2005.

[63] D. Fong, Y. Chan, Y. Hong, P. Yung, K. Fung, K. Chan, Estimating the complete ground reaction forces with pressure insoles in walking, Journal of Biomechanics 41 (2008) 2597–2601.

[64] B. Cookson, Crossing the River, Mainstream Publishing, Edinburgh, 2006.

[65] D. Abrams, Two coupled oscillator models: The millennium bridge and the chimera state, Phd thesis, Cornell University (August 2006).

[66] T. Fitzpatrick, P. Dallard, S. Le Bourva, A. Low, R. Ridsill Smith, M. Willford, Linking London: The Millennium Bridge, Tech. rep., Royal Academy of Engineering (2001).

[67] B. Josephson, Out of step on the bridge, The Guardian (Wednesday 14 June 2000).
URL http://guardian.co.uk/theguardian/2000/jun/14/guardianletters3

[68] F. Danbon, G. Grillaud, Dynamic behaviour of a steel footbridge. Characterisation and modelling of the dynamic loading induced by a moving crowd on the Solferino footbridge in Paris, in: Proceedings of Footbridge 2005, Second International Conference, Venice, 2005.

[69] P. Dziuba, G. Grillaud, O. Flamand, S. Sanquier, Y. Tétard, La passerelle Solférino comportement dynamique (dynamic behaviour of the Solférino bridge), Bulletin Ouvrages Métalliques 1 (2001) 34–57, (in French).

[70] R. Sachse, The influence of human occupants on the dynamic properties of slender structures, PhD thesis, University of Sheffield, UK (April 2002).

[71] S. Živanović, A. Pavić, E. Ingólfsson, Modelling spatially unrestricted pedestrian traffic on footbridges, ASCE Journal of Strucutral Engineering 136 (10) (2010) 1296–1308.

[72] S. Živanović, I. Díaz, A. Pavić, Influence of walking and standing crowds on structural dynamic performance, in: Proceedings of the 27th IMAC Conference, Orlando, USA, 2009.

[73] N. Jørgensen, Human structure interaction: Influence of walking pedestrians on the dynamic properties of footbridge structures they occupy, MSc Thesis, Department of Civil Engineering, Technical University of Denmark (August 2009).

[74] C. Georgakis, E. Ingólfsson, N. Jørgensen, Change in mass and damping on footbridges due to pedestrians: vertical direction, manuscript in preperation (2011).

[75] P. Charles, V. Bui, Transversal dynamic actions of pedestrians. synchronization, in: Proceedings of Footbridge 2005, Second International Conference, Venice, 2005.

[76] Ove Arup and Partners International Ltd., London Borough of Southwalk Millennium Bridge. Prototype test report 2: Damping test results, (Unpublished internal report) (February 2002).

[77] A. Pavic, T. Armitage, P. Reynolds, J. Wright, Methodology for modal testing of the millennium bridge, london, Proceedings of the ICE: Structures and Buildings 152 (2) (2002) 111–122.

[78] A. Pavic, M. Willford, P. Reynolds, J. Wright, Key results of modal testing of the Millennium Bridge, London, in: Proceedings of Footbridge 2002, First International Conference, Paris, 2002.

[79] R. Hobbs, Test on lateral forces induced by pedestrians crossing a platform driven laterally, Tech. rep., Civil Engineering Department, Imperial College London, London, UK, a report for Ove Arup and Partners (August 2000).

[80] M. Willford, Dynamic actions and reactions of pedestrians, in: Proceedings of Footbridge 2002, First International Conference, Paris, 2002.

[81] A. McRobie, G. Morgenthal, J. Lasenby, M. Ringer, Section model tests on human-structure lock-in, Proceedings of the ICE: Bridge Engineering 156 (BE2) (2003) 71–79.

[82] J. Yoshida, M. Abe, Y. Fujino, K. Higashiuwatoko, Image analysis of human induced lateral vibration of a pedestrian bridge, in: Proceedings of Footbridge 2002, First International Conference, 2002.

[83] J. Yoshida, Y. Fujino, T. Sugiyama, Image processing for capturing motions of crowd and its application to pedestrian-induced lateral vibration of a footbridge, Shock and Vibration 14 (2007) 251–260.

[84] E. Ingólfsson, C. Georgakis, J. Jönsson, F. Ricciardelli, Vertical footbridge vibrations: Towards an improved and codifiable response evaluation, in: third International Conference on Structural Engineering, Mechanics and Computation, Cape Town, South Africa, 2007.

[85] D. Newland, Pedestrian excitation of bridges - recent results, in: Proceedings of the Tenth International Congress on Sound and Vibration, 2003, pp. 533–547.

[86] D. Newland, Vibration of the london millennium bridge: cause and cure, International Journal of Acoustics and Vibration 8 (1) (2003) 9–14.

[87] D. Newland, Pedestrian excitation of bridges, in: Proceedings of the Institution of Mechanical Engineers, Part C: Journal of Mechanical Engineering Science, Vol. 218, 2004, pp. 477–492.

[88] A. McRobie, G. Morgenthal, Risk management for pedestrian-induced dynamics of footbridges, in: Proceedings of Footbridge 2002, First International Conference, Paris, 2002.

[89] A. Rönnquist, Pedestrian induced vibrations of slender footbridges, PhD thesis, Norwegian University of Science and Technology (2005).

[90] A. Rönnquist, E. Strømmen, Pedestrian induced lateral vibration of slender footbridges, in: Proceedings of the 25th IMAC Conference, Orlando, USA, 2007.

[91] S. Nakamura, T. Kawasaki, H. Katsuura, K. Yokoyama, Experimental studies on lateral forces induced by pedestrians, Journal of Constructional Steel Research 64 (2008) 247–252.

[92] E. Ingólfsson, C. Georgakis, F. Ricciardelli, J. Jönsson, Experimental identification of pedestrain-induced lateral forces on footbridges, Journal of Sound and Vibration 330 (2011) 1265–1284. doi:10.1016/j.jsv.2010.09.034.

[93] E. Ingólfsson, C. Georgakis, F. Ricciardelli, L. Procino, Lateral human-structure interaction on footbridges, in: Tenth Internation Conference on Recent Advances in Structural Dynamics, Southampton, 2010.

[94] F. Ricciardelli, C. Briatico, E. Ingólfsson, C. Georgakis, Experimental validation and calibration of pedestrian models for footbridges, in: Proceedings of Experimental Vibration Analysis for Civil Engineering Structures, Porto, 2007.

[95] A. Pavic, P. Reynolds, Modal testing of a 34m catenary footbridge, Proceedings of SPIE - the International Scociety for Optical Engineering 4753 (II) (2002) 1113–1118.

[96] S. Živanović, A. Pavic, P. Reynolds, Modal testing and fe model tuning of a lively footbridge structure, Engineering Structures 28 (6) (2006) 857–868.

[97] A. Cunha, E. Caetano, C. Moutinho, F. Magalhaes, The role of dynamic testing in design, construction and long-term monitoring of lively footbridges, in: Proceedings of Footbridge 2008, Third International Conference, Porto, 2008.

[98] EN 1990, EN 1990/A1:2002. Eurocode - Basis of structural design, CEN, European Committee for Standardization (December 2005).

[99] J. Brownjohn, P. Fok, M. Roche, P. Moyo, Long span steel pedestrian bridge at Singapore Changi airport - part 1: Prediction of vibration serviceability problems, The Structural Engineer 82 (16) (2004) 21–27.

[100] J. Brownjohn, A. Pavic, P. Omenzetter, Modeling and measuring dynamic crowd loading on a long span footbridge, in: Proceedings of the 2004 International Conference on Noise and Vibration Engineering, ISMA, 2004, pp. 751–765.

[101] J. Brownjohn, P. Fok, M. Roche, P. Omenzetter, Long span steel pedestrian bridge at Singapore Changi airport - part 2: Crowd loading tests and vibration mitigation measures, The Structural Engineer 82 (16) (2004) 28–34.

[102] J. Brownjohn, S. Zivanovic, A. Pavic, Crowd dynamic loading on footbridges, in: Proceedings of Footbridge 2008, Third International Conference, Porto, 2008.

[103] S. Nakamura, Field measurements of lateral vibration on a pedestrian bridge, The Structural Engineer 81 (22) (2003) 22–26.

[104] A. Rönnquist, Strømmen, L. Wollebæk, Dynamic properties from full scale recordings and FE-modelling of a slender footbridge with flexible connections, Structural Engineering International 4 (2008) 421–426.

[105] A. Rönnquist, L. Wollebæk, K. Bell, Dynamic behaviour and analysis of a slender timber footbridge, in: 9th World Conference on Timber Engineering, 2006.

[106] A. Adao Da Fonseca, C. Balmond, Conceptual design of the new Coimbre fotbridge, in: Proceedings of Footbridge 2005, Second International Conference, Venice, 2005.

[107] A. Adao Da Fonseca, R. Bastos, A. Adao Da Fonseca Jr, N. Neves, Design and contruction of the new Coimbre fotbridge, in: Proceedings of Footbridge 2005, Second International Conference, Venice, 2005.

[108] E. Caetano, A. Cunha, C. Moutinho, F. Magalhaes, Lessons from the practical implementation of passive control system at the new Coimbre footbridge, in: Proceedings of Footbridge 2008, Third International Conference, Porto, 2008.

[109] E. Caetano, A. Cunha, C. Moutinho, Implementation of passive devices for vibration control at Coimbra footbridge, in: Experimental Vibration Analysis for Civil Engineering Structures, 2007, pp. 43–54.

[110] F. Magalhaes, A. Cunha, E. Caetano, Comparison of damping estimates from ambient and free vibration tests in large structures, in: Experimental Vibration Analysis for Civil Engineering Structures, 2007, pp. 307–316.

[111] F. Magalhaes, A. Cunha, E. Caetano, Dynamic testing of the new Coimbre footbridge before implementation of control devices, in: Proceedings of the 25th IMAC Conference, Orlando, Florida USA, 2007.

[112] D. Feichtinger, Bridge design, in: Proceedings of Footbridge 2008, Third International Conference, Porto, 2008.

[113] J. Macdonald, Pedestrian-induced vibrations of the Clifton Suspension Bridge, UK, Proceedings of the ICE: Bridge Engineering 161 (BE2) (2008) 69–77.

[114] W. Strobl, I. Kovaces, H. Andrä, Häberle, Eine Fußgängerbrücke mit einer Spannweite von 230 m (a footbridge with a span of 230 m), Stahlbau 76 (12) (2007) 869–879, (in German).

[115] M. Mistler, D. Heiland, Lock-in-Effekt beings Brücken infolge Fugängeranregung - Schwingungstest der weltlängsten Fugänger- und Velobrücke (lock-in effect due to pedestrian excitation of bridges - vibration test of the world's longest pedestrian and bicycle bridge), in: D-A-CH Tagung, Vienna, 2007, (in German).

[116] L. Franck, Synchronous lateral excitation of footbridges, Semester project report, Applied Computing and Mechanics Laboratory, Swiss Federal Insitute of Technology (2009).
URL `http://imacwww.epfl.ch/Team/Lestuzzi/Semester_Project/SA08_Footbridges_Franck.pdf`

[117] C. Butz, J. Dist, P. Huber, Effectiveness of horizontal tuned mass damper exemplified at the footbridge in Coimbre, in: Proceedings of Footbridge 2008, Third International Conference, Porto, 2008.

[118] T. Roberts, Lateral pedestrian excitation of footbridges, Journal of Bridge Engineering 10 (1) (2005) 107–112.

[119] T. Roberts, Synchronised pedestrian lateral excitation of footbridges, in: Proceedings of the 6th International Conference on Structural Dynamics, Paris, 2005.

[120] T. Roberts, Probabilistic pedestrian lateral excitation of bridges, in: Proceedings of the Institute of Civil Engineers: Bridge Engineering, Vol. 158, 2005, pp. 53–61.

[121] Y. Matsumoto, T. Nishioka, H. Shiojiri, K. Matsuzaki, Dynamic design of footbridges, in: IABSE Proceedings, Vol. P-17/78, 1978, pp. 1–15.

[122] F. Ricciardelli, Lateral loading of footbridges by walkers, in: Proceedings of Footbridge 2005, Second International Conference, Venice, 2005.

[123] J. Sólnes, Stochastic processes and random vibrations, Theory and practice, John Wiley & Sons, Chichester, England, 1997.

[124] C. Butz, Codes of practice for lively footbridges: State-of-the-art and required measures, in: Proceedings of Footbridge 2008, Third International Conference, Porto, 2008.

[125] C. Butz, A probabilistic engineering load model for pedestrian streams, in: Proceedings of Footbridge 2008, Third International Conference, Porto, 2008.

[126] S. Nakamura, Model for lateral excitation of footbridges by synchronous walking, Journal of Structural Engineering 130 (1) (2004) 32–37.

[127] E. Ingólfsson, C. Georgakis, A stochastic load model for pedestrian-induced lateral forces on footbridges, accepted for publication in Engineering Structures (2011).

[128] A. Nayfeh, D. Mook, Nonlinear oscillations, Wiley, New York, 1995.

[129] J. Thomsen, Vibration and stability, Advanced theory, analysis and tools, 2nd Edition, Springer, Berlin, Heidelberg, Germany, 2003.

[130] A. Blekherman, Autoparametric resonance in a pedestrian steel arch bridge: Solferino Bridge, Paris, Journal of Bridge Engineering 12 (2007) 669–676.

[131] Y. Fujino, P. Warnitchai, B. Pacheco, An experimental and analytical study of autoparametric resonance in a 3DOF model of cable-stayed-beam, Nonlinear Dynamics 4 (1993) 111–138.

[132] G. Piccardo, F. Tubino, Parametric resonance of flexible footbridges under crowd-induced lateral excitation, Journal of Sound and Vibration 311 (2008) 353–371.

[133] S. Strogatz, I. Stewart, Coupled oscillators and biological synchronisation, Scientific American 269 (1993) 68–73.

[134] S. H. Strogatz, From Kuramoto to Crawford: exploring the onset of synchronization in populations of coupled oscillators, Physica D 143 (1-4) (2000) 1–20.

[135] S. Strogatz, D. Abrams, A. McRobie, B. Eckhardt, E. Ott, Crowd synchrony on the millennium bridge, Nature 438 (7064) (2005) 43–44.

[136] B. Eckhardt, E. Ott, Crowd synchrony on the London Millennium Bridge, Chaos 16.

[137] B. Eckhardt, E. Ott, S. Strogatz, D. Abrams, A. McRobie, Modeling walker synchronization on the Millennium Bridge, Physical Review E 75 (2007) 21110–1–10. doi:10.1103/PhysRevE.75.021110.

[138] M. Abdulrehem, E. Ott, Low dimensional description of pedestrian-induced oscillation of the Millennium Bridge, Chaos 19.

[139] C. Barker, Some observations on the nature of the mechanism that drives the self-excited lateral response of footbridges, in: Proceedings of Footbridge 2002, First International Conference, Paris, 2002.

[140] J. Macdonald, Lateral excitation of bridges by balancing pedestrians, Proceedings of the Royal Society A 465 (2009) 1055–1073.

[141] R. Johnson, A mathematical modelling of the pedestrian induced lateral vibrations of the millennium bridge, MSc thesis, University of Bristol (2005).

[142] A. Hof, R. van Bockel, T. Schoppen, K. Postema, Control of lateral balance in walking, Gait & Posture 25 (2) (2007) 250–258.

[143] Millennium Bridge wobble explained, Nature newsdoi:10.1038/news.2008.1311.

[144] K. Finnis, D. Walton, Field observations of factors influencing walking speeds, in: 2nd International Conference on Sustainability Engineering and Science, 2007.

[145] E. Papadimitriou, G. Yannis, J. Golias, A critical assessment of pedestrian behaviour models, Transportation Research Part F 12 (3) (2009) 242–255. doi:10.1016/j.trf2008.12.004.

[146] R. Hughes, The flow of human crowds, Annual Review of Fluid Mechanics 35 (2003) 169–182.

[147] R. Lee, R. Hughes, Minimisation of the risk of trampling in a crowd, Mathematical and Computers in Simulation 74 (2007) 29–37.

[148] H. Kuang, Analysis of pedestrian dynamics in counter flow via an extended lattice gas model, Physical Review E 78 (6).

[149] R. Hughes, A continuum theory for the flow of pedestrians, Transportation Research, Part B (Methodological) 36B (6) (2002) 507–535.

[150] L. Huang, S. Wong, M. Zhang, C.-W. Shu, W. Lam, Revisiting hughes' dynamic continuum model for pedestrian flow and the development of an efficient solution algorithm, Transportation Research Part B 43 (2009) 127–141.

[151] F. Venuti, L. Bruno, N. Bellomo, Crowd dynamics on a moving platform: mathematical modelling and application to lively footbridges, Mathematical and Computer Modelling 45 (2007) 252–269.

[152] J. E. Wheeler, Prediction and control of pedestrian-induced vibration in footbridges, ASCE Journal of the Structural Division 108 (1982) 2045–2065.

[153] A. Pachi, T. Ji, Frequency and velocity of people walking, The Structural Engineer 83 (3) (2005) 36–40.

[154] S. Živanović, V. Racic, El-Bahnsay, A. Pavic, Statistical characterisation of parameters defining human walking as observed on an indoor passarelle, in: Experimental Vibration Analysis for Civil Engineering Structures, 2007, pp. 219–225.

[155] A. Pansera, Analisi sperimentale delle caratteristiche del cammino ed azione dei pedoni sulle passerelle pedonali (experimental analysis of gait characteristics and walking-induced actions on footbridges), BSc thesis, University of Reggio Calabria, (in Italian) (2006).

[156] P. Terrier, V. Turner, Y. Schutz, GPS analysis of human locomotion: further evidence for long-range correlations in stride-to-stride fluctuations of gait parameters, Human Movement Science 24 (1) (2005) 97–115.

[157] E. Ingólfsson, Pedestrian-Induced Vibrations of Line-like Structures, MSc thesis, Department of Civil Engineering, Technical University of Denmark (June 2006).

[158] O. Morgenroth, Walking speed and pace of life, Report 'städtestudie', TU Chemnitz, Institute for Psychology, (in German) (2003).

[159] S. Živanović, A. Pavic, P. Reynolds, P. Vujovic, Dynamic analysis of lively footbridge under everyday pedestrian traffic, in: Proceedings of the sixth European conference on structural dynamics, 2005.

[160] F. Venuti, L. Bruno, An interpretative model of the pedestrian fundamental relation, C.R. Mecanique 335 (2007) 194–200.

[161] D. Oeding, Verrkhersbelastung und Dimensionierung von Gehwegen und anderen Anlagen des Fußgangerverkhers, Tech. Rep. 22, Strassenbau und Strassenverkherstechnik (1963).

[162] J. Bertram, A. Ruina, Multiple walking speed-frequency relations are predicted by constrained optimization, Journal of Theoretical Biology 209 (4) (2001) 445–453.

[163] L. Bruno, F. Venuti, The pedestrian speed-density relation: modelling and application, in: Proceedings of Footbridge 2008, Third International Conference, Porto, 2008.

[164] C. Butz, F. Magalhaes, A. Cunha, E. Caetano, A. Goldack, Experimental characterization of the dynamic behaviour of lively footbridges, in: Proceedings of Footbridge 2005, Second International Conference, Venice, 2005.

[165] A. De Donno, D. Powell, A. Low, Design of damping systems for footbridges - conceptual framework, in: Proceedings of Footbridge 2005, Second International Conference, Venice, 2005.

[166] K. Zoltowski, Pedestrian on footbridges, vertical loads and response, in: Proceedings Footbridge 2008, Third International Conference, Porto, 2008.

[167] R. Andersen, Pedestrian-induced vibrations: Human-human interaction, MSc Thesis, Department of Civil Engineering, Technical University of Denmark (2009).

[168] F. Ricciardelli, A. Pansera, An experimental investigation into the interaction among walkers in groups and crowds, in: Tenth Internation Conference on Recent Advances in Structural Dynamics, Southampton, 2010.

[169] M. Ishaque, R. Noland, Behavioural issues in pedestrian speed choice and street crossing behaviour: a review, Transport Reviews 28 (2008) 61–85.

[170] F. Venuti, L. Bruno, N. Bellomo, Crowd-structure interaction: Dynamics modelling and computational simulations, in: Proceedings of Footbridge 2005, Second International Conference, Venice, 2005.

[171] L. Bruno, F. Venuti, Crowd-structure interaction in footbridges: Modelling, application to a real case-study and sensitivity analyses, Journal of Sound and Vibration 323 (1-2) (2009) 475–493. doi:10.1016/j-jsv.2008.12.015.

[172] F. Venuti, L. Bruno, A new load model of the pedestrian lateral action, in: Proceedings of Footbridge 2008, Third International Conference, Porto, 2008.

[173] F. Venuti, L. Bruno, Synchronous lateral excitation on lively footbridges: modelling and application to the T-Bridge in Japan, in: Proceedings of Footbridge 2008, Third International Conference, Porto, 2008.

[174] J. Bodgi, S. Erlicher, P. Argoul, Lateral vibration of footbridges under crowd-loading: Continuous crowd modelling approach, Key Engineering Materials 347 (2007) 685–690.

[175] J. Bodgi, S. Erlicher, P. Argoul, Lateral vibration of footbridges under crowd-loading: on the modelling of the crowd-synchronization effects, in: Experimental Vibration Analysis for Civil Engineering Structures, Porto, 2007, pp. 237–245.

[176] J. Bodgi, S. Erlicher, P. Argoul, O. Flamand, F. Danbon, Crowd structure synchronization: coupling between Eulerian flow modeling and Kuramoto phase equation, in: Proceedings of Footbridge 2008, Third International Conference, Porto, 2008.

[177] J. Bodgi, Synchronization piétons-structure: Application aux vibration des passerelles souples (pedestrian-structure synchronization: Application to vibration of flexible bridges), PhD thesis, Ecole Nationale des Ponts - ParisTech, (in French) (September 2008).

Paper II (Ingólfsson et al., 2008a)

"A preliminary experimental investigation into lateral pedestrian-structure interaction"

E.T. Ingólfsson, C.T. Georgakis & A. Knudsen

In proceedings: *Seventh International Conference on Structural Dynamics, Southampton, UK*

7th European Conference on Structural Dynamics
EURODYN 2008
7-9 July 2008 Southampton

A PRELIMINARY EXPERIMENTAL INVESTIGATION INTO LATERAL PEDESTRIAN-STRUCTURE INTERACTION

E.T. Ingólfsson[1*], C.T. Georgakis[1+], A. Knudsen[2]

[1]Department of Civil Engineering
Technical University of Denmark
Brovej - Building 118, 2800 Kgs. Lyngby, Denmark
E-mail: *eti@byg.dtu.dk, +cg@byg.dtu.dk

[2] Rambøll Danmark A/S
Bredevej 2, 2830 Virum, Denmark
E-mail: andk@ramboll.dk

Keywords: Footbridges, lateral vibration, instrumented platform, DLF

ABSTRACT

This paper presents results from a preliminary experimental study on lateral human-structure dynamic interaction on footbridges using an instrumented platform. The platform has a natural frequency close to the average walking frequency of pedestrians and consists of a suspended concrete girder. With a length of $17\,\mathrm{m}$ and weight of $19.6\,\mathrm{ton}$, the platform provides a realistic comparison to an actual footbridge. Based on experiments with single pedestrians walking across the platform at resonance, the fundamental dynamic load factor is determined using only the recorded acceleration signal. Furthermore, tests were made with small groups of people to investigate their tendency to synchronise their walking to the motion of the platform. By analysing the recorded acceleration response and video data from the tests, the pedestrian pacing rate distribution and correlated pedestrian force have been identified. Finally, the results from this study are compared to previous full-scale as well as section model measurements.

1. INTRODUCTION

In recent years, several bridges have experienced excessive lateral vibrations due to pedestrian induced loadings. Most of these have been attributed to pedestrian "synchronisation" with the vibrating bridge [1–3]. Several researchers within the engineering community have attempted to measure the forces from pedestrians, directly or indirectly, using different experimental setups. Some have used instrumented platforms [4, 5] whereas others have used treadmills [6–8] to simulate the vibration of the structure. The interaction between a pedestrian and a moving structure is complex and may depend on several parameters such as bridge frequency, vibration amplitudes, modal mass and damping. Therefore, in order to understand and quantify this interaction, the platform must provide a realistic comparison to an actual footbridge. Generally,

the platforms used have been light and/or short. For short platforms, a limited number of steps can be recorded and they do not allow for a smooth development of the response. Light platforms have a tendency to provide accelerations in excess of what is usually found on an actual footbridge due to their low modal mass.

In this paper, a new experimental setup is presented. It consists of a $17\,\mathrm{m}$ long instrumented platform with a natural frequency close to the average walking frequency (here defined as half the pacing rate) of human beings, see Fig. 1. The vibration characteristics of the platform are described and results from single pedestrian experiments are presented where the acceleration response is measured for walking with a frequency matching the natural frequency of the platform. In a subsequent analysis of the response, the dynamic load factor (DLF) of the first load harmonic is estimated using a nonlinear data fit. Finally, preliminary investigations into crowd induced vibrations are made, based on experiments with small groups of people.

Figure 1. Instrumented platform.

2. INSTRUMENTED PLATFORM

An instrumented platform has been constructed at the Department of Civil Engineering, Technical University of Denmark. The platform is a double T-girder made of prestressed concrete with the overall length of $17\,\mathrm{m}$ and weight $19.6\,\mathrm{tons}$, see Fig. 1. At one end the platform is supported by two columns that act as a rotational spring in the horisontal plan and at the other end it is suspended by two hangers allowing a horisontal motion of the free end. The setup is schematically drawn in Fig. 2. The acceleration response of the platform was measured at the hanger location, i.e. $16\,\mathrm{m}$ from the simple support of the structure.

2.1 Dynamic properties

For a theoretical estimate of the dynamic properties of the bridge, Lagrange's equations can be used, [9]:

$$\frac{d}{dt}\left(\frac{\partial \mathcal{L}}{\partial \dot{q}}\right) - \frac{\partial \mathcal{L}}{\partial q} = 0 \tag{1}$$

The function $\mathcal{L} \equiv T - V$ is the Lagrangian, T is the kinetic energy, P is the potential energy and $q(t)$ is the generalised coordinate. If it is assumed that the bending stiffness of the concrete deck (in the horisontal plan) is much larger than the stiffness of the remaining system, the platform will move as a rigid body in a triangular mode with $\Phi(x) = x/L$. The modal mass

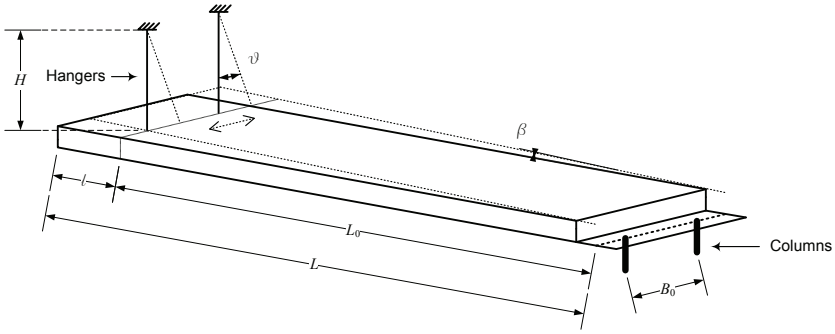

Figure 2. Schematic representation of the platform.

of the structure is determined from the mode shape and the mass distribution as $M = 6530\,\mathrm{kg}$. When using ϑ as the generalised coordinate and the notation from Fig. 2 it is shown in [10] that the natural frequency of the system can be obtained as:

$$f_0 = \frac{\omega_0}{2\pi} = \frac{1}{2\pi}\sqrt{\frac{3}{2}\frac{(2k_{rot}H + mgLL_0)}{mHL^2}} \cong 0.81\,\mathrm{Hz} \tag{2}$$

where $k_{rot} = 3EIB_0^2/2l_{\text{column}}^3$ is the rotational stiffness of the columns with EI and l_{column} as their bending stiffness and length respectively. The total mass of the girder is denoted m.

The natural frequency of the system was also determined experimentally by means of simple free-decay experiments. The natural frequency was determined as $f_0 = 0.87\,\mathrm{Hz}$, i.e. slightly higher than the theoretical estimate. The same experiments revealed a damping ratio $\zeta = 0.79\,\%$.

3. DLFS FROM SINGLE PEDESTRIAN TESTS

A series of single pedestrian tests have been undertaken on the laboratory platform. Initially, five test subjects were asked to cross the platform at predefined pacing rates controlled by a metronome. The walking frequency was selected such that it matches the natural frequency of the structure. Each test subject repeated the test three times.

3.1 Methodology

In the mathematical modelling of the bridge response it is assumed that the force induced by the pedestrian can be written as:

$$F(x,t) = \alpha W \sin(2\pi f_w t)\,\delta(x - v_w t) \tag{3}$$

where α is the DLF, W, f_w and v_w are the pedestrian weight, walking frequency and walking velocity respectively. This is the simplest way of representing the pedestrian load but it neglects the intra-subject variability (reasonable for the first harmonic, [11]), it takes only one load harmonic into account and it assumes that the walking speed is constant. Furthermore, any type of human-structure interaction is neglected, i.e. all parameters are independent of the motion of the structure. This assumption is not necessarily justifiable and several researchers have indicated that there is indeed an interaction that needs to be taken into account, [4, 6, 7]. The

presence of this interaction will be investigated during the subsequent response analysis. In modal coordinates, the pedestrian load from Eq. (3) is written as:

$$P(t) = \int_0^L F(x,t)\Phi(x)\mathrm{d}x = \alpha W \sin\left(2\pi f_w t\right)\Phi\left(v_w t\right) \tag{4}$$

Let $y(t)$ be the envelope of the response time history of the load in Eq. (4) acting at resonance. It was shown in [12] that there is a simple relationship between the envelope of the response and the amplitude of the load:

$$\mathrm{d}y = \left(\frac{1}{2}\frac{F_0}{K} - y\zeta\right)\omega_0 \mathrm{d}t \tag{5}$$

where F_0 is the amplitude of a load function of the type $F(t) = F_0 \sin\omega_0 t$ and K is the modal stiffness. In this case $F_0 = \alpha W \Phi\left(v_w t\right)$. It is noted that Eq. (5) is a first-order differential equation. The envelope of the acceleration response is obtained as the full solution to Eq. (5) multiplied with ω_0^2, thus:

$$\ddot{y}(t) = \frac{\alpha W}{M}\frac{1}{2\pi\zeta\varepsilon}\left(e^{-\omega_0\zeta t} - 1 + \omega_0\zeta t\right) \tag{6}$$

where ζ and ω_0 are the structural damping and the angular frequency respectively and $\varepsilon = 2\zeta n$ with n as the number of steps needed by the pedestrian to cross the bridge.

The purpose of the experiments is to determine the applicability of the mathematical model from Eq. (3) and determine the DLF of the fundamental load harmonic. This is done by analysing the measured acceleration response from the single pedestrian experiments and attempt to fit the envelope function from Eq. (6) to the measured data. To extract the peak values, a digital low-pass filter is used to eliminate higher frequency components and to locate the local maxima in the time series.

The *fitting model* $M(\mathbf{x}, t)$ is a function of time, t, and one or more yet unknown parameters that are determined by the data fit. The residuals are expressed as the difference between the fitting model, $M(\mathbf{x}, t)$, and the actual data points, $\ddot{y}_i$ as:

$$f_i(\mathbf{x}) = \ddot{y}_i - M(\mathbf{x}, t_i), \qquad i = 1, \ldots, m \tag{7}$$

A least square problem is formulated to find $\mathbf{x}^*$, a local minimiser for a function of the form:

$$F(\mathbf{x}) = \frac{1}{2}\sum_{i=1}^{m}\left[f_i(\mathbf{x})\right]^2 \tag{8}$$

In general $\mathbf{x}$ can be a vector of several variables and $M(\mathbf{x}, t)$ can be an arbitrary nonlinear function. In the case presented in this paper, the fitting model is the envelope function in Eq. (6) with only a single parameter to fit, i.e. $\mathbf{x} = [\alpha]$ and the data points $\ddot{y}_i$ are the local maxima extracted from the filtered time series. The structural parameters are as reported in section 2.1.

3.2 Test results

Figure 3 shows an example of a recorded acceleration time history together with the fitted function for test person 1. The results for all five test subjects and the pedestrian related data from the experiments are summarised in Table 1. In all cases, the algorithm used to solve Eq. (8) converged to a solution with an accuracy similar to that of pedestrian 1, indicating that the simple

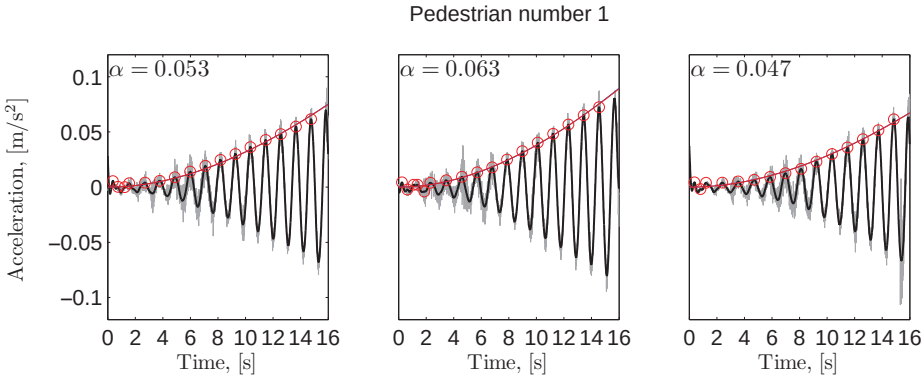

Figure 3: Measured acceleration response. (–) original unfiltered acceleration time history, (–) low-pass filtered acceleration, (o) local acceleration peaks, (–) fitted function.

load model successfully predicts the acceleration response of the structure. Therefore, the result indicate that the DLF did not change with the vibration amplitude and since the pacing rate was fixed by a metronome at resonance, this parameter also remained constant. Thus, during the short passage time of the pedestrians, human-structure interaction did not occur. The vibration felt by the walker was always lower than the comfort criterion threshold of $0.2\,\mathrm{m/s^2}$ according to the Eurocode [13] and in most cases also lower than the lock-in threshold of $0.1\,\mathrm{m/s^2}$ as defined in [14]. A combination of a triangular mode shape, the transient effect associated with the bridge starting at rest and the general low level of vibration probably eliminated any possibility of synchronisation during the single pedestrian tests. Further investigations into synchronisation and lock-in are presented in connection with the crowd experiments in section 4.

Table 1. Pedestrian data and results from the experiments.

Pedestrian no.	Traverse time	Fitted DLF			Average DLF	Weight	Load amplitude
	[s]	[-]	[-]	[-]	[-]	[kg]	[N]
1	16	0.053	0.063	0.047	0.054	54	29
2	12	0.033	0.037	0.038	0.036	68	24
3	11	0.045	0.036	0.038	0.040	73	28
4	15	0.067	0.056	0.045	0.056	83	46
5	13	0.097	0.092	0.082	0.090	103	91
Average value, μ_X					0.0553	76.2	44
Standard deviation, σ_X					0.022	16.3	28
Coefficient of Variation, COV					0.39	0.21	0.64

3.3 Comparative study

In an extensive literature review, [15] different values for the DLFs were summarised. According to [16] the value of the first DLF is $\alpha_1 = 0.039$ but in a later publication, the value $\alpha_1 = 0.1$ is suggested, [17].

Based on treadmill experiments, a relationship between the DLF and the pacing frequency was established, [18]. Due to scatter in the measured data, two equations were presented for the DLF of the first harmonic as function of the structural frequency:

$$\alpha_1 = 0.05 f_w - 0.011 \qquad 0.6\,\mathrm{Hz} \leq f_w \leq 1.1\,\mathrm{Hz} \qquad \text{Mean value} \tag{9}$$

$$\alpha_1 = 0.05 f_w + 0.001 \qquad 0.6\,\mathrm{Hz} \leq f_w \leq 1.1\,\mathrm{Hz} \qquad 95\,\% \text{ fractile} \tag{10}$$

These values are somewhat lower than those reported in [19] where several consecutive footsteps were measured on a rigid platform with the length of $6\,\mathrm{m}$. Figure 4 shows the measured fundamental DLFs as function of the step frequency (pacing rate) according to [19].

The above mentioned DLFs are based on measurements on a rigid surface. There are few examples of lateral DLFs for a vibrating or flexible surfaces in the literature. However, some of the attempts that have been made are summarised in the following. Based on platform tests, an expression for the DLF as function of the walking frequency and the structural acceleration is presented in [5] as:

$$\alpha_1 = 0.145 - 0.1 \exp\left\{ - \left(0.45 + 1.5 \exp\left[-\frac{1}{2} \left(\frac{f_w - f_n}{0.07} \right)^2 \right] \right) a^{1.35} \right\} \tag{11}$$

where a is the structural acceleration and $f_w - f_n$ is the difference between the walking frequency and the natural frequency of the structure. Based on the tests performed at Imperial College [4], a relationship between the first lateral DLF and the displacement amplitudes at two different vibration frequencies were presented, see Fig. 5.

The results from different studies are summarised in Table 2 and it shows that the results from present study generally agree with earlier reported values, both in terms of mean values data scatter.

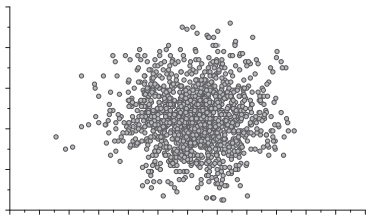

Figure 4: Measured DLFs for the first load harmonic. (Figure from [19])

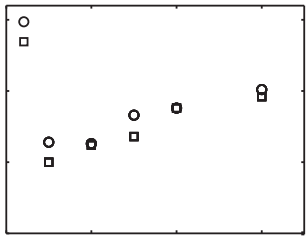

Figure 5: DLFs as function of displacement amplitude of the underlying surface according to [2].

Table 2. Comparison between DLFs based on different studies.

Reference	General expression	$\alpha_1(1.74\,\mathrm{Hz})$	Amplitude range
Bachmann and Ammann, [16]	0.039	0.039	
Bachmann et.al., [17]	0.10	0.10	
Ricciardelli et.al., [18] (Mean value)	$0.05 f_w - 0.011$	0.033	Rigid surface
Ricciardelli et.al. [18] (95 %)	$0.05 f_w + 0.001$	0.045	Rigid surface
Kasperski, [19]	Fig. 4	0.01 - 0.08	Rigid surface
Dallard et.al., [2]	Fig. 5	0.05 - 0.10	0 - 30 mm
Ronnquist and Strömmen, [5]	Eq. (11)		0 - 2 $\mathrm{m/s^2}$
Present study		0.055	0 - 0.1 $\mathrm{m/s^2}$

4. CROWD TEST

Crowd studies were undertaken to investigate the onset of lock-in between the pedestrian and the bridge deck. The test series comprise seven individual tests, each of duration $180\,\mathrm{sec}$. In each test the number of pedestrians on the bridge was kept constant such that a steady vibration state was reached. The number of pedestrians was varied from two in the first test, to eight in the last one. The total of 16 test subjects were used during the tests. Their average weight was $76\,\mathrm{kg}$ with standard deviation $14\,\mathrm{kg}$. The participants were asked to walk in a single line at their own preferred speed. Their arrival time onto the bridge was controlled such that an approximately uniform distribution of pedestrians was obtained. The walking frequencies were determined for each pedestrian from video recordings of the experiments. During the tests, the mean walking frequency was in the range from $0.88\,\mathrm{Hz}$ – $0.93\,\mathrm{Hz}$ with coefficient of variation 0.04 in all of them.

During the closure of the Millennium Bridge in London, several full scale experiments with large crowds of pedestrians were performed. It was found that the lateral pedestrian force has a component in phase with (correlated pedestrian force) and proportional to the velocity of the bridge. The total correlated pedestrian force was derived in [2] as:

$$F_{cor} = 2\zeta M\ddot{q} + M\frac{\Delta\ddot{q}}{\pi} \propto v(t) \tag{12}$$

where M, ζ and $\ddot{q}$ are the modal mass, damping ratio and acceleration respectively and $v(t)$ is the velocity of the structure. This finding led to Arup's stability criterion which can be expressed in terms of a critical number pedestrians that will cause excessive vibrations, [2]:

$$N_{crit} = \frac{4\pi\zeta f_0 M}{k\frac{1}{L}\int_0^L [\Phi(x)]^2\,\mathrm{d}x} \tag{13}$$

Here $k = 300\,\mathrm{Ns/m}$ is the lateral walking force coefficient that defines the linear relationship between the correlated force per person and the velocity of the underlying surface (local velocity), [2]. Using the parameters for the laboratory bridge, a critical number $N_{crit} = 6.7\,\mathrm{ped}$ is obtained. This means that according to Arup's assumptions, excessive vibrations are expected for a "crowd" of 6-7 people continuously on the bridge.

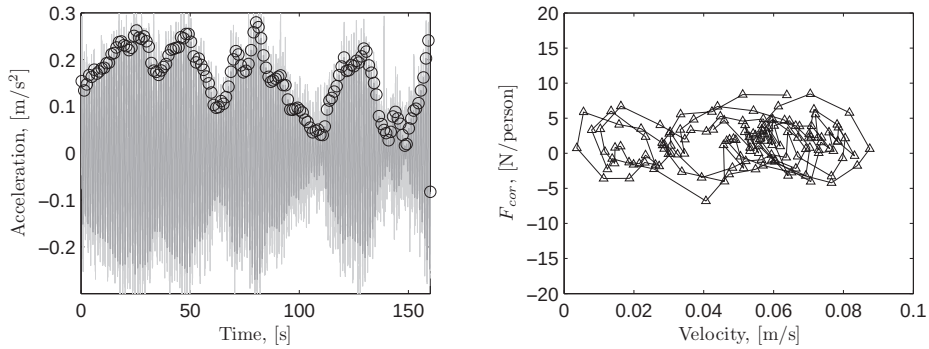

Figure 6: Acceleration response measured during crowd test with seven persons on the bridge (left) and correlated pedestrian force per person as function of the local velocity (right).

The total correlated pedestrian force from the experiments has been calculated using Eq. (12). This force was divided by the number of people involved in the test to get the average modal force and then divided by the root mean square mode shape to convert it into a physical force. The modal acceleration was converted into a modal velocity and multiplied with the same factor. The procedure is similar to the one used for the Millennium Bridge in London and reported in [2].

Figure 6 shows a typical record of the acceleration time history and the lateral pedestrian force as function of the local velocity of the structure. Figure 7 shows a comparison between the results from the Millennium Bridge in London, as presented in [2], and the results from the laboratory studies. As shown, there were no signs of correlation between the force and the velocity of the structure in any of the tests performed on the bridge, indicating that lock-in did not occur for up to eight pedestrians on the bridge and acceleration responses up to $0.28\,\mathrm{m/s^2}$ ($0.20\,\mathrm{m/s^2}$ for 1 s. RMS). It is noted that this acceleration exceeds the synchronisation threshold as defined in [14].

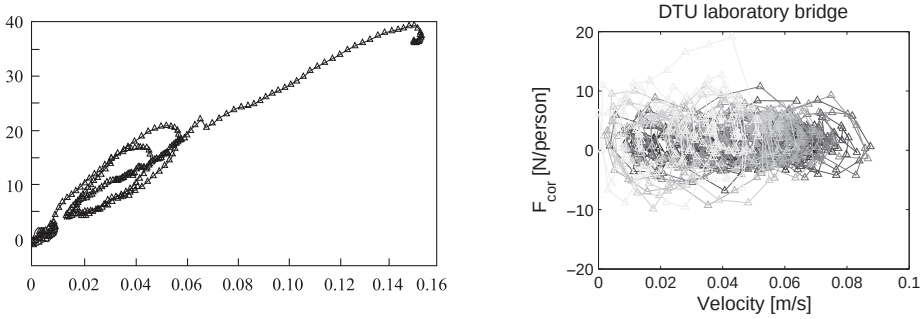

Figure 7: Correlated pedestrian force per person as function of the velocity of the structure. Left: Results presented from the Millennium Bridge (Figure from [2]). Right: All results from the crowd tests using 2-8 pedestrians. Notice the different coordinate scales.

Further investigations included video analysis from the crowd tests to determine the phase angle between pedestrian and the bridge movement for all the pedestrians with a walking frequency matching the natural frequency of the structure. This analysis is presented in [10] and it showed that there was no tendency for people to synchronise their phase with the movement of the structure.

The lack of synchronisation can possibly be attributed to the triangular mode shape which causes a general low level of vibration felt by the walker during the first part of the passage. This means that the high acceleration amplitudes were only felt by the walkers for a limited period of time, not enough to synchronise.

5. CONCLUSIONS

Based on the pedestrian tests, following main conclusions can be drawn:

1. For the experimental configuration described in this paper the simplified model can reproduce the measured acceleration response with a reasonable accuracy, despite that human-structure interaction and imperfections in the walking were neglected.

2. A simple method involving a non-linear single variable data fit can be used to determine the fundamental DLF for test subjects walking at resonance.

3. The measured DLFs agree with values reported in the literature both in terms of mean value and scatter.

4. During the crowd tests, there were no signs of synchronisation (lock-in) between the pedestrians and the structure despite large vibration amplitudes, indicating that the synchronisation depends on more than the immediate acceleration felt by the walker.

The acceleration response measured on the platform is the same order of magnitude as that expected on an actual footbridge. This means that the platform can be used to study human-structure interaction under realistic conditions. Future studies will include more test subjects, a variation of the walking frequency and changes to the structure in terms of mode shape and natural frequency.

REFERENCES

[1] Y. Fujino, B.M. Pacheco, S.I. Nakamura, and P. Warnitchai. Synchronization of human walking observed during lateral vibration of a congested pedestrian bridge. *Earthquake Engineering & Structural Dynamics*, 22(9):741–758, 1993.

[2] P. Dallard, A.J. Fitzpatrick, A. Flint, S.Le. Bourva, A. Low, R.M. Ridsdill-Smith, and M. Willford. The London Millennium Footbridge. *Structural Engineer*, 79(22):20–21, 2001.

[3] S.I. Nakamura and T. Kawasaki. Lateral vibration of footbridges by synchronous walking. *Journal of Constructional Steel Research*, 62(11):1148–1160, 2006.

[4] R.E. Hobbs. Test on lateral forces induced by pedestrians crossing a platform driven laterally. Technical report, Civil Engineering Department, Imperial College London, London, UK, August 2000. A report for Ove Arup and Partners.

[5] A. Rönnquist. *Pedestrian induced vibrations of slender footbridges*. PhD thesis, Norwegian University of Science and Technology, 2005.

[6] A. McRobie, G. Morgenthal, J. Lasenby, and M. Ringer. Section model tests on human - structure lock-in. *Bridge Engineering*, 156:71–79, 2003.

[7] A.D. Pizzimenti. *Experimental analysis of the lateral pedestrian-induced mechanism of excitation of footbridges (Italian)*. PhD thesis, Dipartimento di Ingegneria Civile e Ambientale, Universita' Degli Studi di Catania, 2003.

[8] F. Ricciardelli and A.D. Pizzimenti. Lateral walking-induced forces on footbridges. *Journal of bridge engineering*, 12(6):677–688, 2007.

[9] J.J. Thomsen. *Vibration and stability, Advanced theory, analysis and tools*. Springer, Berlin, Heidelberg, Germany, 2 edition, 2003.

[10] A. Knudsen. Pedestrian-induced lateral vibrations of bridges. MSc thesis, Department of Civil Engineering, Technical University of Denmark, 2007.

[11] J.M.W. Brownjohn, A. Pavic, and P. Omenzetter. A spectral density approach for modelling continuous vertical forces on pedestrian structures due to walking. *Canadian Journal of Civil Engineering*, 31(1):65–77, 2004.

[12] C. Barker. Footbridge pedestrian vibration limits. part 3: Background to response calculations. In *Proceedings of the Second International Conference on the Design and Dynamic Behaviour of Footbridges: FOOTBRIDGE 2005*, Venice, Italy, 6-8 December 2005.

[13] CEN, European Committee for Standardization. *EN 1990/A1:2002. Eurocode - Basis of structural design*, December 2005.

[14] Footbridges, assessment of vibrational behaviour of footbridges under pedestrian loading. Technical guide, Sétra, November 2006.

[15] S. Zivanovic, A. Pavic, and P. Reynolds. Vibration serviceability of footbridges under human-induced excitation: a literature review. *Journal of Sound and Vibration*, 279(1-2):1–74, 2005.

[16] H. Bachmann and W.J. Ammann. *Vibrations in Structures. Induced by Man and Machine*. Structural Engineering Documents. International Association for Bridge and Structural Engineering IABSE, Zrich, Switzerland, 3rd edition, 1987.

[17] H. Bachmann, W.J. Ammann, and et.al. *Vibration Problems in Structures. Practical Guidelines*. Birkhauser, 2nd edition, 1996.

[18] F. Ricciardelli, C. Briatico, E.T. Ingólfsson, and C.T. Georgakis. Experimental validation and calibration of pedestrian models for footbridges. In *Experimental vibration analysis for civil engineering structures*, Porto, Portugal, 24-26 October 2007.

[19] M. Kasperski. Serviceability of pedestrian structures. In *Proceedings of the IMAC-XXV: A conference & Exposition on Structural Dynamics*, Orlando, Florida USA, 19-22 February 2007.

Paper III (Ingólfsson et al., 2011)

"Experimental Identification of pedestrian-induced lateral forces on footbridges"

E.T. Ingólfsson, C.T. Georgakis, F. Ricciardelli & J. Jönsson

Published in: *Journal of Sound and Vibration*

Journal of Sound and Vibration 330 (2011) 1265–1284

Contents lists available at ScienceDirect

Journal of Sound and Vibration

journal homepage: www.elsevier.com/locate/jsvi

Experimental identification of pedestrian-induced lateral forces on footbridges

E.T. Ingólfsson [a,*], C.T. Georgakis [a], F. Ricciardelli [b], J. Jönsson [a]

[a] Department of Civil Engineering, Technical University of Denmark, Building 118, Brovej, 2800 Kgs. Lyngby, Denmark
[b] DIMET, University of Reggio Calabria, Via Graziella - Feo di Vito, 89122 Reggio Calabria, Italy

ARTICLE INFO

Article history:
Received 15 February 2010
Received in revised form
21 September 2010
Accepted 30 September 2010
Handling Editor: J. Macdonald
Available online 10 November 2010

ABSTRACT

This paper presents a comprehensive experimental analysis of lateral forces generated by single pedestrians during continuous walking on a treadmill. Two different conditions are investigated; initially the treadmill is fixed and then it is laterally driven in a sinusoidal motion at varying combinations of frequencies (0.33–1.07 Hz) and amplitudes (4.5–48 mm). The experimental campaign involved 71 male and female human adults and covered approximately 55 km of walking distributed between 4954 individual tests. When walking on a laterally moving surface, motion-induced forces develop at the frequency of the movement and are herewith quantified through equivalent velocity and acceleration proportional coefficients. Their dependency on the vibration frequency and amplitude is presented, both in terms of mean values and probabilistically to illustrate the randomness associated with intra- and inter-subject variability. It is shown that the motion-induced portion of the pedestrian load (on average) inputs energy into the structure in the frequency range (normalised by the mean walking frequency) between approximately 0.6 and 1.2. Furthermore, it is shown that the load component in phase with the acceleration of the treadmill depends on the frequency of the movement, such that pedestrians (on average) subtract from the overall modal mass for low frequency motion and add to the overall modal mass at higher frequencies.

1. Introduction

The widely publicised closure of Paris' Solférino and London's Millennium footbridges in 1999 [1] and 2000 [2] have led to an understanding on the part of engineers and architects of the need to evaluate the potential for footbridge vibrations that can be attributed to pedestrians. Within the scientific community, the closures has also led to the initiation of a new tract of research, focused on the understanding of pedestrian loading, bridge response and their interaction. A plethora of research on the topic now exists [3–10] and as a consequence, numerous other bridges of different length and type have also been found prone to similar excessive lateral vibrations when exposed to large pedestrian crowds [11–15].

Only few national and international codes of practice and official design guidelines currently exist to help the designer address this issue. Most of these are based on the main hypotheses, that pedestrian-induced lateral loads can be modelled as velocity proportional loads or as "negative dampers", resulting from the "synchronised" lateral movement of pedestrians. This pedestrian lateral excitation mechanism is often characterised as synchronous lateral excitation (SLE) or

* Corresponding author. Tel.: +45 4525 1766; fax: +45 4588 3282.
E-mail address: eti@byg.dtu.dk (E.T. Ingólfsson).

0022-460X/$ - see front matter © 2010 Elsevier Ltd. All rights reserved.
doi:10.1016/j.jsv.2010.09.034

Nomenclature

a	parameter in a power law fit
A_j	fitting parameters in a spectral load model
b	parameter in a power law fit
B_j	fitting parameters in a spectral load model
c_p	velocity proportional pedestrian load coefficient
$\overline{c}_p$	mean value of the velocity proportional pedestrian load coefficient
$\hat{c}_p$	estimated error of the velocity proportional pedestrian load coefficient
Co_{Fx}	co-spectral density between F and x
DLF_j	dynamic load factor of load harmonic j
$\overline{\mathrm{DLF}}_j$	mean value of the dynamic load factor of load harmonic j
f	frequency
f_L	frequency of the lateral motion of the treadmill
f_n	natural frequency of a single-degree-of-freedom system
f_{Ny}	Nyquist frequency
f_p	pedestrian pacing frequency
f_w	pedestrian walking frequency
$\overline{f}_w$	mean pedestrian walking frequency
F	pedestrian-induced lateral force
$\hat{F}$	measurement error
F_D	damping force
$F_{D,\mathrm{eq}}$	equivalent pedestrian damping force
F_E	elastic restoring force (spring force)
F_i	lateral force peaks (i=1…3)
F_I	inertia force
$F_{I,\mathrm{eq}}$	equivalent pedestrian inertia force
G_j	amplitude of load harmonic j
H_n	frequency response function of a single-degree-of-freedom system
$\hat{k}$	calibration constant
K_n	stiffness of a single-degree-of-freedom system
m_p	pedestrian body mass
M	mass of stage 3 of the treadmill ergometer device
N_{av}	number of windows used to calculate a particular PSD
p	probability density function
$P_{D,\mathrm{eq}}$	average work done by $F_{D,\mathrm{eq}}$ per unit time
P_F	average work done by F per unit time
Qu_{Fx}	quad-spectral density between F and x
S_F	PSD of F
$S_{F,j}$	PSD of F around load harmonic j
$S_{F\,x}$	cross-spectral density between F and x
$S_{F\dot{x}}$	cross-spectral density between F and $\dot{x}$
t	time
T_{tot}	total signal duration
T_w	fundamental period of lateral pedestrian-induced load
v_p	pedestrian walking speed
W	body weight
x	lateral displacement of the treadmill
$\dot{x}$	lateral velocity of the treadmill
$\ddot{x}$	lateral acceleration of the treadmill
x_0	lateral displacement amplitude of the treadmill
$\dot{x}_0$	lateral velocity amplitude of the treadmill
$\ddot{x}_0$	lateral acceleration amplitude of the treadmill
δf	frequency resolution in a spectrum
Δf	bandwidth
ζ_n	damping ratio of a single-degree-of-freedom system
μ_X	sample mean of X
ξ	parameter in the lognormal distribution
ρ	linear correlation coefficient
ϱ_p	acceleration proportional pedestrian load coefficient
$\overline{\varrho}_p$	mean value of the acceleration proportional pedestrian load coefficient
$\hat{\varrho}_p$	estimated error of the acceleration proportional pedestrian load coefficient
σ_{DLF_j}	standard deviation of the DLF of load harmonic j
σ_F^2	total area of the PSD of F (total signal variance)
$\sigma_{\hat{F}}$	standard deviation of the error of the pedestrian-induced load
$\tilde{\sigma}_F^2$	area of the PSD of F in a specific frequency range
$\tilde{\sigma}_{F,j}^2$	area of the PSD of F around load harmonic j
$\sigma_{F\dot{x}}$	total area of the cross-spectral density between F and $\dot{x}$
$\tilde{\sigma}_{F\dot{x}}$	area of the cross-spectral density between F and $\dot{x}$ within a specific frequency range
$\tilde{\sigma}_{F\ddot{x}}$	area of the cross-spectral density between F and $\ddot{x}$ within a specific frequency range
$\tilde{\sigma}_{u,\mathrm{eq}}^2$	total area of the equivalent power spectral density of u
$\tilde{\sigma}_{u,j}^2$	area of the PSD of u around load harmonic j
$\hat{\sigma}_V$	standard deviation of the measured voltage signal from load cells
σ_X^2	sample variance of X
σ_x	standard deviation of x
$\sigma_{\ddot{x}}$	standard deviation of $\ddot{x}$
ϕ_j	phase angle of load harmonic j
ϕ_{xF}	phase spectrum between x and F
φ	phase angle
χ	parameter in the lognormal distribution
ω	angular frequency
ω_L	angular frequency of the treadmill motion
Cov[]	covariance operator
E[]	expected value operator
$\mathcal{F}$[]	Fourier transform operator
Re[]	real part operator
Var[]	variance operator

human–structure "lock-in" [2,11,16]. The UK National Annex to Eurocode (EN 1991-2) [17], the HIVOSS guidelines [18] and the *fib* (2005) recommendations [19] are for the most part based on this hypothesis. Alternatively, the French Road Agency (Sétra) has published a guideline in which the lateral acceleration, calculated assuming random pedestrian behaviour,

should be limited to 0.10 m/s^2. The value is chosen, so as to avoid SLE [20] and thus the destabilising effect of excessive negative damping. The limit is based on research carried out during the temporary closure of the Solférino Bridge. Results from a limited number of controlled pedestrian crowd tests indicated that there is a transition point at which a rapid increase in the lateral bridge response is triggered. The transition is explained as random pedestrian walking that becomes "synchronised" when lateral bridge accelerations increase beyond 0.10 m/s^2.

Although the current codes of practice and guidelines help to improve the designer's ability to predict the potential for large amplitude lateral footbridge vibrations, it should be recognised that they are based on a limited understanding of the actual phenomenon. This can be understood by examining the origins of the physical models they rely on. Those that utilise the concept of negative damping, employ an empirically derived velocity-proportional pedestrian damping constant c_p=300 N s/m, which represents an averaged value for each pedestrian, derived from back calculations of the measured modal response during specific controlled crowd tests on the Millennium Bridge [2]. The constant is assumed to remain unchanged, regardless of frequency of bridge motion. Furthermore, its determination is highly susceptible to experimentally obtained parameters, such as mode shape, modal mass and pedestrian distribution; rendering the universality of its application questionable. Similarly, the Sétra guidelines rely on a binary frequency-independent acceleration criterion, which suggests that the same probability of synchronisation is assigned to all pedestrians independent of the ratio between their walking frequency and the lateral vibration frequency of the bridge.

In recent years, various researchers have studied the mechanics of pedestrian-induced lateral forces on a laterally vibrating surface. Different hypotheses exist about the complex nature of the human–structure interaction and unlike current codes of practice and design guidelines which are primarily based on empirical full-scale observations, many of these hypotheses are supported by theoretical modelling of the interaction [21–25], which lack the proper experimental evidence to support their applicability.

In this paper, an in-depth examination of frequency-dependent lateral forces produced by a pedestrian are analysed and presented. An extensive experimental campaign was carried out, where the characteristics of the lateral forces from 71 volunteering pedestrians were measured during treadmill walking, both on a fixed surface and during lateral sinusoidal motion at different combinations of frequencies (0.33–1.07 Hz) and amplitudes (4.5–48 mm). Emphasis is placed on the treatment of both the motion-induced forces, defined as equivalent velocity and acceleration proportional coefficients, and those measured on a fixed surface. All of the data are presented in a probabilistic manner which illustrates the randomness associated with both intra- and inter-subject variability.

2. Mechanics of pedestrian-induced lateral forces

2.1. Laterally fixed surface

During walking, a person generates a ground reaction force, or simply GRF, through the acceleration (and deceleration) of the centre of mass of their body. In general, the GRF can be represented by a three-dimensional vector which varies in time and in space due to the forward movement of the person [8].

The lateral components of the GRF are small, compared to the vertical ones, and are generated through the balancing of the body [26]. The shape of a generalised lateral force time history is shown in Fig. 1. A single footstep is characterised by three lateral force peaks, F_1 to F_3, with values around 4–5 percent of the body weight [27]. However, several factors influence the shape of the walking force which is governed by large intra- and inter-subject variability. The intra-subject variability denotes differences in the GRF of the same pedestrian measured at two different time instances and depends on the type of footwear, walking speed and random variations in the gait, mood of the person, etc. [8,28]. The inter-subject variability refers to the variability between different people and depends on physiological parameters of the pedestrians, age, gender, race, etc. [29].

Due to the intra-subject variability, the time history of the walking force is a narrow-band random process, centred around the fundamental lateral loading frequency, f_w (defined as half the pacing frequency, f_p) and its higher harmonics.

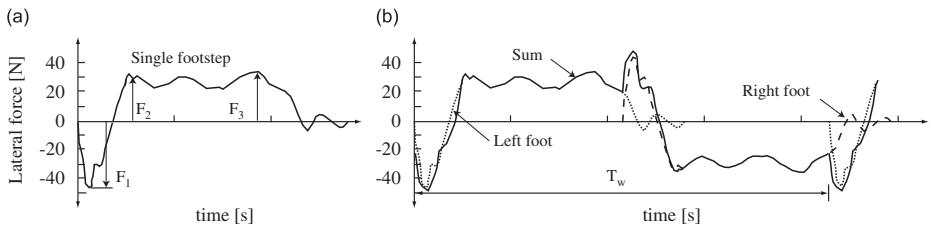

Fig. 1. Typical shape of a walking force from (a) a single footstep and (b) a series of consecutive footsteps (figure reproduced from [5]).

However, lateral walking forces are often modelled as a truncated Fourier series with a fundamental frequency, f_w, based on the simplified assumption that each footstep can be replicated from a single "characteristic" footstep (see Fig. 1):

$$F(t) = \sum_{j=1}^{n} G_j \sin(2\pi j f_w t - \phi_j) \tag{1}$$

where G_j and ϕ_j are the amplitude and phase angle of load harmonic j, respectively, and n is the number of load harmonics included in the truncated Fourier series. In most cases, the load amplitude is defined through the body weight normalised dynamic load factor $DLF_j = G_j/W$. According to Bachmann and Ammann [30], the values of the first five load harmonics are DLF_j={0.039; 0.01; 0.042; 0.012; 0.015}, j=1…5. In a later publication by same authors, the values of $DLF_1 = DLF_3 = 0.1$ are suggested for design purposes [31]. However, no justification for the difference is given. Other studies aimed at finding the DLFs from measured GRFs on stationary platforms indicate that they are independent of the walking speed and vary only slightly between males and females [32–34].

Non-zero load harmonics at even integer harmonics imply that the gait is asymmetric and that the walking is imperfect. This intra-subject variability was addressed by Pizzimenti [35], who used an instrumented treadmill to measure the continuous GRFs of 66 individuals. Ricciardelli and Pizzimenti [28] defined DLFs for an average (perfectly periodic) footprint as the sum of the contributions in the Fourier spectrum of the measured force in a narrow band around the frequency of the respective harmonic. The characteristic values (with 95 percent probability of non-exeedance) of the first five DLFs were reported as DLF_j = {0.04; 0.0077; 0.023; 0.0043; 0.011}, j=1…5. In the frequency domain, Pizzimenti and Ricciardelli [36] present a characteristic power spectral density (PSD), $S_{F,j}(f)$, for the first five load harmonics in a general (non-dimensional) form as

$$\frac{S_{F,j}(f)\cdot f}{\tilde{\sigma}_{F,j}^2} = \frac{2A_j}{\sqrt{2\pi}B_j}\exp\left\{-2\left[\frac{f/jf_w - 1}{B_j}\right]^2\right\} \tag{2}$$

where A_j and B_j are parameters determined by a data fit and $\tilde{\sigma}_{F,j}^2$ is the area of the PSD around the jth harmonic.

2.2. Lateral human–structure interaction

When walking on a laterally oscillating surface, it has been postulated that people tend to spread their legs apart and change their walking frequency and phase, to match that of the floor [16]. This alleged modification of the gait due to floor oscillations has become known within the civil engineering community as human–structure synchronisation. Early works by Fujino et al. [11] describe the concept of synchronisation. Their experimental studies on a human walking on a laterally moving platform showed that the walking frequency became synchronised to the platform frequency for lateral amplitudes in the range of 10–20 mm. This was used to explain the excessive lateral vibrations of the Toda Park Bridge in Japan during periods when the bridge is congested by large crowds. However, details regarding the platform tests have not been presented. Charles and Bui [37] defined the equivalent number of resonance pedestrians from back calculations of the measured response on the Solférino bridge and Danbon and Grillaud [38] used their result to propose a load model, where the number of synchronised resonance pedestrians increases linearly with the bridge displacement amplitude.

Strogatz et al. [21] offered a mathematical framework for the modelling of human–structure interaction, assuming that each pedestrian reacts to a weak stimulus from the bridge, either through the lateral displacement [21] or the acceleration [39]. If the stimulus is strong enough and the natural frequency of the bridge is close to the (original) walking frequency of the individual, the pedestrian locks into synchrony with the structure. The models are presented in the same framework as the theory of coupled oscillators, known from e.g. complex biological systems [40], but they lack any experimental evidence that can confirm their capability to predict pedestrian-induced lateral vibrations. According to Butz [33], only persons with natural walking frequency within 0.1 Hz of the lateral vibration frequency can synchronise with the structural motion. Similar observations were reported by Nakamura et al. [41], who investigated walking on the spot on a laterally moving shaking table. If the hypothesis that the correlated pedestrian force (or equivalent number of resonance pedestrians) increases with the vibration amplitude, due to an increasing number of synchronised pedestrians, is true, then the results by Butz [33] and Nakamura et al. [41] suggest that the susceptibility to SLE depends on the frequency ratio between the pedestrian walking frequency and the frequency of the lateral movement. This is contradictory to the basic assumption upon which current design recommendations are based.

An alternative approach is taken by Barker [42] who uses a simplified mechanical model of the human body centre of mass to show that synchronisation of the step is not a necessary precondition for diverging lateral vibrations to occur. Following along the same line, Macdonald [25] uses an inverted pendulum model to describe the lateral movement of the centre of mass and comes to similar conclusion. He argues that balance control is a matter of foot placement rather than timing of the step. His results are supported by full-scale measurements conducted on the Cliffton Suspension bridge during a period with large crowd-induced lateral vibrations [15].

2.3. Laterally moving surface

The importance of human–structure interaction when modelling pedestrian-induced lateral loading on long span footbridges has already been highlighted. Consequently, many researchers have attempted to measure pedestrian GRFs on

a laterally moving surface. Shortly after the closure of the London Millennium Bridge, platform tests were performed at Imperial College where it was found that the fundamental DLF increases with the lateral vibration amplitude and that at frequency 1.0 Hz there is a 40 percent probability of synchronisation or "lock-in", for vibration amplitudes of 5 mm [43]. However, very few details regarding these experiments have been published.

Similar platform tests were commissioned following the closure of the Solférino bridge in Paris [20], with the main conclusions being that the mean amplitude of the fundamental load harmonic is 35 N and that synchronisation with the platform does generally not occur for lateral accelerations lower than 0.15 m/s^2 [37]. Rönnquist [13] and Rönnquist and Strömmen [44] report that the lateral load increases both with an increase in the lateral acceleration of the structure and also as the walking frequency approaches the natural frequency of the platform. Similarly, Butz [33] reports that the DLF for a synchronised pedestrian depends of the structure and for the non-synchronised pedestrian the fundamental DLF should be taken as measured on a rigid surface. Common for all these tests however, is the fact that no distinction is made between pedestrian forces in phase with velocity or acceleration of the structure.

Phase synchronisation was initially addressed by McRobie et al. [16] who report that the load amplitudes can reach values as high as 300 N and the component in phase with the velocity of the structure can reach 100 N, when the vibration amplitude of the structure is 100 mm. Sun and Yuan [45] performed walking tests with seven individuals, using an instrumented treadmill fixed onto a shaking table. They concluded that for small vibration amplitudes, the relative phase between pedestrian and structure is variable (non-constant), but as the amplitude increases the phase becomes almost constant and the walking frequency changes to the vibration frequency. Furthermore, they find that on average the pedestrian load increases linearly with the acceleration and is 140.8° ahead of the bridge motion (S.D. 17.9°).

The experimental setup presented herewith (Treadmill Ergometer Device as described in Section 3) was initially constructed by Pizzimenti [35] and used in a pilot study with five different test subjects. The lateral GRFs were measured, and Pizzimenti and Ricciardelli [36] identified two different loading mechanisms; the first one centred around the walking frequency and its integer harmonics and the second one, *the self-excited force*, occurring at a frequency equal the vibration frequency. The self-excited force was further subdivided into in-phase and out-of-phase (with the displacement) lateral pedestrian load components. It is reported that the in-phase component of the force obtain negative values over the entire frequency range, which implies that pedestrians act as negative mass on the structure. This is in line with Macdonald's observations [25]. For the out-of-phase-component, pedestrians act as negative dampers, only for one combination of frequency and amplitude. At other frequencies, they add to the overall structural damping [36]. Since only five test subjects were used in the study and a limited number of frequencies and amplitudes were tested, the results can only serve as a qualitative indicator.

3. Current experimental investigations

3.1. Test subjects

During the summer of 2009, 71 healthy human volunteers (45 male and 26 female) with an age distribution according to Table 1, a mean height of 1.73 m (S.D. 0.01 m) and a mean weight of 74.4 kg (S.D. 15.1 kg) participated in an experimental campaign to determine pedestrian-induced lateral forces on a laterally vibrating platform. The lengths of the volunteers' legs were measured as well as the circumference of their wrist and ankle prior to the tests.

All tests which involved human test subjects were carried out in accordance with The Code of Ethics of the World Medical Association (Declaration of Helsinki) for experiments involving humans.

3.2. Experimental setup

A Treadmill Ergometer Device, positioned in the laboratory of the Inter University Research on Building Aerodynamics and Wind Engineering (CRIACIV) at the University of Florence in Prato, Italy, was used to measure the lateral GRF during walking, Fig. 2. The treadmill was built in 2003 at the University of Reggio Calabria [35] and moved to CRIACIV in 2006.

In brief, the treadmill consists of three separate parts, stages 1–3. The base of the treadmill, consisting of steel beams fixed on the laboratory floor is denoted by stage 1. Stage 2, which is a steel frame connected to the base through guide rails, such that it can move laterally, is driven by a motor. This motor controls the lateral vibration frequency of the system as well as the amplitude. Stage 3 consists of the walking surface with the dimension 100 × 180 cm, which is made of a steel frame system covered with plywood panels and a rubber belt. The belt is driven by a motor, which is attached to stage 2

Table 1
Age and gender distribution of test subjects.

	0–18 years	19–35 years	36–55 years	> 55 years	Total
Male	0	29	14	2	45
Female	1	16	9	0	26
Total	1	45	23	2	71

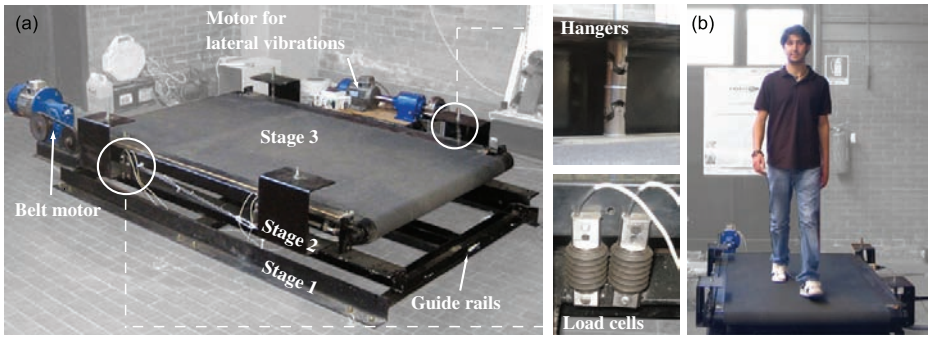

Fig. 2. (a) A treadmill ergometer device and (b) a pedestrian test subject during a walking test.

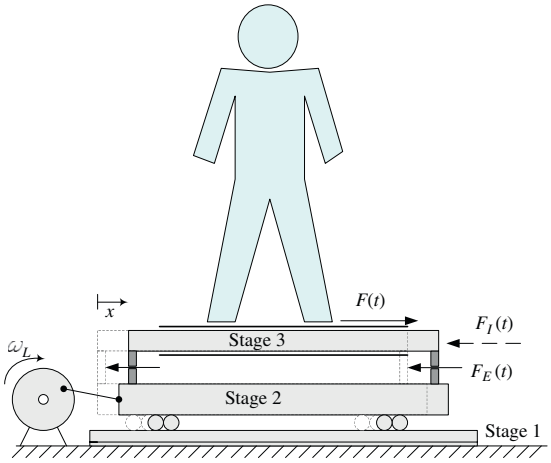

Fig. 3. A schematic overview of the treadmill ergometer device setup and the force equilibrium.

and therefore moves with the motion of the platform. The connection between stages 2 and 3, i.e. the belt and the laterally driven frame is twofold. First of all, it is vertically suspended from the supporting frame (at stage 2) using low friction hinges and secondly it is laterally supported with four flexural load cells. Images of various components of the treadmill are shown in Fig. 2. Both the motion of the belt and the lateral motion of the treadmill are driven by asynchronous 1.1 kW (1.5 HP) motors equipped with gearboxes. Both motors are controlled with inverters for variable belt speed and vibration frequencies, respectively. A schematic representation of the system is shown in Fig. 3. The experimental setup is a slightly modified version of that described by Pizzimenti and Ricciardelli [36] and Ricciardelli and Pizzimenti [28].

3.3. Other equipment

The resulting horizontal lateral force between stages 2 and 3 is measured with four load cells. Each load cell can measure up to 500 N with a sensitivity of 3.7711 mV/N. The motion of the treadmill is measured with two high sensitivity (10 V/g) ICP accelerometers (PCB Piezotronics, type 393B12). The accelerometers are connected to a 4 channel signal conditioner (PCB Piezotronics, type 441A42). Furthermore, the displacement of the treadmill is measured using a laser with sensitivity 100 mV/mm. The walking speed is determined using an encoder that measures the rotation of the steel cylinder which drives the treadmill belt. All signals were acquired with ± 5 V 24-Bit data acquisition modules (National Instruments, cDAQ-9172 and National Instruments, BNC 9234) at a sampling rate of 2048 Hz.

3.4. Test procedure

Subjects were requested to perform two types of walking on the treadmill; one without lateral motion of stage 3 of the treadmill (denoted static tests) and one with lateral sinusoidal movement at various vibration frequencies and amplitudes

Table 2
Test matrix which shows the number of different subjects tested at each particular combination of lateral vibration amplitude and frequency.

Frequency f_L/x_0 (Hz)	Lateral vibration amplitude						
	4.5 mm	10 mm	19.4 mm	28.7 mm	31.0 mm	38.3 mm	48.0 mm
0	Static test—71 subjects						
0.33	45	65	59	35	36	48	60
0.40	45	65	59	35	36	48	60
0.43	45	65	59	35	36	47	59
0.47	45	65	59	35	35	47	58
0.50	45	66	60	35	36	47	58
0.60	46	66	60	35	35	47	22
0.70	46	66	60	34	34	47	18
0.77	45	65	59	34	31	46	14
0.80	46	66	59	34	29	44	11
0.83	46	66	59	34	27	32	8
0.87	46	66	59	33	10	23	4
0.90	46	66	59	33	9	21	3
0.93	46	66	59	33	8	17	2
0.97	46	66	58	21	8	14	2
1.00	46	64	57	21	7	12	2
1.03	45	64	57	15	6	5	0
1.07	45	64	56	14	6	5	0

(denoted dynamic tests). Initially, each subject was asked to walk on the treadmill and select a comfortable walking speed. This walking speed was subsequently used in both the static and the dynamic tests. Only one static test with a duration of 2 min was performed, whereas each subject performed several dynamic tests of 30 s duration, with vibration frequencies in the range 0.33–1.07 Hz and displacement amplitudes between 4.5 and 48 mm. Typically, each test subject spent between 1 and 2 h in the laboratory, depending on their availability and thereby the number of dynamic tests performed. The order in which the dynamic tests were performed was determined by a combination of random and systematic selections. After a successful completion of the static test, the displacement amplitudes of the treadmill were selected randomly. The pedestrian was asked to walk continuously on the treadmill at each particular amplitude whilst the frequency was increased in steps, from the lowest frequency tested to the highest one. Each step lasted 30 s plus a transition time interval during which the frequency was changed. After sweeping through all the frequencies, a short break was taken during which time the amplitude was changed. Generally, each subject was tested at both low, intermediate and large amplitude vibrations. Most of the tests were recorded with a digital video camera and all comments from the test subjects relating to the tests were recorded. The test matrix is given in Table 2, where the number in each cell indicates the number of different subjects tested for that particular combination of frequency and amplitude.

A total of 71 static tests were performed and 4883 dynamic tests, covering the total walking distance of approximately 55 km.

3.5. Data post-processing

Initially, the DC components of all the measured signals were removed and subsequently the signals were re-sampled from the original 2048 to 32 Hz, by applying a digital anti-aliasing lowpass FIR filter. The new (re-sampled) data were further lowpass filtered with a cutoff frequency of 8 Hz for the static tests and 5 Hz for the dynamic tests. The spectral densities presented herewith are generally estimated from an averaged periodogram of the measured time series. The periodograms are obtained by dividing the original time series into a number of windows (possibly overlapping) and calculating the discrete Fourier transform in each of them. No general rules can be made regarding the preferred shape of the window (rectangular, raised cosine, etc.), its size or overlap percentage as it depends on the particular application as well as a trade-off choice between the accuracy of the estimate and the desired frequency resolution [46,47]. Therefore, different methods have been used depending on the particular application and in the following the frequency resolution, δf, number of averages, N_{av}, and the selected window function will be accounted for each time a new spectrum is presented.

By taking advantage of the fact that the pedestrian-induced load is near-periodic with fundamental frequency equal the (average) walking frequency, the most severe type of spectral leakage can be avoided by assuring that each window contains an integer number of vibration cycles. This is achieved by identifying the dominant frequency in the signal from the periodogram of the original time series, which has been zero padded to a much longer length (here 2048 s) for enhancing the frequency resolution. Having identified the dominant frequency, the original time series is truncated such that each window contains (as closely as possible) an integer number of vibration cycles. In the dynamic tests, the fundamental period is taken as that of the lateral treadmill motion, determined from the periodogram of the zero-padded

displacement signal. This ensures that the self-excited portion of the pedestrian-induced load is represented by an integer number of vibration periods.

3.6. Calibration of the treadmill

A dynamic calibration of the treadmill was performed prior to the pedestrian tests to verify the sensitivity of the force transducers and to determine the accuracy of the measurements. The treadmill is constructed such that a sinusoidal base motion with angular frequency ω_L and amplitude x_0 is generated at stage 2, and stage 3 can therefore be treated as a single-degree-of-freedom (SDOF) system subject to the base motion $x(t)$. The stiffness of this SDOF system is governed by the stiffness of the load cells, which for all practical purposes may be treated as rigid. The equilibrium of forces (see Fig. 3) is written according to d'Alambert's principle as [50]

$$F_I(t)+F_D(t)+F_E(t)=F(t) \tag{3}$$

where $F_I(t)$ is the inertia force, obtained as the mass M of stage 3 multiplied with the acceleration $\ddot{x}(t)$, $F_D(t)$ is the damping force which is considered negligible, $F_E(t)$ is the elastic force in the system, i.e. the measured force in the load cells and $F(t)$ is the external (pedestrian-induced) lateral load which acts on stage 3.

A calibration of the treadmill was made for all amplitudes and all frequencies in the range 0.27–1.17 Hz in step of 0.03 Hz and similar post-processing as described in Section 3.5 is adopted. The measured acceleration signal is used to calibrate the load cells. The calibration constant, $\hat{k}$, defined as the transformation of the voltage output from the load cells to force, is determined from the measured standard deviation of the acceleration and strain signals, respectively. For each combination of lateral frequency and amplitude a value for the calibration constant was obtained as

$$\hat{k}_i = M\frac{\sigma_{\ddot{x},i}}{\sigma_{Vi}} \tag{4}$$

where $\sigma_{\ddot{x},i}$ and σ_{Vi} are the measured standard deviations of the acceleration signal and the load cell signals, respectively. The load cells showed a linear behaviour with a linear correlation coefficient $\rho = 0.99997$.

3.7. Static pedestrian walking tests

In the following, the power spectral density (PSD) of the pedestrian lateral force is defined as either a continuous or a discrete single sided spectrum such that

$$\mathrm{Var}[F]=\sigma_F^2=\int_0^{f_{\mathrm{Ny}}} S_F(f)\,\mathrm{d}f \cong \sum_{k=1}^{N/2+1} S_F(f_k)\delta f \tag{5}$$

where $S_F(f)$ is the spectral ordinate at frequency f, f_{Ny} is the Nyquist frequency (half the sampling rate), δf is the frequency resolution of the spectrum and N is the number of samples in the discrete Fourier transform. An example of a typical measured force time history and the corresponding normalised square-root PSD is shown in Fig. 4. The intra-subject variability in the loading is illustrated by the varying load amplitude in the time history and quantified through the distribution of the energy around the main load harmonics.

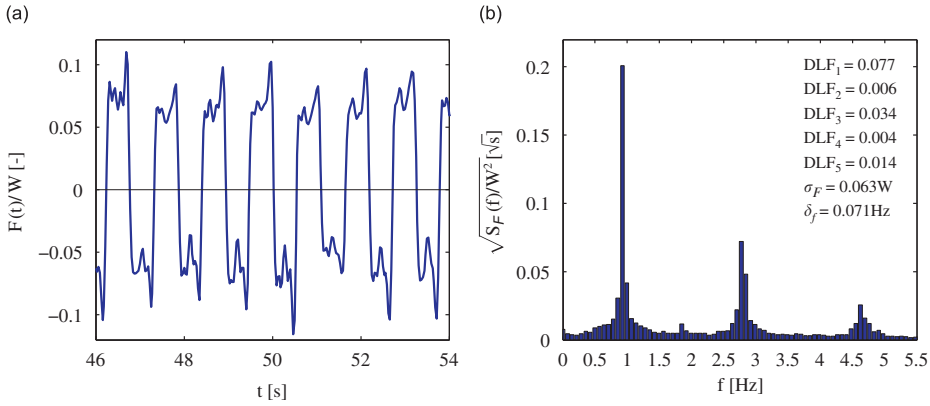

Fig. 4. Example of (a) a measured weight normalised force time-history and (b) the corresponding square-root PSD from a single pedestrian walking on a stationary surface (obtained with $\delta f = 1/15$ Hz and averaged over eight non-overlapping rectangular windows).

3.7.1. Equivalent "perfect" DLF

The intra-subject variability in the load makes a deterministic (and perfectly harmonic) description, similar to that in Eq. (1), only possible through an equivalent load amplitude [28,48]. The amplitude, or the equivalent perfect DLF, is obtained by requiring that the mean-square value of the response, $\tilde{\sigma}^2_{u,j}$, of a SDOF oscillator (with natural frequency, f_n), caused by the component of the measured force around load harmonic j, equals the mean-square response, $\tilde{\sigma}^2_{u,\mathrm{eq}}$, from a perfectly periodic force applied at resonance. The mean-square value of the response from the measured force is obtained as

$$\tilde{\sigma}^2_{u,j} = \int_{f_n - f_w/2}^{f_n + f_w/2} S_F(f)|H_n(f)|^2 \, \mathrm{d}f \tag{6}$$

$$|H_n(f)|^2 = \frac{1}{K_n^2}\left[\left[1-\left(\frac{f}{f_n}\right)^2\right]^2 + 4\zeta_n^2\left(\frac{f}{f_n}\right)^2\right]^{-1} \tag{7}$$

where $H_n(f)$, K_n, f_n and ζ_n are the frequency response function, stiffness, natural frequency and damping of the single-degree-of-freedom system, respectively, and f_w is the pedestrian walking frequency. The equivalent DLF can now be obtained from the following expression:

$$\tilde{\sigma}^2_{u,\mathrm{eq}} = \frac{1}{4K_n^2\zeta_n^2}\frac{\mathrm{DLF}_j^2 W^2}{2} = \tilde{\sigma}^2_{u,j} \tag{8}$$

The equivalent DLF depends on the modal damping and takes into account the filtering effect of the structure and that only load contributions in a narrow band near the natural frequency of the structure contribute to the vibration. As the modal damping ratio ζ_n and thereby the bandwidth may vary between structures, a conservative (upper-bound) value for the equivalent DLF is obtained by requiring that the mean-square value of the measured force, $\tilde{\sigma}^2_{F,j}$, in the total bandwidth between two harmonics ($\Delta f_j = f_w$) equals the mean-square value of the perfectly periodic force:

$$\tilde{\sigma}^2_{F,j}(\Delta f_j) = \int_{(j-1/2)f_w}^{(j+1/2)f_w} S_F(f) \, \mathrm{d}f = \frac{\mathrm{DLF}_j^2 W^2}{2} \tag{9}$$

Therefore, two different equivalent DLFs can be calculated; one according to Eq. (8), denoted the narrow-band model and one according to Eq. (9) denoted the broad-band model, i.e.

$$\mathrm{DLF}_j = \frac{2\sqrt{2}\zeta_n \tilde{\sigma}_{u,j} K_n}{W} \quad \text{narrow-band model} \tag{10}$$

$$\mathrm{DLF}_j = \frac{\sqrt{2}\tilde{\sigma}_{F,j}}{W} \quad \text{broad-band model} \tag{11}$$

The main problem with calculating the narrow-band DLF is that the accuracy of the spectral estimate decreases with a decrease in the bandwidth. This means that for low values of damping, the accuracy of the variance, $\tilde{\sigma}^2_{u,j}$, and thereby the equivalent DLF, relies on an accurate representation of the PSD in a very narrow band around the mean pacing rate. Due to the limited length of the measured force signal (2 min), the desired resolution to calculate the DLF for the narrow-band model is obtained through a combination of averaging, windowing and zero-padding of the data. Firstly, the data are divided into seven windows with 50 percent overlap and pre-multiplied with a Tukey window (a rectangular function with cosine side lobes of width $n_w/4$, where n_w is the number of data points in the window). In each window, the data was subsequently zero-padded to the total length of 16 times the original length (approximately 8 min). The smoothed (average) spectrum was then used to calculate the narrow-band DLFs and the zero-padding thereby works as a smoothening interpolation between the distinct frequencies in the spectrum of the original time series.

3.8. Dynamic pedestrian walking tests

As mentioned in Section 2.3, a pedestrian walking on a laterally driven surface will exert forces at the walking frequency and its integer harmonics, as well as at the frequency of the lateral oscillation. Following Ricciardelli and Pizzimenti [28], the latter force component will be referred to as "the self-excited force". An example of the measured pedestrian force and its PSD is shown in Fig. 5 for a lateral vibration amplitude of 19.4 mm at the frequency 1.06 Hz. The shape of the force time history is considerably different from that of the static tests (Fig. 4), due to the presence of the self-excited force component at the lateral vibration frequency. The two peaks in the PSD also provide clear evidence that the pedestrian walking frequency is not synchronised with that of the treadmill, which is an important observation as many mathematical models rely on that assumption. The potential for human–structure interaction is treated in more detail in Section 4.3.1. Firstly, the nature of the self-excited component of the force must be quantified, as not only the amplitude but also its phase (related to the treadmill motion) is of importance. This is done by dividing it into two terms, one in phase with the

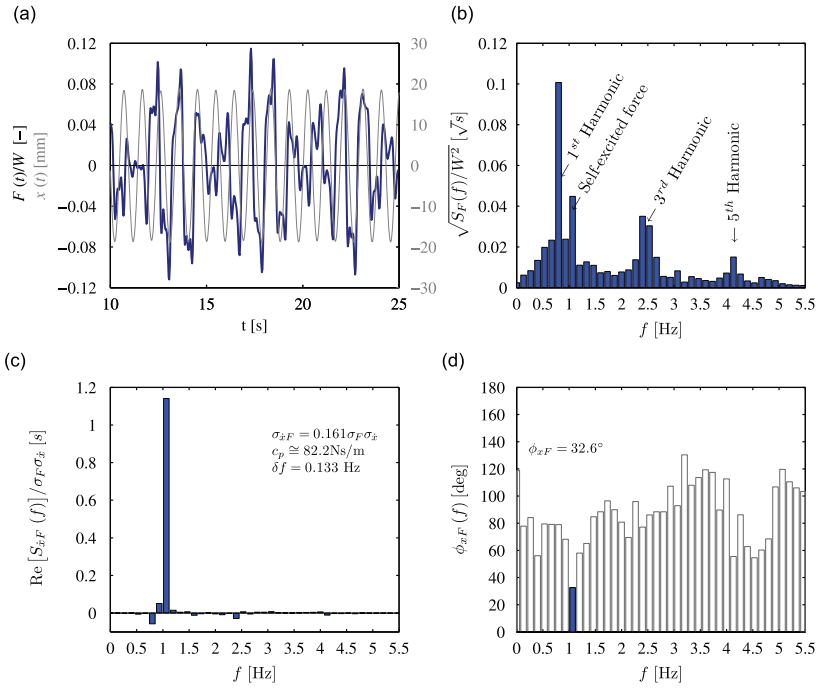

Fig. 5. Example of (a) a measured body-weight normalised force time-history, (b) its corresponding square-root PSD, (c) the normalised cross-spectral density between the measured lateral force and displacement and (d) the corresponding phase spectrum from a single pedestrian walking on a laterally oscillating surface (frequency 1.06 Hz and amplitude 19.4 mm). The spectra in (b)–(d) are obtained with $\delta f = 2/15$ Hz and averaged over four non-overlapping rectangular windows.

acceleration (inertial) and one in phase with the velocity (damping) of the treadmill, by considering the cross-covariance of the force and the treadmill motion.

3.8.1. Work done by pedestrian-induced lateral force

In a situation where a pedestrian is synchronised with the structure (or locked-in), the relative phase between the self-excited pedestrian force and the treadmill movement is constant and the phase angle can be determined. On the contrary, for a non-synchronised pedestrian, the phase angle may vary in time, whilst the pedestrian is still transferring energy into the structure. Therefore, the component in-phase with the velocity of the structure is determined through the average work done by the pedestrian per unit time P_F through integration of the product of the lateral pedestrian force $F(t)$ and the structural velocity $\dot{x}(t)$:

$$P_F = \frac{1}{T_{\text{tot}}} \int_0^{T_{\text{tot}}} F(t)\dot{x}(t)\,\mathrm{d}t \tag{12}$$

The integration in Eq. (12) is more conveniently evaluated in the frequency domain by considering the cross-covariance between the pedestrian force $F(t)$ and the platform velocity $\dot{x}(t)$ (at zero time lag). Recalling that the mean value has been removed from both $F(t)$ and $\dot{x}(t)$, the cross-covariance is written as [49]

$$\mathrm{Cov}[F,\dot{x}] = E[F(t)\cdot\dot{x}(t)] = \lim_{T\to\infty}\frac{1}{T}\int_0^T F(t)\dot{x}(t)\,\mathrm{d}t = \int_{-\infty}^{\infty} S_{F\dot{x}}(f)\,\mathrm{d}f \tag{13}$$

$$S_{F\dot{x}}(f) = \lim_{T\to\infty}\frac{1}{2\pi T}\mathcal{F}^*\{F(t)\}\mathcal{F}\{\dot{x}(t)\} = \mathrm{i}2\pi f\cdot S_{Fx}(f) \tag{14}$$

$$\Rightarrow S_{F\dot{x}}(f) = \mathrm{Co}_{F\dot{x}}(f) - \mathrm{iQu}_{F\dot{x}}(f) = \mathrm{i}2\pi f\cdot\mathrm{Co}_{Fx}(f) + 2\pi f\cdot\mathrm{Qu}_{Fx}(f) \tag{15}$$

$$\phi_{F\dot{x}}(f) = \arctan\frac{\mathrm{Co}_{Fx}(f)}{\mathrm{Qu}_{Fx}(f)} \tag{16}$$

where $\mathcal{F}\{\}$ is a Fourier transform operator, * denotes the complex conjugate and $i^2 = -1$. The cross-spectral density, $S_{F\dot{x}}(f)$, is complex and may be written in terms of its real part, denoted the co-spectral density $\mathrm{Co}_{F\dot{x}}(f)$, and the imaginary part called the quad-spectral density, $\mathrm{Qu}_{F\dot{x}}(f)$. Thereby, the cross-spectral density contains both the cross-amplitude and the phase between the processes $F(t)$ and $\dot{x}(t)$. It is further noted that for practical use of the cross-spectral density, all imaginary parts will cancel out, making only the real part of the spectrum of interest [49]. The last equality in Eq. (15) implies that the cross-spectral density between $F(t)$ and $\dot{x}(t)$ can be evaluated directly from the cross-spectral density between $F(t)$ and $x(t)$, simply by multiplying the spectrum with $i2\pi f$. This is convenient since the lateral treadmill displacement is measured directly, whereas the velocity can only be obtained through numerical differentiation of the measured displacement. The integral in Eq. (12) is now determined through integration of the cross-spectral density, either over the entire frequency domain, $P_F = \sigma_{F\dot{x}}$, or over a specific bandwidth, $\tilde{\sigma}_{F\dot{x}}(\Delta f)$. The latter approach is advantageous as it excludes erroneous contributions from correlated measurement noise or mechanical noise due to the possibility of non-perfect motion of the treadmill, which may occur at frequencies different from the fundamental lateral vibration frequency, see e.g. Fig. 5(c).The bandwidth is selected as $\Delta f = 0.05$ Hz centred at the lateral vibration frequency.

3.8.2. Damping and inertia proportional coefficients

It is now convenient to express the pedestrian force in terms of an equivalent damping force, $F_{D,\mathrm{eq}}(t)$, proportional to the velocity of the treadmill, and an equivalent inertia force, $F_{I,\mathrm{eq}}(t)$, proportional to its acceleration so that

$$F_{D,\mathrm{eq}}(t) = c_p \dot{x}(t) = c_p \dot{x}_0 \sin(\omega_L t + \varphi) \tag{17}$$

$$F_{I,\mathrm{eq}}(t) = \varrho_p m_p \ddot{x}(t) = \varrho_p m_p \ddot{x}_0 \sin(\omega_L t + \varphi + \pi/2) \tag{18}$$

where $\omega_L = 2\pi f_L$ is the angular frequency, $\dot{x}_0$ and $\ddot{x}_0$ are the velocity and acceleration amplitudes of the lateral vibration, φ is an arbitrary phase and m_p is the pedestrian mass. The average work done by the damping force per unit time is $P_{D,\mathrm{eq}} = \frac{1}{2} c_p \dot{x}_0^2$. The velocity proportional constant c_p is now obtained by imposing the condition that the pedestrian load inputs the same energy per unit time as that of the equivalent load within the frequency bandwidth Δf, thus $\tilde{\sigma}_{F\dot{x}}(\Delta f) = P_{D,\mathrm{eq}}$. The portion of the total pedestrian mass $\varrho_p m_p$ that contributes to the added mass of the structure is determined similarly to c_p, i.e.:

$$c_p = \frac{2}{\dot{x}_0^2} \tilde{\sigma}_{F\dot{x}}(\Delta f) \tag{19}$$

$$\varrho_p m_p = \frac{2}{\ddot{x}_0^2} \tilde{\sigma}_{F\ddot{x}}(\Delta f) \tag{20}$$

$$\tilde{\sigma}_{F\dot{x}}(\Delta f) = \int_{f_L - \Delta f/2}^{f_L + \Delta f/2} \mathrm{Re}[S_{F\dot{x}}(f)]\, \mathrm{d}f = -2\pi \int_{f_L - \Delta f/2}^{f_L + \Delta f/2} f\, \mathrm{Qu}_{Fx}(f)\, \mathrm{d}f \tag{21}$$

$$\tilde{\sigma}_{F\ddot{x}}(\Delta f) = \int_{f_L - \Delta f/2}^{f_L + \Delta f/2} \mathrm{Re}[S_{F\ddot{x}}(f)]\, \mathrm{d}f = -4\pi^2 \int_{f_L - \Delta f/2}^{f_L + \Delta f/2} f^2\, \mathrm{Co}_{Fx}(f)\, \mathrm{d}f \tag{22}$$

An example of the application of the spectral analysis for the determination of the force coefficient c_p and the phase angle between the lateral pedestrian force and the treadmill displacement is shown in Fig. 5. According to the definition of the coefficients c_p and ϱ_p, in Eqs. (17)–(18), the self-excited force appears positive on the right-hand side of the equation of motion, thus positive values of c_p and ϱ_p indicate a decrease in the modal damping and mass, respectively.

3.9. Error estimation

From Eq. (3) it is apparent that in the absence of damping and external load, the measured force and the inertial force of stage 3 should be equal in magnitude and opposite in direction. Having calibrated the load cell (see Section 3.6), an estimate of the error can be made by considering the residual force $\hat{F}(t)$, measured for an empty treadmill and defined as

$$\hat{F}(t) = F_I(t) + F_E(t) \tag{23}$$

At each combination of lateral vibration frequency and amplitude, the velocity and acceleration proportional coefficients were calculated according to Eqs. (19)–(20), as well as the total standard deviation of the force. In Fig. 6 the results from these calculations are shown, which indicate the level of error expected in the tests. For the velocity and acceleration proportional load coefficients, the mean errors are -1.0 N s/m (S.D. 4.7 N s/m) and 0.3 kg (S.D. 2.3 kg), whereas the mean error on the total force is 1.2 N (S.D. 0.2 N). For all practical purposes, these errors have been considered acceptable.

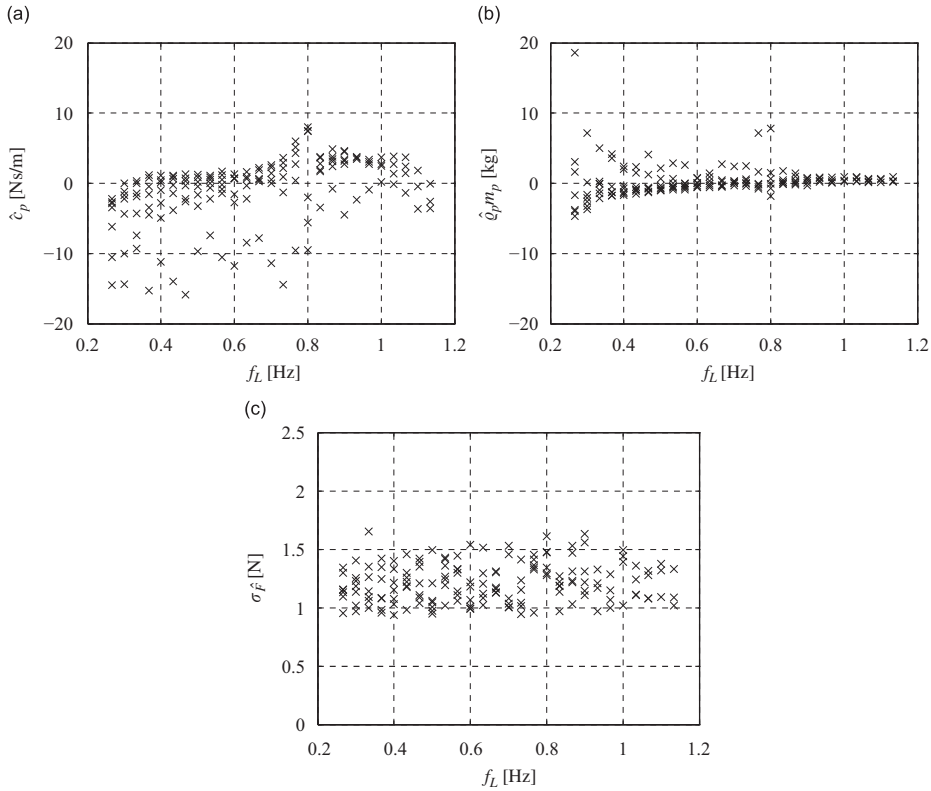

Fig. 6. Measured error for (a) velocity and (b) acceleration proportional load coefficients, respectively, and (c) standard deviation of error on total lateral force.

4. Results and discussion

4.1. Walking speed and frequency

The mean normal walking speed during the tests was 1.27 m/s (S.D. 0.23 m/s) for women and 1.30 m/s (S.D. 0.20 m/s) for men, while the mean normal walking frequency was 0.87 Hz (S.D. 0.09 Hz) for women and 0.85 Hz (S.D. 0.07 Hz) for men. The mean walking speed and walking frequency, $\bar{f}_w$, for all test subjects were 1.29 m/s (S.D. 0.21 m/s) and 0.86 Hz (S.D. 0.08 Hz), respectively, whereas the mean weight of the subjects was 730 N (S.D. 148 N), with a considerable difference between male (808 N and S.D. 110 N) and female subjects (603 N and S.D. 111 N). The probability distribution of the normal walking frequencies, as observed in the tests, can be approximated reasonably with a normal distribution, whereas the walking speed and the subject's weight are more randomly distributed.

A slight correlation between the walking speed and the walking frequency was observed (with linear correlation coefficient $\rho = 0.6612$). In Fig. 7 the pedestrian walking speed versus the walking frequency is shown, together with compiled data from earlier experiments conducted by Pansera [51], Terrier et al. [52] and Ingólfsson [53]. Ingólfsson et al. [54] used a power law of the type $f_w = a v_p^b$ to fit the experimental data (with a = 0.81 and b=0.35) which is also shown in Fig. 7. Opposed to a linear regression, the advantage in using a power law is that it fulfills the boundary condition $v_p(0)$=0, whilst allowing for non-constant values of the stride length.

Furthermore, a slight linear correlation was observed between the pedestrian weight and the RMS value of the pedestrian load ($\rho = 0.6720$). Their relationship is shown in Fig. 7, together with a linear regression, written as $\sigma_F = 0.041$ W. The other physical characteristics, such as length of leg or pedestrian height did not show signs of significant correlation with either the pedestrian force or the walking speed and frequency, confirming similar observations made by Ricciardelli and Pizzimenti [28].

4.2. Static pedestrian walking tests

Little to no correlation between the DLFs and the walking frequency could be observed from the tests. In Fig. 8 the DLFs of the first five load harmonics are shown as a function of frequency (normalised with the mean walking frequency of the

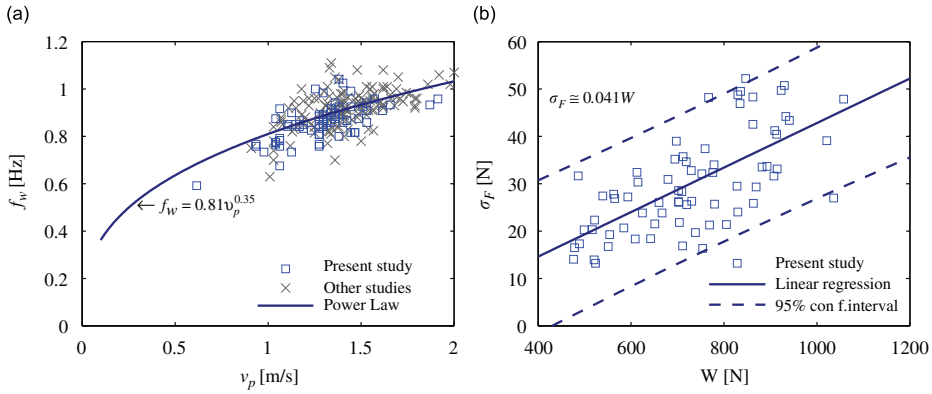

Fig. 7. (a) Relationship between the walking speed and the walking frequency measured in present study and as reported in other studies [54]. (b) Relationship between pedestrian weight and RMS value of the lateral pedestrian force.

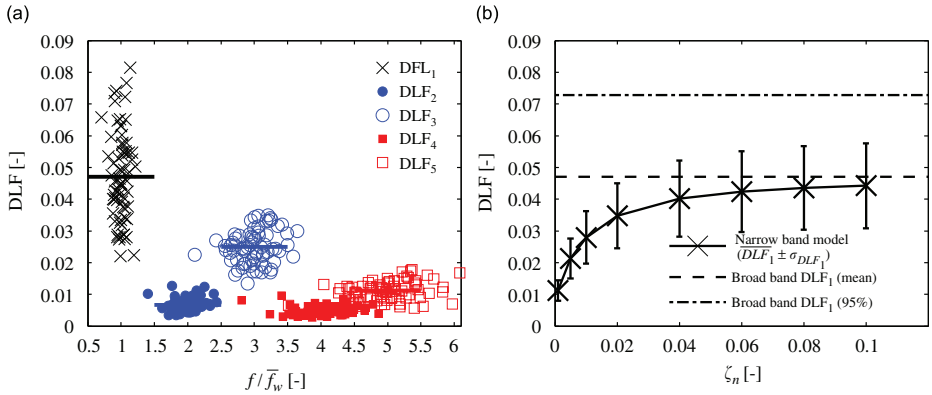

Fig. 8. Equivalent DLF obtained in the static tests using a broad-band model shown as (a) a function of the walking frequency and (b) a function of the damping ratio.

population, $\overline{f}_w$), calculated assuming a broad-band model as described in Section 3.7. Also, in Fig. 8, the fundamental DLF calculated using the narrow-band model is shown as a function of the damping ratio. It is noted that a considerable difference between the DLF calculated using the broad-band and the narrow-band models is observed, particularly at low structural damping ratios, as is characteristic for many long-span footbridges. This observation stresses the importance of intra-subject variability when calculating pedestrian-induced excitation and that the DLFs which are calculated on the basis of the broad-band model can be very conservative. Furthermore, the inter-subject variability in the DLFs is made clear by the large scatter of the measured data and an accurate description of the loading from a group of pedestrians seems only possible through probability distribution functions. The low mean value combined with large scatter suggests the use of a skewed distribution as a fit to the measured data, e.g. the lognormal distribution with the probability density function:

$$p(x) = \frac{1}{x\xi\sqrt{2\pi}} \exp\left[-\frac{[\ln x - \chi]^2}{2\xi^2}\right] \tag{24}$$

The parameters χ and ξ are related to the sample mean $E[X] = \mu_X$ and variance $\mathrm{Var}[X] = \sigma_X^2$ so that

$$\chi = \ln\mu_X - \frac{1}{2}\ln\left(1 + \frac{\sigma_X}{\mu_X^2}\right), \quad \xi^2 = \ln\left(1 + \frac{\sigma_X}{\mu_X^2}\right). \tag{25}$$

The experimentally obtained cumulative distribution functions of DLF_1, DLF_3 and DLF_5 (from the broad-band model) are shown in Fig. 9 together with the fitted lognormal distribution.

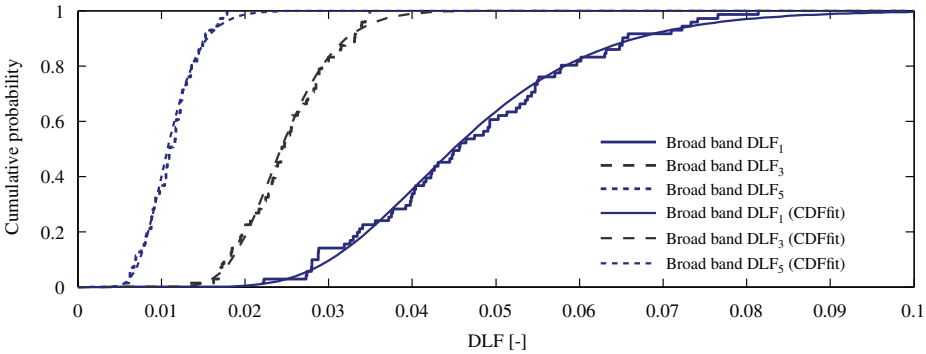

Fig. 9. Cumulative distribution function for the equivalent DLF of the odd harmonics using the broad-band model, shown with fitted log-normal distribution functions.

Table 3
Mean and characteristics values of the measured equivalent DLFs from the static pedestrian tests.

	j=1	j=2	j=3	j=4	j=5
Broad-band model, $\overline{\mathrm{DLF}}_j$ (mean value)	0.047	0.007	0.025	0.005	0.011
Broad-band model, DLF_j (95 percent fractile)	0.073	0.010	0.034	0.007	0.016
Narrow-band model ($\zeta_n = 0.01$), $\overline{\mathrm{DLF}}_j$ (mean value)	0.028	0.003	0.017	0.002	0.008
Narrow-band model ($\zeta_n = 0.01$), DLF_j (95 percent fractile)	0.041	0.006	0.024	0.002	0.012

The mean value of the DLFs and that with a 95 percent non-exceedance probability are shown in Table 3, both for the narrow-band (when assuming $\zeta_n = 0.01$) and the broad-band models. Clearly, there is a difference between these two methods, as illustrated in Fig. 8 and since the DLF depends on the structural damping, the most conservative method in a design situation is to use the broad-band model, in particular if the damping is uncertain or even unknown.

The results from the static tests compare generally well with the values reported by other researchers, see e.g. Section 2.1, both qualitatively in terms of data scatter and frequency dependency and also quantitatively in terms of characteristic values. In particular, the characteristic values of the DLFs reported by Ricciardelli and Pizzimenti [28] from the narrow-band model (with $\zeta_n = 0.01$) agree very well to those reported herewith, as expected since the experimental setups are (near) identical and the test subjects are drawn from a similar pool of persons. It is further shown that the lognormal distribution provides a reasonable fit to the data and may be used to model the probability distribution of the DLFs. This is especially useful when modelling the pedestrian-induced loading in a probabilistic sense e.g. through Monte Carlo simulations. It should be noted that these DLFs were measured in the absence of lateral vibrations and cannot be used for estimating vibrations in footbridges where the self-excited part of the load cannot be neglected.

4.3. Dynamic pedestrian walking tests

Pedestrian walking tests were performed at different lateral oscillation frequencies, f_L, and amplitudes, x_0, with up to 66 test subjects at each particular combination of f_L and x_0 (see Table 2). In each test, both the velocity and acceleration proportional constants c_p and ϱ_p were determined according to Eqs. (19) and (20), respectively. In Fig. 10, the mean value $\overline{c}_p$ for each lateral vibration frequency and amplitude is presented, both as a function of normalised frequency and amplitude. The frequency axis is normalised by the mean walking frequency of the population, $\overline{f}_w$.

In Fig. 10(a), the curves are made of an initial near-linear segment (up to $f_L/\overline{f}_w \cong 0.8$ on the horizontal axis), followed by an almost horizontal segment. The slope of the linear segment and the value of the constant segment increases with decreasing amplitude. At the lowest frequencies $\overline{c}_p$ is negative (i.e. damping is added to the structure), but at higher frequencies ($f_L/\overline{f}_w \gtrsim 0.50$) the coefficient is positive. In addition, in Fig. 10(b) there is a clear correlation between the mean load coefficient and the displacement amplitude at most frequencies. In particular for $f_L/\overline{f}_w > 0.89$, the negative damping decreases with increasing amplitude, which demonstrates the self-limiting nature of the associated structural response. At lower frequencies, the added damping decreases for an increase in the displacement amplitude.

The mean values of c_p presented herewith are lower than 300 N s/m as reported from the London Millennium Bridge [2]. It should be noted that a direct comparison between load coefficients c_p obtained in this study and that reported from the Millennium Bridge is not possible, first of all because on the Millennium Bridge the result is based on a limited number of full-scale experiments and may therefore represent a different fractile than the mean value. Secondly, the value of c_p

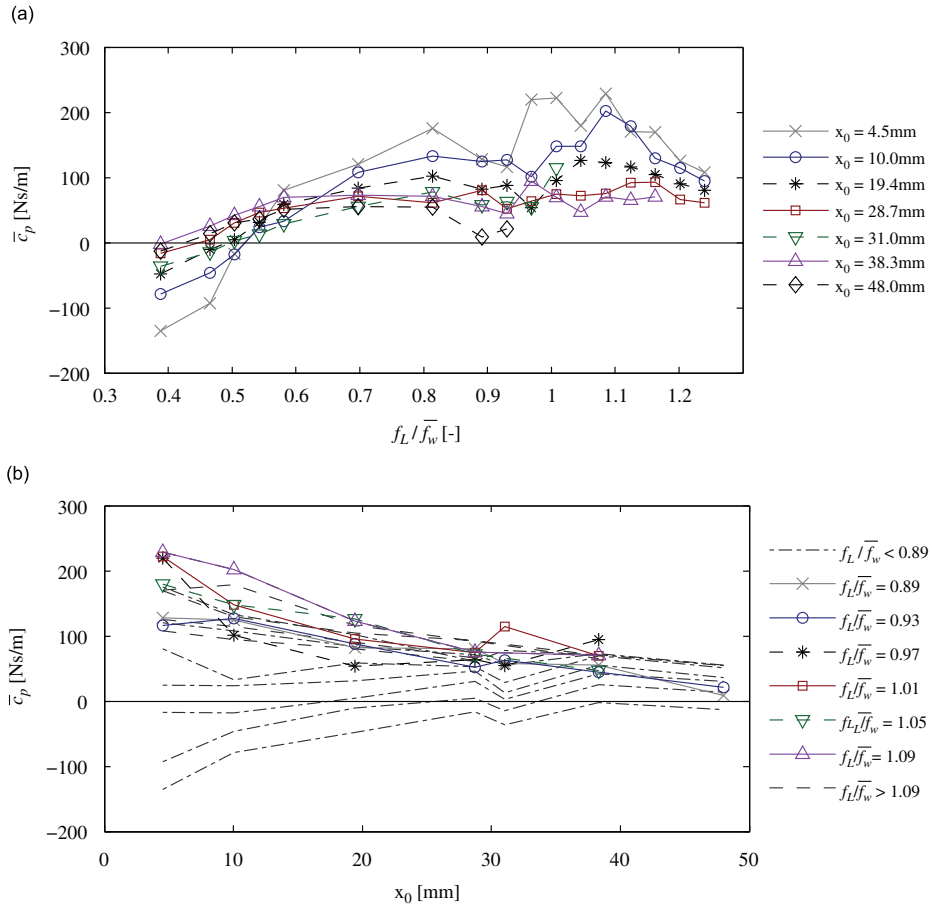

Fig. 10. Average value of the pedestrian load coefficient (a) as a function of the normalised frequency for different lateral displacement amplitudes and (b) as a function of the lateral displacement amplitude for various vibration frequencies.

reported by Dallard et al. [2] is estimated from back calculations of measured response and involves some inaccuracy in several bridge and crowd specific parameters; particularly modal mass, shape, damping and spatial pedestrian distribution. Based on the inverted pendulum model developed by Macdonald [15] the equivalent damping coefficient per pedestrian walking on a laterally moving surface was shown to depend strongly on the lateral oscillation frequency, with a maximum value of around 200 N s/m.

The mean value of the mass proportional constant, $\overline{\varrho}_p$, shows a clear dependency on the lateral vibration frequency. In Fig. 11(a) it is shown that at low frequencies, $\overline{\varrho}_p$ is positive and pedestrians therefore subtract from the overall modal mass of the structure. This effect of the pedestrian mass has been explained as "added stiffness" by Pizzimenti and Ricciardelli [36]. At higher frequencies however it becomes negative and near constant (at around 0.12–0.20), suggesting that pedestrians (on average) add to the modal mass of the structure. The transition from positive to negative values of $\overline{\varrho}_p$ occurs in the frequency range $f_L/\overline{f}_w \sim 0.55-0.85$ and is amplitude dependent, i.e. for large amplitudes, the transition frequency is generally lower. In Fig. 11(b), it is noted that at lower frequencies, $\overline{\varrho}_p$ decrease as the lateral vibration amplitude increases, but at higher frequencies it is near constant. The inverted pendulum model proposed by Macdonald [25] predicts positive values for ϱ_p (i.e. decreased modal mass) in the frequency range $f_L/\overline{f}_w \in [0.3; 1.3]$ and maximum value of 61 percent of the body weight. For lower frequencies, ϱ_p becomes negative with a maximum value of -1 at $f_L/\overline{f}_w = 0$. The results presented herewith contradict this, but as noted by Macdonald [25], the results from the inverted pendulum model depend on the specific control law used for the pedestrian balance control and with a different control scheme, positive values for ϱ_p are predicted in the low frequency range and negative values in the higher frequency range, similar to the results presented herewith.

Although the mean values show some clear frequency and amplitude dependency, it is stressed that a very large inter-subject variability was observed in the tests, illuminated by the large scatter in the measured load coefficients. Therefore,

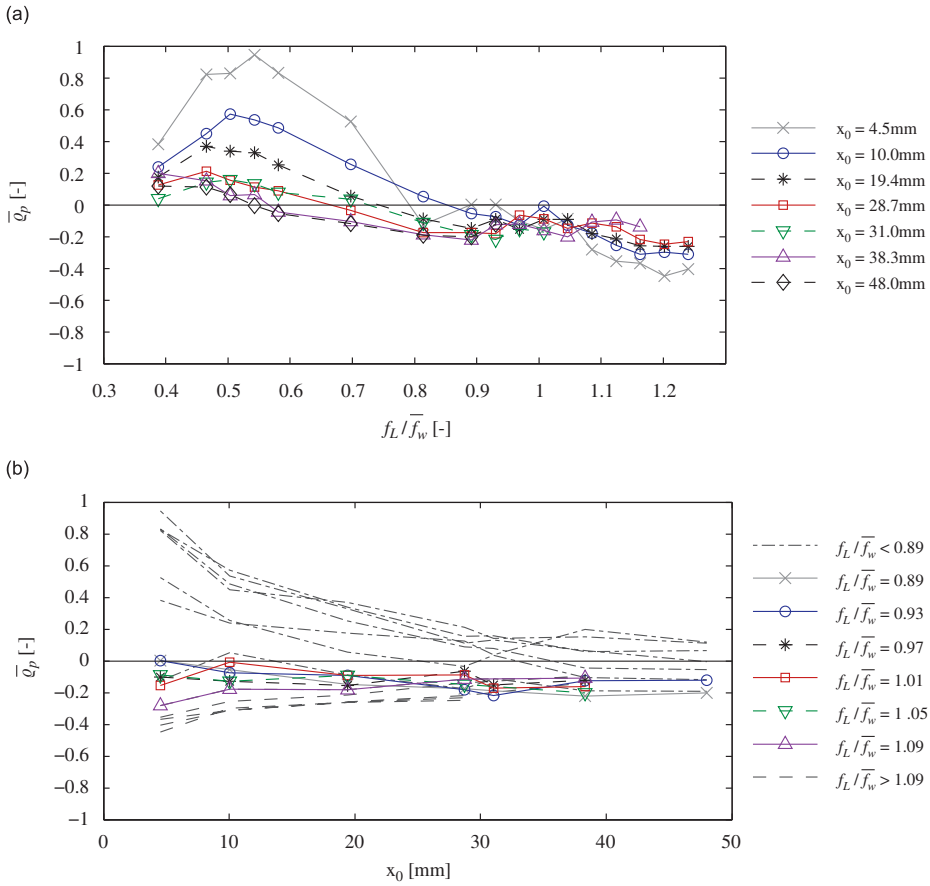

Fig. 11. Average value of the mass proportional coefficient $\overline{\varrho}_p$ (a) as a function of the normalised frequency for different lateral displacement amplitudes and (b) as a function of lateral displacement amplitude for various vibration frequencies.

the load coefficients are best described through their probability distribution and central moments (mean and standard deviation). In Fig. 12(a)–(b), the experimentally obtained probability distributions of c_p and ϱ_p for different frequencies are shown. In Fig. 12(c)–(d) the development of the mean value $\pm$one standard deviation error bar of the same load coefficients are shown as a function of the normalised lateral vibration frequency.

Further analysis reveals that the data scatter is particularly pronounced at low vibration amplitudes. The reason for this is found in the definition of the load coefficients in Eqs. (19) and (20), where it is noted that $\dot{x}_0^2$ and $\ddot{x}_0^2$ appear in the denominator and therefore causes a large magnification at low vibration amplitudes. This phenomenon is illustrated in Fig. 13, showing the mean value of the load and mass coefficients and the single standard deviation boundaries as a function of the lateral velocity and acceleration, respectively. We note that for c_p, the mean value is fairly constant over the entire amplitude range, but the standard deviation decreases as the velocity increases. The mass coefficient, ϱ_p, however, seems to decrease with the acceleration, with a positive value at low accelerations and a negative value in the acceleration range 0.1–0.4 m/s^2.

4.3.1. Qualitative assessment of the potential for human–structure synchronisation

From the tests various qualitative observations regarding the potential for human–structure synchronisation were made. In tests where the natural walking frequency coincided with the walking frequency of the test subject, people reacted differently; some would adjust their steps to match a "comfortable" phase, whilst others walked unaffected by the movement. Those who adjusted their phase to that of the treadmill, did so in different manner, i.e. some people spread the legs further apart whilst others crossed their legs during walking and therefore the load induced is different in these two situations. Furthermore, it was also observed that even the same person did not necessarily react in the same way in two nearly identical situations.

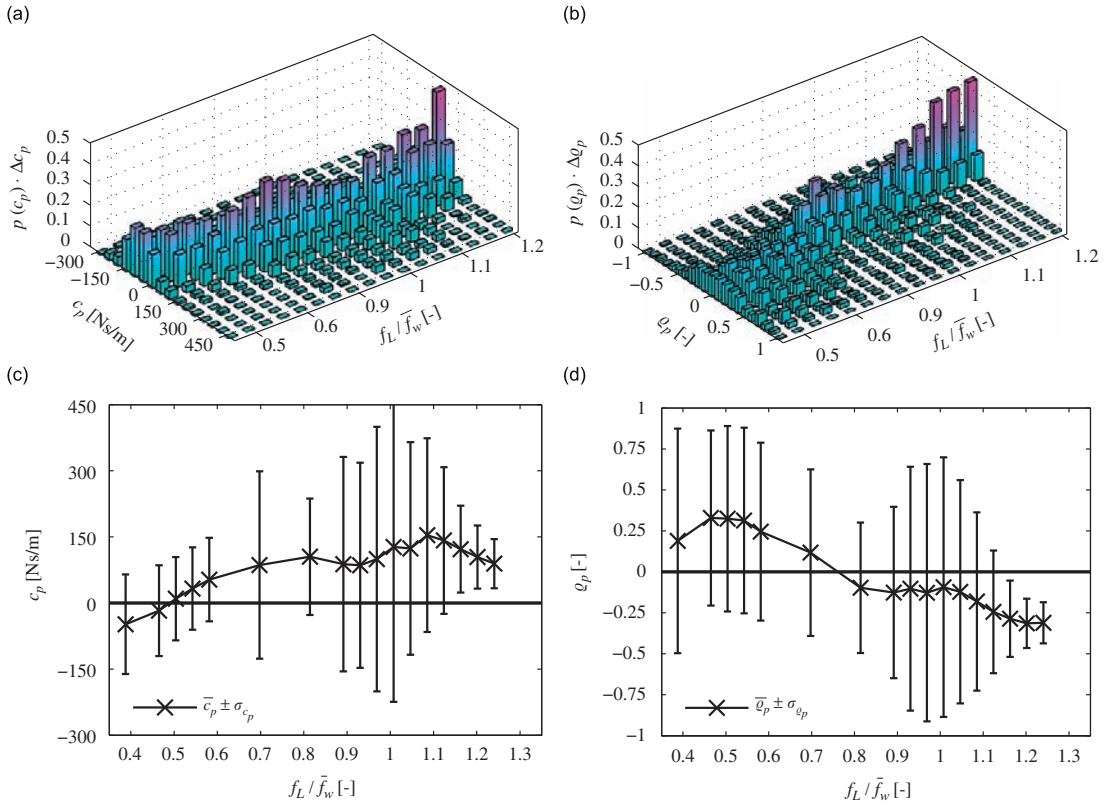

Fig. 12. Probability distributions of (a) damping proportional coefficient, c_p, and (b) inertia proportional coefficient, ϱ_p, at different frequencies shown as functions of the normalised frequency and mean value $\pm$ one standard deviation of (c) c_p and (d) ϱ_p.

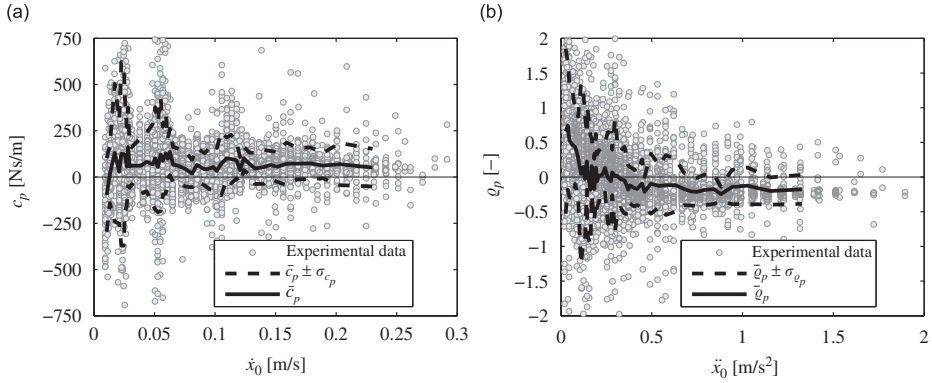

Fig. 13. Mean value $\pm$ one standard deviation of (a) c_p and (b) ϱ_p as functions of the lateral vibration velocity and acceleration, respectively.

Most of the test subjects felt at some point during the tests that they were affected by the lateral vibrations. The combination of low frequency and large amplitude was generally described as uncomfortable and several test subjects mentioned a resemblance to walking on a rocking boat. When the vibration frequency was close to the walking frequency, the vibration was often described as "clearly perceptible" or "annoying". The reason is that the relative phase between the treadmill movement and the steps changes slowly and thereby the reaction force from the treadmill (as felt by the

pedestrian) is constantly changing making it difficult to adapt to the vibration. This frequency range can be described as a potential "lock-in" range where people might tend to adjust their walking frequency to that of the treadmill lateral motion. In the tests presented herewith, this would be possible by adjustment of the stride length. However, a more efficient way would be to adjust the walking speed, which was not possible due to restrictions posed by the nature of the test equipment. Indeed, some of the test subjects made complaints that they would prefer to change their walking speed in an attempt to avoid the uncomfortable feeling of walking at a frequency close to the vibration frequency. Typically, these complaints would only occur during large amplitude vibrations, e.g. $x_0 \geq 19$ mm.

Additionally, it is worth pointing out that, although most of the pedestrians were affected by the lateral vibrations of the treadmill, the large scatter in the data and the visual observations made during the tests suggest that synchronisation of pedestrians walking on a laterally moving surface is neither generic nor obviously deterministic. Instead it is to a large extent governed by randomness and whilst some people feel comfortable adjusting to the platform motions, others are more comfortable walking at their own selected pacing rate. Whilst some people prefer adjusting their phase to match the displacement of the treadmill, others choose to match the acceleration or velocity.

The observed randomness in the behaviour of the pedestrians and lack of obvious signs of human–structure synchronisation, combined with the fact that negative damping could be generated at most frequencies, suggests that synchronisation is not as important as generally believed. To confirm this, further analysis were undertaken on the walking patterns of 7 test subjects that were instrumented with waist-mounted tri-axial accelerometers. These tests revealed that synchronisation is not a pre-condition for the development of velocity (and acceleration) proportional pedestrian forces, which may lead to large amplitude lateral vibrations in footbridges [55].

5. Conclusions

The data presented in this paper are based on measured forces from 71 pedestrians walking on both a laterally fixed and oscillating surface at various amplitudes and frequencies.

Particular attention is paid on quantification of the self-excited component of the pedestrian load through a damping proportional and a mass proportional coefficient, respectively. For both these coefficients, a large scatter is observed at low vibration amplitudes, but decreases as the amplitude increases. Analysis of the self-excited pedestrian load reveals that pedestrians (on average) consistently input energy into the structure in the normalised frequency range between approximately 0.6 and 1.2 and that the component in phase with the structural velocity can be modelled as a velocity proportional force. Interestingly, the coefficient of proportionality, c_p, decreases with an increase in the vibration amplitude and can therefore not be treated as a constant parameter (Fig. 10). Instead the load has a nonlinear component due to this dependency. The decrease in negative damping as the vibration amplitude increases, suggest that the pedestrian-induced loading is self-limiting. The component in phase with the acceleration is analysed and found to depend on the frequency of the structure. It is observed that for low frequencies, pedestrians subtract from the overall modal mass and add to the mass at higher frequency motion, with an amplitude-dependent transition.

The very large scatter in the data suggests that a probabilistic approach is necessary for an accurate estimation of the susceptibility of a footbridge to excessive vibrations. In particular, the critical number of pedestrian needed to trigger SLE may vary considerably depending on the particular crowd occupying the bridge.

Finally, since positive values of $\overline{c}_p$ occur in a broad frequency range, synchronisation of the walking frequency to that of the structure is not necessary for the development of velocity proportional loads, which can be represented in the form of negative damping.

Acknowledgements

The authors gratefully acknowledge Niccoló Bonanni, graduate student at University of Florence for his substantial contribution and enthusiasm in recruiting test persons for the experiments. Further, the authors also thank the people who participated in the tests presented in this study. A special gratitude is directed to the laboratory for Inter University Research on Building Aerodynamics and Wind Engineering (CRIACIV) at the University of Florence in Prato, Italy, who kindly hosted the experimental work, carried out during this research campaign, and in particular Lorenzo Procino chief engineer at CRIACIV is acknowledged for his help and support during this experimental work.

References

[1] P. Dziuba, G. Grillaud, O. Flamand, S. Sanquier, Y. Tétard, La passerelle solférino comportement dynamique (dynamic behaviour of the solférino bridge), *Bulletin Ouvrages Métalliques* 1 (2001) 34–57 (in French).
[2] P. Dallard, A. Fitzpatrick, A. Flint, S. Bourva, A. Low, R. Ridsdill-Smith, M. Willford, The London Millennium footbridge, *The Structural Engineer* 79 (22) (2001) 17–33.
[3] A. Pavic, P. Reynolds, Vibration serviceability of long-span concrete building floors. Part 1: review of background information, *The Shock and Vibration Digest* 34 (3) (2002) 191–211.
[4] A. Pavic, P. Reynolds, Vibration serviceability of long-span concrete building floors. Part 2: review of mathematical modelling approaches, *The Shock and Vibration Digest* 34 (4) (2002) 279–297.

[5] S. Živanović, A. Pavic, P. Reynolds, Vibration serviceability of footbridges under human-induced excitation: a literature review, *Journal of Sound and Vibration* 279 (1–2) (2005) 1–74.
[6] J. Brownjohn, S. Zivanovic, A. Pavic, Crowd dynamic loading on footbridges, *Proceedings of Footbridge 2008, Third International Conference*, Porto, 2008.
[7] M. Kasperski, Safety and serviceability of stand structures, *Proceedings of the 7th European Conference on Structural Dynamics*, Southampton, 2008.
[8] V. Racic, A. Pavic, J. Brownjohn, Experimental identification and analytical modelling of walking forces: literature review, *Journal of Sound and Vibration* 326 (2009) 1–49.
[9] F. Venuti, L. Bruno, Crowd-structure interaction in lively footbridges under synchronous lateral excitation: a literature review, *Physics of Life Reviews* 6 (2009) 176–206.
[10] A. Low, Design for dynamic effects in long span footbridges, *Proceedings of Footbridge 2008, Third International Conference*, Porto, 2008.
[11] Y. Fujino, B. Pacheco, S. Nakamura, P. Warnitchai, Synchronization of human walking observed during lateral vibration of a congested pedestrian bridge, *Earthquake Engineering & Structural Dynamics* 22 (9) (1993) 741–758.
[12] S. Nakamura, Model for lateral excitation of footbridges by synchronous walking, *Journal of Structural Engineering* 130 (1) (2004) 32–37.
[13] A. Rönnquist, Pedestrian Induced Vibrations of Slender Footbridges, PhD Thesis, Norwegian University of Science and Technology, 2005.
[14] Q. Ye, G. Fanjiang, B. Yanev, Investigation of the dynamic properties of the Brooklyn bridge, in: *Sensing Issues in Civil Structural Health Monitoring*, Springer, Netherlands2005, pp. 65–72.
[15] J. Macdonald, Pedestrian-induced vibrations of the Cliffton suspension bridge, UK, *Proceedings of the ICE: Bridge Engineering* 161 (BE2) (2008) 69–77.
[16] A. McRobie, G. Morgenthal, J. Lasenby, M. Ringer, Section model tests on human–structure lock-in, *Proceedings of the ICE: Bridge Engineering* 156 (BE2) (2003) 71–79.
[17] CEN, European Committee for Standardization, NA to BS EN 1991-2:2003 UK. National Annex to Eurocode 1: Actions on structure-Part 2: traffic loads on bridges, May 2008.
[18] C. Butz, C. Heinemeyer, A. Keil, M. Schlaich, A. Goldack, S. Trometer, M. Lukić, B. Chabrolin, A. Lemaire, P. Martin, A. Cunha, E. Caetano, Design of Footbridges-Guidelines and background document, HIVOSS, rFS2-CT-2007-00033, 2007.
[19] Fédération international du béton (*fib*), Guidelines for the design of footbridges, bulletin 32, November 2005.
[20] Sétra, Footbridges, Assessment of vibrational behaviour of footbridges under pedestrian loading, November 2006.
[21] S.H. Strogatz, D.M. Abrams, A. McRobie, B. Eckhardt, E. Ott, Crowd synchrony on the millennium bridge, *Nature* 438 (7064) (2005) 43–44.
[22] F. Venuti, L. Bruno, N. Bellomo, Crowd dynamics on a moving platform: mathematical modelling and application to lively footbridges, *Mathematical and Computer Modelling* 45 (2007) 252–269.
[23] J. Bodgi, S. Erlicher, P. Argoul, O. Flamand, F. Danbon, Crowd structure synchronization: coupling between Eulerian flow modeling and Kuramoto phase equation, *Proceedings of Footbridge 2008, Third International Conference*, Porto, 2008.
[24] G. Piccardo, F. Tubino, Parametric resonance of flexible footbridges under crowd-induced lateral excitation, *Journal of Sound and Vibration* 311 (2008) 353–371.
[25] J. Macdonald, Lateral excitation of bridges by balancing pedestrians, *Proceedings of the Royal Society A* 465 (2009) 1055–1073.
[26] F. Harper, W. Warlow, B. Clarke, The forces applied to the floor by the foot in walking. 1. Walking on a level surface, Technical Report, National Building Studies-Research paper 32, Department of Scientific and Industrial Research, 1961.
[27] E. Chao, R. Laughman, E. Schneider, R. Stauffer, Normative data of knee joint motion and ground reaction forces in adult level walking, *Journal of Biomechanics* 16 (2) (1983) 219–233.
[28] F. Ricciardelli, A. Pizzimenti, Lateral walking-induced forces on footbridges, *Journal of Bridge Engineering* 12 (6) (2007) 677–688.
[29] C. Sahnaci, M. Kasperski, Random loads induced by walking, *Proceedings of the 6th European Conference on Structural Dynamics*, Southampton, 2005.
[30] H. Bachmann, W. Ammann, *Vibrations in Structures. Induced by Man and Machine, Structural Engineering Documents, International Association for Bridge and Structural Engineering (IABSE)*, third ed., Zürich, Switzerland, 1987.
[31] H. Bachmann, A. Pretlov, H. Rainer, Appendix G: dynamic forces from rhythmical human body motions, *Vibration Problems in Structures: Practical Guidelines*, Birkhäuser, 1996.
[32] A. Crowe, M.M. Samson, M.J. Hoitsma, A.A. van Ginkel, The influence of walking speed on parameters of gait symmetry determined from ground reaction forces, *Human Movement Science* 15 (1996) 347–367.
[33] C. Butz, Beitrag zur Berechnung fußgängerinduzierter Brückenschwingungen (on the calculation of pedestrian-induced vibration of bridges), PhD Thesis, RWTH Aachen, 2006 (in German).
[34] C. Sahnaci, M. Kasperski, Excitation of buildings and pedestrian structures from walking and running, *Proceedings of Experimental Vibration Analysis for Civil Engineering Structures*, Porto, 2007, pp. 209–218.
[35] A. Pizzimenti, Analisi sperimentale dei meccanismi di eccitazione laterale delle passerelle ad opera dei pedoni (experimental analysis of the lateral pedestrian-induced mechanism of excitation of footbridges), PhD Thesis, Department of Civil and Environmental Engineering, University of Catania, 2003 (in Italian).
[36] A. Pizzimenti, F. Ricciardelli, Experimental evaluation of the dynamic lateral loading of footbridges by walking pedestrians, *Proceedings of the 6th International Conference on Structural Dynamics*, Paris, 2005.
[37] P. Charles, V. Bui, Transversal dynamic actions of pedestrians. synchronization, *Proceedings of Footbridge 2005, Second International Conference*, Venice, 2005.
[38] F. Danbon, G. Grillaud, Dynamic behaviour of a steel footbridge. Characterisation and modelling of the dynamic loading induced by a moving crowd on the Solferino footbridge in Paris, *Proceedings of Footbridge 2005, Second International Conference*, Venice, 2005.
[39] B. Eckhardt, E. Ott, S. Strogatz, D. Abrams, A. McRobie, Modeling walker synchronization on the millennium bridge, *Physical Review E* 75 (2007) 21110-1–21110-10 10.1103/PhysRevE.75.021110.
[40] S.H. Strogatz, From Kuramoto to Crawford: exploring the onset of synchronization in populations of coupled oscillators, *Physica D* 143 (1–4) (2000) 1–20.
[41] S. Nakamura, T. Kawasaki, H. Katsuura, K. Yokoyama, Experimental studies on lateral forces induced by pedestrians, *Journal of Constructional Steel Research* 64 (2008) 247–252.
[42] C. Barker, Some observations on the nature of the mechanism that drives the self-excited lateral response of footbridges, *Proceedings of Footbridge 2002, First International Conference*, Paris, 2002.
[43] M. Willford, Dynamic actions and reactions of pedestrians, *Proceedings of Footbridge 2002, First International Conference*, Paris, 2002.
[44] A. Rönnquist, E. Strømmen, Pedestrian induced lateral vibration of slender footbridges, *Proceedings of the 25th IMAC Conference*, Orlando, USA, 2007.
[45] L. Sun, X. Yuan, Study on pedestrian-induced vibration of footbridge, *Proceedings of Footbridge 2008, Third International Conference*, Porto, 2008.
[46] C. Chatfield, *The Analysis of Time Series. An Introduction*, sixth ed., Texts in Statistical Science, Chapman & Hall, CRC, 2004.
[47] D.E. Newland, *An Introduction to Random Vibrations, Spectral and Wavelet Analysis*, third ed., Longman Scientific & Technical, Essex, England, 1993.
[48] P.-E. Eriksson, Vibration of Low-frequency Floors—Dynamic Forces and Response Prediction, PhD Thesis, Chalmers University of Technology, Department of Structural Engineering, Göteborg, March 1994.
[49] E. Strömmen, *Theory of Bridge Aerodynamics*, Springer, 2006.
[50] R.W. Clough, J. Penzien, *Dynamics of Structures*, second ed., Civil Engineering Series, McGraw-Hill International Editions, 1993.
[51] A. Pansera, Analisi sperimentale delle caratteristiche del cammino ed azione dei pedoni sulle passerelle pedonali (experimental analysis of gait characteristics and walking-induced actions on footbridges), BSc Thesis, University of Reggio Calabria, 2006 (in Italian).
[52] P. Terrier, V. Turner, Y. Schutz, GPS analysis of human locomotion: further evidence for long-range correlations in stride-to-stride fluctuations of gait parameters, *Human Movement Science* 24 (1) (2005) 97–115.

[53] E. Ingólfsson, Pedestrian-induced Vibrations of Line-like Structures, MSc Thesis, Department of Civil Engineering, Technical University of Denmark, June 2006.
[54] E. Ingólfsson, C. Georgakis, J. Jönsson, F. Ricciardelli, Vertical footbridge vibrations: towards an improved and codifiable response evaluation, *Third international Conference on Structural Engineering, Mechanics and Computation*, Cape Town, South Africa, 2007.
[55] E. Ingólfsson, C. Georgakis, F. Ricciardelli, L. Procino, Lateral human-structure interaction on footbridges, *Tenth International Conference on Recent Advances in Structural Dynamics*, Southampton, 2010.

Paper IV (Ingólfsson et al., 2010b)

"Lateral human-structure interaction on footbridges"

E.T. Ingólfsson, C.T. Georgakis, F. Ricciardelli & L. Procino

In proceedings: *tenth International Conference on Recent Advances in Structural Dynamics, Southampton, UK*

10th International Conference
12-14 July 2010
Southampton
RASD 2010

LATERAL HUMAN-STRUCTURE INTERACTION ON FOOTBRIDGES

E.T. Ingólfsson[1*], C.T. Georgakis[1], F. Ricciardelli[2] and L. Procino[3]

[1]Department of Civil Engineering
Technical University of Denmark
Building 118, 2800 Kgs. Lyngby, Denmark
E-mail: eti@byg.dtu.dk

[2]DIMET
University of Reggio Calabria
Via Graziella Feo di Vito, 89123 Reggio Calabria, Italy

[3]CRIACIV
University of Firenze
Via di Santa Marta 3, 50139 Firenze, Italy

Keywords: Footbridge, human-structure interaction, lateral vibration, synchronisation

ABSTRACT

In recent years, several high-profile footbridges have suffered from unexpected excessive pedestrian-induced lateral vibrations. There is a commonly accepted view that the synchronisation of pedestrians to the lateral movement of a structure is necessary for the onset of a form of instability which may lead to large lateral responses. Several recently published load models are based on this assumption. Yet, few experimental studies exist to support this hypothesis. Therefore, an extensive experimental campaign, involving 71 test subjects, has been carried out to determine the lateral forces generated by pedestrians during walking on an instrumented moving treadmill. The treadmill was driven sinusoidally in a lateral motion at various vibration frequencies and amplitudes. Visual observations made during the experiments and testimonies from the walkers, as well as subsequent analysis of video recordings, suggested that synchronisation is not as pronounced as generally believed. To confirm this, further analyses were undertaken on the walking patterns of 10 test subjects that were instrumented with waist-mounted tri-axial accelerometers. In this paper, the results from these tests are presented. The tests reveal that synchronisation is not a pre-condition for the development of large amplitude lateral vibrations on footbridges, as walking frequencies and phase angles remain largely unaffected by lateral motion at most frequencies

and amplitudes. Instead, large amplitude vibrations are the result of correlated pedestrian forces in the form of "negative damping" that can be generated at all frequencies.

1. INTRODUCTION

Pedestrian-induced lateral excitation has become a major concern in the design of footbridges, following the temporary closure of Paris' Solférino and London's Millennium footbridges in 1999 [1] and 2000 [2]. Subsequent research has revealed that numerous other bridges of different sizes and shapes are prone to similar excessive lateral vibrations when exposed to large pedestrian crowds [3]. The vibrations have often been attributed to a synchronisation between the pedestrian and the bridge, commonly denoted "lock-in" or "Synchronous Lateral Excitation" (SLE), referring to the observation that pedestrians seem to modify their gait to match the frequency and phase to that of the bridge [4, 5]. This has lead to the development of several sophisticated pedestrian load models, which rely on this assumption [6–8]. Nevertheless, there is a general dispute regarding the fundamental nature of human-structure interaction and the importance of synchronisation.

Controlled pedestrian crowd tests performed on the London Millennium Bridge in 2000 validated the observation made on the opening day, that for a certain number of pedestrians, the bridge response was limited, whereas a small increase in the number of pedestrians (beyond a critical number) often resulted in diverging lateral response [2]. An important finding from the pedestrian tests, is that the pedestrian force was strongly related to the velocity of the structure, suggesting that pedestrians act as "negative dampers" on the structure. This supports the idea that excessive lateral vibrations occur when a critical number of pedestrians produce sufficient negative damping to cancel the inherent structural damping. An equally important observation is that the vertical response of the structure at twice the modal frequency did not show any disproportionate increase, as an expected consequence of synchronised walking frequencies. Similar observations on the lack of synchronised vertical loads during excessive lateral vibrations, have been reported on other occasions [9, 10], but largely ignored in the load models that rely on synchronised stepping.

Only a few days after the closure of the Millennium Bridge, the first attempt to explain the excessive vibrations was offered by Josephson [11]: "the problem has little to do with crowds walking in step: it is connected with what people do as the try to maintain balance if the surface on which they are walking starts to move". A very simplified model was proposed by Barker [12], which demonstrates a feasible mechanism of human walking on a laterally moving surface. Surprisingly, the model produces correlated pedestrian forces (i.e. net positive energy input by the pedestrians) for an uncorrelated crowd walking at frequencies away from the vibration frequency. This idea was further developed by Macdonald [13], who produced a plausible theoretical model for predicting both velocity and acceleration proportional pedestrian loads, through the use of human balance control. The main problem with these models is that they lack experimental evidence to support and justify their applicability.

In this paper, the hypothesis that synchronisation is necessary for generating correlated pedestrian forces is put to the test, by analysing the movement of single pedestrians walking on a laterally moving treadmill at various combinations of frequencies (0.33 to 1.1 Hz) and amplitudes

(4.5 to 48 mm). Emphasis is placed on determining the correlation between the movement of a the pedestrians and that of the treadmill using a set of two tri-axial accelerometers; one mounted on the waist of the test person and one mounted on the treadmill. The results are presented and related to the lateral forces produced by the pedestrians, quantified through equivalent velocity and acceleration proportional coefficients.

2. EXPERIMENTAL STUDIES USING AN INSTRUMENTED TREADMILL

A treadmill, positioned in the laboratory of the Inter University Research Centre for Building Aerodynamics and Wind Engineering (CRIACIV) in Prato, Italy was used to measure pedestrian-induced lateral forces during walking, Fig. 1.

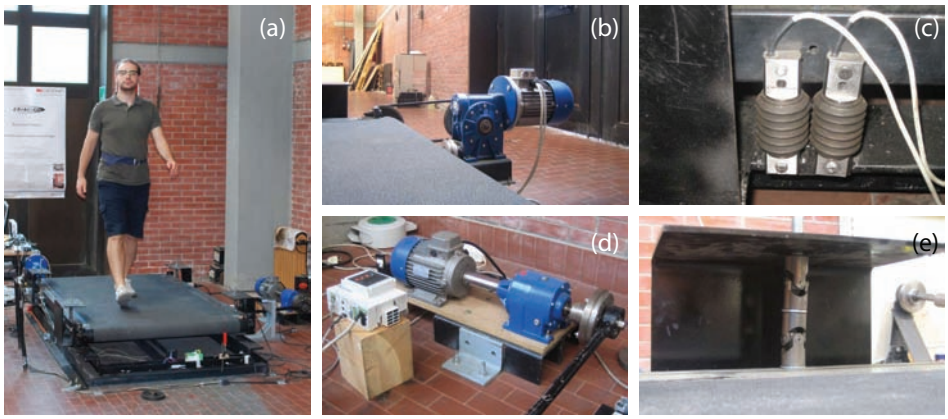

Figure 1: Picture of (a) experimental setup during a pedestrian walking tests, (b) motor for controlling belt speed, (c) motor for controlling lateral oscillation of treadmill, (d) flexural load cells and (e) low friction hinges.

The treadmill consists of three stages; stage one (the treadmill base) is fixed to the laboratory floor, stage two is a laterally driven steel frame mounted on the base through guide rails and stage three consists of the walking surface (100x180 cm). Stage three is made of a steel frame system covered with plywood panels and a rubber belt. Stage three is vertically suspended from the supporting frame (at stage 2) using low friction hinges, but also laterally supported with 4 flexural load cells ($3.7711\,\mathrm{mV/N}$). Both the motion of the belt and the lateral motion of the treadmill are driven by asynchronous $1.1\,\mathrm{kW}$ ($1.5\,\mathrm{HP}$) motors which are controlled with inverters for variable belt speed and vibration frequencies respectively. Various components of the system are shown in Fig. 1. The lateral motion of the treadmill is measured with two ICP accelerometers (PCB Piezotronics, type 393B12, $10\,\mathrm{V/g}$) and one displacement laser (sensitivity $100\,\mathrm{mV/mm}$). All signals were acquired with $\pm 5\,\mathrm{V}$ 24-Bit data acquisition modules (NI, cDAQ-9172 and NI, BNC 9234) at sampling rate $2048\,\mathrm{Hz}$.

During summer 2009, a total of seventy-one healthy volunteers (45 males and 26 females)

participated in an experimental campaign with two types of walking on the treadmill; one without lateral motion (denoted static tests) and one with lateral sinusoidal movement denoted dynamic tests). Each walker participated in one static test with a duration of 2 min and several dynamics tests of 30 s duration at various combinations of oscillation frequencies (0.33 to 1.07Hz) and displacement amplitudes (4.5 to 48 mm). Additionally, most of the tests were recorded with a digital video camera and all comments from the volunteers relating to the tests were noted. A total of 71 static tests were performed and 4883 dynamic tests, covering the total walking distance of approximately 55 km. A detailed description of the tests and a presentation of the results from the entire experimental campaign is provided elsewhere [14].

The results presented in this paper, are based on a detailed study of the walking patterns for seven test subjects, using a set of two triaxial accelerometers; one attached firmly to the waist of the test subject and one attached to the treadmill (stage two), see Fig. 2. The accelerometers, which are wireless and time synchronised, were developed for the study of crowd synchronisation at the Department of Civil Engineering of the Technical University of Denmark [15].

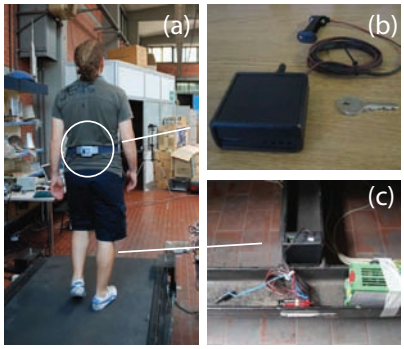

Figure 2: Pictures showing (a) Pedestrian test subject during a walking test, (b) a view of the accelerometer which is attached to the waist of the test subject and (c) the accelerometer which is attached to stage two of the treadmill.

3. ASSESSMENT OF HUMAN-STRUCTURE SYNCHRONISATION

When walking on a laterally oscillating surface, it has been postulated that people tend to spread their feet apart and change their walking frequency and phase, to match that of the floor [5]. This alleged modification of the gait due to floor oscillations has become known within the engineering community as human-structure synchronisation. According to Pizzimenti and Ricciardelli [16], synchronisation may occur if the frequency of the lateral motion approaches the walking frequency of the pedestrians, causing motion induced forces to develop at the frequency of the lateral motion.

Unlike synchronisation, (dynamic) human-structure interaction is more general and is related to the change in the pedestrian-induced loading due to bridge vibration and its potential effect on structural parameters, i.e. mass, damping and stiffness. This means, that a two-way interaction

between a pedestrian and the laterally moving structure occurs, which does not necessarily develop into synchronisation. In a situation where a pedestrian is synchronised with the structure (or locked-in), the relative phase between the motion of the treadmill and that of the pedestrian is constant, and the phase angle can be determined. On the contrary, for a non-synchronised pedestrian, the phase angle may vary in time. The instantaneous phase, $\phi_s(t)$, of a signal, $s(t)$, can be obtained as:

$$\phi_s(t) = \arctan \frac{\tilde{s}(t)}{s(t)} \tag{1}$$

where $\tilde{s}(t)$ is the Hilbert transform of $s(t)$ [17]. The phase difference between the lateral movement of the pedestrian, u, and the treadmill, x, can now be expressed trough their instantaneous phases:

$$\phi_{u,x}(t) = \phi_u(t) - \phi_x(t) \tag{2}$$

Further, a measure of the overall synchronisation is introduced through the mean phase coherence, $R_{u,x}$, defined as [17]:

$$R_{u,x} = \left| \frac{1}{N} \sum_{j=0}^{N-1} e^{i\phi_{u,x}(j\Delta t)} \right| \tag{3}$$

where Δt is the sampling interval, N is the number of samples and $i = \sqrt{-1}$. It is noted that the condition $R = 1$ is reached if and only if the time series are completely synchronised, i.e. for strict phase locking. The condition $R = 0$ is obtained for a uniform distribution of phases, [17].

In Fig. 3, a characteristic example of the results from a pedestrian walking test is shown. In this particular test, the lateral vibration amplitude is fixed at $x_0 = 10$ mm and the frequency of the lateral motion of the treadmill is gradually increased from 0.33 to 1.07 Hz in 17 increments. In each increment, a measurement of 30 s duration is recorded. This is illustrated in Fig. 3 (a) and (b), showing the recorded lateral acceleration time histories of the treadmill, $\ddot{x}$, and that of the walker's body, $\ddot{u}$. In Fig. 3 (c) the instantaneous phases between the treadmill and the body are shown as a function of time, where it is noted that the frequency of the lateral motion increases gradually, whereas the frequency of the body sway is near constant. For comparison, the pedestrian walking frequency as measured in the static test, is shown with a dashed line. As illustrated in this particular experiment, and generally observed in all the tests, the frequency of the body sway is (near) constant during the entire test session, suggesting a limited effect of the treadmill motion on the walking frequency. In Fig. 3 (d) the instantaneous phase difference, $\varphi_{\ddot{u},\ddot{x}}$, between $\ddot{u}$ and $\ddot{x}$ is shown as a function of time and in Fig. 3, (e) the corresponding mean phase coherence, $R_{\ddot{u},\ddot{x}}$, is shown. At low vibration frequencies $R_{\ddot{u},\ddot{x}}$ is negligible and the phase variation occurs quickly due to the large difference between the two frequencies. As the lateral vibration frequency approaches the walking frequency, the phase change is slower and $R_{\ddot{u},\ddot{x}}$ increases. Similarly, as the lateral vibration frequency increases beyond the walking frequency, $R_{\ddot{u},\ddot{x}}$ decreases again. When the walking frequency matches the lateral oscillation frequency of the treadmill, $R_{\ddot{u},\ddot{x}}$ is almost unity and the level of the instantaneous phase difference does not

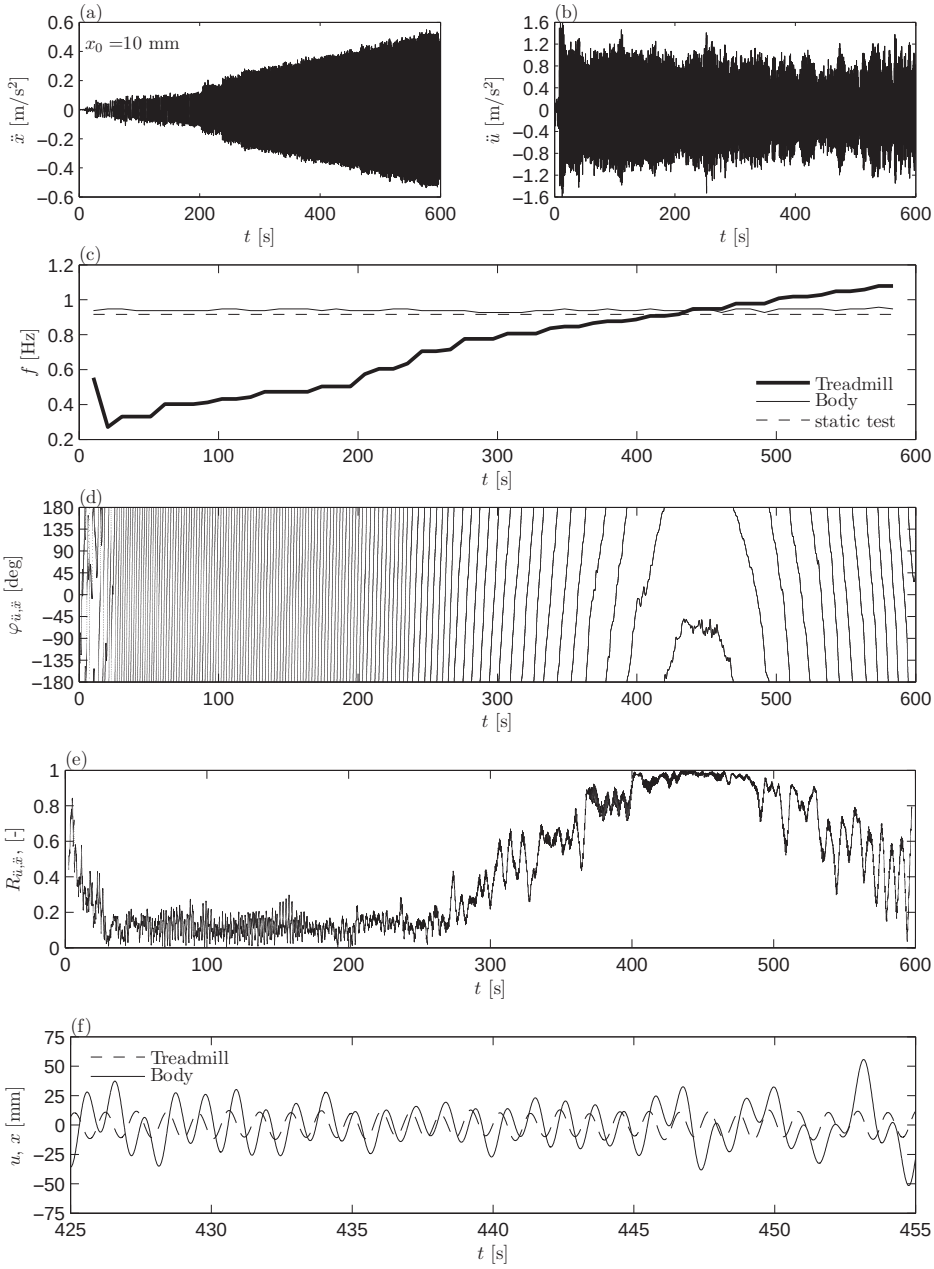

Figure 3: Results from a walking test with $x_0 = 10$ mm showing (a) lateral acceleration of the treadmill, $\ddot{x}$, and (b) lateral acceleration of the walker's waist, $\ddot{u}$, (c) instantaneous phase of $\ddot{x}$ and $\ddot{u}$, (d) instantaneous phase difference, (e) mean phase coherence and (f) displacement time-histories of u and x.

drift; although the phase does not remain strictly constant. In Fig. 3 (f), the lateral displacement, obtained through numerical integration of the measured acceleration, of both the treadmill and the body is shown during a time period where the walking frequency is close to the lateral vibration frequency. Although the mean phase coherence is large, the movement of the pedestrian is not perfectly synchronised to the movement of the treadmill, instead there is considerable amplitude and phase variation.

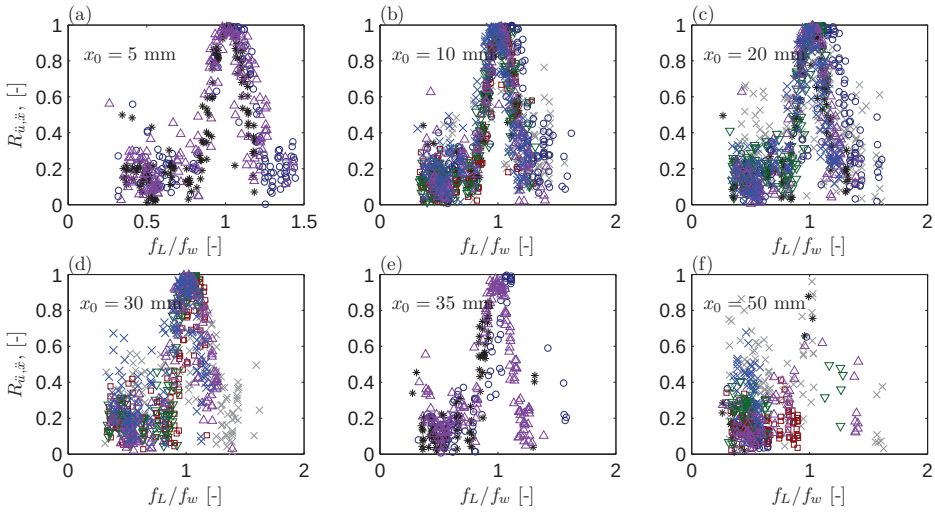

Figure 4: Mean phase coherence as function of the normalised frequency for different lateral vibration amplitudes. Each marker type represents one pedestrian.

The observations leading from the analyses of the characteristic example can be assumed generic, as they remain unchanged for all the test subjects, i.e. the mean phase coherence is low when the lateral vibration frequency is away from the normal walking frequency of the pedestrian and increases gradually as the two frequencies approach each other. This also implies that the walking frequency is dominated by the preferred walking frequency of the pedestrian rather than the oscillation of the treadmill. In Fig. 4, the mean phase coherence is shown as a function of the normalised frequency, where this effect is clearly illustrated. It is also noted that in a small frequency range (approximately $f_L/f_w \in [0.9; 1.1]$), the mean coherence is large ($R_{\ddot{u},\ddot{x}} > 0.9$) and therefore human-structure synchronisation might develop in this range. Even though, a large phase coherence is necessary, it is not a sufficient condition for synchronisation. A large phase coherence can be the result of a pedestrian walking naturally at a frequency that happens to match that of the motion and which can be attributed to chance rather than synchronisation. The mean phase coherence can thereby be used to determine the range for which human-structure synchronisation can occur.

The results presented in Fig. 3 and Fig. 4 relate to the correlation between the movement of the walker's waist and that of the treadmill. It should be noted, though, that during the tests

the lateral ground reaction force generated by the pedestrians was also measured. In Fig. 5 (a), the lateral force measured during a 30 s time interval is shown for the same walker used in the characteristic example above. This corresponds to the time interval with the maximum phase coherence ($x_0 = 10\,\text{mm}$, $f_L/f_w \cong 1$). During this test, the pedestrian-induced lateral force is found to be in almost complete anti-phase (180 degrees) with the lateral displacement, which essentially means that when the treadmill is at its mid-position and moving to the right, the person puts his or her left foot on the ground. Similarly, when the treadmill is at its mid-position and moving to the left, the person puts his or her right foot on the ground. The external force produced by the pedestrian is thereby in phase with the acceleration of the treadmill and can be treated as an additional (negative) inertial force which reduces the overall modal mass of the structure which the pedestrian occupies. Similarly, if the pedestrian puts his foot (left or right) to the ground when the velocity is zero (i.e. at maximum displacement amplitude), the pedestrian force is proportional to the structural damping, positive or negative, depending on the sign of the acceleration. In the general case however, the instantaneous phase and/or amplitude is variable (as illustrated in Fig. 5 (b)) and the pedestrian induced force cannot readily be classified as added inertia or damping. Instead, a deterministic quantification is only possible in terms of equivalent forces.

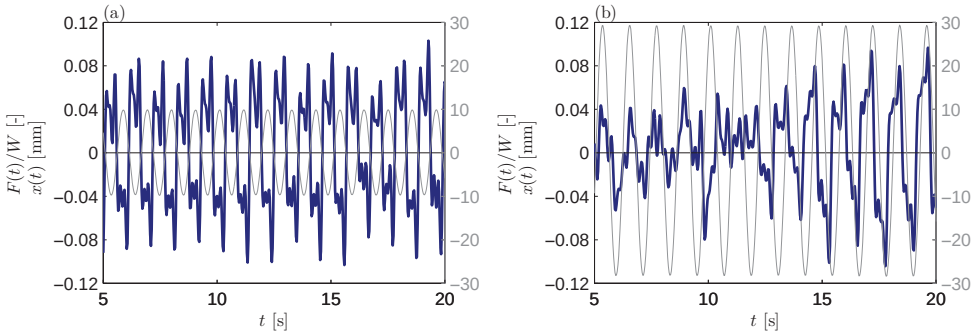

Figure 5: Two different examples of measured time-histories of the pedestrian-induced lateral force shown with the lateral displacement of the treadmill.

4. EQUIVALENT PEDESTRIAN DAMPING AND INERTIAL FORCE

As proposed by Ingólfsson et al. [14], an equivalent damping force, $F_{D,eq}(t)$, proportional to the velocity of the treadmill and an equivalent inertia force, $F_{I,eq}(t)$, proportional to its acceleration are therefore defined as:

$$F_{D,eq}(t) = c_p \dot{x}(t) = c_p \dot{x}_0 \sin(\omega_L t + \varphi) \tag{4}$$

$$F_{I,eq}(t) = \varrho_p m_p \ddot{x}(t) = \varrho_p m_p \ddot{x}_0 \sin(\omega_L t + \varphi + \pi/2) \tag{5}$$

where $\dot{x}_0$ and $\ddot{x}_0$ are the velocity and acceleration amplitudes of the treadmill respectively and φ is an arbitrary phase. The average work done per time unit of the damping force upon a harmonic

displacement at the same frequency and phase is $P_{D,eq} = 1/2 c_p \dot{x}_0^2$. The velocity proportional constant, c_p, is now obtained by imposing that the pedestrian load inputs the same energy per unit time, P_F, as that of the equivalent load. The average work, P_F, is obtained through convolution of the measured pedestrian-induced lateral force and the treadmill velocity:

$$P_F = \frac{1}{T_{tot}} \int_0^{T_{tot}} F(t)\dot{x}(t)\ \mathrm{d}t \tag{6}$$

where T_{tot} is the duration of a pedestrian test. The portion of the total pedestrian mass, $\varrho_p m_p$, that contributes to added mass on the structure is determined through convolution of the pedestrian force and the acceleration of the structure. Thus, c_p and $\varrho_p m_p$ are now obtained as:

$$c_p = \frac{2}{\dot{x}_0^2} \frac{1}{T_{tot}} \int_0^{T_{tot}} F(t)\dot{x}(t)\ \mathrm{d}t = \frac{2\mathrm{Cov}\left[F(t), \dot{x}(t)\right]}{\dot{x}_0^2} \tag{7}$$

$$\varrho_p m_p = \frac{2}{\ddot{x}_0^2} \frac{1}{T_{tot}} \int_0^{T_{tot}} F(t)\ddot{x}(t)\ \mathrm{d}t = \frac{2\mathrm{Cov}\left[F(t), \ddot{x}(t)\right]}{\ddot{x}_0^2} \tag{8}$$

where Cov[ ] is a covariance operator.

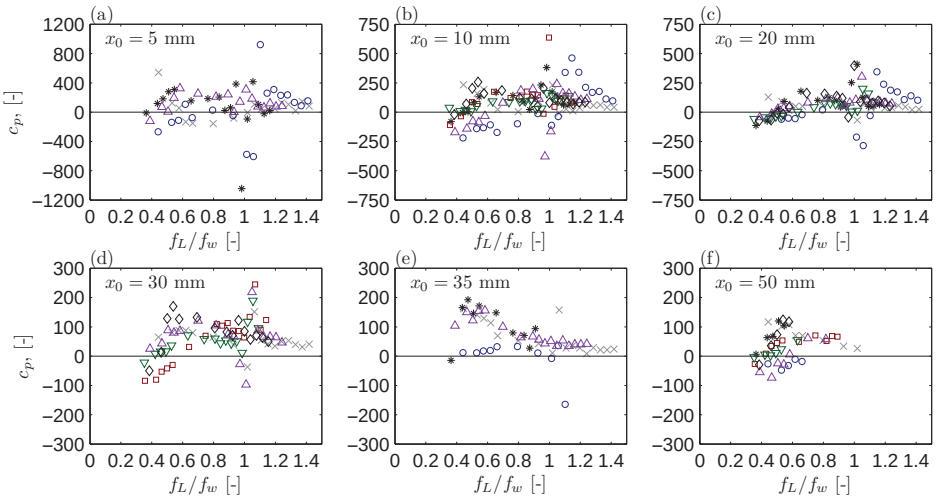

Figure 6: Velocity proportional load coefficient, c_p, as a function of the normalised frequency for different lateral vibration amplitudes. Each marker type represents one pedestrian.

In Fig. 6 the velocity proportional coefficients, obtained from the analyses of the walking patterns of the test pedestrians, are shown. For most frequencies and amplitudes, the pedestrian

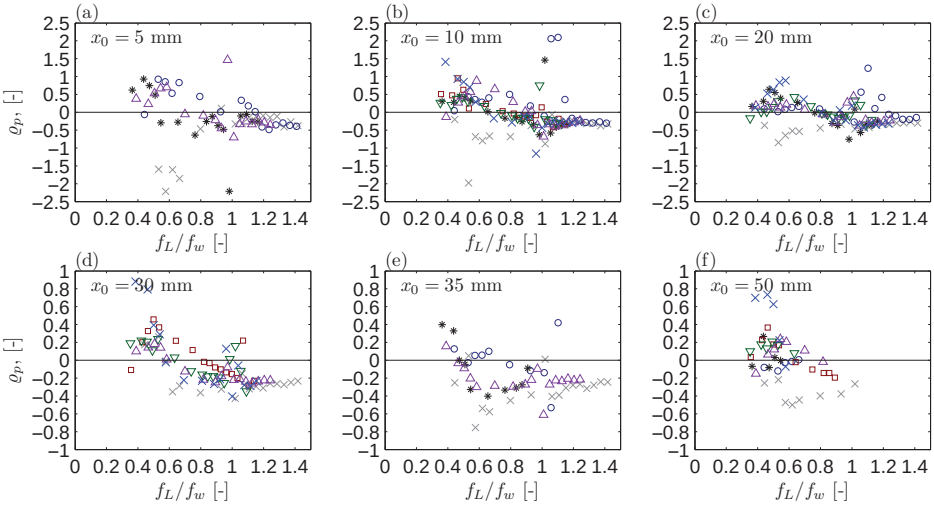

Figure 7: Acceleration proportional load coefficient, ϱ_p, as a function of the normalised frequency for different lateral vibration amplitudes. Each marker type represents one pedestrian.

load coefficient is positive, suggesting that pedestrians generally act as negative dampers. In particular, it is interesting to note that this is not only true at the frequency range with a large mean phase coherence, but throughout the frequency range. This suggests that the synchronisation of the lateral movement of the body to the motion of a bridge is not a necessary condition for the generation of forces proportional to the lateral velocity, which could potentially cause negative structural damping on a bridge. This has indeed been suggested before, [3, 10, 12, 13], but to the authors' knowledge, not yet been verified experimentally under controlled conditions. In Fig. 7, the mass proportional coefficient, ϱ_p, is shown as a function of normalised frequency, for varying vibration amplitudes. Generally, ϱ_p is positive in the low frequency region, but at higher frequencies it is mostly negative.

The results presented in Fig. 6 and Fig. 7 also indicate that the phase coherence is important and in the frequency range around $f_L/f_w \cong 1$, large values of c_p occur, although these may obtain both positive and negative values. This suggests that, when the phase angle between the pedestrian and the structure is (near) constant, the covariance is larger and thereby the potential for large numerical values of c_p increases. In this case, the nature of the synchronisation (i.e. the timing of the footstep compared to the movement of the treadmill) decides the phase angle between the pedestrian induced load and the structural movement and thereby whether the pedestrian adds to, or decreases the overall structural damping and modal mass.

5. CONCLUSIONS

In this paper, the hypothesis that synchronisation is necessary for generation of correlated pedestrian forces (and thus large amplitude lateral footbridge vibrations) has been tested, by analysing

the movement of seven pedestrians walking on a moving treadmill. The movement of the pedestrians and their correlation with the motion of the treadmill was analysed using a set of two tri-axial accelerometers; one attached to the waist of each walker and one attached to the treadmill. After a detailed analysis of the movement of the pedestrians some general conclusions can be made:

1. A large phase coherence between pedestrian and bridge motion can only be obtained when the frequency of the lateral motion is close to the natural pedestrian walking frequency (as measured on a fixed treadmill). Since a large mean-phase coherence is a necessary condition for synchronisation, it can be concluded that the pedestrian walking frequency and phase angle are largely unaffected by the lateral movement of the treadmill and that synchronisation can only occur when the relationship between the normal walking frequency and the vibration frequency is near unity. However, negative damping from the pedestrians was observed over nearly the entire frequency range, indicating that synchronisation is not a necessary pre-condition for initiation of excessive lateral vibrations.

2. Models of pedestrian loading that rely solely on human-structure phase-synchronisation are therefore insufficient, particularly for structural frequencies away from the the first load harmonic. Furthermore, the scatter in the equivalent lateral forces obtained from the tests suggests that the pedestrian-induced loading is governed by randomness. Therefore, a probabilistic approach that relies on experimentally obtained forces and takes into account the randomness in the loading, seems necessary for an accurate estimation of the susceptibility of a footbridge to excessive lateral vibrations.

6. ACKNOWLEDGEMENTS

The authors gratefully acknowledge Niccoló Bonanni, graduate student at University of Firenze for his substantial contribution and enthusiasm in recruiting test persons for the experiments. Further, the authors also thank the people who participated in the experiments presented in this study.

REFERENCES

[1] P. Dziuba, G. Grillaud, O. Flamand, S. Sanquier, and Y. Tétard. La passerelle Solférino comportement dynamique. *Bulletin Ouvrages Métalliques*, 1:34–57, 2001. (in French).

[2] P. Dallard, A.J. Fitzpatrick, A. Flint, S.Le. Bourva, A. Low, R.M. Ridsdill-Smith, and M. Willford. The London Millennium Footbridge. *The Structural Engineer*, 79(22):17–33, 2001.

[3] J. Brownjohn, S. Zivanovic, and A. Pavic. Crowd dynamic loading on footbridges. In *Proceedings of Footbridge 2008, Third International Conference*, Porto, July 2008.

[4] Y. Fujino, B.M. Pacheco, S.I. Nakamura, and P. Warnitchai. Synchronization of human walking observed during lateral vibration of a congested pedestrian bridge. *Earthquake Engineering & Structural Dynamics*, 22(9):741–758, 1993.

[5] A. McRobie, G. Morgenthal, J. Lasenby, and M. Ringer. Section model tests on human-structure lock-in. *Proceedings of ICE: Bridge Engineering*, 156(BE2):71–79, 2003.

[6] B. Eckhardt, E. Ott, S.H. Strogatz, D.M. Abrams, and A. McRobie. Modeling walker synchronization on the Millennium Bridge. *Physical Review E*, 75, 2007.

[7] F. Venuti, L. Bruno, and P. Napoli. Pedestrian lateral action on lively footbridges: A new load model. *Structural Engineering International*, 17:236–241, 2007.

[8] J. Bodgi, S. Erlicher, P. Argoul, O. Flamand, and F. Danbon. Crowd structure synchronization: coupling between eulerian flow modeling and Kuramoto phase equation. In *Proceedings of Footbridge 2008, Third International Conference*, Porto, July 2008.

[9] J.M.W. Brownjohn, P. Fok, M. Roche, and P. Omenzetter. Long span steel pedestrian bridge at Singapore Changi airport - part 2: Crowd loading tests and vibration mitigation measures. *The Structural Engineer*, 82(16):28–34, 2004.

[10] J.H.G. Macdonald. Pedestrian-induced vibrations of the clifton suspension bridge, uk. *Proceedings of ICE: Bridge Engineering*, 161(BE2):69–77, 2008.

[11] Out of step on the bridge. The Guardian, Wednesday 14 June 2000.

[12] C. Barker. Some observations on the nature of the mechanism that drives the self-excited lateral response of footbridges. In *Proceedings of Footbridge 2002, First International Conference*, Paris, November 2002.

[13] J.H.G. Macdonald. Lateral excitation of bridges by balancing pedestrians. *Proceedings of the Royal Society A*, 465:1055–1073, 2009.

[14] E.T. Ingólfsson, C.T. Georgakis, F. Ricciardelli, and J. Jönsson. Experimental identification of pedestrain-induced lateral forces on footbridges. Submitted to Journal of Sound and Vibration, 2010.

[15] R.K. Andersen. Pedestrian-induced vibrations: Human-human interaction. MSc thesis, Department of Civil Engineering, Technical University of Denmark, 2009.

[16] A.D. Pizzimenti and F. Ricciardelli. Experimental evaluation of the dynamic lateral loading of footbridges by walking pedestrians. In *Proceedings of the 6th International Conference on Structural Dynamics*, Paris, 2005.

[17] F. Mormann, K. Lehnertz, P. David, and C.E. Elger. Mean phase coherence as a measure for phase synchronization and its application to the EEG of epilepsy patients. *Physica D*, 144:358–369, 2000.

Paper V (Ingólfsson and Georgakis, 2011)

"A stochastic load model for pedestrian-induced lateral forces on footbridges"

E.T. Ingólfsson, C.T. & Georgakis

In press: *Engineering Structures*

ARTICLE IN PRESS

Engineering Structures ▮ (▮▮▮▮) ▮▮▮–▮▮▮

Contents lists available at ScienceDirect

Engineering Structures

journal homepage: www.elsevier.com/locate/engstruct

A stochastic load model for pedestrian-induced lateral forces on footbridges

E.T. Ingólfsson *, C.T. Georgakis

Department of Civil Engineering, Technical University of Denmark, Building 118, Brovej, 2800 Kgs. Lyngby, Denmark

ARTICLE INFO

Article history:
Received 13 December 2010
Received in revised form
19 June 2011
Accepted 1 July 2011
Available online xxxx

Keywords:
Footbridges
Lateral vibration
Load model
Stochastic
Pedestrian

ABSTRACT

In the past decade, several researchers have studied the phenomenon of excessive pedestrian-induced lateral vibrations and full-scale measurements of various bridges under crowd loading have been carried out. These tests have verified the existence of a form of instability for which a transition between limited and excessive lateral vibrations occurs for a small increase in the number of people occupying the bridge. This disproportionate increase in the lateral vibration amplitude is caused by a dynamic interaction between the pedestrian and the laterally moving structure, although the governing mechanism which generates the load is still somewhat disputed.

Theoretical work has also been undertaken, but unlike current codes of practice and design guidelines, which are primarily based on the empirical full-scale observations, many of the theoretical hypotheses lack the proper experimental evidence to support their applicability. Recently, an extensive experimental campaign was carried out, in which the lateral forces generated by pedestrians during walking on a laterally moving treadmill were determined for various combinations of lateral frequencies (0.33–1.07 Hz) and amplitudes (4.5–48 mm). It was shown that large amplitude vibrations are the result of correlated pedestrian forces in the form of "negative damping", with magnitudes that depend on the relationship between the pacing frequency and the frequency of the lateral movement.

Herewith, a novel stochastic load model for the frequency and amplitude dependent pedestrian-induced lateral forces is presented. The lateral forces are modelled as a sum of an "equivalent static force" and "motion-induced" (or self-excited) forces which are quantified through equivalent pedestrian damping and mass coefficients. The parameters in the model are based directly on measured lateral forces from a large group of pedestrians. Thereby, the model is currently the most statistically reliable analytical tool for modelling of pedestrian-induced lateral vibrations. Through simplified numerical simulations, it is shown that the modal response of a footbridge subject to a pedestrian crowd is sensitive to the selection of the pacing rate distribution within the group, the magnitude of ambient wind loads and the total duration of the load event. In a particular simulation, the selection of these parameters ultimately affects the critical number of pedestrians needed to trigger excessive vibrations. Finally, as an example, it is shown that the prediction of the critical number of pedestrians matches well with observations made during the opening of the London Millennium Bridge.

1. Introduction

In long-span footbridges, the possibility of excessive pedestrian-induced lateral vibrations is a serious threat to the design and therefore provisions for the installation of mechanical damping devices and full scale dynamic testing has become an integrated part of their design process [1–3]. As the bridge spans increase, the avoidance of crowd-induced lateral vibrations becomes more difficult and the necessary amount of additional damping easily exceeds the limit of what is practically possible or economically acceptable [4]. In some cases, this means that modifications in the initial structural layout may be necessary, e.g. to provide additional horizontal stiffness. Alternatively, an informed decision can be made to accept that excessive lateral vibrations may occasionally occur. In this case dampers may be avoided or introduced to provide the minimum amount of damping needed to avoid the problem on a daily basis. This strategy was adopted for the newly built Tri-Country arch footbridge in Weil-am-Rhein in Germany, which features a record breaking clear span of 230 m [5]. Shortly after its opening, full scale pedestrian tests were carried out, in which the possibility of excessive lateral vibrations was verified. However, the conditions under which excessive vibrations occurred were associated with a large crowd density with a low probability of occurrence and hence no dampers were installed [5].

For design purposes, a successful implementation of this strategy, relies on an accurate representation of the pedestrian-induced load and the criterion for the number of pedestrians needed to trigger excessive lateral vibrations. However, current state-of-the-art guidelines [6–10] offer only a limited insight into this field, as they are primarily based on empirical observations

* Corresponding author. Tel.: +45 4525 1766; fax: +45 4588 3282.
E-mail address: eti@byg.dtu.dk (E.T. Ingólfsson).

0141-0296/$ – see front matter © 2011 Elsevier Ltd. All rights reserved.
doi:10.1016/j.engstruct.2011.07.009

Please cite this article in press as: Ingólfsson ET, Georgakis CT. A stochastic load model for pedestrian-induced lateral forces on footbridges. Engineering Structures (2011), doi:10.1016/j.engstruct.2011.07.009

Nomenclature

α	coefficient of a stochastic process
β	coefficient of a stochastic process
δ	Dirac delta function
Δf	frequency resolution
Δt	time separation
ζ_{CL1}	modal damping ratio for the fundamental lateral vibration mode of the London Millennium Bridge
ζ_n	modal damping for mode n
ζ_{tot}	overall modal damping ratio, modified by the self-excited force
θ_0	fitting parameters in stochastic load model
θ_1	fitting parameters in stochastic load model
θ_2	fitting parameters in stochastic load model
θ_3	fitting parameters in stochastic load model
μ_{c_p}	sample mean of the velocity proportional pedestrian load coefficient
μ_{DLF_j}	average DLF of load harmonic j
μ_{f_w}	mean loading frequency (gait cycle frequency)
μ_{W_p}	mean body weight
ξ_j	parameter in the lognormal distribution
ρ	linear correlation coefficient
ϱ_p	acceleration proportional pedestrian load coefficient
σ	standard deviation
Σ_{nm}	covariance structure
σ_{DLF_j}	standard deviation of DLF of load harmonic j
$\tilde{\sigma}^2_{F,j}$	area of the PSD of F around load harmonic j
σ_{f_w}	standard deviation of the loading frequencies (gait cycle frequencies)
σ_{W_p}	standard deviation of body weights
τ	time separation variable
ϕ_0	fitting parameters in stochastic load model
ϕ_1	fitting parameters in stochastic load model
ϕ_2	fitting parameters in stochastic load model
ϕ_3	fitting parameters in stochastic load model
Φ_n	mode shape for mode n
χ_j	parameter in the lognormal distribution
ψ	arbitrary phase angle
ω_c	coefficient of a stochastic process
ω_n	modal frequency for mode n
A_j	fitting parameter in a spectral load model
B_j	fitting parameter in a spectral load model
c	damping per unit length
c_p	velocity proportional pedestrian load coefficient
DLF_j	dynamic load factor of load harmonic j
EI	bending stiffness
F	pedestrian-induced lateral load
f	frequency
f_0	frequency of lateral vibration
f_{CL1}	natural frequency of the fundamental lateral vibration mode of the London Millennium Bridge
F_j	pedestrian-induced lateral force for the jth load harmonic
F_p	pedestrian-induced lateral load
f_p	pacing frequency
F_{st}	equivalent static pedestrian-induced lateral force
f_w	fundamental loading frequency (gait cycle frequency) $f_w = f_p/2$
g	acceleration of gravity 9.82 m/s^2
L	bridge length
l_s	pedestrian step length
m	bridge mass per unit length
M_n	modal mass of mode n
m_p	pedestrian body mass
M_{tot}	overall modal mass, modified by the self-excited force
N	total number of data points
N_{cr}	critical number of pedestrians
N_{Harm}	total number of load harmonics
N_p	number of pedestrians on the bridge
p	probability density function
p_n	modal load for mode n
Q	general load function
q_0	amplitude of modal displacement
q_n	modal displacement for mode n
R	autocorrelation
$S_{F,j}$	PSD of F around load harmonic j
S_F	PSD of F
t	time
t_0	pedestrian arrival time onto the bridge
t_d	pedestrian passage time
T_{tot}	total duration of a time series
u	lateral displacement
u_0	lateral displacement amplitude
v_p	forward walking speed
w	an independent standard Gaussian variable
W_p	pedestrian body weight
X	stochastic parameter
x	space variable
Y	stochastic parameter

from a limited number of pedestrian crowd tests carried out in the beginning of the new Millennium, following the temporary closures of both the Solferino bridge in Paris [11] and later the London Millennium Bridge [12].

Research in this field can generally be split into three categories, (i) full-scale measurements of existing bridges subjected to crowd induced loading, (ii) experimental investigations of single pedestrians under controlled (laboratory) circumstances and (iii) mathematical modelling of the pedestrian-induced lateral load. As reviewed by Ingólfsson [3], a significant amount of research has been carried out in each of the three categories, but there is a missing link which interconnects them, particularly between the mathematical models on one side and actual field observations on the other.

As an example, excessive lateral vibrations have often been attributed to human–structure synchronisation, referring to the observation that pedestrians seem to modify their gait to match the frequency and phase to that of the bridge [13,14]. This has led to the development of several pedestrian loading models, which rely on this assumption [15–18]. In the French design guidelines [8], an acceleration criterion which defines the transition between random and synchronised pedestrian walking is provided (as 0.1–0.2 m/s^2). Nevertheless, there is a general dispute regarding the fundamental nature of human–structure interaction and the importance of synchronisation. To the best of the authors' knowledge, none of the full scale tests that have been carried out to date, have been able to verify the assumption that pedestrians synchronise their walking frequency and phase to that of the laterally moving surface. On the contrary, many researchers have questioned the necessity of phase synchronisation [19–21] and recently Ingólfsson et al. [22] showed that synchronisation of pedestrians is not a necessary condition for the development of excessive pedestrian-induced vibrations.

It has been proposed that nonlinear coupling (autoparametric resonance), in which vertical or torsional modes predominantly excited by vertical forces can cause autoparametric resonance in

Please cite this article in press as: Ingólfsson ET, Georgakis CT. A stochastic load model for pedestrian-induced lateral forces on footbridges. Engineering Structures (2011), doi:10.1016/j.engstruct.2011.07.009

lateral vibration modes. This would occur for vertical load amplitudes larger than a certain threshold, provided that the ratio between the natural frequencies of the lateral and vertical vibration modes are related through an integer number (e.g. 1:2) [23,24]. Piccardo and Tubino [25] presented a load model for which a portion of the lateral load was written as the product of a sinusoidal loading term (with frequency equals half the pacing frequency) and the lateral displacement of the bridge. This displacement proportionality is a nonlinear phenomenon which can cause excitation of vibration modes at frequencies other than that of the sinusoidal loading term. The model was used to demonstrate that lower frequency modes, e.g. the fundamental mode of the London Millennium Bridge at 0.5 Hz, can be excited from walking at the frequency 1 Hz. Both models are purely theoretical and lack experimental evidence to support and justify their applicability. The displacement proportional load in the model of Piccardo and Tubino [25] is based on experimental observations [26,27] in which it was shown that the amplitude of the pedestrian-induced load increases linearly with the displacement amplitude. However, this does not justify the multiplication of the two time histories upon which the model is based.

Macdonald [28], proposed that the lateral ground reaction force (GRF) from the pedestrians could be modelled as the support force of an inverted and actively controlled pendulum, which is representative of the movement of the pedestrians' centre of mass. He argued that, instead of the timing of the footstep, the placement of the foot is affected by the lateral motion of the underlying surface. A simple benchmark test was used to verify that self-excited forces in the form of negative damping could be developed when the model was applied on a laterally moving surface, even at frequencies different from half the assumed pacing frequency. The model is appealing in that it is based on a feasible mechanical model where the GRFs match qualitatively well to measurements for a stationary surface. However, further justification for the selection of particular modelling parameters, e.g. the balance control scheme, is needed to verify the general applicability of the model and to include the randomness associated with human walking.

Motivated by the general lack of statistically reliable data, an extensive experimental campaign was carried out by Ingólfsson et al. [29], to determine the lateral forces generated by pedestrians during walking on a laterally moving treadmill at different combinations of lateral vibration frequencies and amplitudes.

In this paper, a novel time-domain load model is presented for the frequency and amplitude dependent pedestrian-induced lateral forces. The model is presented in a stochastic framework and is based on an in-depth quantitative analysis of the experimental data collected by Ingólfsson et al. [29]. Despite its probabilistic nature, the load model is simple in that the load is represented through its Power Spectral Density (PSD) as measured in the absence of lateral motion, whereas the pedestrian–structure interaction is taken into account through velocity and acceleration proportional loads. These motion-induced pedestrian loads thereby act to increase or decrease the modal damping and mass of the structure. The application of the load model is demonstrated through numerical response simulations, and the sensitivity of various input parameters, as well as its capability to predict excessive footbridge vibrations are discussed.

2. Time-domain load model for pedestrian-induced lateral vibrations

Conveniently, the pedestrian-induced lateral force can be divided into two different components: an equivalent static force, centred at frequency f_w and its integer harmonics and one which occurs at the frequency of the lateral motion, denoted the "self-excited force". The frequency f_w is related to the gait cycle duration and represents the frequency of two nominally identical events in the walking process [30]. Thereby, $f_w = f_p/2$, where f_p is the pedestrian pacing rate (or step frequency). The equivalent static force represents the lateral force exerted by a pedestrian on a rigid surface, whereas the motion-induced loads are those attributed to the movement of the structure. This subdivision of the force is commonly used in the field of wind engineering [31], but was first used to describe pedestrian-induced loading of footbridges by Pizzimenti and Ricciardelli [32]. The self-excited force is due to an interaction between the pedestrian and the laterally moving structure and can be further subdivided into two orthogonal components, one in phase with the velocity, $\dot{u}$, and the other in phase with the acceleration, $\ddot{u}$, of the structure. By treating the motion-induced portion of the load as velocity and inertia proportional loads, the total pedestrian-induced lateral load, $F(t)$, can be written as the equivalent static force plus the additional equivalent damping and inertia forces respectively:

$$F(t) = F_{st}(t) + \underbrace{c_p\,(f_0/f_w, u_0)\cdot\dot{u}}_{\text{equivalent damping}} + \underbrace{m_p\varrho_p\,(f_0/f_w, u_0)\cdot\ddot{u}}_{\text{equivalent inertia}}. \quad (1)$$

The functions $c_p\,(f_0/f_w, u_0)$ and $\varrho_p\,(f_0/f_w, u_0)$ define the self-excited forces and depend on the vibration frequency, f_0, the gait cycle frequency, f_w, and the displacement amplitude, u_0. The function $F_{st}(t)$ represents the time history of the equivalent static force, modelled as a narrow-band random process, centred at frequency f_w and m_p is the pedestrian body mass.

2.1. Equivalent static force

Due to the repetitive and near-harmonic nature of the pedestrian-induced forces, they are often approximated as a sum of perfectly periodic harmonic contributions, i.e. as a truncated Fourier series [16,33]. As discussed by Ingólfsson et al. [29], the intra-subject variability in the measured footfall forces makes a deterministic and perfectly periodic representation of the load only possible through equivalent load amplitudes that depend on the structural damping. This damping dependency of the equivalent load amplitude makes the perfectly periodic model unsuitable in a general load model.

Instead the pedestrian-induced load can be represented in the frequency domain directly through its PSD. Pizzimenti and Ricciardelli [32] suggested that a Gaussian shaped function can be used to fit the individual load harmonics of the PSD. Herewith, a similar version is proposed, where the function, $S_{F,j}(f)$, represents the fitted PSD around load harmonic j, i.e.:

$$\frac{S_{F,j}(f)\cdot f}{\tilde{\sigma}^2_{F,j}} = \frac{2A_j}{\sqrt{2\pi}B_j}\exp\left\{-2\left[\frac{f/(jf_w)-1}{B_j}\right]^2\right\}. \quad (2)$$

The parameters A_j and B_j are determined by the data fit and $\tilde{\sigma}^2_{F,j}$ is the area of the PSD around the jth harmonic. This formulation is similar to that proposed by Vickery and Clark [34] to fit the spectrum of generalised lift force, as used in wind engineering models of vortex excitation.

In Fig. 1, the experimentally obtained PSDs are shown as functions of the normalised frequency, $f/(jf_w)$, together with the average spectrum for each of the first five load harmonics, ($j = 1, \ldots, 5$).

The fitted PSDs using the expression in Eq. (2) are also shown in Fig. 1 for the first five load harmonics. The parameters A_j and B_j were determined through a nonlinear least square fit and represent the average shape of the PSD. The variance $\tilde{\sigma}^2_{F,j}$, which is a measure of the overall energy content in the load process, can be taken such that it represents a certain probability of exceedance, depending on the particular situation.

Please cite this article in press as: Ingólfsson ET, Georgakis CT. A stochastic load model for pedestrian-induced lateral forces on footbridges. Engineering Structures (2011), doi:10.1016/j.engstruct.2011.07.009

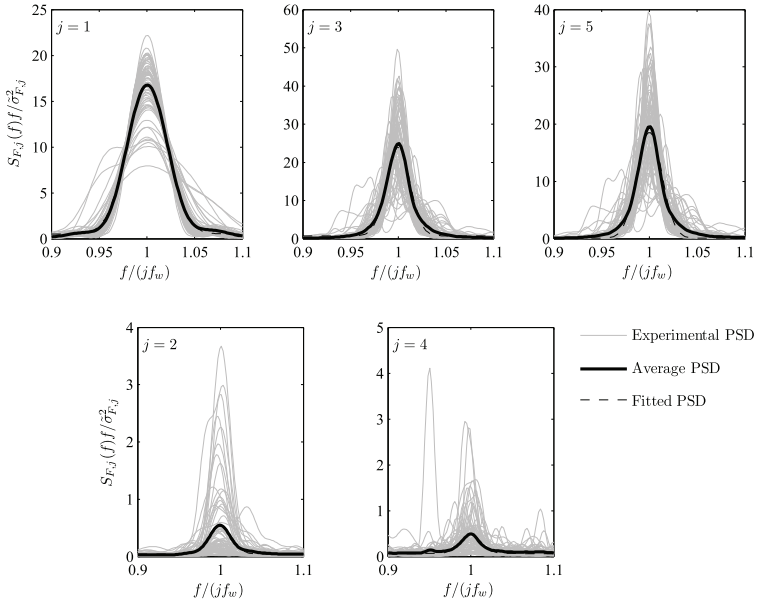

Fig. 1. Experimental PSD (obtained as the average of seven 50% overlapping rectangular windows, zero-padded to obtain the desired resolution) of the first five load harmonics for each pedestrian shown with the average PSD for all pedestrians and the fitted Gaussian shaped spectrum.

Ingólfsson et al. [29] showed that the probability distribution of the body weight normalised variance (expressed through equivalent perfectly periodic DLF_j) of load harmonic j, can be modelled through a log-normal distribution with the following probability density function:

$$p(\mathrm{DLF}_j) = \frac{1}{\mathrm{DLF}_j\,\xi_j\sqrt{2\pi}}\exp\left[-\frac{\left[\ln \mathrm{DLF}_j - \chi_j\right]^2}{2\xi_j^2}\right]. \quad (3)$$

The parameters χ_j and ξ_j are related to the sample mean, μ_{DLF_j}, and variance, $\sigma^2_{\mathrm{DLF}_j}$, so that

$$\chi_j = \ln \mu_{\mathrm{DLF}_j} - \frac{1}{2}\ln\left(1+\frac{\sigma_{\mathrm{DLF}_j}}{\mu^2_{\mathrm{DLF}_j}}\right), \qquad \xi_j^2 = \ln\left(1+\frac{\sigma_{\mathrm{DLF}_j}}{\mu^2_{\mathrm{DLF}_j}}\right). \quad (4)$$

The variance of the load can then be obtained from the DLF as $\tilde{\sigma}^2_{F,j} = W_p^2\mathrm{DLF}_j^2/2$, where W_p is the pedestrian body weight. In Fig. 2, the experimentally obtained cumulative probability of DLF_j is shown for the first five load harmonics together with fitted cumulative distribution functions (CDFs).

The pedestrian body weight, W_p, is generally a random variable, with a probability distribution that depends on the particular population to be modelled. No significant correlation between the body weight and the DLF has been reported. Therefore, these quantities can be treated as independent random variables when modelling the pedestrian-induced load. The fitting parameters A_j and B_j as well as the lognormal coefficients χ_j and ξ_j needed to generate the spectral density for the first five load harmonics are summarised in Table 1.

To the authors' knowledge, there exist no analytical time-domain models, which are capable of capturing both the temporal shape of the walking force and its frequency content. Therefore, emphasis is placed on an accurate representation of the frequency content, which is obtained by using the experimentally determined PSDs directly to reconstruct the load.

Table 1
Summary of parameters for the Gaussian shape spectrum for representation of the pedestrian-induced lateral force.

	$j=1$	$j=2$	$j=3$	$j=4$	$j=5$
A_j	0.900	0.020	0.774	0.0258	0.612
B_j	0.043	0.031	0.026	0.064	0.026
χ_j	−3.061	−5.004	−3.674	−5.315	−4.492
ξ_j	0.3078	0.2876	0.2169	0.2655	0.2818

A pseudo-random time series of the equivalent static load from a single pedestrian, can be generated as follows [35]:

$$F(t) = \sum_{k=0}^{N-1}\sqrt{2S_F(f_k)\,\Delta f}\cdot\cos(2\pi f_k t + \psi_k) \quad (5)$$

$$S_F(f_k) = \sum_{j=i}^{N_{\mathrm{Harm}}} S_{F,j}(f_k) \quad (6)$$

$$\Delta f = \frac{1}{N\Delta t} = \frac{2}{T_{tot}}. \quad (7)$$

The parameters ψ_k are randomly generated phase angles, drawn from a uniform distribution, $f_k = k\Delta f$, $k = 0\ldots N-1$ is the distinct frequency from which the power spectrum ordinates are calculated, N is the total number of data points, N_{Harm} is the total number of load harmonics (here $N_{\mathrm{Harm}} = 5$) and T_{tot} is the total duration of the time series. The power spectral density function $S_{F,j}(f)$ is defined in Eq. (2) and depends on the shape (parameters A_j and B_j in Table 1) and the magnitude $\tilde{\sigma}^2_{F,j} = W_p^2\mathrm{DLF}_j^2/2$, defined through their individual probability distributions (parameters χ_j and ξ_j in Table 1).

In Fig. 3, a time-domain comparison is made between a sample of measured pedestrian-induced lateral force and a pseudo-random time series using the method outlined in this section (Eq. (5)).

Please cite this article in press as: Ingólfsson ET, Georgakis CT. A stochastic load model for pedestrian-induced lateral forces on footbridges. Engineering Structures (2011), doi:10.1016/j.engstruct.2011.07.009

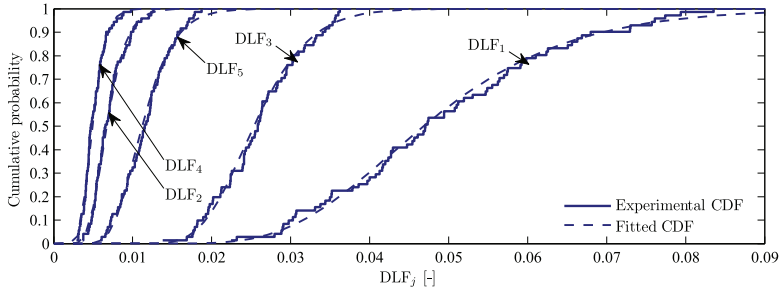

Fig. 2. Experimental and fitted CDF functions for the equivalent perfectly periodic DLF of the first five load harmonics.

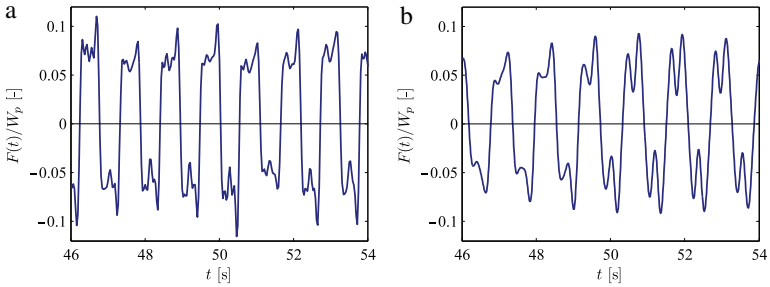

Fig. 3. Samples from (a) a measured [29] and (b) a pseudo-random time-history of the weight normalised pedestrian-induced lateral force (obtained using $f_w = 0.85$ Hz, $\Delta t = 1/64$ s and $N = 16\,837$).

2.2. Equivalent damping

The load model in Eq. (1) is based on the assumption that motion-induced pedestrian loads can be modelled as velocity and acceleration proportional, defined through the coefficients c_p and ϱ_p. From the experimental work of Ingólfsson et al. [29], it was shown that c_p and ϱ_p are functions of both the frequency and amplitude of the lateral motion. In Fig. 4, the results from the study of Ingólfsson et al. [29] are presented, showing the sample mean value of the velocity proportional load coefficient, μ_{c_p}, as functions of both normalised frequency and lateral displacement amplitude. The vibration frequency, f_0, is normalised with half the average free pacing frequency μ_{f_w} of the pedestrian test subjects.

2.2.1. Statistical characterisation of damping coefficient

In a microscopic modelling perspective, it is more convenient to relate the vibration frequency to the normal pacing frequency of each individual rather than the population mean. Therefore, the raw data from the study of Ingólfsson et al. [29] has been revisited. Herewith, the test results have been divided into nine different frequency regions depending on the ratio f_0/f_{wi} in each individual test, where $f_{wi} = f_{pi}/2$ is the normal gait cycle frequency of test subject i. The nine regions are defined through bands bracketed by normalised frequency pairs {0–0.45}, {0.45–0.55}, {0.55–0.65}, {0.65–0.75}, {0.85–0.95}, {0.95–1.05}, {1.05–1.15}, {1.15–∞}. In each frequency bin, the mean value of the damping coefficient has been calculated at each particular vibration amplitude.

The number of frequency bins was selected as a trade-off between the desire to obtain an acceptable frequency resolution and the need for a sufficient number of samples in each bin, since this influences the reliability of the statistics. The total number of distinct data points, from which the pedestrian load coefficients are obtained, is 4724. With 9 frequency intervals, the average number of samples per frequency bin is 525. As the number of tests at each combination of frequency and amplitude varied, the number of samples used to calculate each distinct mean value, varied from 15–197 with an average value of 75 samples.

In each frequency bin, a simple linear function can be used to represent the relationship between the sample mean, μ_{c_p} of the measured velocity proportional load coefficient and the lateral vibration amplitude u_0. Owing to the large scatter in the data, a stochastic model of the following type is proposed:

$$Y = \theta_0 + \theta_1 u_0 + X\sigma \tag{8}$$

where σ is an amplitude dependent standard deviation and the term $X\sigma$ therefore represents a random deviation with zero mean ($E[X] = 0$) and covariance, $\mathrm{Cov}[X(t_n), X(t_m)] = \mathbf{\Sigma}_{nm}$, [36]. The scatter in the data decreases with the vibration amplitude which can conveniently be approximated with an exponentially decreasing standard deviation:

$$\sigma = \theta_2 \exp[\theta_3 u_0]\,. \tag{9}$$

The parameters θ_0 and θ_1 have been obtained by fitting Eq. (8) (with $X = 0$) to the mean values of c_p in each frequency range and θ_2 and θ_3 were subsequently determined by fitting Eq. (9) to the measured standard deviations of c_p. The stochastic model for generating pedestrian damping coefficient can now be written as

$$c_p(f_0/f_w, u_0) = \theta_0(f_0/f_w) + \theta_1(f_0/f_w)\,u_0 + X \cdot \theta_2(f_0/f_w) \cdot \exp[\theta_3(f_0/f_w)\,u_0]\,. \tag{10}$$

In Fig. 5, the average damping coefficient calculated in each frequency range is shown as a function of the lateral vibration amplitude together with ± one standard deviation error bar. Also in Fig. 5, both the linear fits to the mean values, as well as the exponential fits to the standard deviations are indicated.

In time-domain modelling, c_p is a function of time t as the amplitude u_0 is generally a non-constant function of time. The time series of c_{pi} is generated at discrete time instances, t_k, and depends

Please cite this article in press as: Ingólfsson ET, Georgakis CT. A stochastic load model for pedestrian-induced lateral forces on footbridges. Engineering Structures (2011), doi:10.1016/j.engstruct.2011.07.009

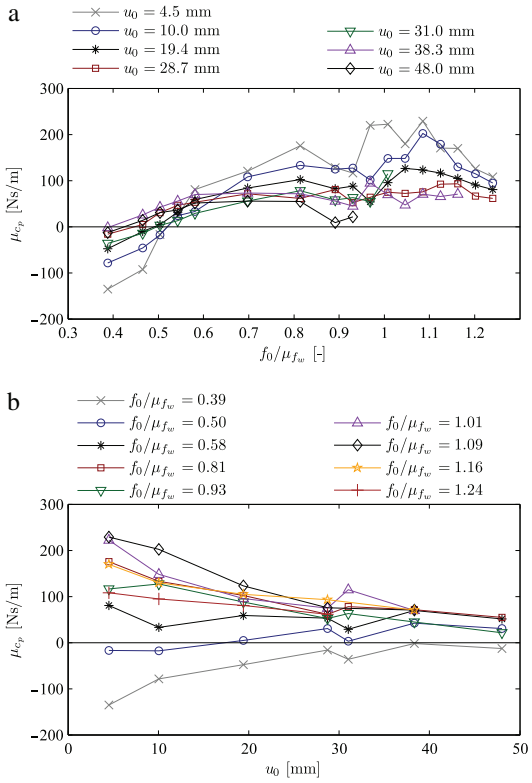

Fig. 4. Mean value of the velocity proportional coefficient μ_{c_p} as a function of normalised frequency (top) and as a function of amplitude (bottom) (based on data from Ingólfsson et al. [29]).

on the frequency ratio f_0/f_{wi}, the displacement amplitude, $u_{0i}(t_k)$, felt by pedestrian i at time t_k. In addition, a random variation $X(t_k)$ takes into account deviations of the instantaneous load coefficient from the mean value. The pedestrian tests from which the results in Fig. 5 are based upon, were carried out at constant vibration amplitude, and represent an average value of c_p taken over a time period of 30 s [29]. Therefore, when generating a series of instantaneous values of $c_{pi}(t_k)$ ($k = 1 \ldots N$), some assumptions relating to the temporal correlation of X must be introduced. Qualitatively, this correlation can be obtained if X is generated as a first-order autoregressive process (or discrete-time Gaussian Markov process), $X_{i+1} - \alpha X_i = \beta w_i$ where w_i are independent standard Gaussian variables and α and β are coefficients of the process. In continuous time, this corresponds to passing a white noise through a linear first-order filter, with an exponential autocorrelation function, $R(\tau) = \exp[-\omega_c \tau]$. The coefficients α and β for the discrete process may be obtained by solving the Yule–Walker equations [37]. The recursive formula (with time separation Δt) can be re-written in the following format [38]:

$$X_{k+1} = \exp[-\omega_c \Delta t] X_k + w_i \sqrt{1 - \exp[-2\omega_c \Delta t]}. \tag{11}$$

The parameter ω_c is selected such that the desired temporal correlation is obtained.

The use of Eqs. (10) and (11) to generate a time series of the pedestrian damping coefficient is illustrated in Fig. 6 for different values of w_c and compared with mean value $\mu_{c_p}(t) = \theta_0 + \theta_1 u(t)$, i.e. with $X = 0$. The example shows how a time series, $c_{pi}(t_k)$, is generated when the displacement amplitude $u_{0i}(t_k)$ follows a half-sine. This corresponds to the displacement amplitude felt by a pedestrian crossing a footbridge (at constant forward speed) with a half-sine mode shape and constant vibration amplitude of 50 mm. In the example, the initial value of the random variation is $X_1 = X(t_1) = X(0) = -0.688$ and thereby the initial value of the pedestrian load coefficient is $c_p(t_1) = c_p(0) = -335.8$ N s/m. The two extremes, $\omega_c = 0$ and $\omega_c \to \infty$, correspond to situations with full and no temporal correlation respectively. In the first case, the stochastic variable X remains constant and the pedestrian damping coefficient follows a deterministic path along a certain fractile of the $c_p(f_0/f_w, u_0)$-curve, determined by the initial value of X (here $X_1 = -0.688$). When $\omega_c \to \infty$, X_k are independent standard Gaussian variables. By allowing for non-zero values of ω_c an intra-subject variability is introduced, as illustrated in Fig. 6. Currently, the parameter ω_c, which controls the degree of intra-subject variability, can only be determined qualitatively.

2.3. Equivalent inertia

Similarly to the velocity proportional coefficient the acceleration proportional coefficient, ϱ_p, was determined by Ingólfsson et al. [29]. The coefficient is defined such that negative values of ϱ_p imply an overall increase in the modal mass of the structure whereas positive values imply that the pedestrian acts as to reduce the overall modal mass. The stochastic model to generate ϱ_p is similar to that in Eq. (10):

$$\varrho_p(f_0/f_w, u_0) = \phi_0(f_0/f_w) + \phi_1(f_0/f_w)\, u_0 + X \cdot \phi_3(f_0/f_w) \cdot \exp[\phi_4(f_0/f_w)\, u_0] \tag{12}$$

with parameters ϕ_0 and ϕ_1 determined by fitting an expression similar to that in Eq. (8) (with $X = 0$) to the measured mean values of ϱ_p. The parameters ϕ_2 and ϕ_3 were determined by fitting an expression of the type in Eq. (9) to the measured standard deviations. The stochastic variable X is a discrete-time Gaussian Markov process, with the recursive format as given in Eq. (11). In Fig. 7 the average value of the acceleration proportional coefficient, calculated in each frequency bin, is shown as a function of the lateral vibration amplitude. Also in Fig. 7, the fitted expressions through the mean values and the standard deviations, respectively are shown.

In Table 2, the numerical values of the fitting parameters in the stochastic models in Eqs. (10) and (12) are summarised. In all cases (except two), a significant linear correlation between the fitted variables was observed with mean value $\rho = 0.88$ (S.D 0.06 for c_p and 0.07 for ϱ_p).

In two of the frequency ranges, the correlation is low ($\rho < 0.5$) and therefore the amplitude independent mean values of the velocity and acceleration proportional coefficients have also been provided (in brackets). These values have been used in the load model presented herewith.

3. Application of the load model: basic assumptions

3.1. The footbridge structure

The lateral deflection, $u(x, t)$, of the footbridge structure is assumed to satisfy the equation of motion for linear and viscously damped straight beam with distributed elasticity $EI(x)$, mass $m(x)$ and damping $c(x)$, neglecting rotational inertia, axial force effects and shear deformations [39]:

$$\frac{\partial^2}{\partial x^2}\left[EI(x)\frac{\partial^2 u(x,t)}{\partial x^2}\right] + m(x)\frac{\partial^2 u(x,t)}{\partial t^2} + c(x)\frac{\partial u(x,t)}{\partial t} = Q(x,t) \tag{13}$$

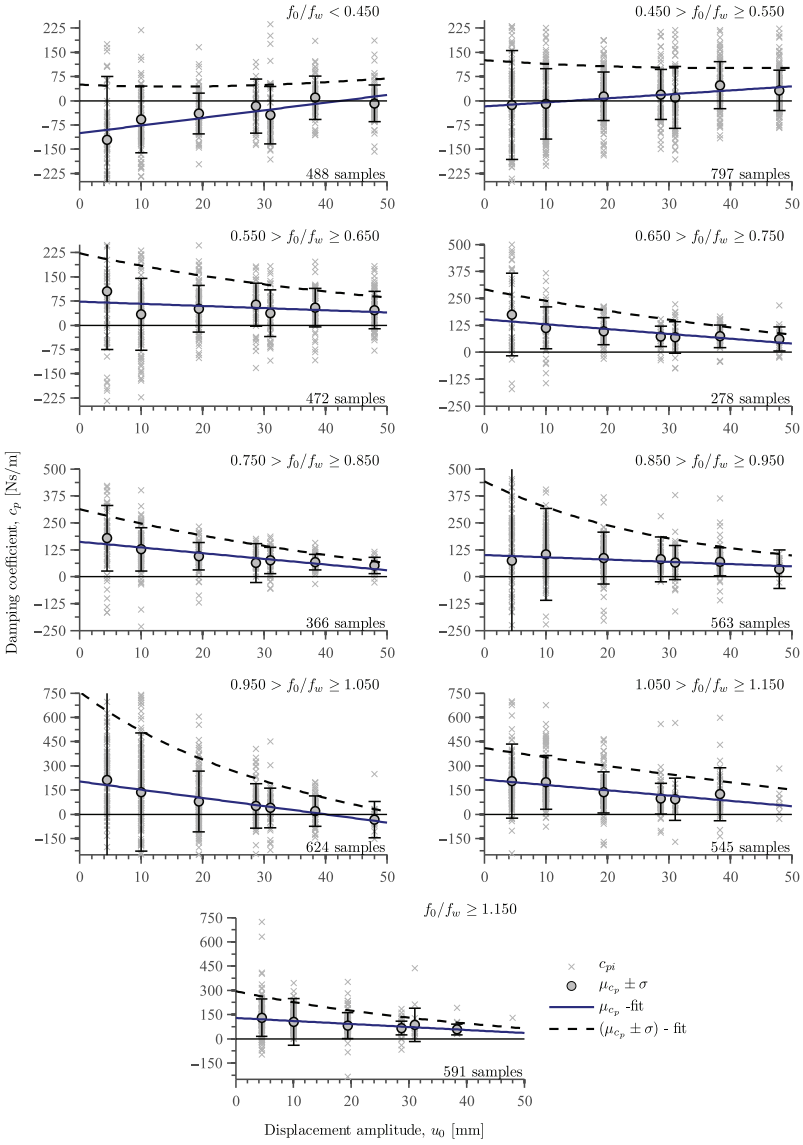

Fig. 5. Pedestrian damping coefficients as functions of the lateral vibration amplitudes in various frequency intervals.

where $Q(x,t)$ is the external load function. If the structural damping is assumed to be proportional, the equation of motion can be decoupled into n ordinary second-order differential equations:

$$\ddot{q}_n(t) + 2\zeta_n\omega_n\dot{q}_n(t) + \omega_n^2 q_n(t) = p_n(t) \tag{14}$$

$$u(x,t) = \sum_{n=1}^{\infty} \Phi_n(x) q_n(t) \tag{15}$$

where ζ_n, ω_n, $q_n(t)$ and $\Phi_n(x)$ are the modal damping, angular frequency, modal displacement and mode shape of vibration mode n, respectively. The mass normalised modal load, $p_n(t)$, is defined as

$$p_n(t)M_n = \int_0^L Q(t,x)\Phi_n(x)\mathrm{d}x \tag{16}$$

where M_n is the modal mass of mode n and L is the bridge length. In the following treatment, it is assumed that only a single vibration mode contributes significantly to the response and therefore the subscript n is omitted from hereon.

3.2. Modal pedestrian load

It is assumed that each pedestrian walks with a constant speed across the bridge, thus the spatial distribution of the pedestrian

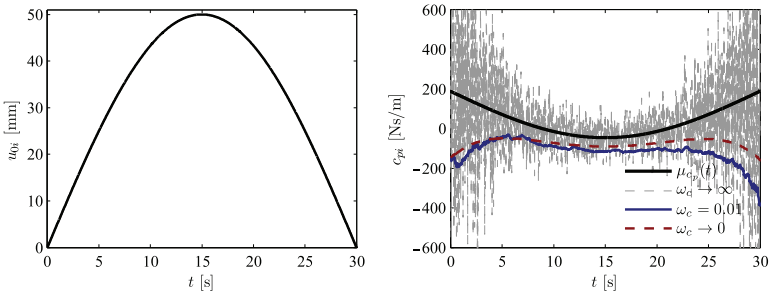

Fig. 6. Variation of displacement amplitude (left) and simulated pedestrian load coefficient for different temporal correlations (right), with $\Delta t = 1/64$ s and $0.95 \leq f_0/f_w < 1.05$.

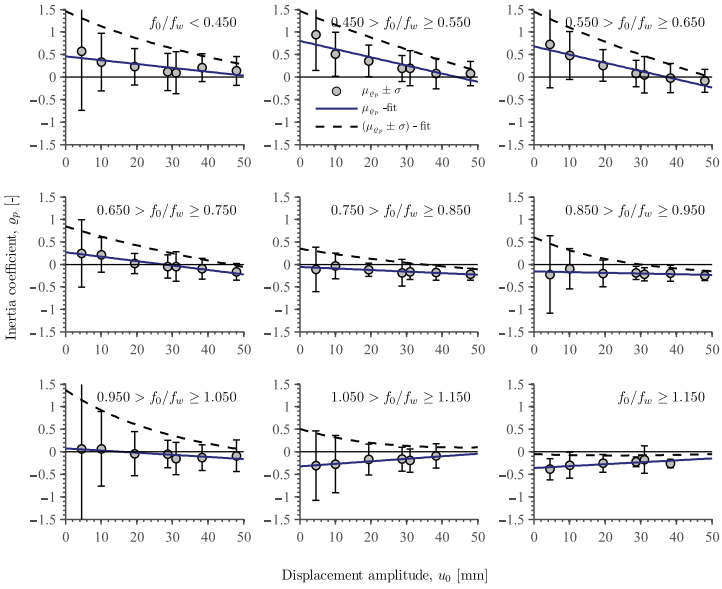

Fig. 7. Pedestrian inertia coefficients as functions of the lateral amplitudes in various frequency ranges.

Table 2
Parameters of the regression model in Eq. (9).

Frequency range f_0/f_w	θ_0 (N s/m)	θ_1 (N s/m^2)	θ_2 (Ns/m)	θ_3 (m^{-1})	ϕ_0 (–)	ϕ_1 (m^{-1})	ϕ_2 (–)	ϕ_3 (m^{-1})
<0.45	−100	2360	150.3	−21.6	0.460	−8.5	1.003	−28.1
0.45–0.55	−18	1237	143.2	−18.2	0.801	−18.1	0.662	−20.5
	(14.3)	(0)						
0.55–0.65	73	−667	150.7	−23.5	0.680	−18.2	0.773	−25.2
0.65–0.75	152	−2240	139.4	−24.7	0.270	−9.8	0.574	−24.8
0.75–0.85	162	−2643	151.4	−30.6	−0.057	−3.5	0.408	−24.3
0.85–0.95	101	−1055	342.0	−38.2	−0.158	−1.5	0.763	−44.6
					(−0.197)	(0)		
0.95–1.05	203	−5080	555.9	−42.3	0.074	−4.7	1.30	−36.9
1.05–1.15	214	−3284	195.3	−13.1	−0.324	5.6	0.832	−35.4
≥ 1.15	129	−1858	166.5	−35.5	−0.362	4.3	0.309	−23.1

load is determined by the Dirac delta function. The load induced by a single pedestrian therefore becomes:

$$Q(x,t) = \begin{cases} F(t)\delta\left(x - v_p t\right) & \text{for } t_0 \leq t \leq t_0 + t_d \\ 0 & \text{for } t > t_0 + t_d,\ t < t_0 \end{cases} \tag{17}$$

where v_p and t_0 are the pedestrian walking speed and arrival time respectively and $t_d = L/v_p$ is the pedestrian passage time. It is assumed that the pedestrian load can be written as shown in Eq. (1), i.e. as a sum of an equivalent static force and motion-induced forces in the form of equivalent damping and inertia:

$$\begin{aligned} F(t) &= F_{st}(t) + c_p \dot{u}(t) + m_p \varrho_p \ddot{u}(t) \\ &= F_{st}(t) + c_p \Phi(x)\dot{q}(t) + m_p \varrho_p \Phi(x)\ddot{q}(t). \end{aligned} \tag{18}$$

Please cite this article in press as: Ingólfsson ET, Georgakis CT. A stochastic load model for pedestrian-induced lateral forces on footbridges. Engineering Structures (2011), doi:10.1016/j.engstruct.2011.07.009

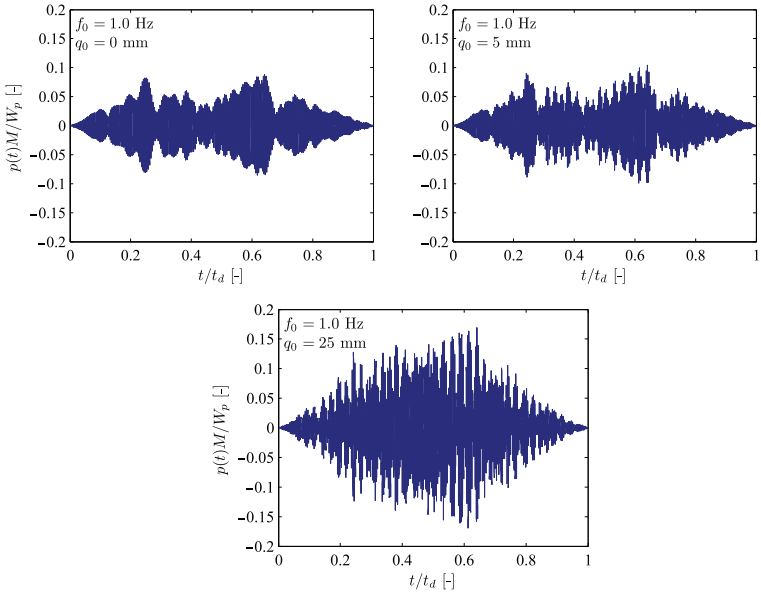

Fig. 8. Pseudo-random time series of the modal pedestrian-induced lateral force from a single pedestrian crossing a half-sine mode shape for different (constant) vibration amplitudes.

The modal load from a single pedestrian can now be written as

$$p(t)M = \int_0^x Q(x,t)\Phi(x)\mathrm{d}x = \begin{cases} F_{st}(t)\Phi(v_p t) + \left(c_p\dot{q}(t) + m_p\varrho_p\ddot{q}(t)\right)\left[\Phi(v_p t)\right]^2 \\ \quad \text{for } t_0 \le t \le t_0 + t_d \\ 0 \quad \text{for } t > t_0 + t_d,\ t < t_0. \end{cases} \tag{19}$$

The coefficients c_p and ϱ_p are determined from the stochastic models in Eqs. (10) and (12), respectively. The total load from a group of pedestrians is obtained as the sum of the load from each individual. Due to the vibration dependency of the load, linear superposition of the response from each individual is not possible, but instead the total pedestrian-induced load must be evaluated in each time step.

In Fig. 8, three different pseudo-random time series are shown for the weight normalised modal load ($p(t)M/W_p$) according to Eq. (19), at different constant vibration amplitudes. For the generation of the figure, the loading frequency was taken as $f_w = 0.85$ Hz and the body-weight normalised pedestrian load coefficients were taken as $c_p/W_p = 0.1$ s/m and $\varrho_p/g = 0.1$ s^2/m, respectively. The mode shape is assumed to be a half-sine. Without bridge motion, the modal load is governed by the equivalent static load, as generated through the use of Eq. (3), but as the vibration amplitude is increased (at frequency $f_0 = 1.0$ Hz), the self-excited portion of the load becomes more pronounced.

3.3. Other modelling assumptions

3.3.1. Body weight

The distribution of the pedestrian's weight is assumed to follow a normal distribution. In this paper, the mean value and standard deviations are taken as $\mu_{W_p} = 727$ N and $\sigma_{W_p} = 145$ N respectively, based on statistical data for the Danish population [40].

3.3.2. Walking frequency distributions

With frequency dependent load coefficients c_p and ϱ_p, the distribution of pacing frequencies in the crowd (mean value μ_{f_w} and standard deviation σ_{f_w}), are important modelling parameters. For spatially unrestricted pedestrians, these parameters can be determined by the free walking speed and the normal gait parameters of each individual. Typical values for the average gait cycle frequencies are in the range 0.9–1.0 Hz (S.D. 0.05–0.10 Hz) and may depend on factors such as the travel purpose, visual surroundings [41], or geographic location and the particular "pace of life" [42]. With footbridges being restricted by physical boundaries (e.g. the hand rails), the spatially unrestricted walking is only possible when a limited number of pedestrians occupy the bridge. Several studies have shown that the forward walking speed of the group decreases from the free walking speed to zero as the crowd density approaches a certain "jam density" [43–45]. However, less is known about the relationship between the pacing frequency distribution and the crowd density. Recent research suggests that the mean value decreases with increasing density and that the standard deviation either remains constant [45] or decreases [46]. It has been suggested that synchronisation amongst pedestrians occurs in large density crowds, but according to [46], this only occurs in pairs or very small clusters of people. Therefore, in the simulations presented herewith, the assumption about random pedestrian arrivals and mutually independent (and uniformly distributed) phase difference between pedestrians is maintained and assumed unaffected by the crowd density. However, as the average walking speed may vary with the crowd density, several different pacing frequency distributions are investigated. In the simulations, the gait cycle frequency distribution is assumed to follow a normal distribution with mean value μ_{f_w} and standard deviation σ_{f_w}.

3.3.3. Step length and walking speed

There is a physical relationship between the step length, l_s, and the forward speed, v_p, of the pedestrian, which can be written in

Please cite this article in press as: Ingólfsson ET, Georgakis CT. A stochastic load model for pedestrian-induced lateral forces on footbridges. Engineering Structures (2011), doi:10.1016/j.engstruct.2011.07.009

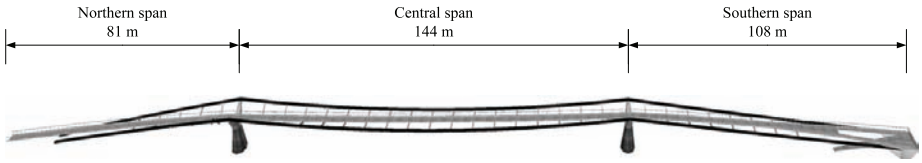

Fig. 9. The London Millennium Footbridge.

Table 3
Modal properties of the Millennium Bridge without added damping.
Source: Table reproduced with permission from Ove Arup and Partners.

Description	Abbreviation	Frequency (Hz)	Damping(%)	Modal mass (tonnes)
First lateral mode of central span	CL1	0.48–0.49	0.75–0.77	128–130
Second lateral mode of central span	CL2	0.95–0.99	1.3	145–148
First lateral mode of Southern span	SL1	0.80–0.81	0.6–0.7	172
First lateral mode of northern span	NL1	1.04	0.32*	113*

* The damping was estimated from poor quality data and the modal mass was obtained from an FE analysis.

terms of the pacing frequency as

$$v_p = f_p l_s = 2 f_w l_s. \tag{20}$$

Both the pacing frequency and the step length change with the walking speed which is modelled through the following empirical relationship [47]:

$$l_s = 0.25 f_p^{1.86} = 0.91 f_w^{1.86}. \tag{21}$$

3.3.4. Arrival time

The numerical simulations are based on the assumption that each pedestrian in the load model can be modelled independently. Each pedestrian walks at a constant speed and the arrival of pedestrians to the bridge is modelled as a Poisson process. This means that the arrival time of each pedestrian is a mutually independent random variable, with uniform probability distribution, whereas the inter-arrival time follows the exponential distribution.

4. Numerical response simulations

Herewith, the performance of the model is demonstrated through numerical response simulations. The response simulations employ the fundamental modes of the London Millennium Bridge, as this structure was highly susceptible to pedestrian induced vibrations and has exhibited strong vibrations in several different vibration modes. Furthermore, as the bridge has been subject to intensive investigations in the past decade it will serve as a suitable platform for comparison with other numerical models and full-scale measurements.

A number of different simulations are carried out. Initially, it is assumed that all pedestrians walk at a common forward speed with identical step frequencies to demonstrate some basic features of the load model. Subsequently, the effects of background noise, the duration of the load event and the distribution of pacing frequencies on the response characteristics are investigated and discussed.

4.1. Modal properties of the London Millennium Bridge

The London Millennium Bridge is an extremely shallow suspension bridge with a total length of approximately 324 m. It is divided into 3 spans, the north span (80 m), the central span (144 m) and the south span (100 m); see Fig. 9. On its opening day and during subsequent full-scale pedestrian crowd tests, excessive lateral vibrations were observed in four vibration modes; on the southern span at a frequency around 0.8 Hz, at the central span in the first and second modes at frequencies around 0.5 Hz and 0.95 Hz respectively and more rarely on the northern span at a frequency of around 1.0 Hz [12].

Extensive modal identification of the empty structure revealed a series of vibration modes susceptible to lateral as well as vertical human-induced dynamic loads, [48,49]. In Table 3, the experimentally determined modal properties for the first four lateral vibration modes are summarised.

4.2. Fundamental lateral vibration mode (CL1)

A single response simulation is carried out using the fundamental lateral mode of the Millennium Bridge (CL1) as a benchmark. This mode is characterised by its low natural frequency ($f_{CL1} = 0.5$ Hz) and structural damping ($\zeta_{CL1} = 0.76\%$). As a first test, the crowd size is gradually increased from 25 to 300 pedestrians, in steps of 25 every 5 min. Within each five minutes, the flow of pedestrians is uniform, i.e. the inter-arrival times between the pedestrians are kept constant. As a benchmark test, it is further assumed that all pedestrians walk at the same forward speed (1.14 m/s) and have identical gait cycle frequencies (0.85 Hz), corresponding to constant step length (0.67 m). However, the pedestrian body mass, the equivalent perfectly periodic DLFs and the self-excited force coefficients (c_p and ϱ_p) are treated as random variables as described in Sections 2 and 3.3 respectively.

In Fig. 10, the modal acceleration response of the footbridge is shown as well as the total number of pedestrians on the bridge. Both the linear footbridge response is shown (i.e. in the absence of self-excited force components) as well as the nonlinear response where the self-excited pedestrian load is included. From the response time history, there is generally no difference between the linear response and the nonlinear one during the first 40 min of simulation. However, approximately 45 min into the simulations, the response increases considerably and within a few minutes the acceleration exceeds an amplitude of approximately 0.2 m/s^2 (21 mm), which could easily be characterised as excessive lateral vibrations. From the spectrogram of the modal acceleration (Fig. 10 bottom), it is demonstrated that, during low level vibrations, the dominant frequency components are those at the frequency of the main harmonics. As the number of people on the bridge increases, the self-excited portion of the load becomes more important and during large vibrations, this component (at the modal frequency) dominates the response.

The self-excited force is responsible for alterations in the modal mass and damping ratio of the structure. Therefore, equivalent and time dependent values for the instantaneous modal mass and

Please cite this article in press as: Ingólfsson ET, Georgakis CT. A stochastic load model for pedestrian-induced lateral forces on footbridges. Engineering Structures (2011), doi:10.1016/j.engstruct.2011.07.009

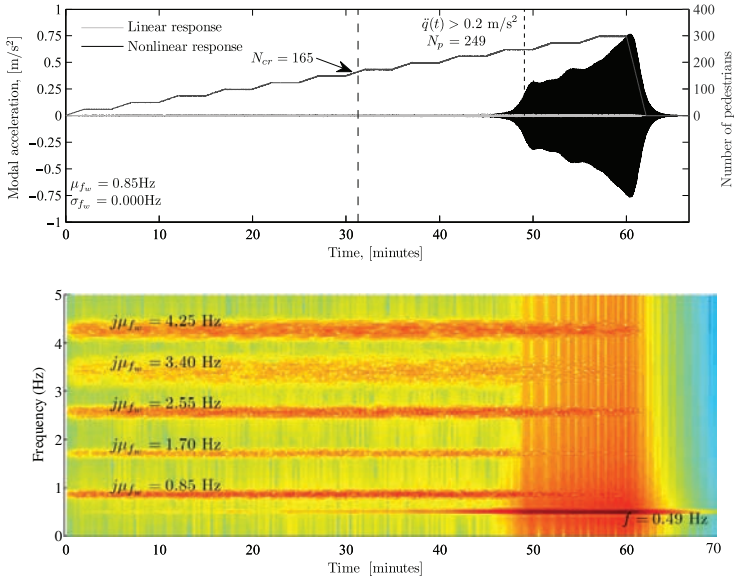

Fig. 10. Modal acceleration time history (top) and spectrogram (bottom) of mode CL1, subject to a gradually increasing size of pedestrians walking with a common pacing rate.

damping can be calculated as the initial modal mass and damping modified by the acceleration and velocity proportional self-excited pedestrian force components:

$$M_{tot}(t) = \left(M - \sum_{i=i}^{N_p(t)} m_{pi} \varrho_{pi}(t) \left[\Phi(v_{pi}t)\right]^2\right) \tag{22}$$

$$\zeta_{tot}(t) = \frac{1}{2\omega M}\left(C - \sum_{i=i}^{N_p(t)} c_{pi}(t) \left[\Phi(v_{pi}t)\right]^2\right) \tag{23}$$

where $N_p(t)$ indicates the number of pedestrians present on the bridge at any given time instance, t.

A single realisation can only offer a qualitative view into the nature of the bridge response and the development of the overall modal mass and damping and therefore the aforementioned simulations have been repeated 200 times. In Fig. 11(top), the change in the modal mass is shown through the modification in the natural frequency of the system and in Fig. 11(bottom) the change in the overall modal damping ratio is depicted. The figure shows the individual realisations, the mean value as well as the 5% and 95% quantiles. In addition, the realisation which corresponds to the response in Fig. 10 is also emphasised in Fig. 11.

It is noted that the effect of the pedestrians on the natural frequency is quite minimal, but it is worth noting that they act to decrease the apparent structural mass and thereby raise the modal frequency. In Fig. 11 (bottom), it is noted that the modal damping generally decreases with the number of people on the bridge but there are considerable fluctuations due to the randomness in the pedestrian load coefficients.

4.2.1. Critical number of pedestrians and prediction of excessive vibrations

Traditionally, the critical number of pedestrians needed to cause zero damping is calculated by using Arup's formula [12]:

$$N_{cr} = \frac{2\zeta\omega M}{\mu_{c_p} \frac{1}{L} \int_0^L [\Phi(x)]^2 dx}. \tag{24}$$

With $\mu_{c_p} = 73$ Ns/m taken as the mean value of the pedestrian load coefficient in the relevant frequency range (see θ_0 in Table 2), the critical number of pedestrians in CL1 is predicted as 165.

By considering the development of the overall damping as shown in Fig. 11 (bottom), a similar definition of the critical number of pedestrians may be adopted, by determining the condition for which the damping becomes negative ($\zeta_{tot}(t) \leq 0$).

It is interesting to note that in the benchmark simulation, already at $N_p = 98$, the overall damping turns negative, implying the potential for instability, but in this case the damping quickly turns positive again, excessive vibrations are avoided and the amplitudes remain limited. When the overall damping approaches zero, the structures becomes extremely sensitive to any load which acts at the modal frequency, e.g. from ambient wind which may cause large vibration before zero structural damping is reached. On the other hand, the damping may turn negative and remain negative for a certain amount of time before large vibrations occur. As illustrated in Fig. 11, the first zero crossing in the benchmark simulation occurs after approximately 17 min. After 40 min, the damping remains more or less negative. Excessive vibrations occur a few minutes later.

Therefore, if the critical number of pedestrians is defined as that needed to exceed a certain acceleration threshold, e.g. the comfort criterion as specified according to Sétra [8] (0.15–0.20 m/s^2), a completely different result may be obtained, then for the zero-damping criterion. In this case, the number of pedestrians on the bridge when the acceleration exceeds a threshold of 0.20 m/s^2 is approximately 249 pedestrians.

When considering the 5% and 95% quantiles of the modal damping, the time for which the damping turns negative varies from around 21 min up to around 42 min. The average number of pedestrians needed to cause negative damping is consistent with the initial estimate of 165 pedestrians as indicated with the vertical dashed line in Fig. 11.

4.2.2. Effect of background noise

The basic assumption of the pedestrian loading model is that the lateral load is concentrated in narrow bands around the gait

Please cite this article in press as: Ingólfsson ET, Georgakis CT. A stochastic load model for pedestrian-induced lateral forces on footbridges. Engineering Structures (2011), doi:10.1016/j.engstruct.2011.07.009

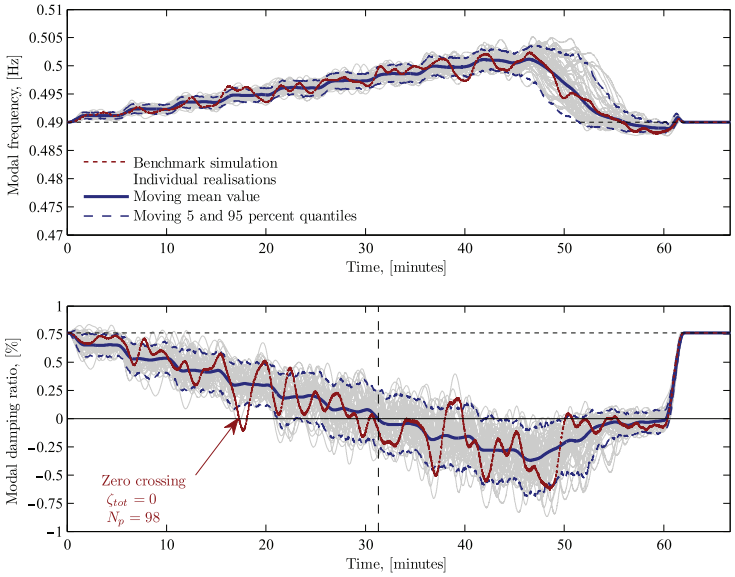

Fig. 11. Changes in the modal frequency and damping due to the self-excited portion of the pedestrian-induced lateral force during a response simulation of CL1 subject to a gradually increasing size of pedestrians walking with a common pacing rate.

cycle frequency, its integer harmonics and at the frequency of the structure in the form of velocity and acceleration proportional loads. When the loading frequency is well separated from the modal frequency, the only modal excitation (in the model) is that from the self-excited loads. In reality however, there are other possible sources of modal excitation that may prove to be important for the bridge response and the potential for large vibrations when the overall modal damping approaches zero.

In particular, wind loads provide ambient vibrations in the structure and even at moderate wind speeds the resulting load is small but non-negligible. Opposed to the pedestrian load, the wind is broad band and therefore excites all structural modes. The resulting load effect is highly damping dependent, which means that as the overall damping approaches zero (due to the self-excited pedestrian force), the response from ambient loads at the modal frequency increases and large vibrations develop quicker than in the absence of a direct resonance loading. In Fig. 12, this is illustrated, where an uncorrelated pseudo-random noise (with constant spectral density between 0 and 2 Hz) with different magnitudes are added to the total modal load before solving the equation of motion. The magnitude of the background noise, measured as the standard deviation of the total force in the bandwidth between 0 and 2 Hz, is 100 N and 500 N in Fig. 12 (top) and (bottom) respectively.

By comparing the response in Fig. 10 with those in Fig. 12, it is noted that as the magnitude of the background noise increases, the time at which the acceleration criteria is exceeded decreases, although the self-excited forces remain unchanged. Similarly, the number of pedestrians present on the span at the time of exceedance also decreases with the magnitude of the background noise.

In the absence of background noise, the loading at resonance is purely velocity proportional and therefore the transition from stable (and limited) vibrations to excessive vibrations occurs rapidly as the increase in vibration amplitude grows exponentially (see Fig. 10 (top) for $t \cong 47$ min). A damped system subjected to resonance loading experiences a linear increase in the vibration amplitude. Therefore, when the background noise is added, the initial build-up of large amplitudes will be a combination of a linear increase from the resonance part of the background noise and an exponential increase from the self-excited load. The transition between limited and excessive vibrations occurs slower as the magnitude of the background noise increases; see e.g. the comparison between the two time histories in Fig. 12.

4.2.3. *Effect of the duration of the load event*

The duration of the load event affects the results of the simulations, e.g. when the background noise is large, excessive vibrations will occur when the overall damping decreases. Furthermore, the randomness in the underlying load process is responsible for a certain time dependency, often expressed in terms of the return period of a certain event. In other words, an increase in the length of the numerical simulation increases the probability of occurrence of certain vibration amplitudes (or value of the total damping). This means that the critical number of pedestrians needed to either cancel the inherent structural damping or cause an exceed of a certain acceleration threshold generally decreases with an increased duration of the load event. This effect needs to be carefully considered when interpreting the results of both full scale testing of real-life bridges as well as those obtained from stochastic response simulations. In Fig. 13, two simulations are presented, one in which the simulation time is twice that of the original simulation (top) and another with a duration of twelve times the original simulation time (bottom). In both cases, an increase in the duration of the simulation has the effect of decreasing the number of people on the bridge for which the acceleration threshold is exceeded.

4.2.4. *Effect of the distribution of walking frequencies*

The simulations presented so far assume that all pedestrians walk at the same forward speed and with identical pacing frequencies. If a distribution of frequencies within the crowd is introduced ($\mu_{f_w} = 0.85$ Hz and $\sigma_{f_w} = 0.075$ Hz), the simulated response is that in Fig. 14. It is noted that by introducing a distribution in the pacing frequencies, the walking speed varies

Please cite this article in press as: Ingólfsson ET, Georgakis CT. A stochastic load model for pedestrian-induced lateral forces on footbridges. Engineering Structures (2011), doi:10.1016/j.engstruct.2011.07.009

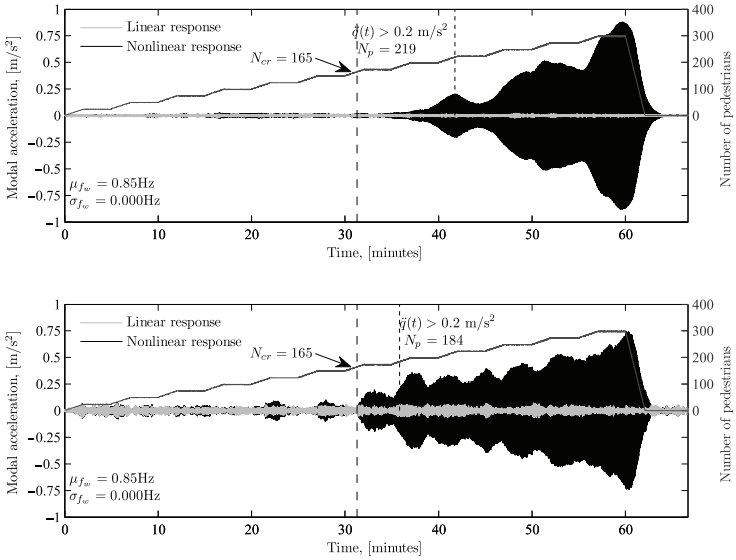

Fig. 12. Modal acceleration time history of mode CL1, subject to a gradually increasing crowd of identical pedestrians with added background noise from ambient wind of modal intensity 100 N (top) and 500 N (bottom) respectively.

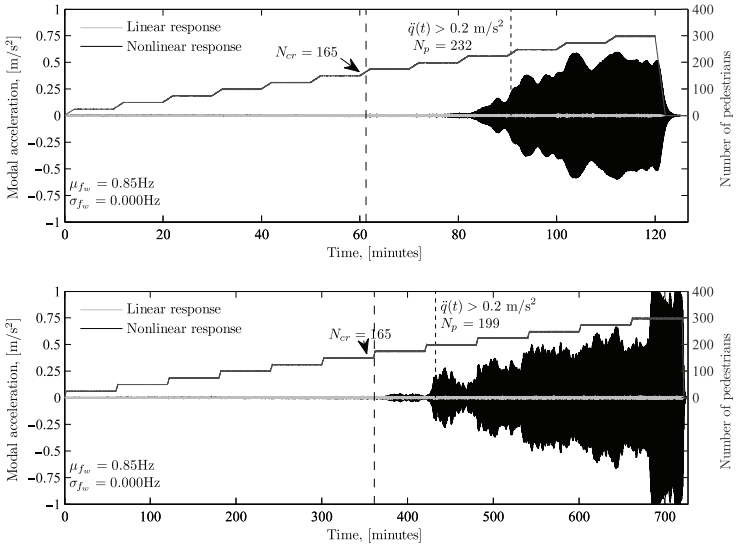

Fig. 13. Modal acceleration time history of mode CL1, subject to a gradually increasing crowd of identical pedestrians for two different simulation lengths.

according to the relationships in Eqs. (21) and (20). To control the number of pedestrians on the bridge in the simulation, the average flow rate is kept constant, such that the average number of pedestrians on the bridge varies from 0 to 300 in steps of 25 every fifth minute. This means that the actual number of pedestrians on the bridge is non-constant as shown in Fig. 14. This is a consequence of the randomness associated with the Poisson arrival process which governs the pedestrian arrival.

In general, the distribution of walking frequencies within a group is a non-deterministic quantity which may vary considerably between different groups of people depending on the particular crowd morphology, its density, the travelling purpose, meteorological conditions, etc. Therefore, a broad range of different gait cycle frequency distributions have been modelled, ranging from $\mu_{f_w} = 0.5$ Hz, corresponding to a very dense crowd, to $\mu_{f_w} = 1.0$ Hz, which represents an upper limit of the average walking frequency in a group of spatially unrestricted pedestrians. The standard deviation of gait cycle frequencies was kept constant ($\sigma_{f_w} = 0.075$ Hz). Furthermore, uncorrelated pseudo-random noise, with constant spectral density between 0 and 2 Hz, was added to the pedestrian induced modal load to simulate ambient excitation of the bridge. The magnitude of this load was selected as 100 N. This

Please cite this article in press as: Ingólfsson ET, Georgakis CT. A stochastic load model for pedestrian-induced lateral forces on footbridges. Engineering Structures (2011), doi:10.1016/j.engstruct.2011.07.009

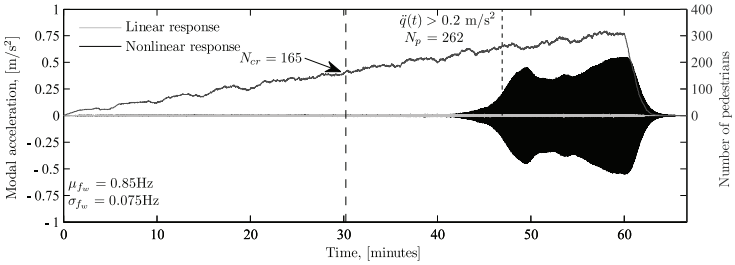

Fig. 14. Simulated modal acceleration response of CL1 subject to a gradually increasing number of people with normally distributed walking frequencies ($\mu_{f_w} = 0.85$ Hz and $\sigma_{f_w} = 0.075$ Hz).

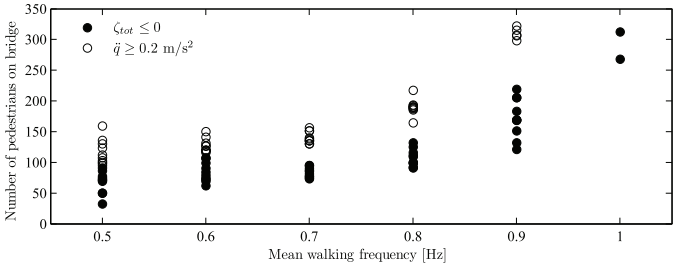

Fig. 15. Critical number of pedestrians for CL1 as functions of the average walking frequency.

value provides realistic values of ambient vibration response as expected on a footbridge. In each simulation, the number of pedestrians present on the bridge at the time instances of (i) initial zero-crossing of the overall damping and (ii) first exceedance of the acceleration threshold ($a \geq 0.2$ m/s^2) are collected.

In Fig. 15, the results are shown for sixty different crowd simulations for six distinct average pacing frequencies, illustrating the effect of both the distribution of pacing frequencies as well as the definition of bridge instability. Generally, as the gait cycle frequency approaches the modal frequency, the critical number of pedestrians decreases. However, the randomness in the underlying load process is responsible for a considerable scatter in the critical number of pedestrians between individual nominally identical simulations.

4.3. Fundamental modes of side-spans (NL1 and SL1)

The fundamental mode of the central span is characterised as a low frequency mode, as it features a natural frequency well below the freely selected average gait cycle frequency of normal pedestrians. Thereby, CL1 is only excited by the self-excited pedestrian-induced loads. The fundamental vibration frequencies of the side spans are within the range of average walking (SL1 at 0.80 Hz and NL1 at 1.04 Hz) and are therefore both excited by direct resonance from the equivalent pedestrian-induced load and from the self-excited forces. In Fig. 16, two examples of simulated modal acceleration responses are shown for a gradually increasing crowd, similar to that used for CL1 (and shown in Fig. 10). In both cases, excessive vibrations occur, but generally NL1 is more prone to vibrations than SL1, due to its extremely low modal damping combined with a low modal mass compared to the other modes (see Table 3). Qualitatively, the simulated response for these modes is similar to that of CL1, i.e. the critical number of pedestrians calculated from Arup's formula (146 for SL1 and 73 for NL1) is generally lower than the number of people on the bridge during the initiation of large vibrations. Furthermore, it is noted that large vibration amplitudes occur more quickly. Due to the randomness in the underlying load process and sensitivity in the simulations to the pacing frequency distribution, the background noise and the duration of the load event, the time series presented in Fig. 16 mainly serve as a demonstration of the capability of the model.

To demonstrate the frequency dependency of the results, a series of load simulations, in which the critical number of pedestrians (i) needed to cancel the inherent structural damping and (ii) needed to cause lateral vibrations in excess of the acceleration threshold 0.2 m/s^2, have been carried out. In Fig. 17, the results for all three modes (CL1, NL1 and SL1) are shown as functions of the average gait cycle frequency. In the simulations, it has been assumed that the standard deviation of the gait cycle frequencies is 0.075 Hz, such that it renders a realistic crowd morphology. The modal damping ratio of NL1 has been reported as 0.32 (see Table 3), which is based on poor quality data obtained from forced excitation of the central span. In the results presented in Fig. 17, a damping ratio of 0.7% has been used, which is close to that of SL1.

5. Discussion

5.1. Load model and statistical characterisation

The load model presented in this paper is simple and is based on the main assumption that pedestrian-induced lateral forces consist of two primary contributions, the "equivalent static" force and the "self-excited" force. Its main strength is that the coefficients in the load model are determined from a large database of almost 5000 time series of measured GRFs from seventy-one different people. The complication in the model is the inclusion of the randomness and the large inter and intra-subject variability which was observed from the data.

However, this randomness is important, particularly that related to the self-excited forces, as the standard deviations of the measured load coefficients are of the same order of magnitude as the mean value. A further complication to the model is the strong dependency of the pedestrian load coefficients on both the

Please cite this article in press as: Ingólfsson ET, Georgakis CT. A stochastic load model for pedestrian-induced lateral forces on footbridges. Engineering Structures (2011), doi:10.1016/j.engstruct.2011.07.009

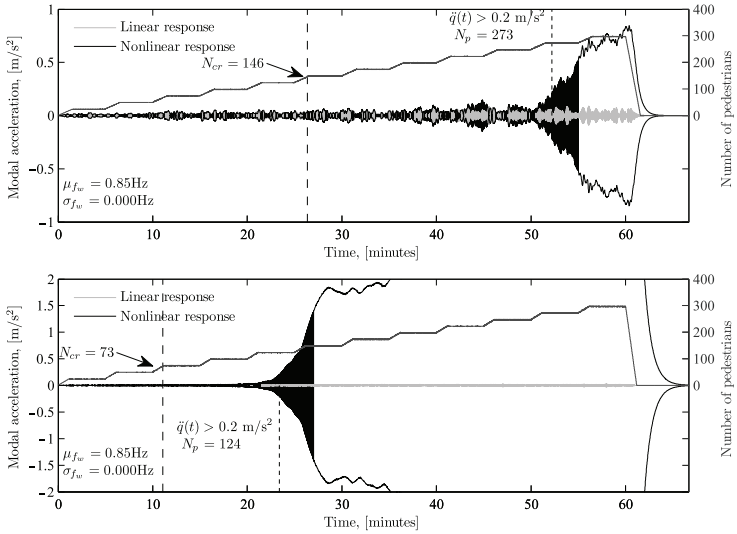

Fig. 16. Simulated response of SL1 (top) and NL1 (bottom) for a gradually increasing crowd of pedestrians with common walking frequencies ($\mu_{f_w} = 0.85$ Hz).

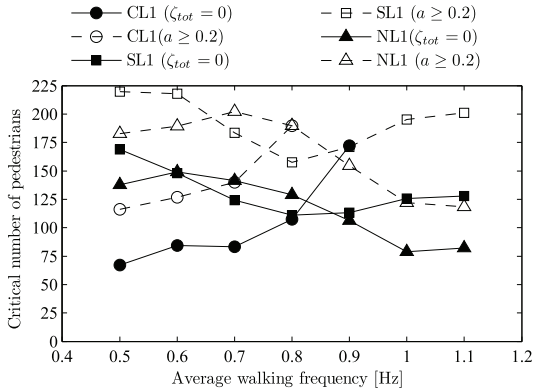

Fig. 17. Critical number of pedestrians for CL1, NL1 and SL1 as function of the average walking frequency.

frequency of the lateral motion as well as the amplitude. This dependency was dealt with by splitting the measured data into nine distinct frequency intervals, in which the data is treated separately and independently. As illustrated in Figs. 5 and 7, the amplitude dependency of the pedestrian load coefficients is such that the mean values and standard deviations generally decrease numerically with increasing vibration amplitudes. The generalised linear function, which is used to fit average values, and the exponential function used to fit the development of the standard deviations provide reasonable fits to the data in most of the frequency intervals. To avoid splitting the data into distinct frequency bins, different fitting functions could be used, which capture both the frequency and amplitude dependency of the load factors. However, a simple format is chosen herewith such that the main features of the load process can be captured, without overcomplicating the mathematical expressions.

When the load from a single pedestrian is generated, the Gaussian variable X, represents the deviation of the load coefficient from the mean value. By including a temporal correlation, through its representation as a discrete Gaussian Markov process, the possibility of including intra-subject variability in the pedestrian load coefficients is introduced in a fairly simple way; see Eq. (11). As illustrated in Fig. 6, by tuning the parameter ω_c, different levels of temporal correlation (and thereby intra-subject variability) can be obtained, with $\omega_c = 0$ being a limit case in which intra-subject variability is neglected.

In this model, the pedestrian-induced load depends only on the ratio between the lateral vibration frequency and the pacing frequency, but not on the walking speed of the individual. Furthermore, the PSD of the equivalent static force is assumed to remain unchanged with frequency ratio, amplitude and walking speed of the pedestrians.

5.2. Numerical simulations as a prediction tool

As presented herewith, the load model in Eq. (1) can efficiently be used for predicting the potential for excessive lateral vibrations of footbridges. However, there are several parameters that need to be taken into account and quantified. As already shown, the distribution of the pacing rate is an important modelling parameter, but equally important is the definition of instability and the probability associated with the event (i.e. the combination of a particular crowd density and pacing rate distribution) in which instability is triggered. If instability is defined as the condition for which the overall damping becomes negative, it is sufficient to analyse the time series of the overall bridge damping and estimate the first-excursion probability. However, as already noted, if the damping is sufficiently small, large vibrations may occur due to small resonance loads, e.g. from ambient wind, before the damping turns negative. On the other hand, if the damping turns negative during a short period of time, without the development of strong vibrations, then the bridge remains stable. Alternatively, instability may be defined through an acceleration criterion, i.e. through a comfort criterion. In this case, the comfort criterion should be carefully defined as little data exists on the vibration perceptions and annoyance of pedestrians subject to lateral footbridge vibrations.

In Fig. 17, it was shown that there is a large difference between the critical number of pedestrians in different simulations.

Please cite this article in press as: Ingólfsson ET, Georgakis CT. A stochastic load model for pedestrian-induced lateral forces on footbridges. Engineering Structures (2011), doi:10.1016/j.engstruct.2011.07.009

However, common for all modes is that instability can be triggered for less than 200 pedestrians, which is consistent with the observations made on the London Millennium Bridge [50].

Finally, the simulations presented herewith have only dealt with a simplified representation of the dynamics of the pedestrian crowd. It has been assumed that the forward speed of the pedestrians and pacing frequency remain constant and that no interaction between the pedestrians occur. However, as pointed out in this paper and on other occasions [3], a pedestrian crowd is a dynamic system for which local variations in the crowd density may occur with subsequent modifications in the walking patterns of the individuals. These effects should be included in cases where the pedestrian crowd is expected to undergo considerable local or global variations in its density or if it is expected that the structural vibrations affect the walking pattern of each individual.

5.3. Multi-modal excitation

It should be noted that the mathematical model, in its current form, is only applicable for lateral vibrations of a single mode and that the effect of multi-modal response on the pedestrian-induced load is unknown. This is caused by the nature of the experiments for which the quantification of the pedestrian load coefficients is based upon. In these tests, a single harmonic lateral vibration was imposed on the treadmill and therefore the resulting load coefficients should be related to lateral motion at that particular frequency and not in combination with other modes. The model should therefore be used on a mode-by-mode basis and, for multi-modal response, the susceptibility of each vibration mode can be checked independently.

For a generalisation of the load model, further tests should be carried out, in which multi-mode vibration is imposed on the walking surface and the resulting pedestrian-load coefficients quantified and compared with those of the single-mode response. This may prove practically difficult as the number of tests to be carried out, to cover a reasonable number of cases, may be excessively large. Another strategy would be to use the measured data, and the load model presented herewith, to calibrate a feasible mechanical model of the lateral GRF on a laterally moving surface. This model can subsequently be used in more general settings, such as multi-modal response or combined vertical and lateral motion.

Finally, the model cannot take into account nonlinear modal coupling, the possibility of parametric excitation, excitation of lateral modes through vertical loads, etc. Without excluding the possibility that these phenomena may contribute to a quicker or a different development of excessive lateral vibrations, there is not enough empirical data to justify their inclusion in the modelling framework.

6. Conclusions

The main conclusions from the study can be summarised in the following.

1. A stochastic load model has been presented for modelling of the frequency and amplitude dependent pedestrian-induced lateral forces of footbridge. The model is shown to successfully predict excessive lateral vibrations in a number of benchmark tests.
2. The self-excited pedestrian force has been quantified through an extensive experimental campaign and is represented in a stochastic framework, which resembles the large inter and intra-subject variability in the empirical data.
3. Several parameters influence the response characteristics, in particular the distribution of pacing frequencies in the group, duration of the load event, definition of instability and the level of background noise.
4. In order to use the mathematical model as a tool for predicting the susceptibility of a footbridge to excessive lateral vibrations, a series of simulations must be carried out to fully comprehend the randomness associated with the pedestrian-induced load and uncertainties in the modelling assumptions.
5. The critical number of pedestrians predicted for the first three modes of the London Millennium Bridge compare generally well with observations reported from the opening day.

References

[1] Powell D, De Donno A, Low A. Design of damping systems for footbridges. Experience from Gatwick and Jjburg. In: Proceedings of Footbridge 2005, second international conference. 2005.
[2] De Donno A, Powell D, Low A. Design of damping systems for footbridges — conceptual framework. In: Proceedings of Footbridge 2005, second international conference. 2005.
[3] Ingólfsson E. Pedestrian-induced lateral vibrations of footbridges. Ph.D. thesis, Dep Civil Eng, Technical University of Denmark; 2011.
[4] Low A. Design for dynamic effects in long span footbridges. In: Proceedings of Footbridge 2008, third international conference. 2008.
[5] Strobl W, Kovaces I, Andrä H, Häberle. Eine Fußgängerbrücke mit einer Spannweite von 230 m (a footbridge with a span of 230 m). Stahlbau 76(12). 2007 p. 869–79 [in German].
[6] EN 1991-2, NA to BS EN 1991-2:2003 UK. National annex to Eurocode 1: actions on structure — Part 2: traffic loads on bridges. CEN, European Committee for Standardization; 2008.
[7] FIB, Guidelines for the design of footbridges, bulletin 32. Fédération international du béton (fib); 2005.
[8] Sétra. Footbridges. Assessment of vibrational behaviour of footbridges under pedestrian loading. November 2006.
[9] Butz C, Heinemeyer C, Keil A, Schlaich M, Goldack A, Trometer S. et al. Design of footbridges — guidelines and background document. HIVOSS, rFS2-CT-2007-00033. 2007.
[10] Brownjohn J, Caetano E, Cespedes X, Charles P, Cunha A, Duflot P, et al. Footbridge vibration design. Taylor and Francis; 2009.
[11] Dziuba P, Grillaud G, Flamand O, Sanquier S, Tétard Y. La passerelle Solférino comportement dynamique (dynamic behaviour of the Solférino bridge). Bull Ouvrages Métall 2001;1:34–57 [in French].
[12] Dallard P, Fitzpatrick A, Flint A, Bourva S, Low A, Ridsdill-Smith R, et al. The London Millennium footbridge. Struct Eng 2001;79(22):17–33.
[13] Fujino Y, Pacheco B, Nakamura S, Warnitchai P. Synchronization of human walking observed during lateral vibration of a congested pedestrian bridge. Earthq Eng Struct Dyn 1993;22(9):741–58.
[14] McRobie A, Morgenthal G, Lasenby J, Ringer M. Section model tests on human-structure lock-in. Proc ICE: Bridge Eng 2003;156(BE2):71–9.
[15] Eckhardt B, Ott E, Strogatz S, Abrams D, McRobie A. Modeling walker synchronization on the millennium bridge. Phys Rev E 2007;75: 21110-1-10.
[16] Venuti F, Bruno L, Napoli P. Pedestrian lateral action on lively footbridges: a new load model. Struct Eng Int 2007;17:236–41.
[17] Bodgi J, Erlicher S, Argoul P, Flamand O, Danbon F. Crowd structure synchronization: coupling between Eulerian flow modeling and Kuramoto phase equation. In: Proceedings of Footbridge 2008, third international conference. 2008.
[18] Trovato A, Erlicher S, Argoul P. Modeling the lateral pedestrian force on rigid and moving floors by a self-sustained oscillator. In: ECCOMAS thematic conference on computational methods in structural dynamics and earthquake engineering. 2009.
[19] Barker C. Some observations on the nature of the mechanism that drives the self-excited lateral response of footbridges. In: Proceedings of Footbridge 2002, first international conference. 2002.
[20] Brownjohn J, Fok P, Roche M, Omenzetter P. Long span steel pedestrian bridge at Singapore Changi airport – part 2: crowd loading tests and vibration mitigation measures. The Struct Eng 2004;82(16):28–34.
[21] Macdonald J. Pedestrian-induced vibrations of the Clifton Suspension bridge, UK. Proc ICE: Bridge Eng 2008;161(BE2):69–77.
[22] Ingólfsson E, Georgakis C, Ricciardelli F, Procino L. Lateral human-structure interaction on footbridges. In: Tenth international conference on recent advances in structural dynamics. 2010.
[23] Blekherman A. Swaying of pedestrian bridges. J Bridge Eng 2005;10(2): 142–50.
[24] Blekherman A. Autoparametric resonance in a pedestrian steel arch bridge: Solferino bridge, Paris. J Bridge Eng 2007;12:669–76.
[25] Piccardo G, Tubino F. Parametric resonance of flexible footbridges under crowd-induced lateral excitation. J Sound Vib 2008;311:353–71.
[26] Hobbs R. Test on lateral forces induced by pedestrians crossing a platform driven laterally. Tech rep, Civil Engineering Department, Imperial College London, London, UK, a report for Ove Arup and Partners. August 2000.
[27] Newland D. Pedestrian excitation of bridges. Proc Inst Mech Eng, Part C 2004; 218:477–92.
[28] Macdonald J. Lateral excitation of bridges by balancing pedestrians. Proc Roy Soc A 2009;465:1055–73.

Please cite this article in press as: Ingólfsson ET, Georgakis CT. A stochastic load model for pedestrian-induced lateral forces on footbridges. Engineering Structures (2011), doi:10.1016/j.engstruct.2011.07.009

[29] Ingólfsson E, Georgakis C, Ricciardelli F, Jönsson J. Experimental identification of pedestrian-induced lateral forces on footbridges. J Sound Vib 2011;330: 1265–84.
[30] Racic V, Pavic A, Brownjohn J. Experimental identification and analytical modelling of walking forces: literature review. J Sound Vib 2009;326:1–49.
[31] Strömmen E. Theory of bridge aerodynamics. Springer; 2006.
[32] Pizzimenti A, Ricciardelli F. Experimental evaluation of the dynamic lateral loading of footbridges by walking pedestrians. In: Proceedings of the 6th internat conf struct dyn. 2005.
[33] Bachmann H, Pretlov A, Rainer H. Appendix G: dynamic forces from rhythmical human body motions. In: Vibration problems in structures: practical guidelines. Birkhäuser; 1996.
[34] Vickery B, Clark A. Lift of across-wind response of tapered stacks. Proc Amer Soc Civil Eng J Struct Div 1972;98:1–20.
[35] Shinozuka M, Deodatis G. Simulation of stochastic processes by spectral representation. Appl Mech Rev 1991;44(4):191–204.
[36] Madsen H. Time series analysis. Texts in statistical science, Chapman & Hall/CRC; 2007.
[37] Chatfield C. The analysis of time series. An introduction. 6th ed. Texts in statistical science, Chapman & Hall/CRC; 2004.
[38] Hogsberg J, Krenk S. Adaptive tuning of elasto-plastic damper. Int J Non-Linear Mech 2007;42:928–40.
[39] Clough RW, Penzien J. Dynamics of structures. 2nd ed. Civil engineering series, McGraw-Hill International Editions; 1993.
[40] Susy. The national health interview survey. Tech rep., Danish National Institute of Public Health; 2000.
[41] Pachi A, Ji T. Frequency and velocity of people walking. The Struct Eng 2005; 83(3):36–40.
[42] Kasperski M. Serviceability of pedestrian structures. In: Proceedings of the 25th IMAC conference. 2007.
[43] Venuti F, Bruno L. An interpretative model of the pedestrian fundamental relation. C.R. Mecanique 2007;335:194–200.
[44] Bruno L, Venuti F. The pedestrian speed–density relation: modelling and application. In: Proceedings of Footbridge 2008, third international conference. 2008.
[45] Andersen R. Pedestrian-induced vibrations: human–human interaction. M.Sc. thesis. Dep Civil Eng, Technical University of Denmark; 2009.
[46] Ricciardelli F, Pansera A. An experimental investigation into the interaction among walkers in groups and crowds. In: Tenth internation conference on recent advances in structural dynamics. 2010.
[47] Ingólfsson E, Georgakis C, Jönsson J, Ricciardelli F. Vertical footbridge vibrations: towards an improved and codifiable response evaluation. in: Third international conference on structural engineering, mechanics and computation. 2007.
[48] Pavic A, Armitage T, Reynolds P, Wright J. Methodology for modal testing of the millennium bridge, London. Proc ICE: Struct Build 2002;152(2):111–22.
[49] Pavic A, Willford M, Reynolds P, Wright J. Key results of modal testing of the millennium bridge, London. In: Proceedings of Footbridge 2002, first international conference. 2002.
[50] Dallard P, Fitzpatrick T, Flint A, Low A, Smith R, Willford M, et al. London Millennium bridge: pedestrian-induced lateral vibration. J Bridge Eng 2001; 6(6):412–7.

Please cite this article in press as: Ingólfsson ET, Georgakis CT. A stochastic load model for pedestrian-induced lateral forces on footbridges. Engineering Structures (2011), doi:10.1016/j.engstruct.2011.07.009

In this thesis the phenomenon of excessive pedestrian-induced lateral vibrations as observed on several high-profile footbridges e.g. Paris' Solferino Bridge (1999) or the London Millennium Bridge (2000) is investigated. As a part of this research, an extensive experimental campaign, involving 71 test subjects, has been carried out to determine the lateral forces generated by pedestrians during walking on a laterally moving treadmill. Various combinations of lateral vibration frequencies (0.33-1.07 Hz) and amplitudes (4.5-48 mm) were tested and the entire campaign covered approximately 55 km of walking distributed on almost 5000 individual tests.

In particular, the experimental campaign showed that large amplitude vibrations are the result of correlated pedestrian forces in the form of "negative damping" that can be generated irrespective of the relationship between the walking frequency and the frequency of the lateral movement.

DTU Civil Engineering
Department of Civil Engineering
Technical University of Denmark

Brovej, Building 118
2800 Kgs. Lyngby
Telephone 45 25 17 00

www.byg.dtu.dk

ISBN: 9788778773104
ISSN: 1601-2917